Regulation of the Mg^{2+} transporter TRPM7 by growth factors- implications in vascular function in health and disease

Zhiguo Zou

MBBCh, MSc

Submitted in fulfilment of the requirements of the degree of

Doctor of Philosophy

British Heart Foundation Glasgow Cardiovascular Research Centre

Institute of Cardiovascular and Medical Sciences,

College of Medical, Veterinary and Life Sciences,

University of Glasgow

May 2020

Abstract

Transient receptor potential melastatin 7 (TRPM7) is a ubiquitously expressed bi-functional protein (chanzyme, channel + kinase) comprising a cation channel and a C-terminal α-kinase domain. As an ion channel, TRPM7 conducts primarily divalent cations such as Mg^{2+}, Ca^{2+} and Zn^{2+}. The kinase domain has been found to influence activity of downstream target proteins including calpain-2, annexin-1, myosin IIA, phospholipase Cγ2 (PLCγ2) and eukaryotic elongation factor 2-kinase (eEF2-k). The relevance of TRPM7 in the cardiovascular system has been demonstrated by an increasing number of studies. Our group has previously identified TRPM7 as a key regulator of Mg^{2+} homeostasis and growth in vascular smooth muscle cells (VSMCs). We show that TRPM7 exerts protective effects against Ang II-induced hypertension, endothelial dysfunction and cardiac hypertrophy and that vasoactive agent bradykinin regulates TRPM7 and its downstream target annexin-1, playing an important role in VSMC Mg^{2+} homeostasis, cell migration and invasion. The implication of TRPM7 in regulating blood pressure was also highlighted recently with a study showing that leptin induces hypertension through TRPM7 in carotid body.

Growth factors, such as vascular endothelial growth factor (VEGF) and epidermal growth factor (EGF), through activating their receptors VEGF receptor (VEGFR) and EGF receptor (EGFR) respectively, which belong to the receptor tyrosine kinase (RTK) family, trigger a variety of downstream signalling including PLCγ/protein kinase C (PKC), RAS/RAF/mitogen-activated protein kinase kinase (MEK)/mitogen-activated protein kinase (MAPK), phosphoinositide 3-kinase (PI3K)/protein kinase B (AKT)/mammalian target of rapamycin (mTOR), Janus kinase (JAK)/signal transducer and activator of transcription (STAT) and Src family kinases (SFKs). The activation of RTK exerts significant biological effects on many cellular processes including cell division, proliferation, migration, differentiation and ion homeostasis, and plays a pivotal role in embryo development, wound healing and tumour biology.

There is a paucity of information about the relationship between growth factors and TRPM7 in the vasculature, and whether the interaction has a role in vascular health and disease. We hypothesize that in VSMCs VEGF and EGF exert regulatory effects on TRPM7 activity, and the process mediates ion homeostasis and the activation of cellular signalling, which consequently influences cell function and vessel health. While under

pathological conditions such as hypertension, the growth factor-RTK-TRPM7 axis could be aberrantly expressed and result in deleterious consequences.

This study identified novel roles of growth factors (VEGF and EGF) in VSMCs which is specifically mediated by TRPM7. We demonstrate that VEGF and EGF through activating the RTKs (VEGFR and EGFR respectively) upregulate TRPM7 expression and phosphorylation in VSMCs and consequently regulate ion homeostasis (Mg^{2+} and Ca^{2+}) through TRPM7 channel activation. With regards to the downstream effects, we show the crucial involvement of TRPM7 in the effects mediated by EGF, including activation of extracellular signal-regulated kinase 1/2 (ERK1/2) and migration and proliferation in VSMCs, processes that are associated with vessel morphology. We also show that the VEGF-regulated TRPM7 plays an important role in the endothelium-independent vascular relaxation.

Our study demonstrates that the Growth Factor/RTK system is both upstream and downstream of TRPM7 in the vasculature. Taking advantage of different approaches, we identify the direct interaction between EGFR and TRPM7 in VSMCs and the interaction is enhanced by EGF in a c-Src dependent manner. Our experiments provide visible evidence that the interaction between EGFR and TRPM7 occurs at cell membrane, confirming that TRPM7 functions as a cell surface protein. Importantly, our data indicate that TRPM7 acts as an upstream regulator of RTK, since TRPM7 kinase is indispensable for EGFR expression and c-Src activation in VSMCs and lack of TRPM7 kinase activity is associated with reduced EGFR phosphorylation in the vessels. Our data also highlight that the property of TRPM7 as a kinase is specifically involved in these vascular effects.

We explored the potential clinical relevance of the RTK-TRPM7 crosstalk. First, we show that the EGFR-TRPM7-ERK1/2 pathway is enhanced in VSMCs from hypertensive rats, which is associated with increased intracellular Ca^{2+} and cell migration, suggesting that aberrant activity of this pathway might be involved in the pathophysiology of hypertension. Secondly, this study takes advantage of placental tissues from two different animal models of preeclampsia and show that dysregulation of VEGFR and TRPM7 is present in the placenta under preeclamptic conditions. Our experiments suggest that the VEGFR-TRPM7 crosstalk might be important for future studies aimed at pathophysiological mechanisms and therapeutic targets of preeclampsia.

Taken together our findings identify TRPM7 as a novel signalling target of growth factors EGF and VEGF in the vascular system. Importantly TRPM7 is differentially

regulated by EGF and VEGF, which likely contributes to diverse vascular functional consequences of RTK-TRPM7 signalling. Data from our studies advance the field of TRMP7, Mg^{2+} regulation and vascular biology and delineate new molecular mechanisms whereby growth factors impact vascular function in health and disease.

Table of Contents

List of Tables

List of Figures

List of Publications

Zou ZG, Rios FJ, Montezano AC, Touyz RM. TRPM7, Magnesium, and Signalling. International journal of molecular sciences. 2019;20(8). pii: E1877.

Rios FJ, **Zou ZG**, Harvey AP, Harvey KY, Nosalski R, Anyfanti P, Camargo LL, Lacchini S, Ryazanov AG, Ryazanova L, McGrath S, Guzik TJ, Goodyear CS, Montezano AC, Touyz RM. Chanzyme TRPM7 protects against cardiovascular inflammation and fibrosis. Cardiovascular research. 2020 Mar 1;116(3):721-35.

Zou ZG, Rios FJ, Neves KB, Alves-Lopes R, Ling J, Baillie GS, Gao X, Fuller W, Camargo LL, Gudermann T, Chubanov V, Montezano AC, Touyz RM. EGF/EGFR interplays with TRPM7 to regulate the proliferation and migration of vascular smooth muscle cells. Arteriosclerosis, Thrombosis, and Vascular Biology (submitted).

Rios FJ, **Zou ZG**, Harvey AP, Harvey KY, Camargo LL, Neves KB, Nichol S, Cheah A, Zahraa M, Ryazanov AG, Ryazanova L, Gudermann T, Chubanov V, Montezano AC, Touyz RM. TRPM7 is protective against cardiovascular damage induced by aldosterone/salt. Circ Res (submitted).

Invited Conference Presentations

Zou ZG, Neves KB, Alves-Lopes R, Graham D, Montezano AC, Rios FJ, Touyz RM. Vascular effects of VEGF and EGF are mediated through TRPM7. [Oral presentation] XV International Magnesium Symposium, Internatio*nal Society for the Development of Research on Magnesium 2019.*

Zou ZG, Rios FJ, Neves KB, Alves-Lopes R, Camargo LL, Montezano AC, Touyz RM. TRPM7 is involved in EGF and VEGF regulation of calcium and magnesium homeostasis and VSMC signalling. [Poster presentation] *European Council for Cardiovascular Research 2019.*

Rios FJ, **Zou ZG**, Neves KB, Alves-Lopes R, Camargo LL, Montezano AC, Touyz RM. TRPM7 is involved in the effects of VEGF and EGF in vascular cells. [Poster presentation] *American Heart Association 2019.*

Zou ZG, Rios FJ, Neves KB, Alves-Lopes R, Ling J, Baillie GS, Camargo LL, Gudermann T, Chubanov V, Montezano AC, Touyz RM. Interaction between TRPM7 and

Epidermal Growth Factor Receptor mediates Vascular Smooth Muscle Cell activation and proliferation. [Accepted oral presentation] *International Society of Hypertension 2021*.

Awards

Jean Durlach Award (Best oral presentation at the XV International Magnesium Symposium, NIH, USA).

Acknowledgement

First and foremost, I wish to express my sincere appreciation to my supervisor Professor Rhian Touyz for providing me the excellent opportunity to continue PhD study in her lab. Over the past 4 years, I have received continuous support, guidance and encouragement from Professor Touyz and she is always keen and prompt to help. With her supports, I was able to present at several international conferences and achieved the Best Oral presentation in NIH. Professor Touyz has also kindly provided me with one-year funding allowing me to finish PhD study without financial stress. Moreover, her experience that it took her 10 years of tremendous effort before getting back to clinic in Canada has encouraged me so much, letting me know that goals can be achieved only with hardwork, dedication and discipline.

I wish to write a truly special thank you to Dr Augusto Montezano and Dr Francisco Rios. This work would have been entirely impossible without both of them. As my supervisors and lab mentors, they have been providing me daily guidance by email or face to face communication. Thank you Dr Montezano for treating me as a friend, making great effort to improve my critical thinking and academic writing and offering me the tremendous help in all facets of my research. My sincere gratitude goes to Dr Rios, who has taught me technical skills and how to be a better scientist every day. Dr Rios always encourages me with his unique and inspiring ideas, especially when I felt confused and lost confidence to move forward. He also shows great patience despite my immaturity as a young scientist in the early days, and he always tries his best to answer my questions, even some of which seems not clever.

I would like to thank senior lab members Dr Rheure Lopes and Dr Karla Neves, for always being kind to me, answering all my questions with patience, helping me with the myography study and inviting me to those unforgettable parties. The sweetest couple, also my officemates, have helped me so much throughout the past 4 years and without them, my PhD life would have been more tough. Thanks go to Dr Rashida Lathan, for being one of my best friends in Glasgow and kindly inviting me to her flat, where I have enjoyed many wonderful movies. Thanks go to Dr Livia De Lucca Camargo, Dr Adam Harvey and Dr Aikaterini Anagnostopoulou for teaching me several techniques and answering me many academic questions.

I wish to specifically acknowledge the irreplaceable technical staff: Mrs Jackie Thomson for always being there to provide lab supports; Mrs Wendy Beattie for her patience in answering me many questions regarding lab techniques and Scottish culture and traditions; Mrs Laura Haddow for her expertise in myography and microscopy and bringing me a cake in our first Christmas dinner; John McAbney and Ross Hepburn for the helpful hands in my experiments; Mrs Carol Jenkins for teaching me English jokes and leaving me warm memories, and Linda Hood, my Scottish teacher, for teaching me tough but interesting Scottish words and expressions.

Special thanks to my friends, Yu, Hanna, Xing, Jiayue, Jithin, Giacomo, Blessy, and Angela. Very nice to meet you in Glasgow, my second hometown. Those times we spent together outside the lab, drinking beer in a bar, watching movie in Rashida' flat and chatting about anything but experiments, make me feel that life is still beautiful especially when I was struggling with frustration and stress. All of you have become parts of the most beautiful memories I have in Glasgow and in my life.

Huge thanks go to my Dad and Mom. You never put any pressure of marriage or financial issues on me, and always encourage me to pursue my dream, wherever it is in the UK, America or China. Especially, my mom has come to Glasgow three times to look after the little boy, bringing him wonderful lunch each day. Without love and supports from my family, life could have been more difficult for me.

Finally, I want to express my gratitude to the China Scholarship Council scholarship, which has covered my living cost during my PhD study.

Authors's Declaration

I declare that this thesis has been written entirely by myself and is a record of the work performed by myself except where explicit reference has been made. This thesis has not been previously submitted for a higher degree at any institution. The research was carried out in the Institute of Cardiovascular and Medical Sciences, College of Medical, Veterinary and Life Sciences at the University of Glasgow under the supervision of Professor Rhian M. Touyz, Dr Augusto Montezano and Dr Francisco Rios.

Zhiguo Zou

May 2020

Abbreviation

2-APB	2-Aminoethoxydiphenyl borate
ACh	Acetylcholine
ADP	Adenosine diphosphate
ADPKD	Autosomal dominant polycystic kidney disease
AES	Aromatase excess syndrome
AF	Atrial fibrillation
Akt	Protein kinase B
Ang II	Angiotensin II
ANXA1	Annexin A1
APK	Atypical protein kinases
ARDS	Adult respiratory distress syndrome
AT1R	Ang II type-1 receptor
ATP	Adenosine triphosphate
BBB	Blood-brain barrier
BMI	Body mass index
cAMP	Cyclic adenosine monophosphate
cDNA	Complementary DNA
CNNM4	Ancient conserved domain protein/cyclin M 4
CPK	Conventional protein kinases
Cyro-EM	Cyro-electron microscopy
DAG	Diacylglycerol
DCT	Distal convolute tubule
EC	Endothelial cell
EDHF	Endothelium derived hyperpolarizing factor
EDRF	Endothelium-derived relaxing factor
eEF-2	Elongation factor-2
EGF	Epidermal growth factor
EGFR	epidermal growth factor receptor
eNOS	Endothelial nitric oxide synthase

EPC	Endothelial progenitor cell
EPHR	Erythropoietin-producing hepatocellular receptor
ER	Endoplasmic reticulum
ERK	Extracellular signal-regulated kinase
ET-1	Endothelin 1
FDA	Food and Drug Administration
FGFR	Fibroblast growth factor receptor
Flt3	FMS-like tyrosine kinase 3,
FSGS	Focal segmental glomerulosclerosis
GAPDH	Glyceraldehyde-3-phosphate dehydrogenase
GFR	Glomerular filtration rate
GPCR	G-protein-coupled receptor
Grb2	Growth factor receptor-bound 2
GSK3	Glycogen synthase kinase 3
GTP	Guanosine triphosphate
HAK	Heart alpha-kinase
HB-EGF	Heparin-binding EGF-like growth factor
HEPES	N'-2-Hydroxyethylpiperazine-N'-2 ethanesulphonic acid
HUVEC	Human umbilical vein endothelial cell
IGFR	Insulin-like growth factor receptor
InsR	Insulin receptor
IP3	Inositol 1,4,5-trisphosphate
IRH	Isolated recessive hypomagnesemia
IRS1	InsR substrate 1
IRR	Insulin receptor-related receptor
JAK	Janus kinase
JNK	c-Jun N-terminal kinase
LAK	Lymphocyte alpha-kinase
MagT1	Magnesium transporter subtype 1
MAK	Muscle alpha-kinase
MAP2K	MAP kinase kinase

MAP3K	MAP kinase kinase kinase
MAPK	Mitogen-activated protein kinase
MEK	Mitogen-activated protein kinase kinase
MHCK A	Myosin heavy chain kinase A
MHR	Melastatin homologous regions
MLIV	Mucolipidosis type IV
MPO	Myeloperoxidase
mTOR	mammalian target of rapamycin
MuSK	Muscle-specific kinase
NGFR	Nerve growth factor receptor
NICE	National Institute for Health and Care Excellence
NO	Nitric oxide
NSCC	Non-selective cationic channel
OGD	Oxygen-glucose deprivation
Ox-LDL	Oxidised low-density lipoprotein
PCR	Polymerase chain reaction
PDGFR	Platelet-derived growth factor receptor
PDK1	3-phosphoinositide-dependent kinase 1
PE	Preeclampsia
PI3K	Phosphoinositol-3-kinase
PIGF	Placental growth factor
PIP2	Phosphatidylinositol 4,5-bisphosphate
PIP3	Phosphatidylinositol 3,4,5-triphosphate
PKA	Protein kinase A
PKC	Protein kinase C
PKD	Protein kinase D
PLC	Phospholipase C
PMT	Photomultiplier tube
ROS	Reactive oxygen species
RTK	Receptor tyrosine kinase
RUPP	Reduced uterine perfusion pressure

S1P	Sphingosine-1-phosphate
SAN	Sinoatrial node
SAPK	Stress-activated protein kinase
sEng	Soluble endoglin
SFKs	Src family tyrosine kinases
sFlt1	Soluble vascular endothelial growth factor receptor-1
SH2	Src homology region 2
shRNA	Short hairpin RNA
siRNA	Small interfering RNA
SK	Calcium-activated potassium channels
SLC41A1	Solute carrier family 41 member A1
SLC41A3	Solute carrier family 41 member A3
SNP	Sodium nitroprusside
SOCE	Store-operated calcium entry
SOS	Son of Sevenless
STAT	Signal transducer and activator of transcription
TGFα	Transforming growth factor- α
TGF-beta	Transforming growth factor-beta
TKD	Tyrosine kinase domain
TKI	Tyrosine kinase inhibitor
TMA	Terminal mesenteric arteriole
TRPA	Transient receptor potential ankyrin
TSC	Tuberous sclerosis complex
TRPM6	Transient receptor potential melastatin 6
TRPM7	Transient receptor potential melastatin 7
TRPV	Transient receptor potential vanilloid
TRPML	Transient receptor potential mucolipin
TRPP	Transient receptor potential polycystine
TXA2	Thromboxane A2
VCAM-1	Vascular cell adhesion molecule-1
VEGF	Vascular endothelial growth factor

VEGFI	VEGF inhibitor
VEGFR	Vascular endothelial growth factor receptor
VGCC	Voltage-gated calcium channel

Chapter One

1 Introduction

Magnesium (Mg^{2+}) is one of the most abundant minerals in the body, which is critically involved in normal cardiovascular functions such as vascular tone and contractility. Altered Mg^{2+} status has been associated with the incidence of cardiovascular diseases including hypertension (1). Cellular levels of Mg^{2+} are tightly regulated and maintained within a narrow range through a specialized Mg^{2+} transport system composed of a series of transporters, and we have demonstrated that the ubiquitously expressed Mg^{2+} transporter transient receptor potential melastatin 7 (TRPM7) acts as a functionally important regulator of Mg^{2+} homeostasis in the vascular system (2). Receptor tyrosine kinases (RTKs) such as vascular endothelial growth factor receptor (VEGFR) and epidermal growth factor receptor (EGFR) and their ligands VEGF and EGF respectively, have been shown to modulate the activity of TRPM7 and its sister homologue TRPM6. Of importance, therapeutic inhibition of EGFR in cancer patients leads to significant hypomagnesemia (3) with mechanisms involving renal TRPM6. However, whether VEGF and EGF through RTKs regulate TRPM7 in the vascular system has not been thoroughly investigated yet.

1.1 Magnesium in health and disease

1.1.1 Magnesium and cell biology

Magnesium (Mg^{2+}) is the fourth most abundant cation in the body and the second most common intracellular divalent cation. The normal adult human body contains ~ 20 mmol/kg of fat-free tissue, with a total Mg^{2+} of approximately 1000 mmols (22~26g) (4-6). As the second most prevalent cation in the intracellular fluid, Mg^{2+} has versatile biological functions, including contributions to DNA and RNA tertiary structures, protein tertiary or quaternary structures and fluidity, stability of phospholipid bilayers and regulation of enzymes and signalling molecules (7, 8). Mg^{2+} is the most frequently found metal ion cofactor and involved in more than 300 enzyme systems in the body (9, 10). Mg^{2+} can affect enzyme activity through binding to ligand such as ATP in ATP-requiring enzymes, including Na^+/K^+ ATPase, creatine kinase, protein kinase and cyclases, regulating diverse biochemical reactions (7, 9, 11, 12). The ability of Mg^{2+} to form complexes with phosphate-containing species, such as ATP, and consequently facilitate transphosphorylation reactions which are crucial to cell physiology, is the best recognised function (7, 11). Mg^{2+} can also form complexes ADP and GTP, which are necessary for the activity of enzymes involved in energy metabolism (11). Another important property contributing to the essential physiological role of Mg^{2+} is its role as nature's physiologic

Ca^{2+} blocker (13). Mg^{2+} and Ca^{2+} levels in the body are jointly regulated through competition for intestinal absorption and renal reabsorption, and Mg^{2+} competes with Ca^{2+} for binding sites on proteins and membranes, thus inhibiting Ca^{2+} activity.

Due to the importance of Mg^{2+} in the body, cellular levels of Mg^{2+} need to be tightly regulated and maintained within a narrow range despite a wide range of variations in external Mg^{2+} concentration. This control is achieved through a balance of Mg^{2+} uptake, intracellular storage and Mg^{2+} efflux, which is dependent on specialized Mg^{2+} transporter system across biological membranes (Figure 1.1) (14, 15).

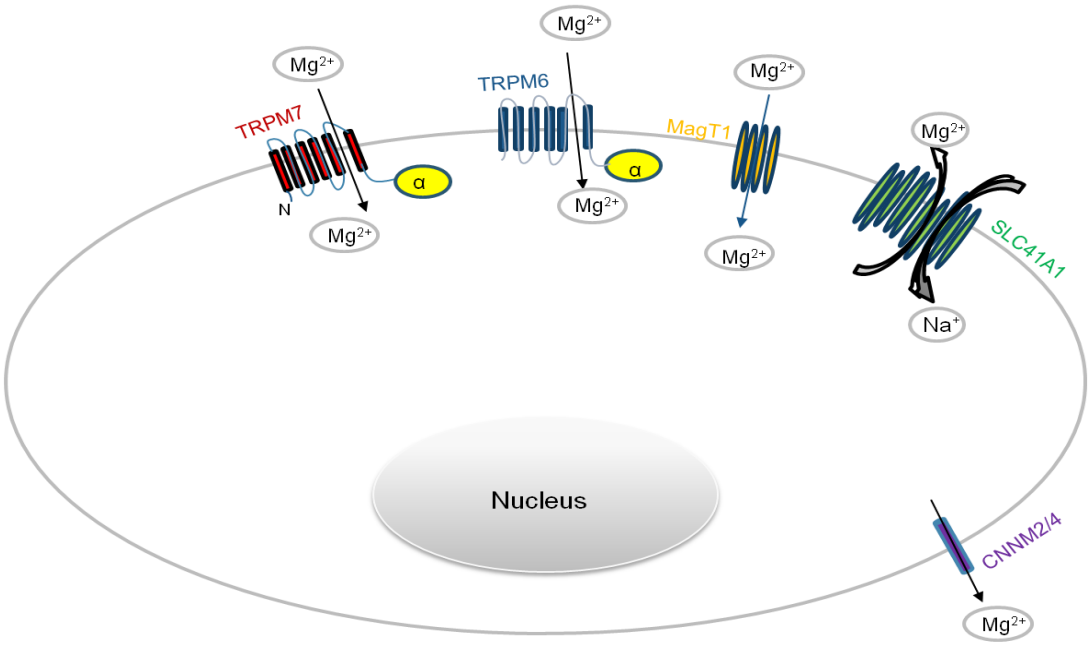

Figure 1.1 Main magnesium transporters across biological membranes. Transient receptor potential melastatin -6 (TRPM6) and -7 (TRPM7), have 6 transmembrane domains and harbour a C-terminal α-kinase domain. Magnesium transporter 1 (Mag T1), is composed of 4 or 5 transmembrane domains based on different transmembrane prediction methods, regulating Mg^{2+} influx. Solute carrier family 41 member A1 (SLC41A1), structurally has 10 putative transmembrane domains, which has been characterized as a Na^{+}/Mg^{2+} exchanger. Ancient conserved domain protein/cyclin M 2 (CNNM2) and 4 (CNNM4) are strongly expressed in the renal and intestinal epithelia respectively, considered as basolateral Mg^{2+} extruders.

Magnesium transporter subtype 1 (MagT1) was first discovered in 2005 when Goytain *et al.* used microarray analysis to identify candidate genes that were upregulated with low

Mg^{2+} (16). *MagT1* gene is located on human chromosome Xq13.1-13.2 and mouse XD. The encoded protein is composed of 4 or 5 transmembrane domains based on different transmembrane prediction methods, with no sequence similarity to any known Mg^{2+} transport proteins (17, 18). Northern analysis show that MagT1 is highly expressed in liver, heart, kidney and colon, and less expressed in intestine, spleen, brain and lungs (16, 19). MagT1 is found in the plasma membrane of mammalian cells, and is particularly abundant in epithelial cells (17). The available studies suggest that MagT1 protein possesses channel-like characteristics and is highly selective for Mg^{2+} (19) and its deficiency is associated with reduction of total and free intracellular Mg^{2+} concentration and inhibition of embryonic development (20). In humans, loss-of-function mutations in *MagT1* are associated with an immune deficiency called "X-linked immunodeficiency with magnesium defect, intellectual disability and skin disorders (18, 21).

The 41st family of solute carriers member 1 (SLC41A1), which structurally has 10 putative transmembrane domains, has been characterized as an Na^{+}/Mg^{2+} exchanger medicating Mg^{2+} efflux (15, 22). SLC41A1 is part of the central component of vertebrate Mg^{2+} transport systems. It is highly expressed in the body, especially in renal epithelial tissues and it is upregulated during Mg^{2+} deficiency (23, 24). Mutation of SLC41A1 and knockdown of SLC41A1 in experiment models can lead to defects in the maintenance of Mg^{2+} homeostasis and are linked to Mg^{2+} associated diseases (25, 26). SLC41A3, another isoform of SLC41, which is predominantly expressed in the DCT (distal convoluted tubule), has also been confirmed as a novel player in Mg^{2+} homeostasis. SLC41A3 knock out mice suffer from isolated hypomagnesemia, and it has recently been demonstrated that SLC41A3 is a mitochondrial Mg^{2+} efflux system, in a Na^{+}-dependent manner (27, 28).

TRPM6 and TRPM7, which are members of the transient receptor potential (TRP) superfamily, composed of Mg^{2+} permeable channel and α-kinase domain, and share ~50% sequence homology, have been highlighted as important channels regulating Mg^{2+} homeostasis (14, 29). The ion channel has six transmembrane segments, with the peptide between segments 5 and 6 forming the channels pore, which is highly permeable to Mg^{2+}. The kinase domain TRPM6 and TRPM7 harbours is an atypical α-type serine/threonine protein kinase in their respective carboxyl termini, which has been shown to form a dimer that can autophosphorylate and phosphorylate protein substrates (30). In the following sections, we will further discuss these two Mg^{2+} transporters and the TRP family in more detail.

1.1.2 Overview of TRP family

Transient receptor potential (TRP) gene was first described in Drosophila melanogaster in the late 1960s. It took about two decades before Rubin et al. showed that *trp* gene encodes a 1275 amino acid protein that has eight transmembrane segments in 1989 (31, 32), which functions as Ca^{2+}-permeable cations channel and is necessary for maintained excitation during intense illumination in the photoreceptors of drosophila (33). Despite the variations in protein sequence homology between 35% and 80%, TRP channels share common structure, comprising six transmembrane domains, with a cation conduction pore formed between the fifth and sixth transmembrane segments and intracellular located $–NH_2$ and –COOH termini (34, 35). According to amino acid sequence homology, the mammalian TRP superfamily is divided into six subfamilies: TRPMC (Canonical), TRPV (Vanilloid), TRPM (Melastatin), TRPA (Ankyrin), TRPP (Polycystic) and TRPML (Mucolipin) (Figure 1.2) (34). It has been demonstrated that almost all mammalian cells express at least one member of the TRP channel superfamily. The majority of TRP channels are localised in the plasma membrane, where they can sense external stimuli, such as light, sound, chemical, temperature and touch, and play an essential role in modulating the entry of cations such as Ca^{2+} and Mg^{2+} (36). Activated TRP channels are able to change the membrane potential, translocate important signalling ions cross the cell membrane and modulate intracellular enzyme activity. By doing so, TRP channels contribute to a plethora of fundamental processes, including pure sensory functions (taste transduction, temperature sensation and pheromone signalling etc.), cations homeostasis, and motile functions such as muscle contraction and vasomotor control (36).

The critical importance of the TRP family is further supported by the implications of TRP channels in a wide range of human diseases, which are also known as channelopathies. Defects in the encoding gene of TRP channels, resulting in “loss-of-function” or “gain-of-function” ion channels have been linked to six diseases: 1) mutations in TRPC6 cause the human proteinuric kidney disease called focal segmental glomerulosclerosis (FSGS); 2) mutations in the chanzyme TRPM6, which is critical for Mg^{2+} homeostasis, result in hypomagnesemia with secondary hypocalcemia; 3) autosomal dominant polycystic kidney disease (ADPKD), which is the most common inherited form of kidney failure, results from mutations either in the channel TRPP2 or the associated protein TRPP1; 4) mucolipidosis type IV (MLIV), an autosomal-recessive neurodegenerative lysosomal storage disorder, is associated with mutations in TRPML1; 5) aromatase excess syndrome, an autosomal-dominant disease characterized by enhanced extraglandular aromatization of

steroids is linked to a potential rearrangement between TRPM7 and CYP19 genes; and 6) Guamanian amyotrophic lateral sclerosis (ALS-G) and Guamanian parkinsonism dementia (PD-G) were linked to TRPM7, although one study based on parametric linkage analysis did not support the association between TRPM7 and the disease in the Kii peninsula of Japan (37-40). The mechanisms underlying the involvement of TRP channels in these diseases remain unclear, however, cellular and somatosensory dysregulation, dysfunctions in Ca^{2+} signalling, disturbance of cations (Ca^{2+} and Mg^{2+}) homeostasis and impairment of cellular functions are likely to play a role.

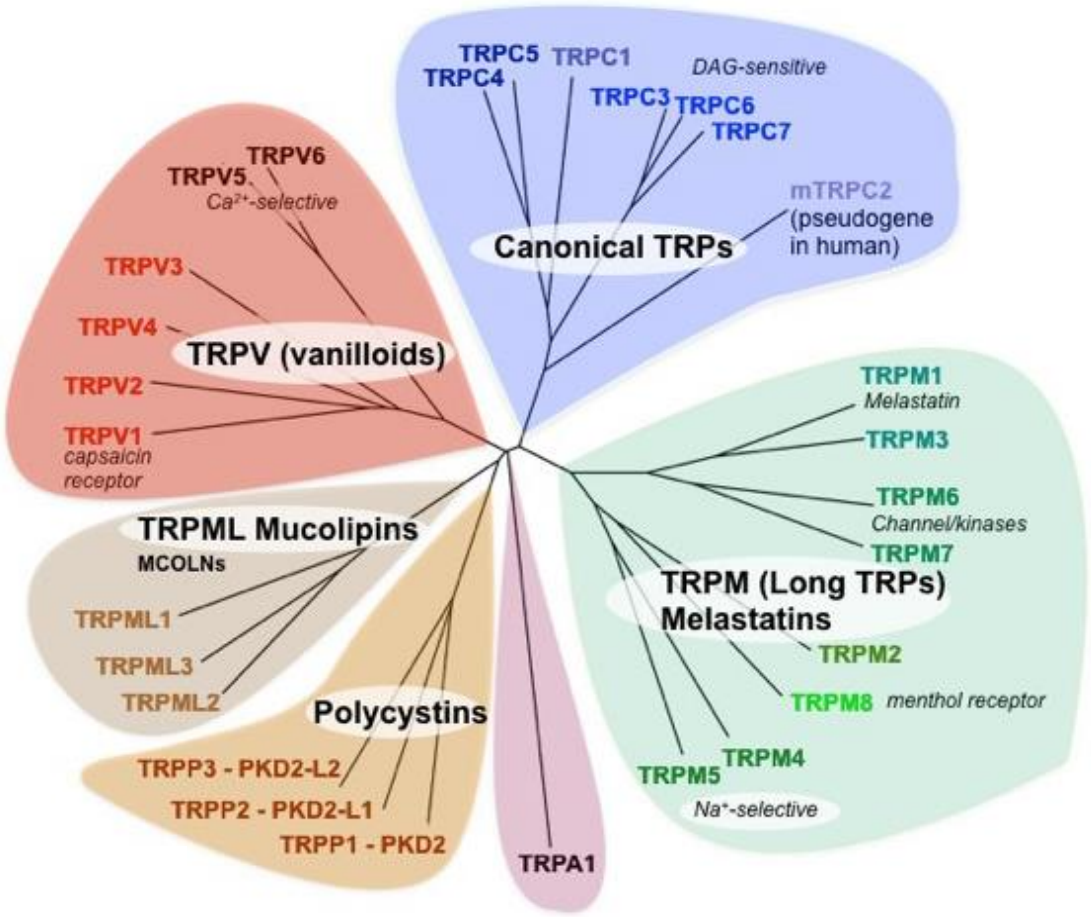

Figure 1.2 A schematic representation of the TRP superfamily in mammalian species. Based on their sequence homology mammalian TRP channels fall into six subfamilies, including TRPC (Canonical), TRPV (Vanilloid), TRPM (Melastatin), TRPML (Mucolipin), TRPP (Polycystic) and TRPA (Ankyrin), with each subfamily containing one or more members. Modified from (41).

1.1.3 TRPM subfamily: TRPM7 and TPRM6

1.1.3.1 Overview of TRPM7 and TRPM6

TRPM7 and TRPM6 are the closest homologue in the TRPM subfamily. TRPM7 and TRPM6 are also called chanzymes (41, 42), as they comprise a cation channel with six transmembrane domains fused to a C-terminal atypical α-kinase domain (43).

The TRPM7 human gene consist of 39 exons located on chromosome 15, encoding a 1863 amino acid protein with a molecular weight of 210 kDa, which is expressed in all cell types examined so far (30, 44). As postulated for other TRP channel, TRPM7 is believed to form a tetrameric complex by four TRPM7 subunits (44). The cytoplasmic N-terminus of TRPM7 consists of a hydrophobic region (H1), and four melastatin homologous regions (MHR), that are highly homologous to other members of TRPM subfamily and have undefined biological significances (45). Downstream of H1 segment are six transmembrane domains, and the channel pore (aa 1039–1056) is formed between transmembrane domain 5 and 6, with 3 negatively charged amino acids located in the pore forming segment regulating divalent cation selectivity (30). After the last transmembrane domain, the C-terminus portion of TRPM7 contains a highly conserved TRP domain (aa 1109–1128) which is common to other TRP family members, followed by a coiled-coil (CC) connecting loop (aa 1198-1250), serine and threonine-rich domains (aa 1380-1596) and eventually the α-kinase domain (aa 1597-1821) (Figure 1.3) (45, 46). Moreover, the crystal structure of the TRPM7 kinase domain showed that the N-terminal catalytic core is very similar to that of classical protein kinases in structure, including actin-fragmin kinase and aminoglycoside kinase, whereas the C-terminal lobe resembles metabolic enzymes with ATP-grasp folds (46, 47). Recently, the cryo-electron microscopy (cryo-EM) structure of mouse TRPM7 has been reported, showing that Mg^{2+} occupies the centre of the conduction pore, and prominent external disulphide bond found in the pore helix is required for channel function as a common feature among the TRPM subfamily (42).

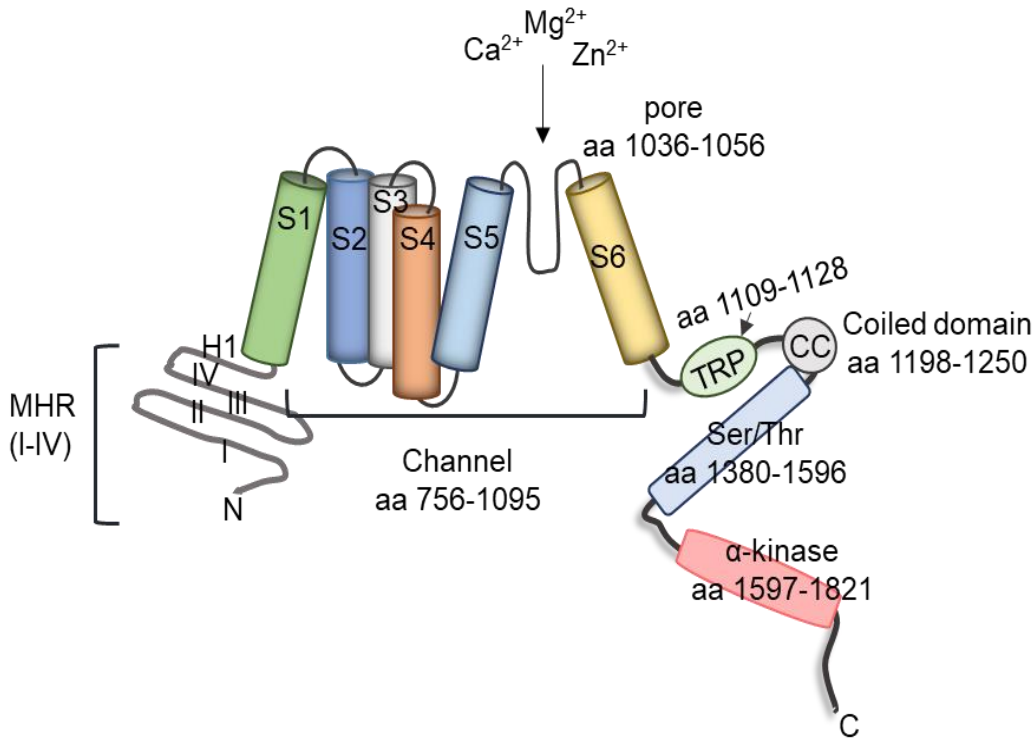

Figure 1.3 A schematic diagram to illustrate the structure of the TRPM7 channel and kinase. The TRPM7 protein contains four melastatin homologous regions (MHR), followed by a hydrophobic region (H1). There are six transmembrane segments (aa 756-1095), with the channel pore formed between domain 5 and domain 6, which are mainly permeable to Zn^{2+}, Mg^{2+}, and Ca^{2+}. Downstream of the last transmembrane domain, is the highly conserved TRP domain (aa 1109-1128), followed by a coiled-coil (CC) domain (aa 1198-1250), serine- and threonine-rich domains (aa 1380-1596), and the α-kinase domain (aa 1597-1821).

The human TRPM6 gene comprises 39 exons and is located on chromosome 9, encoding a large protein of 2022 amino acids (48). TRPM6 shares 52% overall identity with TRPM7, and similarly comprises six transmembrane domains fused to the C-terminal α-kinase, with a conduction pore formed between transmembrane segment 5 and 6 (49). TRPM6 was first confirmed as important regulator of Mg^{2+} homeostasis due to its association with hypomagnesemia with secondary hypocalcemia (HSH). Loss-of-function mutations in TPRM6 gene (also knowns as CHAK2), was identified in patients with HSH by genetic analysis. HSH patients suffer from primary defect in intestinal Mg^{2+} absorption and renal Mg^{2+} wasting (29, 50). TRPM6 is mainly expressed in the colon and the renal distal convolute tubule (DCT), specifically localised to the brush-border membrane and the apical membrane respectively, and is responsible for active transcellular Mg^{2+}

absorption in the intestine and active reabsorption in kidneys (19, 51, 52). In contrast to channel function, the role of TRPM6 kinase and how TRPM6 channel and kinase activity are linked remain unclear. Alessi et al. demonstrate a structural co-ordination between channel and kinase activity. Hoenderop et al. indicate that the α-kinase domain itself but not kinase activity is required for the regulation of TRPM6 by intracellular ATP. TRPM6 autophosphorylation is involved in the receptor for activated C-kinase 1 (RACK1)-induced inhibition of TRPM6 activity (53-55). Recently, Clapham et al. showed that the C-terminus of TRPM6 is proteolytically cleaved *in vivo*, and the freed kinase moves to the nucleus and phosphorylates specific histone residues, regulating gene transcription (56). To date, little is known about the substrates of TRPM6 kinase (57, 58).

1.1.3.2 Interaction between TRPM7 and TRPM6

TRPM6 kinase has an important role in the function of TRPM7 and TRPM6/TRPM7 complexes. TRPM6 homomultimeric complexes are not stable and requires TRPM7 to form membrane hetero-oligomeric channel complex, where the TRPM6 kinase domain determines the Mg^{2+}/ATP sensitivity (14, 59). The crucial role of TRPM7 to the complex formation of both channels in cell physiology was demonstrated *in vitro* by molecular studies showing that TRPM6 deficiency in trophoblasts stem cells results in reduction of TRPM6/7 currents while the deficiency in TRPM7 completely abolished the TRPM6/7 currents (60). Moreover, TRPM6 and TRPM7 present both several phosphorylation sites in the entire structure of the protein, and besides autophosphorylation, TRPM7 can also be transphosphorylated by TRPM6 (61). This was demonstrated in co-transfection experiments, which showed that cells transfected with TRPM7-K1646R kinase dead mutant was transphosphorylated at serine and threonine motifs by TRPM6 expression. Importantly, TRPM7-K1646R mutants do not exhibit autophosphorylation properties. These phosphorylated residues were present in the N-terminal, channel, and C terminus, and the kinase domain of the TRPM7-K1646R (61). In this study, the mass spectrometric analysis of homomeric and heteromeric TRPM7 and TRPM6 channels revealed several prominent phosphorylation sites on TRPM7 that are modified through transphosphorylation by TRPM6, which is believed to release trafficking signals to direct the assembled TRPM6/TRPM7 heteromers to the cell membrane (Figure 1.4) (61). However, transphosphorylation of TRPM6 by TRPM7 is very weak, and the interaction between TRPM7 and other Mg^{2+} transporters has rarely been reported, except for the observation that in DT40 B cells and colon carcinoma cells, the TRPM7 deficiency was associated with increased expression of MagT1 (62, 63). TRPM6 kinase activity also

regulates peripheral TRPM7 trafficking and TRPM7-dependent cell growth under hypomagnesic conditions in HEK-293 cells and chicken DT40 B cells (64).

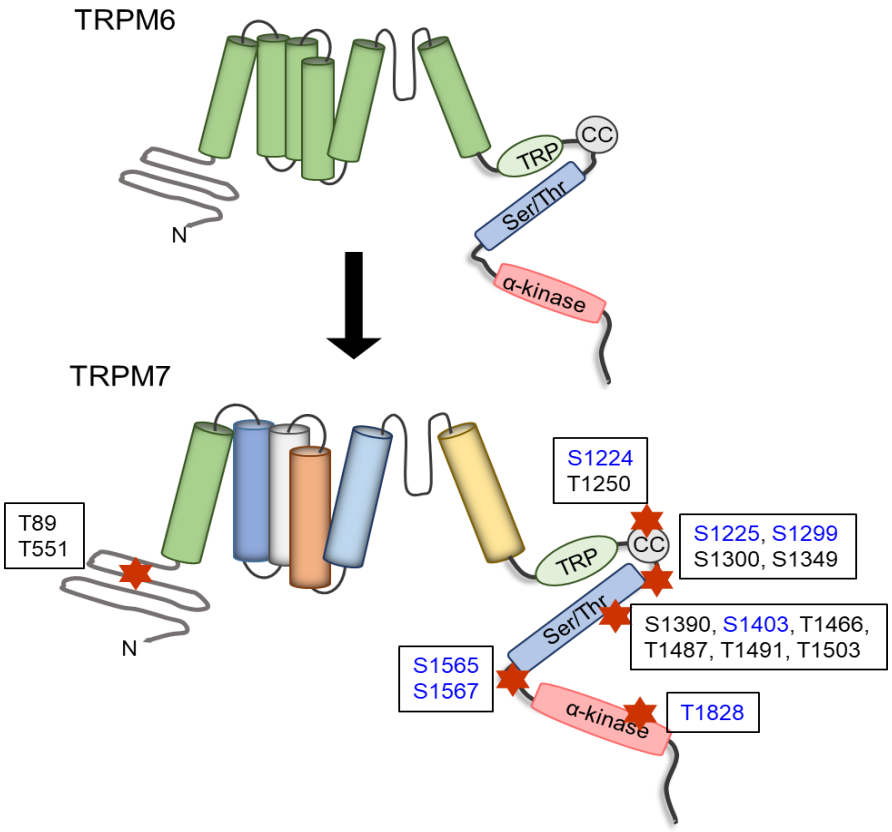

Figure 1.4 Transphosphorylation of TRPM7 by TRPM6. TRPM7 and its sister homologue, share ~50% sequence identity, with similar structure containing both 6-domian channel and an atypical α-kinase. Several sites on TRPM7 as indicated can be transphosphorylated by TRPM6, contributing to the regulation of TRPM7/TRPM6 complex.

1.1.4 TRPM7 channel domain and ion homeostasis

As an ion channel, TRPM7 is generally permeable to metal cations, conducting Zn^{2+}>Mg^{2+} >Ca^{2+}, and other essential cations including Co^{2+}, Ba^{2+}, Sr^{2+}, Ni^{2+}, and Cd^{2+} (65, 66). It was initially proposed that TRPM7 regulate, and itself to be regulated by, intracellular Mg^{2+} content, with Mg-ATP below 1 mM significantly activating the channel (67). TRPM7 has been shown to mediate cellular Mg^{2+} homeostasis in many cell types, including tumour cells, leukocytes, platelets, endothelial cells, vascular smooth muscle cells (VSMCs), cardiac myocytes, cardiac fibroblasts and osteoblasts, under both physiological and pathological conditions (2, 67-74). For example, in endothelial cells, knock-down of TRPM7 significantly inhibited Mg^{2+} influx, and TRPM7 amounts were regulated by extracellular Mg^{2+} levels (74, 75). *In vivo*, the TRPM7 kinase-deficient mice

demonstrated lower Mg^{2+} concentration in plasma, urine and bones, and displayed a proliferation arrest phenotype which could be rescued by Mg^{2+} supplementation (76, 77). Dysregulation of vascular TRPM7 and its kinase substrate annexin-1 was present in an inherited model of hypomagnesemia (78). Cryo-EM structure of mouse TRPM7 showed that the centre of the TRPM7 conduction pore is occupied by partially hydrated Mg^{2+} ions, which supports TRPM7 as an important regulator in Mg^{2+} homeostasis (42). However, the role of TRPM7 as an exclusive regulator of Mg^{2+} homeostasis was questioned by the evidence that deletion of TRPM7 did not affect acute uptake of Mg^{2+} or the maintenance of total cellular Mg^{2+} in T cells, and a recent study demonstrating TRPM7 as intracellular Zn^{2+} storage vesicles (66, 79). However, this may relate to the cell type used in these studies. For example, in T lymphocytes Mg^{2+} homeostasis is typically regulated by MagT1 (80).

In addition to modulating Mg^{2+} transport across cell membranes, TRPM7, together with other Ca^{2+} permeable and membrane located channels, regulate the Ca^{2+} entry in many cell types (81, 82). TRPM7 was demonstrated as the major Ca^{2+}-permeable channel in human atrial fibroblasts, while silencing TRPM7 by shRNA largely abolished both the endogenous TRPM7 currents and Ca^{2+} entry (83). In particular, TRPM7 medicates Ca^{2+} influx during receptor stimulation: 1) in cardiac fibroblasts TRPM7 is functionally active and controls both Mg^{2+} and Ca^{2+} influx induced by angiotensin II at different time period (69); 2) in neuroblastoma cells, activated TRPM7 following bradykinin stimulation mediates Ca^{2+} influx in a kinase-independent manner (84) and 3) Ca^{2+} entry triggered by lipopolysaccharide (LPS) is controlled by TRPM7, with pharmacological channel inhibitor significantly diminishing cytosolic Ca^{2+} elevation (85). Intriguingly, although TRPM7 itself was not recognised as a store-operated calcium channel (SOCE), the kinase has been shown to modulate SOCE, contributing to Ca^{2+} homeostasis and cellular function (86, 87).

TRPM7 also exhibits a high Zn^{2+} conductance, suggesting that it plays a role in cellular Zn^{2+} homeostasis or Zn^{2+}-related physiological functions. The role of TRPM7 in intracellular Zn^{2+} dynamics was first established in mouse cortical neurons, where activation of TRPM7 channels increases intracellular Zn^{2+}, and knockdown of TRPM7 using short hairpin RNA reduces TRPM7-like current and intracellular Zn^{2+} concentration (88). Furtherly, a recent study showed that TRPM7 is intracellular Zn^{2+}-storage vesicle, which sequesters Zn^{2+} during cytosolic overload, and releases Zn^{2+} under oxidizing conditions (66). Several members from the TRPM subfamily have been associated with Zn^{2+}. Drosophila TRPM channels are very permeable to Zn^{2+} and a loss-of-function of the

channel disrupts intracellular Zn^{2+} homeostasis (89). TRPM2 is capable of conducting Zn^{2+}, Zn^{2+} inhibits TRPM2 channel currents, and activation of TRPM2 leads to Zn^{2+} release from intracellular store (90-92). TRPM5, a monovalent cation permeable channel, can be blocked by extracellular Zn^{2+}, with the interaction sites located in the outer pore loop of TRPM5 (93).

1.1.5 TRPM7 kinase domain and its substrates

The TRPM7 and TRPM6 C-terminal kinase belongs to a specific subfamily of atypical protein kinases (APKs) known as alpha-kinases, which is a family of protein kinases with a unique catalytic domain homologous to the *Dictyostelium discoideum* myosin heavy chain kinase (MHCK), and little similarity to conventional protein kinases (CPKs) (42, 47, 94). The name alpha-kinase was proposed for the family because MHCK and elongation factor-2 (eEF-2), the first two members of the alpha-kinase family identified in 1995 and 1997 respectively, were found to phosphorylate amino acids located within alpha-helices (95). This is contrary to CPKs, which have been shown to phosphorylate substrate residues usually located within loops, β-turns or irregular structures (94, 95). To date, six human alpha-kinases have been reported, including eEF-2, alpha-kinase 1 (lymphocyte alpha-kinase, LAK or ALPK1), alpha-kinase 2 (heart alpha-kinase, HAK or ALPK2), alpha-kinase 3 (muscle alpha-kinase, MAK or ALPK3), TRPM6 and TRPM7 (46).

As indicated previously, the N-terminal catalytic core of the TRPM7 kinase domain is very similar in structure to that of classical protein kinases, including actin-fragmin kinase and aminoglycoside kinase, whereas the C-terminal lobe resembles metabolic enzymes with ATP-grasp folds (46, 47). The TRPM7 α-kinase predominantly phosphorylate Ser/Thr residues on α-helices. Activation of TRPM7 can induce autophosphorylation with multiple autophosphorylation sites identified in the cytoplasmic domain, and phosphorylation of other proteins (96, 97). To date, TRPM7 kinase has been shown to phosphorylate: 1) Annexin-1 at the conserved serine residue 5 located within the N-terminal α-helix and modulate the function of annexin-1 (98); 2) Myosin IIA at Thr1800, Ser1803 and Ser1808 in a short stretch of amino acids within the α-helical tail and regulate myosin IIA filament stability and localisation (99); 3) Eukaryotic elongation factor 2 (eEF2)'s cognate kinase eEF2-k on Ser77 under low Mg^{2+} (100); 4) SMAD2 at the C-terminal Ser465/467 motif in a dose dependent manner (101) and 5) Phospholipase C γ2 (PLCγ2) in its C2-domian on Ser1164 (Figure 1.5) (102). Additionally, TRPM7 has been shown to activate m-calpain (calpain-2) through stress-dependent stimulation of p38, mitogen-activated protein kinase

(MAPK) and c-Jun N-terminal kinase (JNK), which has an important role in regulating cell adhesion (103, 104).

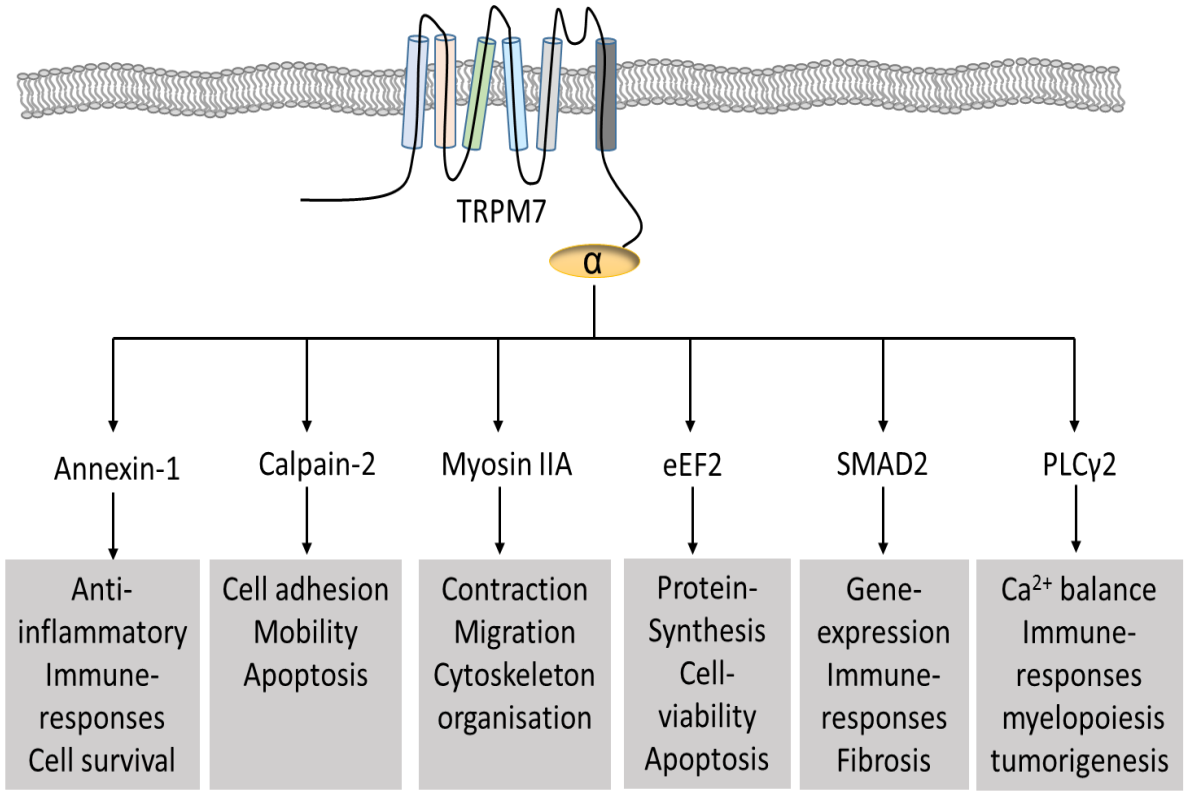

Figure 1.5 TRPM7 and substrates downstream of its kinase domain. To date, TRPM7 kinase has been found to phosphorylate annexin-1, myosin IIA, eEF2, SMAD2 and PLCγ. TRPM7 also activates calpain-2. All these substrates play important roles in various (patho)physiological processes, such as immune responses, cell survival, apoptosis, cell adhesion, protein synthesis, Ca^{2+} homeostasis, vascular contraction and cell migration.

1.1.6 Interaction between kinase domain and channel domain

The functional significance of the coupling between the TRPM7 channel domain and kinase domain has been extensively discussed. There is still much controversy regarding the interdependence of the kinase and channel domains. Matsushita et al. compared cells expressing wild type TRPM7 and mutant TPRM7 with mutation at specific sites disrupting the kinase domain activity and found that loss of kinase activity did not affect TRPM7 channel function and sensitivity to divalent cations (Figure 1.6). Additionally, no differences were found in basal intracellular free Ca^{2+} concentration and the channel function (105). These data were further confirmed by *in vivo* studies, where mouse with TRPM7 kinase-dead mutant showed normal development with normal serum total Mg^{2+} and Ca^{2+} levels (106). However, a significant number of studies also support a link between TRPM7 channel and its C-terminal kinase domain. Scharenberg et al. found that

HEK293 cells overexpressing mutant human TRPM7 K1648R and G1799D exhibit deficient Mg^{2+}/Mg.ATP-dependent suppression of channel activity, and concluded that the phosphotransferase activity of the kinase domain could influence channel activity (107). Other studies supported the interplay between the kinase and channel include: 1) the cleavage of TRPM7 kinase is associated with substantially increasing ion channel activity (108), 2) Mg^{2+} nucleotides and halides regulate TRPM7 channel through the kinase domain (109, 110), and 3) Cyclic adenosine monophosphate (cAMP)/protein kinase A (PKA) regulate TPRM7 which requires a functional kinase domain (111). Furthermore, Ryazanov et al. showed that heterozygous $TRPM7^{\Delta kinase}$ mice developed signs of hypomagnesemia with a defect in intestinal Mg^{2+} uptake, reduced TRPM7 currents with increased sensitivity to Mg^{2+}-induced inhibition (76) and reduced intracellular Mg^{2+} concentration (112). Thus, it seems that although the catalytic activity of the kinase is not essential for the channel gating, the kinase domain somehow modulates and "fine tunes" channel function in a complex manner.

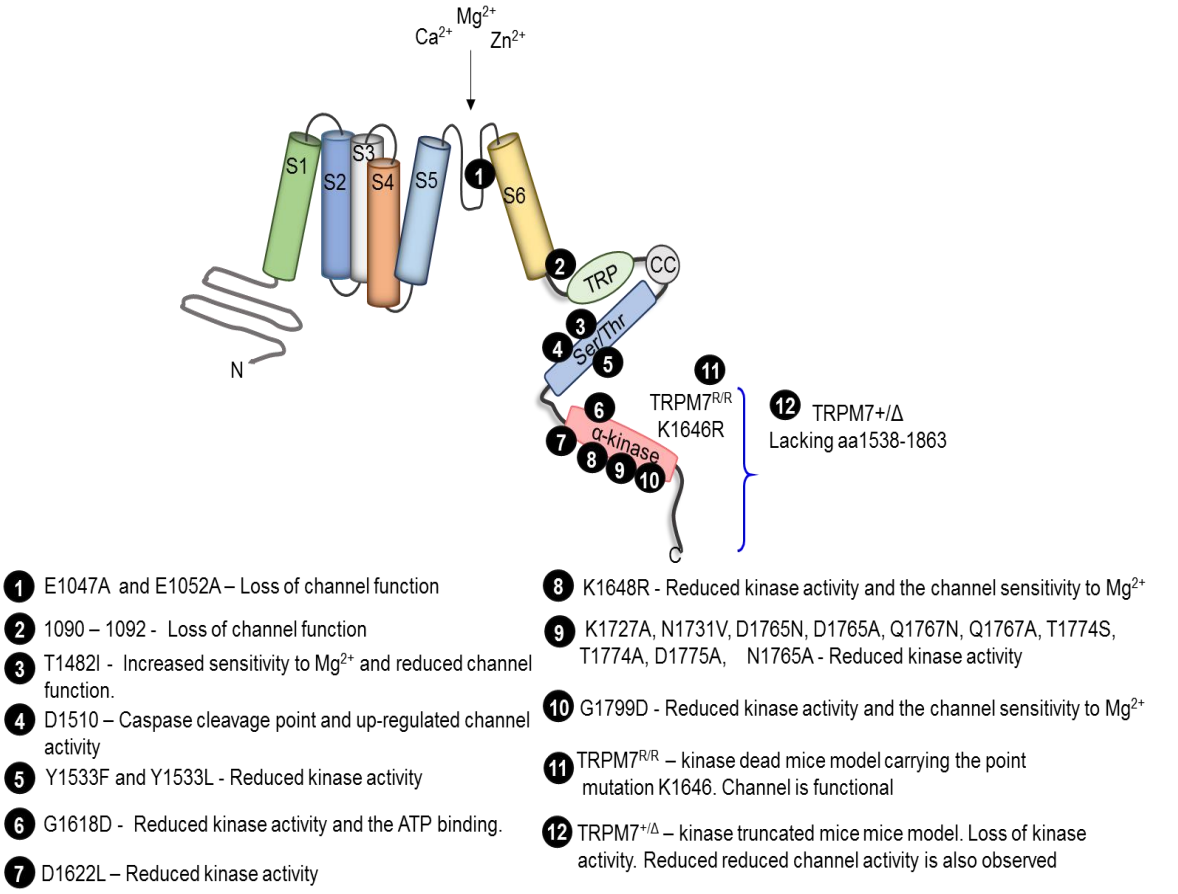

Figure 1.6 Schematic diagram showing mutations identified in TPRM7. Mutations of TRPM7 that have been reported are highlighted. Numbers indicate the single amino acid or region that influence the TRPM7 channel or kinase activity (46).

1.1.7 TRPM7 in physiological processes

1.1.7.1 Overview of the physiological role of TRPM7

The indispensable role of TRPM7 in cellular biology, could be attributed to its channel properties, particularly in mediating the homeostasis of divalent cations Mg^{2+}, Zn^{2+}, and Ca^{2+}. Mg^{2+} and Zn^{2+} are catalytic and structural cofactor of a great number of enzymes, including those involved in cellular signalling pathways and transcription factors (113, 114) and the deprivation of these cations suppress cell cycle progression leading to growth failure (115, 116). The requirement of Zn^{2+} is most likely due to its essential role in maintaining the conformation and activity of enzymes, transcription factors and cytokines involved in the process (117). Mg^{2+} is a crucial divalent cation needed for the activity of protein kinases, and the importance of Mg^{2+} in the regulation of kinase activity occurs in four steps (Figure 1.7): i) Mg-ATP binds to the enzyme, ii) the kinase binds to its substrate protein and catalyses the transfer of the phosphoryl group, iii) substrate protein is phosphorylated and Mg^{2+} is freed, and iv) Mg-ADP is released with the completion of the catalytic cycle (46).

In addition, Ca^{2+}, another important divalent cation regulated by TRPM7, participates in the regulation cell function in several ways, with evidence showing that basal cytosolic Ca^{2+}, transmembrane Ca^{2+} influx, nucleoplasmic Ca^{2+} and endoplasmic reticulum (ER) Ca^{2+} homeostasis all play major roles in vital cellular functions such as cell cycle progression, cell proliferation, division and apoptosis (118-120). In particular, intracellular Ca^{2+} has been considered as a major effector of stimulus-induced physiological changes in a variety of cell types, involved in the regulation of a wide range of important eukaryotic cellular processes including gene expression, membrane excitability and dendrite development (121, 122).

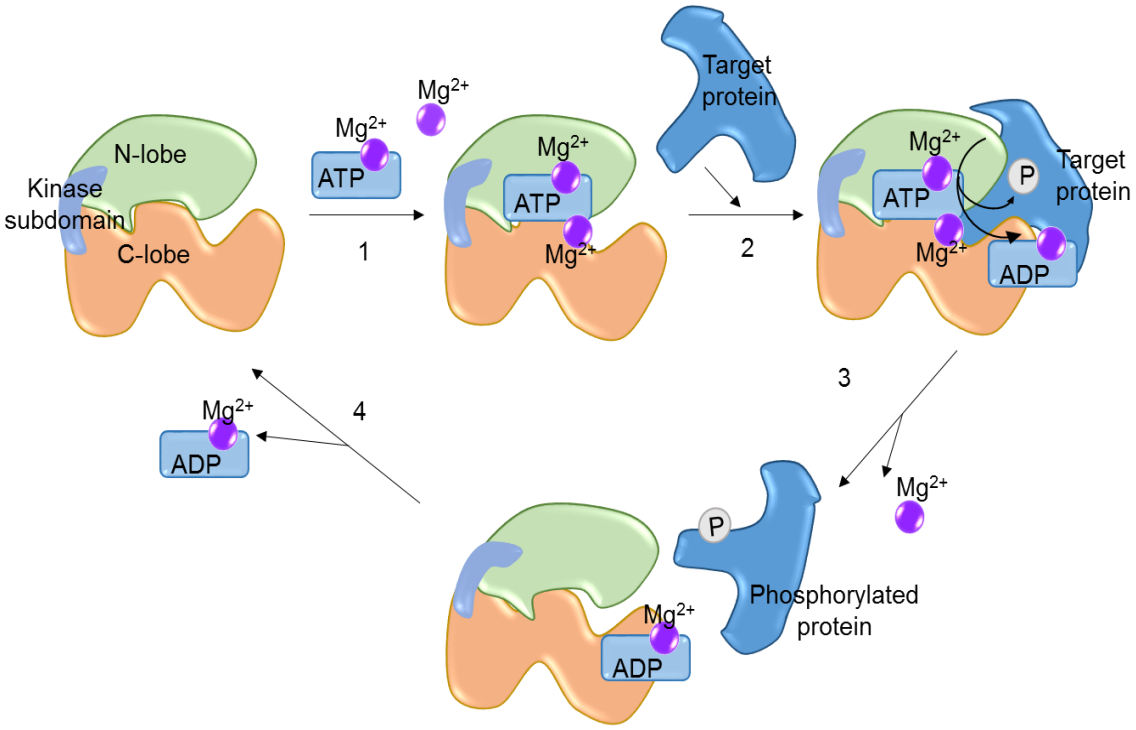

Figure 1.7 Contribution of Mg^{2+} in the kinase catalytic activity. Enzymatic activation and phosphoryl transfer require two Mg^{2+} molecules. The catalytic cycle of kinase activity involving Mg^{2+} is divided into four steps: 1) Mg-ATP binds to the enzyme, 2) the kinase binds to its substrate protein and catalyses the transfer of the phosphoryl group, 3) substrate protein is phosphorylated and Mg^{2+} is freed, and 4) Mg-ADP is released with the completion of the catalytic cycle. Copied from (46).

1.1.7.2 TRPM7 in vital cellular processes: proliferation, migration and differentiation

The dominant role of TRPM7 as ion transporter has been linked to important cellular processes. In one of the earliest studies focusing on the cell biological role of TRPM7, the genetic disruption of TPRM7 was shown to induce cell growth arrest, which could be rescued by Mg^{2+} supplementation (107). Consistently, Ryazanova et al. showed that the proliferation arrest phenotype was displayed in embryonic stem cells with deficient TRPM7 kinase domain (76). The critical involvement of TRPM7 in cell proliferation was also demonstrated in other cell types including human osteoblast-like cell, colon cancer cell and mouse cortical astrocyte (73, 123, 124). Runnels et al. found that silencing TRPM7 in fibroblasts enhances cell resistance to apoptotic stimuli in a Mg^{2+}-dependent manner through decreasing ROS levels (125). In addition, TRPM7 mediated-Ca^{2+} homeostasis is also closely linked to cellular function. TRPM7 regulates non-voltage-gated spontaneous Ca^{2+} influx, facilitating cell growth, while silencing TRPM7 reduces the magnitude of Ca^{2+} influx and reduces the rate of cell proliferation with retarded G(1)/S cell

cycle progression (126). Similarly, Takahashi et al. found that siRNA-mediated TRPM7 knockdown eliminates spontaneous Ca^{2+} entry and consequently retards cell growth and suppresses erythroid differentiation, possibly through inhibiting ERK activity in a human leukaemia cell line K562 (127). Sun et al. showed that cholesterol increases Ca^{2+} entry via TRPM7 channel, which regulates the proliferation, migration and viability of human prostate cells (128).

TRPM7 is also closely associated with cell migration. In VSMCs, Zhang et al. found that TRPM7 regulates oxidised low-density lipoprotein (Ox-LDL)-induced migration through MEK-ERK pathways (129), and Touyz et al. showed that bradykinin-induced cell migration is mediated by TRPM7 (130). In prostate cancer cells, TRPM7 deficiency reversed the epithelial-mesenchymal transition (EMT) status and consequently inhibited cell migration and invasion (131). In glioblastoma cells, naltriben, a TRPM7 activator enhanced migration and invasion, by mechanisms dependent on MAPK/ERK signalling pathway, without effects on cell viability and proliferation (132). The regulation of cell migration by TRPM7 has been reported in neuroblastoma cell (133), bladder cancer cell (134), and human non-small cell lung cancer cells (135). To further investigate whether TRPM7 regulates migration via its channel function or via its kinase domain, Guilbert et al. overexpressed TRPM7 wild type or kinase-truncated form in breast cancer cells. Notably, overexpression of kinase truncated TRPM7 reduced cell migration, while overexpression of wild type TRPM7 significantly enhanced it. These experiments suggested the crucial role of TRPM7 kinase rather than the channel domain in cell migration (136).

The essential role of TRPM7 in cell differentiation and embryonic development has been addressed in several studies: global disruption of TRPM7 in mice causes embryonic lethality before embryonic day 7 (79, 137), consistently homozygous TRPM7 kinase knockout mice demonstrates early embryonic lethality (76) and cardiac-targeted knock out of TRPM7 impairs embryonic cardiac development (138). The implication of TRPM7 in the regulation of cell differentiation has been highlighted in various cell types. In mesenchymal stromal cells, TRPM7 mediates shear stress and modulates osteogenic differentiation, and silencing TRPM7 accelerates osteogenic differentiation (139). In VSMCs, Mg^{2+} negatively regulates osteogenic differentiation through TRPM7, interleukin-18 enhances osteogenic differentiation by activating TRPM7, and TRPM7 knockdown partially blocks high concentration of d-glucose-induced development of the proliferative phenotype (140-142). TRPM7 has also been shown to modulate differentiation in hepatic cells, lung fibroblasts, dental pulp stem cells and T cells (79, 143-145). Some of these

studies investigated underlying mechanisms of the involvement of TRPM7 in cell differentiation, and indicated that the contribution of cations such as Ca^{2+} and Mg^{2+} and the interaction between TRPM7 and cellular signalling kinases are important (127, 140-142, 144, 146). Additionally, Mg^{2+} supplementation was found to promote osteogenic differentiation via the activation of Notch signalling in MSCs, which was decreased by non-specific TRPM7 inhibitor 2-APB (139, 147-149). In human dental pulp stem cell, silencing TRPM7 inhibited proliferation, migration, and osteogenic differentiation, supporting TRPM7 a role in the dental pulp repair process (145).

1.1.8 TRPM7, cancer and stem cell biology

Since the late 1980s with observations that ion channels are aberrantly expressed in cancer cell lines, a variety of channel types continue to be implicated in neoplastic progression and critically contribute to the acquirement of the main hallmarks of cancer cells, including metabolic re-programming, sustained angiogenesis, limitless replicative potential, apoptosis resistance, cell migration and invasiveness (150, 151). In particular, the role of TRPM7 as well as several other members of the TRPM family, have been demonstrated in various types of human malignant tumours (152). Increasing evidence indicates that TRPM7 is aberrantly over-expressed in different types of cancer, such as breast carcinoma, gastric carcinoma, lung, colon, prostate and ovarian cancer, and glioblastoma. Genetic and pharmacologic studies have shown that TRPM7 inhibition results in reduced proliferation, growth, migration and invasion in cancer cells (134, 153). Furthermore, TRPM7 is required for self-renewal and differentiation of cancer stem cells (CSCs), which is important for tumour initiation, growth and recurrence (154). Critical role of TRPM7 has been observed in mesenchymal stromal cells (MSCs), where it senses mechanical stimuli such as intermittent fluid shear stress and membrane tension to regulate Ca^{2+} influx and phosphorylation of cellular signalling kinases, Smad1/5 and p38 MAPK, and TRPM7 knockdown reduces MSCs proliferation and viability and triggers cell death. In glioma stem cell, Liu et al. found that TRPM7 activates JAK2/STAT3- aldehyde dehydrogenase1 (ALDH1) and/or Notch signalling pathways, contributing to the regulation of cell proliferation, migration and invasion (155). In lung cancer cells, Chen et al. indicated that TRPM7 regulates the cancer stem cell-like and metastatic phenotypes through positively modulating the Hsp90α/uPA/MMP2 signalling pathway, while pharmacological inhibition of TRPM7 with Waixenicin A is able to supress this pathway as well as the CSCs phenotype (156).

1.1.9 TRPM7 and its substrates in the cardiovascular system

1.1.9.1 TRPM7 in cardiac development and cardiac dysfunction

The role of TRPM7 in different organ systems has been identified in important experiments using TRPM7 tissue specific deletion. Animals with specific TRPM7 deficiency in T cells exhibited impaired thymocytes development and a progressive depletion of thymic medullary cells (79). Using Cre-LoxP techniques, Chubanov et al. demonstrated that mice with TRPM7 deletion in intestines exhibited early growth failure and death after birth, while no obvious phenotypes were observed in mice with TRPM7 kidney-specific deletion (157). However, none of these studies could elucidate the underlying mechanisms whereby global deletion of TRPM7 induces embryonic lethality.

To date, embryonic lethality was only observed in mice with cardiac-targeted knock-out of TRPM7 (138). Interestingly, effects of cardiac-specific TRPM7 deletion is timing dependent. Early cardiac TRPM7-deletion (before embryonic day 9) results in congestive heart failure and death at embryonic day 11.5 (E11.5) due to hypo-proliferation of the compact myocardium, while late TRPM7-inactivation (about E13) in cardiogenesis produces viable mice with normal cardiac phenotypes, and TRPM7 knock-out at intermediate time-point (between E9 and E12.5) leads to cardiomyopathy in half of the mice, associated with impaired repolarization and cardiac arrhythmias (138). Furthermore, TRPM7 has also been shown to be required for maintaining cardiac automaticity in sinoatrial node (SAN) (158). *In vivo*, TRPM7 deletion in zebrafish, murine global cardiac TRPM7 knock-out and SAN-restricted TRPM7 deletion could disrupt cardiac automaticity indirectly via regulation of Hyperpolarization Activated Cyclic Nucleotide Gated Potassium Channel 4 (HCN4), a hyperpolarization-activated channel responsible for basal automaticity in mouse SAN (158). In addition, the critical role of TPRM7 in cardiac function has been highlighted by the involvement of TRPM7 in several cardiac diseases: 1) TRPM7 regulates SAN fibrosis induced by Ang II in rats with sick sinus syndrome through Smad2-mediated mechanisms (159); 2) TRPM7 acts as the major Ca^{2+} permeable channel in human atrial fibroblasts and is likely to participate in transforming growth factor-beta1 (TGF-beta1)-elicited fibrogenesis in human atrial fibrillation (AF) (83, 160); 3) there was an inverse correlation between cardiac TRPM7 expression and left ventricular dysfunction in patients with ischaemic cardiomyopathy (161) and 4) reduced TRPM7 expression is associated with cardiac fibrosis through mediating inflammation, collagen production and Mg^{2+} deficiency (69, 162).

1.1.9.2 TRPM7, vascular Mg^{2+} homeostasis and hypertension

Hypertension is a major risk factor to common chronic cardiovascular diseases including myocardial infarction, stroke, vascular dementia and chronic kidney disease. It is a multifactorial disease, in which many systems including vascular, neurohumoral, renal, metabolic, cardiac and immune have been implicated in its development. Epidemiological and clinical studies demonstrate a negative correlation between intracellular Mg^{2+} and blood pressure. Reduced plasma and tissue Mg^{2+} levels have been associated with increased blood pressure in various experimental models (163-165). In the vascular system, Mg^{2+} negatively regulates vascular tone through its Ca^{2+} antagonistic property and induces vascular smooth muscle cell (VSMC) growth (166).

Despite the critical role of Mg^{2+} in vascular function, molecular mechanisms regulating vascular Mg^{2+} remain unclear. In 2005, Touyz et al. first showed that TRPM7 is expressed in rat, mouse and human VSMCs (2). Downregulation of TRPM7 by siRNA reduced both basal level of Mg^{2+} and Mg^{2+} influx, whereas there were no significant differences of Ca^{2+} responses relative to control cells (2). Touyz et al. also compared TRPM7 and TRPM6 expression in VSMCs from Wistar Kyoto rats (WKY) and spontaneously hypertensive rat (SHR). Although TRPM6 was also observed in rat VSMCs, basal level of TRPM7 rather than TRPM6 was lower in VSMCs from SHR compared to WKY, associated with significantly reduced intracellular Mg^{2+} (166). Three possible mechanisms were proposed to explain the changed TRPM7 expression in SHR, including modulation of TRPM7 by Ang II and other vasoactive agents, alterations in TRPM7 gene and protein expression, and disturbance of intracellular Mg^{2+} homeostasis (167). Moreover, in an animal model of inherited hypomagnesemia, low intracellular Mg^{2+} level was associated with altered vascular expression of TRPM7 and its substrate annexin-1 (78). The involvement of TPRM7 in vascular function is further supported by the fact that fluid flow-related mechanical stimuli and vasoactive agents are able to modulate TRPM7 activity. Clapham et al. showed that TRPM7 translocated to the region of plasma membrane in response to shear stress, and TRPM7 current amplitude was increased by fluid flow in VSMCs (168). Shear stress is proposed to be sensed by extracellular matrix interaction molecules of the cell and signal to cytoskeletal proteins, which consequently leads to activation of motor proteins that transport TRPM7 to the plasma membrane (168). Touyz et al. found that bradykinin via bradykinin type 2 receptor regulates TRPM7 and its substrate annexin-1 through PLC-, PKC- and c-Src-dependent pathways, which influences VSMCs migration (130), Ang II upregulated TRPM7 expression via Ang II type 1

receptor-mediated ERK1/2 signalling in VSMCs from WKY, which was blunted in VSMCs from SHR (166), and aldosterone infusion in mice resulted in downregulation of renal TRPM7, which was associated with increased inflammation and fibrosis (169).

A direct role of TRPM7 vascular function and blood pressure was established through a novel mice model, which is heterozygous for the deletion of the TRPM7 kinase domain (TRPM7Δkinase), and preserves channel function with truncated kinase domain (76, 77). Exaggerated blood pressure induced by Ang II was found in mice heterozygous for TRPM7 kinase with channel mal-function (TRPM7Δkinase mice). These mice also exhibited worsening left ventricular function and pronounced cardiac hypertrophy in comparison with Ang II-infused WT mice. These altered phenotypes were associated with reduced eNOS phosphorylation and increased expression of inflammatory marker vascular cell adhesion molecule-1 (VCAM-1) (77). In the animal model of inherited hypomagnesemia, low Mg^{2+} status was associated with increased blood pressure, vascular remodelling, elevation in vascular expression of TRPM7 and reduction of the substrate annexin-1, suggesting that TRPM7 and its substrate may contribute to Mg^{2+}-related pathologies (78). In addition, TRPM7 substrate calpain may also play an important role in the development of hypertension. Scalia R et al. showed myeloperoxidase (MPO), a major neutrophil effector protein which is elevated in hypertension (170), induced endothelial dysfunction through a calpain-mediated manner (171). Calpain was also shown to regulate inflammatory process and was a key downstream mediator in Ang II-induced cardiovascular remodelling. On the opposite, transgenic mice expressing high levels of calpastatin, a calpain-specific inhibitor, exhibited reduced vascular remodelling and ventricular hypertrophy induced by Ang II infusion (172). Therefore, all these evidences suggest a link between TRPM7 and pathological processes during the development of hypertension, and underlying mechanisms may involve both TRPM7-mediated Mg^{2+} homeostasis and the kinase activity (Figure 1.8).

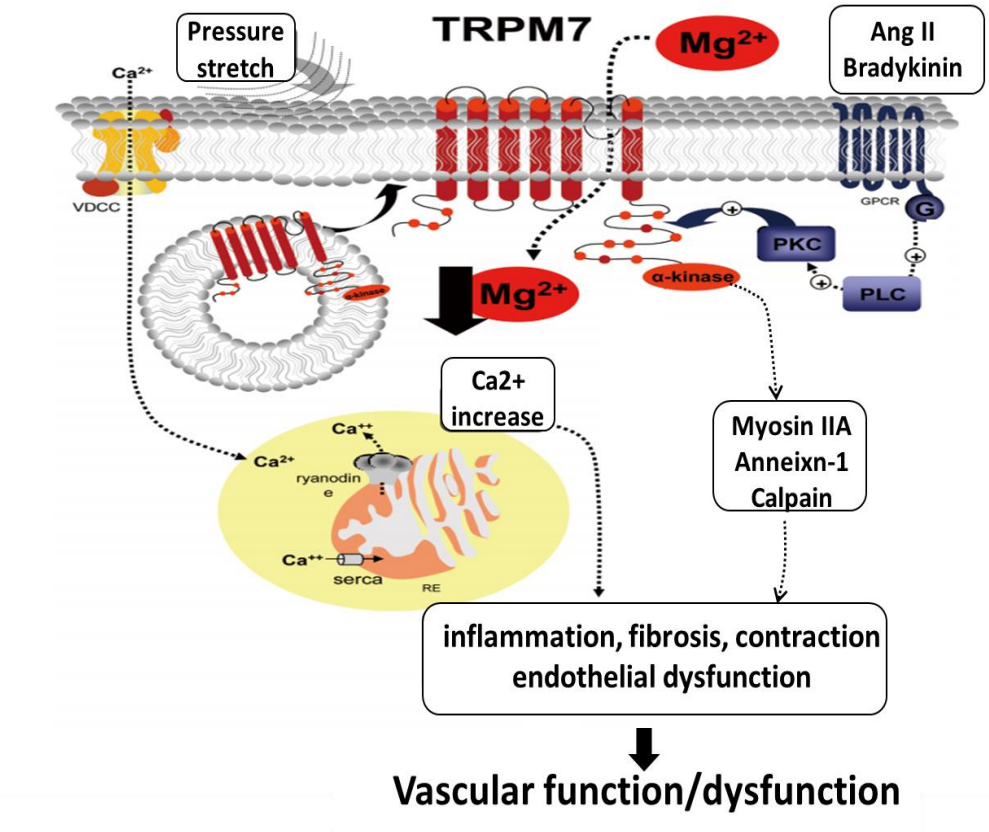

Figure 1.8 TRPM7 has been implicated in vascular pathologies in hypertension. Fluid flow-related mechanical stimuli and vasoactive agents including Ang II and bradykinin (BK), can regulate TRPM7 activity. TRPM7, through mediating Mg^{2+} influx and Mg^{2+} sensitive process and influencing the activity of several substrates such as myosin IIA, annexin-1 and calpain, contributes to pathological processes implicated in the development of hypertension. Modified from (14).

1.1.9.3 Ca^{2+} mediated by TRPM7 and vascular contraction

Contraction of VSMCs is triggered by an increase in intracellular free Ca^{2+} concentration, which consequently leads to actin-myosin cross-bridge formation (173). Under physiological conditions, intracellular Ca^{2+} and Ca^{2+} signalling are finely controlled by plasma membrane Ca^{2+}-permeable channels, transporters, exchangers and intracellular stores (173). However, perturbed intracellular Ca^{2+} homeostasis marked by increased Ca^{2+} influx, augmented Ca^{2+} release from intracellular stores such as sarcoplasmic reticulum and enhanced Ca^{2+} signalling, is associated with an anomalous vascular tone, as has been observed in genetic, experimental and human hypertension (173, 174). The involvement of Ca^{2+} in hypertension development is furtherly evidenced by the effective antihypertensive action of drugs blocking L-type Ca^{2+} channel (175).

Members of the TRP channel family including TRPM4, TRPC1, TRPC6, TRPC3 and TRPC5 have been implicated in blood pressure regulation (44, 176, 177). Excluding TRPM4, which appears to regulate blood pressure through affecting sympathetic tone (176), the other four TRP channels were shown to mediate blood pressure in a Ca^{2+}-dependent manner. In Trpc6−/− deficient mice, an elevation of about 7 mmHg in basal mean atrial blood pressure was observed, and this was explained by the compensatory overexpression of TRPC3, which led to enhanced basal and agonist-induced Ca^{2+} entry into smooth cells (176). Schmidt et al. showed that a lack of TRPC1 in mice leads to stronger hyperpolarisation, extensive Ca^{2+} influx, and increased release of endothelium derived hyperpolarizing factor (EDHF), resulting in decreased blood pressure (176, 178). Changes in Ca^{2+} influx was also observed in non-vascular cells, Liu and colleagues found that in monocytes from hypertensive patients and rats, TRPC3 and TRPC5 expression are increased and contributing to an enhanced Ca^{2+} influx (179, 180).

Thus, considering the permeability of TRPM7 to Ca^{2+}, the fact that TRPM7-mediated Ca^{2+} signals plays a critical role in cardiovascular disease such as atrial fibrillation (83) and the involvement of TRPM7 in hypertension established by our group (77), it is reasonable to suspect that Ca^{2+} homeostasis-mediated by TRPM7 in the vasculature may also has a role in the regulation of blood pressure by mechanisms that are still elusive.

1.1.9.4 TRPM7-kinase substrates and cardiovascular dysfunction

Calpain is a Ca^{2+} dependent neutral cysteine protease composed of a large catalytic subunit (80 kDa) and a small regulatory subunit (30 kDa) (181). Among the calpain family, two major isoforms calpain μ (or 1) and calpain m (or 2) are ubiquitously expressed (there is one paper also suggesting that calpain-10 is ubiquitous) (182), whereas the other isoforms are tissue-specific (172). Under basal conditions, all calpain isoforms are predominantly located in the cytosol as inactive proenzymes and translocate to the membrane after activation, where it undergoes autoproteolysis with removal of 9 to 15 amino acids of the N-terminus domain (171, 183). Calpain activity is tightly controlled by calpastatin, a specific endogenous inhibitor containing 4 equivalent inhibitory domains (184). However, excessive activation of calpains has been implicated in pathophysiological processes underlying cardiovascular disease (CVDs), such as endothelial dysfunction and vascular remodelling. Scalia and colleagues found that Ang II treatment in mice significantly increased vascular calpain activity through Ang II type-1 receptor (AT1r), causing endothelial dysfunction with increased leukocyte-endothelium interactions and

disruption of the endothelial cell barrier, a process attenuated by either AT1r blocker losartan or calpain inhibitor ZLLal (181). Calpain was also shown to cause endothelial dysfunction and vascular inflammation in a genetic rat model of type 2 diabetes (185, 186). In addition to a widely studied association with endothelial dysfunction, calpain has been closely linked to vascular remodelling, by acting as a critical downstream mediator in Ang II-induced cardiovascular remodelling (172). The role of calpain in vascular remodelling was also observed in experimental models of pulmonary arterial hypertension (PAH) (187). Furthermore, activation of calpain-1 was demonstrated in human carotid artery atherosclerotic lesions, and a deficiency of calpain inhibitor calpastatin was demonstrated in patients with essential hypertension and genetic hypertensive rats (188, 189).

Based on the critical role of calpain activity in endothelial dysfunction and vascular remodelling, targeting the calpain/calpastatin system has been proven promising in the treatment of CVDs. In transgenic mice expressing high levels of calpastatin, Ang II-induced left ventricular hypertrophy and vascular remodelling were blunted compared to wild type (172). In piglets undergoing cardiopulmonary bypass surgery, calpain inhibition was shown to reduce plasma endothelin-1 and pulmonary vascular resistance, associated with preserved pulmonary function(190).

Annexins (ANX) represent a large family of Ca^{2+}-dependent phospholipid-binding proteins, which are found in most eukaryotic organisms and share a similar structure involving a conserved C-terminal domain with Ca^{2+} biding sites and a variable N-terminal domain (191, 192). Annexin A1 (ANXA1), the first characterized member of the annexin superfamily, is a 37 kDa glucocorticoid-regulated protein, which has been shown to be phosphorylated by TRPM7 at a conserved serine residue (Ser5) located within the N-terminal amphipathic alpha-helix of ANXA1 (98, 193). Interestingly, protective properties of ANXA1 has been observed in the vasculature (193). ANXA1 displays potent anti-inflammatory and pro-resolving properties, possibly through mechanisms involving the inhibition of pro-inflammatory mediators release, tissue repair and inhibition of leukocyte recruitment (193, 194). In particular, ANXA1 and its N-terminal-derived peptide have been shown to attenuate early atherogenesis and plaque formation (195, 196), protect cardiomyocyte in mice subjected to ischemia-reperfusion injury (197), and play a protective role in healing after wire injury in mice (198). In an animal model of hypomagnesemia, reduced expression of ANXA1 in the vasculature was associated with increased vascular inflammation, impaired endothelial function and increased blood pressure (78). In addition, another member of annexin family, annexin A5 was also shown

to attenuate vascular inflammation and remodelling and improve endothelial function in a mouse model of vascular injury (199).

Therefore, calpain and ANXA1 are able to exert significant effects on vascular function and have been considered as attractive therapeutic targets for CVDs. However, despite the observation that in inherited model of hypomagnesemia vascular reduction of ANXA1 was associated with elevated TRPM7 and TRPM7 regulated cell adhesion through calpain by mediating the local influx of Ca^{2+} (78, 103), how calpain and ANXA1 contribute to the function and regulation of TRPM7 in the vasculature remains unclear. Further investigation is necessary to build a better understanding of TRPM7 and its substrates as an integrated system in the vasculature.

1.2 Receptor tyrosine kinase and downstream signalling

1.2.1 Classification of RTKs

Protein kinases are key enzymes in phosphorylation and regulation of a variety of cellular processes by catalyzing phosphate transfer from the adenosine triphosphate (ATP) to serine (85%), threonine (11.8%) and tyrosine (1.8%) residues on protein substrates (200, 201). Although the majority of protein kinases phosphorylate serine or threonine residues, 90 tyrosine kinases were found in the human genome, of which 58 are receptor types (RTKs) and 32 non-receptor types (202, 203). Based on structural features, RTKs in humans have been classified in 20 subfamilies, including epidermal growth factor receptor (EGFR), vascular endothelial growth factor receptor (VEGFR), platelet-derived growth factor receptor (PDGFR), nerve growth factor receptor (NGFR), fibroblast growth factor receptor (FGFR), insulin-like growth factor receptor (IGFR), discoidin domain receptor (DDR), muscle-specific kinase (MuSK) and erythropoietin-producing hepatocellular receptor (EPHR) (Figure 1.9) (202).

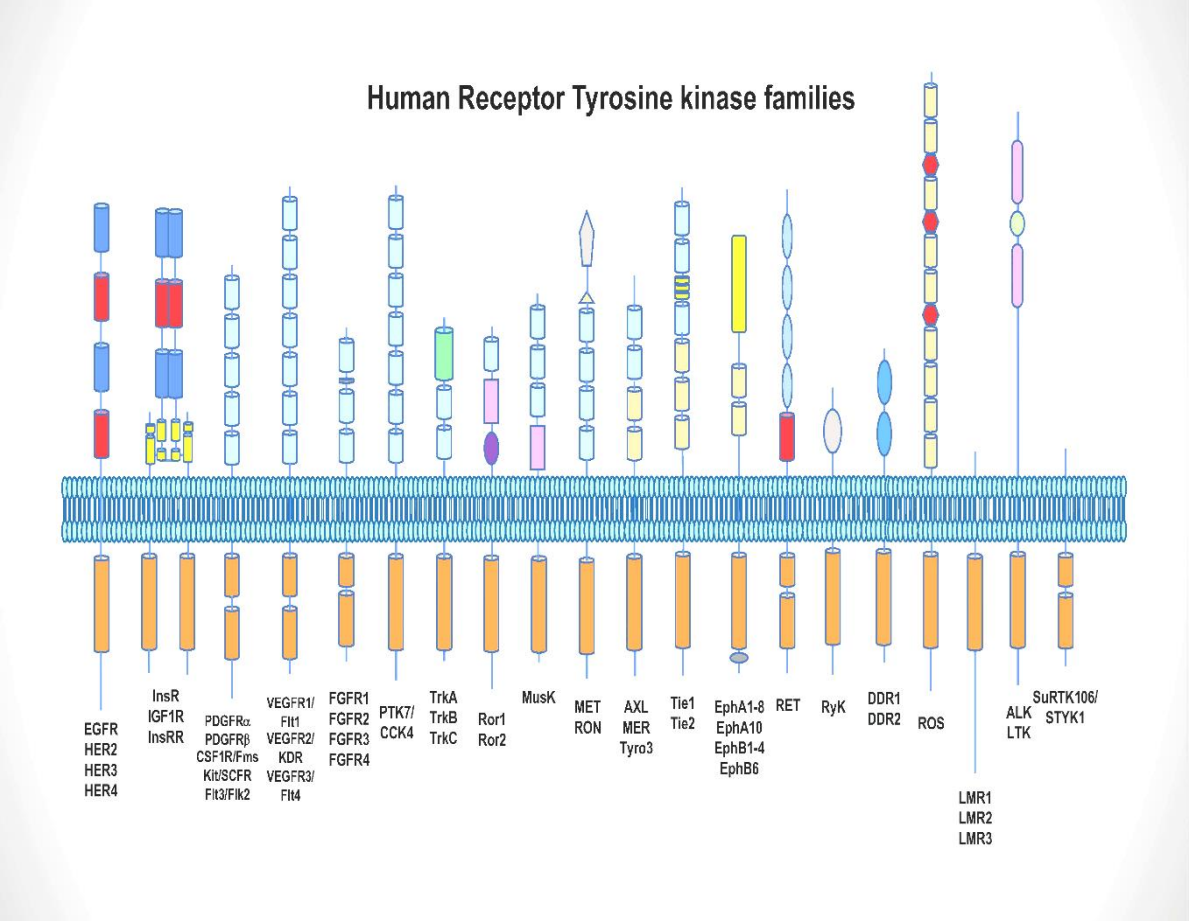

Figure 1.9 Schematic representation of the family of human receptor tyrosine kinase. Human receptor tyrosine kinases (RTKs) are divided into 20 different subfamilies. Orange cylinders are intracellular tyrosine kinase-homologous domains. Modified from (204).

1.2.2 Structure of RTKs

RTKs are membrane receptors with a similar molecular architecture, which consist of three major domains, including an extracellular ligand-binding domain, and an intracellular tyrosine kinase domain separated by a transmembrane domain (Figure 1.10) (205). The majority of RTKs are present at the cell surface as a single polypeptide chain and are monomeric in the absence of ligand, with exceptions including the subfamilies Met and insulin receptor (InsR). Met is the receptor for hepatocyte growth factor, and its subfamily members are heterodimers typically consisting of a short extracellular 50 kDa α-chain and a transmembrane 140 kDa β-chain, linked together by disulphide bridges (206-208). The InsR subfamily of RTKs such as the insulin-like growth factor-1 receptor (IGF1R) and insulin receptor-related receptor (IRR), comprise two α and two β subunits, which are disulphide-linked and form an $\alpha_2\beta_2$ heterotetramer (209). The extracellular portion of RTKs exhibits significant diversity, depending on the classes of RTKs, and contains a wide array of discrete folding modules such as immunoglobulin (Ig)-like domains, fibronectin type III-like domains, cysteine-rich domains and EGF-like domains (206). The extracellular region is joined to the intracellular region by an α-helix transmembrane domain, which is composed by 20 amino acids (202). The transmembrane domain has been shown to contribute to the stability of full-length dimers of RTKs, and maintain a signalling-competent structure (210). In contrast to the extracellular domain, the cytoplasmic portion of RTKs has a more uniform structure. Connected to the transmembrane helix, is the juxtamembrane region composed of 40-80 amino acids, which is followed by the tyrosine kinase domain (TKD) and a carboxy-terminal region. The tyrosine kinase domain consists of 12 subdomains, which is organised into two lobes and connected by the kinase insert subdomain. The small N-terminal lobe consisting of β-sheets and one α helix, binds, stabilises and orients the ATP-Mg^{2+} complex. The large C-terminal lobe, mainly composed of α helices, participates in the chelation of ATP, and catalyses the transfer of the phosphate group from the ATP to the receptor chains (202, 211).

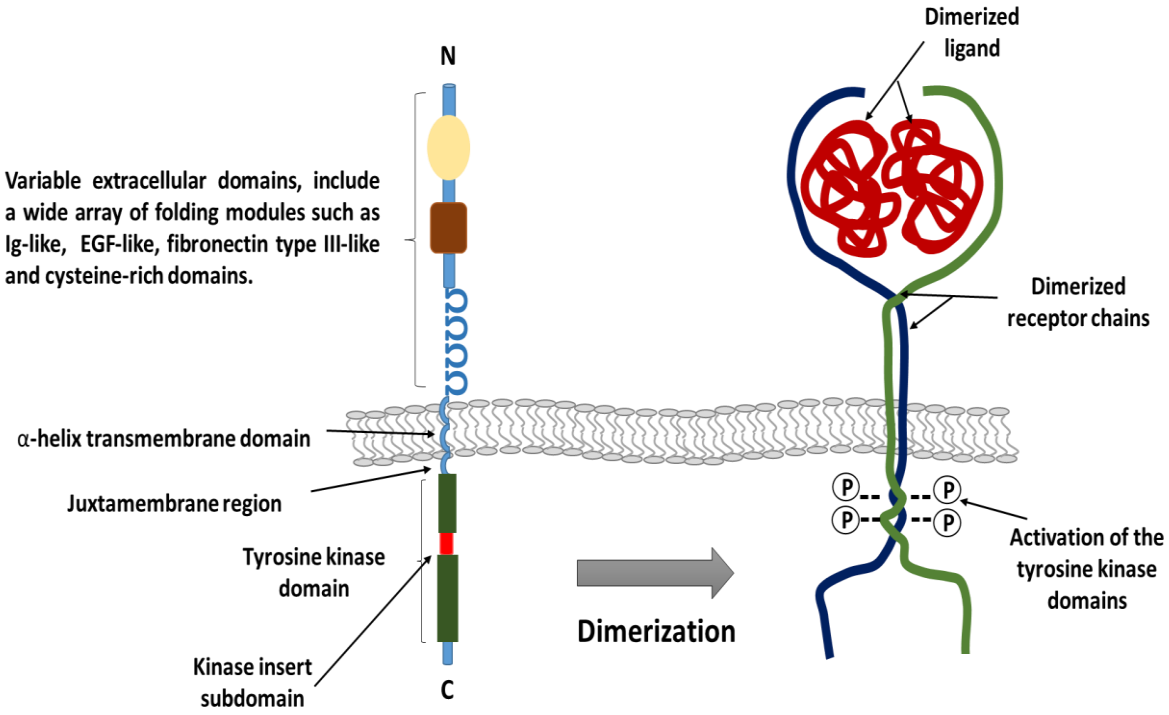

Figure 1.10 General structure of RTKs. RTKs consist of three major domains, include an extracellular ligand-binding domain, a transmembrane domain, and an intracellular tyrosine kinase domain. The extracellular domain contributes to ligand recognition, and exhibits significant diversity depending on the RTK class. The transmembrane domain is α-helix chain comprising 20 amino acids, followed by the juxtamembrane region composed of 40-80 amino acids. The tyrosine kinase domain has 12 subdomains, which is organised into two lobes and connected by the kinase insert subdomain. In general, ligand binding to RTKs at the extracellular level induces receptor dimerization, which further leads to activation of the intracellular tyrosine kinase domain through releasing cis-autoinhibition.

1.2.3 General mechanisms of action

In general, RTKs are activated through ligand-induced oligomerization, typically, dimerization (Figure 1.10), and four models of RTK dimerization have been proposed (212, 213): The receptor dimerization could be completely ligand mediated without any contact between the extracellular domains; Entirely receptor mediated and the two activating ligands make no direct contribution to the dimer formation; Two additional proposed models are both ligand-mediated and receptor-mediated components with or without the participation of accessory molecules (212, 213). Importantly, a subset of RTKs, such as the insulin receptor subfamily, forms dimers without activating ligands, however, the pre-

formed dimers, which are either ‘active’ or ‘inactive’ are stabilized or activated relatively by ligand binding through conformational changes (212, 214).

Dimerization of the RTK chains increases the respective local concentrations of TKDs, and also promotes allosteric effects, which induces the autophosphorylation of tyrosine residues located on the opposite receptor chain, a process known as transphosphorylation. Consequently, key tyrosine residues in the activation loop are phosphorylated, resulting the stabilization of activation loop in an optimal structure conformation for catalysis and an accessible C-lobe for protein substrates. Additionally, phosphorylation of tyrosine residues located on non-catalytic domains including the juxtamembrane and the kinase insert subdomain, provides various anchoring sites for cytoplasmic target proteins. However, some RTKs do not require transphosphorylation of the activation loops for activation, such as the EGFR/ErbB family. Uniquely, the EGFR TKD forms an asymmetric dimer where the C-lobe of one kinase domain, named the ‘Activator’, physically contacts the N-lobe of the other kinase domain, named the ‘Receiver’, leading to conformational changes in the N-lobe of the Receiver kinase. The allosteric change disrupts the cis-autoinhibition seen in the monomer, and induces activation of the Receiver kinase domain (202, 207, 212, 213).

In the absence of cognate ligands, the intracellular TKD is uniquely cis-autoinhibited by intramolecular interactions specific for each receptor. Different autoinhibitory mechanisms have also been described (205, 212). The activation loop contains a roughly central tyrosine residue, and determines the active or inactive state of the kinase domain (202). For RTKs such as InsR and FGFR1, the TKD autoinhibition is mediated by the activation loop, which makes physical contact with the activation site of the TKD, where a key tyrosine residue in the activation loop is phosphorylated and occludes the active site, blocking access of both ATP and protein substrates (213). For RTKs such as MuSK, the FMS-like tyrosine kinase 3 (Flt3) and EPHR, the TKD autoinhibition is regulated by juxtamembrane sequences, which make close contact with the active site of the TKD, and stabilize an inactive conformation. In addition, a third form of reversible cis-autoinhibition is observed in Tie2. A region in the carboxyl terminus of Tie2 that contains tyrosine autophosphorylation sites, occludes substrate access to the active site of the TDK, and plays a negative regulatory role in Tie2 signalling (205, 213, 215).

1.2.4 RTKs downstream signalling

After activation, RTKs recruit numerous cytoplasmic proteins containing Src homology region 2 (SH2) or phosphotyrosine-binding (PTB) domains that specifically

bind to tyrosine phosphorylated receptor chains. These proteins either have intrinsic enzymatic activity such as Src and PLCγ, or serve as docking proteins such as FGFR substrate 2 (FRS2) and InsR substrate 1 (IRS1), that function as 'assembly platforms' and recruit additional enzymes (202, 212, 213, 216). Activated RTKs are able to trigger a wide range of downstream signalling pathways, mainly include PLCγ/PKC, RAS/RAF/MEK/MAPK, PI3K/AKT/mTOR, and JAK/STAT (Figure 1.11) (217).

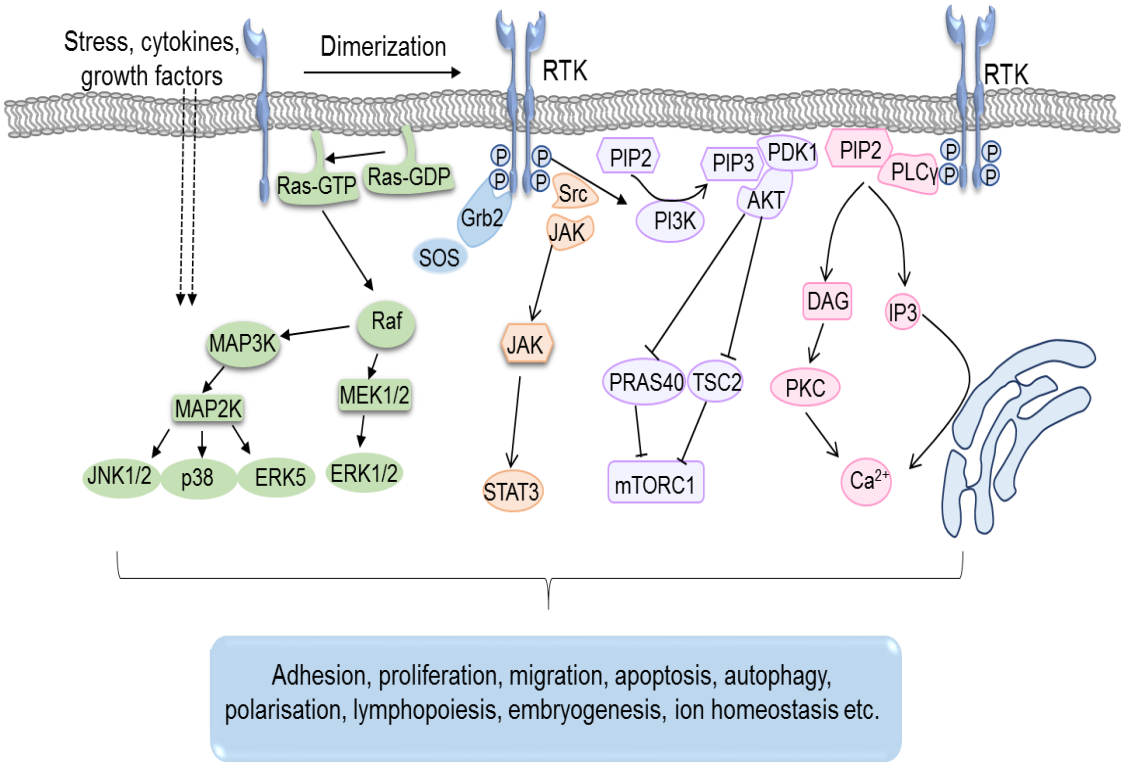

Figure 1.11 Schematic representation of main signalling pathways downstream of RTKs activation. Ligand-binding induced dimerization triggers transphosphorylation of tyrosine residues located on the receptor chain, resulting in activation of RTKs. Downstream signalling cascades activated by RTKs mainly include PLCγ/PKC, RAS/RAF/MEK/MAPK, PI3K/AKT/mTOR, JAK/STAT and the Src pathway. The functional response of these signals are essentially involved in the regulation of a variety of physiological processes. Figure copied from (46).

1.2.4.1 The RAS/RAF/MEK/MAPK pathway

The mitogen-activated protein kinase (MAPK) cascade include three tiers of serine/threonine kinases, and the third tier mammalian MAPK are divided into four groups: the extracellular signal-related kinases (ERK1/2), Jun amino-terminal kinases (JNK1/2/3),

p38-MAPK and ERK5. Each MAPK module consists of three tiers of protein kinases termed MAP kinase kinase kinase (MAP3K), MAP kinase kinase (MAP2K) and MAPK. The MAPK signalling pathway is activated by a number of extracellular signals, including hormones, tumour-promoting substances, differentiation factors, and growth factors such as EGF and the PDGF (218-220). Growth factors bind to and activate their RTKs, which bind to the adaptive protein growth factor receptor-bound 2(Grb2) and recruit Son of Sevenless homolog protein (SOS). Activated SOS interacts with its downstream target Ras, a small GTP binding protein, which is transformed to the active conformation by exchanging GDP for GTP (221). In turn, Ras recruits the serine/threonine protein kinase Raf, also known as MAP3K, to the membrane, where it becomes activated by phosphorylation. Activated Raf phosphorylates MAP2K MEK1 and MEK2 at specific serine residues in the activation loop. MEK1/2 in turn catalyse the phosphorylation of ERK1 and ERK2 at both threonine and tyrosine residues within the TEY motif (218). Activated ERK1/2 phosphorylate a variety of substrates in the cytoplasm, cellular membrane and the cytoskeleton. Phosphorylated ERK1/2 also translocates to nucleus and activates various transcription factors involved in cellular processes such as cell proliferation, differentiation and migration (202, 222). In addition, the MAPK pathway also activates p38 MAPK, JNK and ERK5, all of which involve the classical pathway components, MAP3K and MAP2K. However, relative to ERK1/2, which is mainly triggered by growth factor via RTKs, there are other important stimuli such as cell stress and inflammatory cytokines that activate ERK5, JNK and p38 MAPK independent of Ras (223, 224).

1.2.4.2 The PI3K/AKT/mTOR pathway

The phosphoinositol-3-kinase (PI3K)/Akt/mammalian target of rapamycin (mTOR) signalling pathway is initiated by the binding of extracellular growth factors to RTKs, including EGFR, VEGFR, IGFR and PDGFR. Activated RTKs recruit the Class I PI3K to the plasma membrane, where the PI3K subunit p110 catalyses the phosphorylation of phosphatidylinositol 4,5-bisphosphate (PIP2) to phosphatidylinositol 3,4,5-triphosphate (PIP3). PIP3 then provides docking sites for signalling proteins with pleckstrin-homology (PH) domains including AKT (Protein kinase B,PKB) and 3-phosphoinositide-dependent kinase 1 (PDK1) at the membrane, where PDK1 phosphorylates and activates AKT (225, 226). Activated AKT then dissociates from the plasma membrane, and phosphorylates many other downstream proteins, such as glycogen synthase kinase 3 (GSK3), the forkhead family of transcription factors (FOXOs) and mTOR. mTOR is a serine/threonine

kinase, that exists in two distinct complexes, including complex 1 (mTORC1) and complex 2 (mTORC2). AKT activates mTOR through phosphorylation of both the proline-rich Akt substrate of 40 kDa (PRAS40), a component of mTORC1, and tuberous sclerosis complex 2 (TSC2) to attenuate the inhibitory effects on mTORC1. Multiple components of the PI3K/AKT/mTOR pathway activated by RKTs play a pivotal role in the regulation of cell growth, proliferation, transcription, motility, protein synthesis and autophagy (217, 226-228).

1.2.4.3 The PLCγ/ PKC pathway

Binding of growth factors to their RTKs including PDGFR, FGFR, EGFR and VEGFR can also activate the phospholipase-Cγ (PLCγ)/protein kinase C (PKC) pathway. Upon growth factor stimulation, the phosphorylated tyrosine residues of RTKs act as high-affinity binding sites and interact with the SH2 domains of PLCγ, leading to its activation. PLCγ then hydrolyses PIP2 into two second messengers, inositol 1,4,5-trisphosphate (IP3) and diacylglycerol (DAG). Consequently, IP3 can bind to its receptor on the endoplasmic reticulum (ER) surface, whereas DAG can mediate the activation of PKC (229, 230). This process has a key role in regulating intracellular Ca^{2+}. PKC activates voltage-dependent Ca^{2+} channels, leading to extracellular Ca^{2+} influx. Binding of IP3 to its receptor triggers the release of Ca^{2+} from ER to increase cytosol Ca^{2+} level. Depletion of Ca^{2+} in ER can further triggers store-operated calcium entry (SOCE) (231-233). Besides Ca^{2+} balance, the PLCγ/ PKC pathway is also involved in the regulation of cell polarisation, proliferation, lymphopoiesis and embryogenesis (234-236).

1.2.4.4 The JAK/STAT and the Src pathways

Src family tyrosine kinases (SFKs) include 11 protein kinases, with eight members such as BLK, FGR, FYN, HCK, LCK, LYN, SRC and YES known as the core SFKs and the other three members, PTK6 (BRK), FRK and SRMS considered as SFK-related kinases (237). SRC family members are recruited on RKTs including PDGFR, EGFR, FGFR, IGFR and MuSK, via an interaction between their SH2 domains and phosphorylated residues of activated receptor chains. The association consequently releases intramolecular interaction between the SH2 domain and the tail, and triggers conformational modifications to initiate SFK activation. Of importance, more studies show that the activation of SFKs by RTKs is more complex, which involves Ras and Ral GTPases, and the tyrosine phosphatase Shp2 (202, 238). On the other hand, SFKs could also regulate the activity and signalling of RTKs, such as EGFR, PDGFR and IGFR. c-Src has been shown

to mediate the phosphorylation of EGFR on specific tyrosine residues, and modulate EGFR intracellular signalling pathways (239). The activation of Src family members can transmit mitogen signals, and plays a major role in the regulation of DNA synthesis, cell survival, adhesion, differentiation and motility (202, 240).

The Janus kinase/signal transducer and activator of transcription (JAK/STAT) is additional signalling pathway associated with RTKs activation. The activation of some RTKs such as EGFR and PDGFR, induces JAK-independent tyrosine phosphorylation of STATs, whereas there is evidence showing that FGFR activates STATs in a JAK-mediated manner (241, 242). Once activated, STATs enter the nucleus, form dimers or more complex oligomers and bind to specific regulatory sequences in target genes, regulating the transcription (243).

1.2.5 Growth factors (VEGF and EGF) and Ca^{2+}/Mg^{2+} homeostasis

In the previous section, we discussed the PLCγ/ PKC pathway downstream of RTKs activation. This pathway was found to play important role in the regulation of Ca^{2+} homeostasis, including the release of Ca^{2+} from intracellular stores, such as ER, and extracellular Ca^{2+} influx via membrane based Ca^{2+} channels. As mentioned earlier, RTKs family contain a significant portion of receptors for growth factors, such as VEGF, EGF, and PDGF, and to further highlight the role of RTKs-triggered signalling in ion mobilisation, we will continue to discuss how these growth factors affect cellular ions, with a focus on Ca^{2+} and Mg^{2+}.

1.2.5.1 Growth factors and Ca^{2+} homeostasis

VEGF has been shown to mediate intracellular Ca^{2+} in different types of cells, including endothelial cells (244-246), VSMCs (247), cardiomyocytes (248), neurons (249) and trophoblast cells (250). In endothelial cells, VEGF-A triggers a biphasic Ca^{2+} signal in human umbilical vein endothelial cell (HUVEC), with an initial transient peak dependent on store-mediated Ca^{2+} release, followed by a sustained plateau dependent of Ca^{2+} influx from the extracellular space (245, 251) (Figure 1.12). Intracellular Ca^{2+} release, mainly from ER, relies on the generation of IP3 and the activation of IP3-operated Ca^{2+} channel (IP3 receptor), whereas Ca^{2+} influx is believed to occur through SOC and/or non-selective cationic channel (NSCC) (245, 251). In particular, the TRP family channel has also been involved in VEGF-induced Ca^{2+} elevation. Bates et al. showed that TRPC6 is an indispensable component of cation channels contributing to VEGF-mediated cytosolic Ca^{2+} increase (246), and a similar role of TRPC was also observed by Son et al. in

hippocampal neurons (249). In addtion, VEGF appears to mediate Ca^{2+} mobilisation by distinct mechanisms in different cell types. For instance, Chandra et al. showed that in VSMCs VEGF stimulated extracellular Ca^{2+} influx with no intracellular Ca^{2+} release (247).

Similarly, the EGF-induced cytosol Ca^{2+} increase was also reported to exhibit two components including store-based Ca^{2+} release due to activation of the PLCγ/IP3 pathway, and a net Ca^{2+} influx from the outer medium through SOC and/or non-SOC (252). Studies focusing on the underlying mechanisms showed that the EGF-mediated Ca^{2+} entry could be regulated by several systems such as sphingosine and annexin VI (253, 254), and EGF-induced activation of SOC involves PKC (255). Particularly, TRP family channels TRPP2 and TRPV4 were shown to form a functional complex, which is activated by EGF in a EGFR- and MAP kinase- dependent manner, consequently contributing to EGF-mediated Ca^{2+} influx (256). In addition, other growth factors including FGF, IGF and PDGF have also been demonstrated in the regulation of Ca^{2+} homeostasis (244, 257, 258).

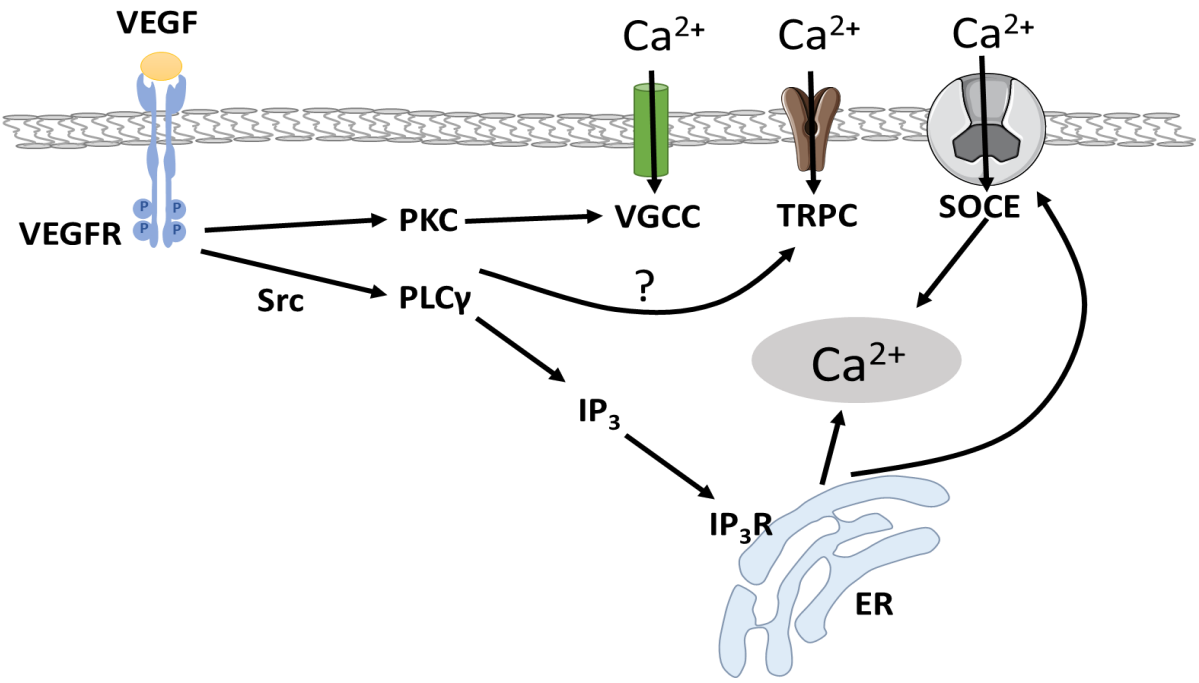

Figure 1.12 VEGF increases cytosolic Ca^{2+} through different mechanisms in endothelial cells. VEGF activates downstream Src and PLCγ, consequently resulting in the generation of IP_3, which binds to IP_3 receptor located on intracellular Ca^{2+} store and triggers Ca^{2+} release. Depletion of Ca^{2+} from intracellular store also induces store-operated Ca^{2+} entry (SOCE), which may contribute to the sustained plateau phase of Ca^{2+} elevation. In addition, voltage-gated Ca^{2+} channel (VGCC) activated by PKC and TRPC channel are also involved in Ca^{2+} influx mediated by VEGF. The question mark indicates that mechanisms of this pathway remains unclear.

1.2.5.2 Growth factors and Mg^{2+} homeostasis

The critical role of EGF in maintaining systemic balance of Mg^{2+} has been well studied. In 2007, Bindels and his colleagues identified EGF as a magnesiotropic hormone involved in total body Mg^{2+} balance. They performed linkage analysis and mutation analysis in two individuals with isolated recessive hypomagnesemia (IRH), and released the homozygous mutation C3209T in exon 22, which was absent in ethnically matched control chromosomes (259). Bindels et al. further showed that EGF is consistently coexpressed with the marker of distal convoluted tubule (DCT) in the kidney, where the fine-tuning of the Mg^{2+} excretion takes place and approximately 10% of the filtered Mg^{2+} load is reabsorbed (259). Mutations in EGF gene lead to abrogated stimulation of the EGFR located in DCT, consequently resulting in inadequate activation of TRPM6, the known predominant Mg^{2+} transporter in renal absorption of Mg^{2+} (52, 259). Furthermore, the critical role of EGF in regulating Mg^{2+} balance is also supported by the fact that cancer patients receiving EGFR inhibitors, such as cetuximab and panitumumab, develop severe hypomagnesemia as reported in randomized trials and meta-analysis (3, 260). In addition, EGF-modulated Mg^{2+} homeostasis is also observed in different types of cells (261, 262).

VEGF-induced intracellular Mg^{2+} elevation was observed in HUVECs by Hong et al, showing that VEGF-A165 released Mg^{2+} from intracellular store in a dose-dependent manner, without impact on Mg^{2+} influx (263). Further investigation into the underlying mechanisms indicated that VEGF influences Mg^{2+} through activation of the RTK/PI3K/ PLCγ pathway (263). However, unlike VEGF, PDGF was found to increase intracellular Mg^{2+} in human osteoblast cells only in the presence of extracellular Mg^{2+}, suggesting a dependence on Mg^{2+} influx (264). It was further demonstrated that PDGF is able to affect the expression of TRPM7, and mediate Mg^{2+} influx through TRPM7, a process associated with cell proliferation, migration and adhesion (264).

1.2.6 Growth factors (VEGF and EGF) and cell function

In recent years, it has been known that growth factors such as VEGF, EGF, PDGF, IGF and FGF, through activation of RTKs downstream signalling pathways, play a critical role in the regulation of cellular functions including cell proliferation, migration, apoptosis and differentiation in a variety of cell types. In this section, we will discuss in more detail the effects of growth factors (VEGF and EGF) in cell functions, with a focus on cell proliferation and migration.

1.2.6.1 VEGF and cell function

There is no doubt that VEGF plays an essential role in regulating basic cellular functions such as proliferation, migration and apoptosis, which has been demonstrated by both experimental and clinical studies in various types of cells, including multipotential stromal cells (MSCs) (265), breast cancer cells (266), neural stem cells (267), endothelial cells (268), multiple myeloma cell lines (269), human chromic myeloid leukaemia cell line (270), human hepatocellular carcinoma cells (271), and smooth muscle cells (272, 273). In endothelial cells, VEGF induces endothelial cell migration and proliferation through the activation the PI3K/Akt pathway and the MAPK pathway. Additionally, Wang and colleagues found that VEGF activates the PLCγ/PKC/protein kinase D (PKD) pathway and contributes to the phosphorylation of histone acetyltransferases and histone deacetylase-7 (HDAC7), a key regulator of gene expression in maintaining vascular integrity, which regulates VEGF responsive genes and is required for EC proliferation and migration (268). Cellular enzymes such as endothelial nitric oxide synthase (eNOS), neuropilin-1 (NRP-1) and Src homology region 2 domain-containing phosphatase 1 (SH-PTP1), are also involved in VEGF-induced endothelial cell proliferation and/or migration (274). Interestingly, underlying mechanisms of VEGF-induced cell function might also vary depending on the cell types. Anderson et al. showed that in human multiple myeloma cell lines, VEGF directly triggers cell proliferation and migration through the RAF/MEK/MAPK pathway and a PKC-dependent ERK-independent pathway respectively, which is different from pathways involved in ECs as discussed earlier (269, 275).

VEGF acts as the key regulator of both physiological and pathological angiogenesis by stimulating endothelial cell proliferation or by inhibiting endothelial cell apoptosis (276, 277). Gupta et al. showed that VEGF prevents ceramide- and starvation-induced apoptosis in human microvascular ECs by activating MAPK/ERK and inhibiting stress-activated protein kinase (SAPK)/JNK. A similar inhibitory role of VEGF in apoptosis was also observed in cardiomyocytes (278) and adenocarcinoma cells (279), and *in vivo* in mice and rats (280). Consistent with these findings, inhibition of VEGF gene expression by sequence-specific siRNA and VEGF deprivation *in vivo* using soluble VEGF receptors were shown to induce apoptosis (281, 282). Of importance, the regulatory role of VEGF in apoptosis may also depend on cell type or experimental conditions, because Narasimhan and colleagues showed that VEGF stimulated ERK1/2 signalling and promoted apoptosis in cerebral ECs under oxygen-glucose deprivation (OGD)-induced ischemic conditions (283).

1.2.6.2 EGF and cell function

EGF has been shown to regulate cell function such as cell migration and proliferation both *in vitro* and *in vivo* (284-286). Distinct cellular pathways involved in EGF-stimulated cell migration and/or proliferation depending on cell types have been described: 1) in hair follicle outer root sheath (ORS) cells, EGF promoted cell proliferation and migration through the Wnt/β-catenin signalling (287), 2) in the periodontal ligament (PDL) derived endothelial progenitor cell (EPC)-like cells, EGF promoted cell proliferation and migration through MEK/ERK- and JNK-dependent signals (288), 3) in renal epithelial cells, EGFR action mediated cell proliferation and migration by PI3K and p38 MAPK respectively (289), 4) in human lens epithelial cells, EGF was found to induce cell migration via ERK and PI3K/Akt pathways (290), and 5) in intestinal epithelial cells, EGF-stimulated cell migration required Src family kinase-dependent p38 MAPK signalling (291). Moreover, EGF was able to exert its influence on cell migration through transactivation of other RTKs. Sendtner et al. showed that in cortical precursor cells EGF activates Trk receptors in a Src-mediated manner, consequently increasing cell surface levels of TrkB and promoting its signalling responsiveness, which is an important physiological process that allow newborn cortical neurons to migrate and find their accurate position (292).

EGF acts as a potent mitogen promoting cell proliferation and survival in different types of cells and the overactivation of EGF signalling has been found in breast, head and neck, prostate and non-small cell lung cancer (293). Under normal conditions, EGF signalling is able to activate proliferation and blocks apoptosis (294, 295). However, EGF has been shown to induce apoptosis in some cell lines that overexpress the EGF receptor (296). Cell lines with naturally overexpressed EGFR such as human epidermoid carcinoma (A431) cells and human breast cancer cells (MDA-MB-468) have been well studied with consistent evidence showing that EGF induces apoptosis by different mechanisms, supposed to involve STAT1 and STAT3 respectively (297-301). In addition, p38 MAPK was also shown to mediate the ligand-induced apoptosis in cells overexpressing EGFR (302). Furthermore, the role of EGF on apoptosis also depends on experimental conditions. Cao et al. found that EGF promoted the growth of squamous carcinoma cell in suspension cultures, while it suppressed cell growth and induced apoptosis in monolayer culture (299). Gulli and colleagues showed that in A431 cells, only high concentration of EGF (10 nM) could lead to morphological features of apoptosis, while a lower concentration (0.01 nM) increased cell proliferation (297). A similar dose-dependent effect of EGF on apoptosis

was also observed by Zhao et al. in transfected Chinese hamster ovary cell line expressing EGFR (303).

1.2.7 RTKs as target for anti-cancer therapy

Under normal physiological conditions, the activation of RTKs and downstream signalling pathways controls a wide range of essential biological functions, including cell growth, motility, apoptosis, and differentiation, as discussed earlier. On the other hand, dysregulated RTKs signalling has been observed in various types of human cancers, and correlates with the development and progression of cancer (304). In the recent years, drugs targeting RTKs have become one of the most promising strategies in the treatment of cancer, and the efficacy has been proved in many clinical trials. However, a significant portion of patients receiving RTK-targeted drugs also develop unexpected side effects, such as hypertension and hypomagnesemia, by unclear mechanisms. In this section, we will briefly summarize current knowledge of the activation of RTKs and RTKs-targeted treatment in cancer.

1.2.7.1 Activation of RTKs in cancer

In normal cells, the activity of RTKs and downstream cellular signalling is tightly regulated by the mechanisms described earlier, and by additional cellular enzymes including phosphatases (212). However, since the first connection between mutated RTK and human cancer was established in 1984, aberrant signalling of RTKs has been reported in nearly all forms of human cancer, such as breast, bladder, lung, glial, colorectal, gastric, ovarian, prostate and cervical cancer (Table 1.1) (204, 305). In most cases, these aberrations result in constitutive or strongly enhanced capacity of RTKs signalling associated with transforming potential, leading to malignant transformation (306). In general, four principal mechanisms by which RTKs become potent oncogenes have been demonstrated in human cancer: activation of RTKs by gain-of-function mutation, overexpression and genomic amplification of RTKs, chromosomal rearrangements and autocrine activation (212). In addition, several emerging mechanisms potentially contributing to the activation of RTKs in cancer have been reported, including dysregulation of microRNAs, alterations in tumour microenvironment and signal attenuation by negative regulators (212).

1.2.7.2 Targeting RTKs signalling as cancer treatment

Based on the increasing knowledge of the structure and functionality of RTKs, several approaches towards the prevention and interception of dysregulated RTKs signalling in cancer have been demonstrated, including the development of selective components that target either the extracellular ligand-binding domain, the C-terminal tyrosine kinase or the substrate-binding site (306). In brief, RTKs have been targeted by monoclonal antibodies that prevent ligand binding and the activation downstream signalling pathways, and small molecule tyrosine kinase inhibitors (TKI) that specifically target the ATP-binding site of the intracellular TKD (212). To date, the US Food and Drug Administration (FDA) has approved many TKIs and monoclonal antibodies to treat a wide range of human cancers (Table 1.1). In addition, alternative strategies targeting RTKs signalling are also explored, such as immunotoxins and antisense oligonucleotides (306).

RTKs	Cancer	RTK-targeted Drugs
EGFR family (EGFR/ErbB/HER)	HER1: Breast, bladder, lung, and glial cancer HER2: Breast, gastric, ovarian, endometrial esophageal, and lung cacer	Cetuximab (Erbitux) Panitumumab (Vectibix) Gefitnib (Iressa) Erlotinib (Tarceva) Trastuzumab (Herceptin) Lapatinib (Tykerb) Vatalanib
VEGFR	Bladder, brain, breast, colon, gastric, lung, ovarian, and prostate cancner head and neck carcinoma	Sorafenib (Nexavar) Sunitinib (Sutent) Bevacizumab (Avastin) Pazopanib
PDGFR	Glioblastoma, Infantile myofibromatosis	Imatinib (Gleevec) Sunitinib (Sutent) Pazopanib
FGFR	Lung, breast, ovarian, bladder, endometrial and cervical cancer, glioblastoma	Brivanib

Table 1.1 Aberrant expression of RTKs in human cancers, and examples of RTK-targeted molecular therapies, including TKIs and monoclonal antibodies approved by FDA. Summarized from (307) and (308).

1.2.8 Involvement of RTKs in vascular (patho)biology and hypertension

RTKs are indispensably involved in the control of most fundamental cellular processes, including cell cycle, migration, metabolism, proliferation and differentiation (309). In the context of hypertension, signalling cascades activated by RTKs are implicated in structural, mechanical and functional abnormalities underlying vascular changes associated with elevated blood pressure, such as vascular hypertrophy, inflammation and endothelial dysfunction (310).

1.2.8.1 EGFR signalling and hypertension

1.2.8.1.1 EGFR and its ligand are expressed in vascular system

The mammalian ligands that bind to EGFR consist of several peptide growth factors, including EGF, transforming growth factor- α (TGFα), heparin-binding EGF-like growth factor (HB-EGF), betacellulin (BTC), amphiregulin (AR), epigen, epiregulin (EPR) and the four neuregulins (311, 312). Most EGF family of ligands as well as all four members of the EGFR family (ErbB1, ErbB2, ErbB3, and ErbB4) have been identified in multiple cell types within the vascular wall including VSMCs and ECs (313). In VSMCs, EGFR signalling activated by EGF or transactivated by other vasoactive agents such as Ang II, bradykinin, and endothelin 1(ET-1) has been shown to regulate many physiological processes including proliferation, migration, Ca^{2+} homeostasis, contraction and ROS production (313). In ECs, enhanced EGFR activation is involved in nitric oxide (NO) homeostasis, an important process associated with inflammation, migration, proliferation and angiogenesis (314). In addition, EGFR is also expressed in macrophages, immune cells that are abundant in atherosclerotic plaques, contributing to the development of atherosclerosis (315), and EGFR inhibition was found to attenuate atherosclerosis via affecting macrophages-mediated ROS production and inflammation (316).

1.2.8.1.2 EGF acts as a vasoconstrictor

Accumulating evidence has highlighted the EGFR signalling as a critical contributor to hypertension. In addition to the well-characterized mitogenic effects in the vasculature, members of the EGF family have also been described as direct vascular mediators (317-320). EGF has been consistently demonstrated as a potent vasoconstrictor by several studies. Berk et al. found that EGF significantly induced contraction of rat aortic strips which maximally was equivalent to 40% of that caused by Ang II (319). Florian and colleagues showed that EGF induced contraction in aorta from rats dependent of MEK and L-type Ca^{2+} channel (320), and Amin et al. showed that myogenic tone of coronary arteriole was significantly reduced under inhibition of either EGFR or the downstream JAK-STAT3 complex (318). Opposite effects have also been observed, Zhou and colleagues showed that HB-EGF promotes both pressure- and flow-induced vasodilation in terminal mesenteric arterioles (TMA) from adults rats (317).

1.2.8.1.3 Enhanced EGFR signalling in hypertension

In the context of blood pressure, enhanced EGFR phosphorylation and expression have been observed in the cardiovascular system of spontaneously hypertensive rats (SHR), while specific knockout of EGFR in VSMCs results in arterial hypotension in mice (314, 321, 322). EGFR was also shown to mediate vascular dysfunction and cardiac remodelling induced by aldosterone/salt and Ang II respectively, strategies widely used to establish experimental model of hypertension (323, 324). Furthermore, transactivation of EGFR by a variety of vasoactive agents such as Ang II, endothelin-1, Sphingosine-1-phosphate (S1P), and phenylephrine has been associated with phenotypes including contraction, inflammation, fibrogenesis and hyperproliferation that have been observed in hypertension (325-329). In addition, many studies have investigated EGFR as potential therapeutic target for cardiovascular diseases. EGFR inhibition using different strategies was found to attenuate cardiac hypertrophy and hypertension induced by Ang II (330, 331), prevent the development of left ventricular hypertrophy in SHR (332), prevent renal vascular fibrosis in nitric oxide (NO) deficiency-induced hypertension in rats (333), attenuate atherosclerosis via reducing inflammation and oxidative stress in mice model of atherosclerosis (316) and decrease cardiac remodelling in streptozotocin-induced cardiomyopathy in mice (334).

Interestingly, although activation of EGFR signalling is observed in animal model of hypertension, and treatments inhibiting EGFR have been shown to be of benefits in hypertension, EGFR deficiency under basal conditions are associated with deleterious vascular effects. Waved-2 mice, a spontaneous mutant with 90% reduced EGFR activity, present with reduced eNOS expression and poor response to acetylcholine-induced vascular relaxation (314), and specific deletion of EGFR in VSMCs and cardiomyocytes results in arterial hypotension and cardiac hypertrophy (322). Therefore, it seems that under physiological conditions, EGFR and downstream signalling play an indispensable role in the normal function of the vascular system, while in the context of hypertension, this EGFR signalling is aberrantly activated and contributes to pathological processes associated with hypertension.

1.2.8.2 VEGFR inhibitor-induced hypertension in cancer patients

1.2.8.2.1 Role of VEGF in vascular function is controversial

While EGF is considered as a potent vasoconstrictor and enhanced EGFR activation is present in animal model of hypertension, findings related to the relationship between

VEGF signalling and hypertension are controversial. Zhao and colleagues found that Ang II infusion in wild type mice upregulates local expression of VEGF and its receptor, which consequently mediate proinflammatory processes and contribute to Ang II-induced vascular inflammation and remodelling (335). Proinflammatory effects of VEGF were also observed during the development of atherosclerotic plaque (336). Contradictory effects were also observed. *In vivo* studies indicated that VEGF delivery after endothelial injury promotes endothelial regeneration and accelerates the recovery of endothelium-dependent relaxation, supporting VEGF a vasculoprotective role (335). Furthermore, Brock et al. showed that recombinant VEGF induced a dose-dependent relaxation in canine coronary arteries previously contracted with prostaglandin $F_{2\alpha,}$ through stimulating endothelium-derived relaxing factor (EDRF)/NO release, a process supposed to have important influence on the vasoreactivity of coronary and other vascular beds (337).

1.2.8.2.2 Hypertension with VEGF inhibition

Interestingly, EGFR and VEGFR as members of RTKs family share common downstream signalling cascades, and both are important therapeutic targets in cancer, however, while EGFR inhibition has been shown to have potential beneficial effects in cardiovascular disease, VEGF inhibitors (VEGFIs) unexpectedly induce hypertension in cancer patients. Both monoclonal antibodies (mAbs) and VEGFR tyrosine kinase inhibitors (TKIs, drugs targeting intracellular kinase domain of RTK) can increase blood pressure, which usually occurs during the first weeks of treatment, with an incidence between 30%-80% in patients treated by VEGFR-targeted drugs, as reported in various clinical trials (Table 1.2) (338, 339). Blood pressure elevation was even explored as a surrogate marker for efficacy of VEGF-targeted antibodies in some studies (340). Mechanisms underlying VEGFR inhibition-induced hypertension are still elusive. Facemire et al. found that antibody against VEGFR2, which is the major VEGFR, could cause rapid and sustained increase in blood pressure of approximately 10 mmHg in mice, by influencing nitric oxide (NO) synthase expression and NO activity (341). Touyz et al. showed that VEGFIs impairs vasodilation and enhances vasoconstriction through redox-sensitive processes mediated by NADPH oxidase (Nox) (342). In addition, increased production of the potent vasoconstrictor ET1, changes in intracellular Ca^{2+}, decreased microvessel (rarefaction), and enhanced sensitivity to salt have also been implicated in VEGFI-induced hypertension (343).

Author	Treatment	Number of Patients	Hypertension	
			All Grade (%)	>= 3 (%)
Motzer et al., 2009	Sunitinib	375	112 (30)	45 (12)
Gore et al., 2015	Sunitinib	4543	1104 (24)	267 (6)
Akaza etal., 2015	Sunitinib	1671	584 (35)	168 (10)
Sternberg et al., 2013	Pazopanib	290	116 (40)	13 (4)
Escudier et al., 2007	Sorafenib	451	76 (17)	16 (4)
Procopio et al., 2007	Sorafenib	136	36 (26)	2 (1.4)
Beck et al. 2011	Sorafenib	1145	223 (19.5)	70 (6.1)
Motzer et al., 2013	Sorafenib	257	88 (34)	46 (18)
Rini et al., 2011	Axitynib	359	145 (40)	56 (16)
Huston et al., 2013	Axitynib	189	92 (49)	26 (13)
Motzer et al., 2013	Pazopanib	554	257 (46)	82 (15)

Table 1.2 Incidence of hypertension in VEGFI-associated hypertension in phase III/IV clinical trials. Adjusted from (344).

1.2.9 VEGFR signalling, magnesium and preeclampsia

1.2.9.1 Overview of preeclampsia

Preeclampsia (PE), a hypertensive disorder of pregnancy, is defined as a systemic syndrome characterized by new-onset of hypertension (systolic blood pressure >140 mm Hg and/or diastolic blood pressure >90 mm Hg on two occasions at least 4h apart and less than 7 days apart) after 20 weeks' gestation associated with proteinuria or maternal organ dysfunction such as thrombocytopenia, renal insufficiency, impaired liver function, pulmonary oedema and cerebral/visual symptoms, which resolves completely by the 6^{th} postpartum week (Figure 1.13) (345, 346). Based on the time of onset or recognition of the disease, PE is clinically divided into two subtypes: early onset (<34 weeks of gestation) and late onset (>34 weeks of gestation), representing different aetiologies and phenotypes. While late onset PE accounts for the majority of PE cases, early onset PE carries a significantly higher risk of adverse maternal and foetal outcomes (347, 348). PE can also be classified as mild or severe, depending on the severity of the symptoms presented by patients (349). According to the National Institute for Health and Care Excellence (NICE) guidance, maternal risk factors for PE include chronic kidney disease, diabetes, chronic hypertension, multiple pregnancy, age of 40 years or older, pregnancy interval of more than 10 years, body mass index (BMI) of $\geqslant$35 kg/m^2 and family history of PE (350). Worldwide, PE affects between 2% and 10% of all pregnancies, with the incidence 7 times higher in developing countries than in developed countries (351). PE can progress to eclampsia, which represents the consequence of brain injury caused by preeclampsia and manifests as new onset of generalized tonic colonic seizures (352). PE/eclampsia is considered as one of the 3 leading causes of maternal mortality, which accounts for more than 50,000 maternal deaths each year and makes a similarly important contribution to perinatal deaths (353, 354).

PE is a multisystemic disorder involving multiple systems, including adult respiratory distress syndrome (ARDS), pulmonary oedema, cerebral thrombosis or haemorrhage, renal dysfunction, hepatic dysfunction, thrombocytopenia and disseminated intravascular coagulopathy (DIC) (350, 355). In particular, PE is associated with significantly increased risk of hypertension and CVDs later in life (356, 357). In a previous systematic review and meta-analysis involving over 258,000 women with PE, Wu et al. found that PE was independently associated with an increased risk of future heart failure, coronary heart disease, cardiovascular disease death and stroke after adjusting for age, BMI, and diabetes

mellitus (358). Additionally, a previous meta-analysis examining multiple prospective and retrospective cohort studies demonstrated an increased risk of hypertension in women with prior PE (359). It is important to note that PE and CVDs share several common risk factors including obesity, metabolic abnormalities, dyslipidaemia and insulin resistance, and underling mechanisms such as endothelial dysfunction, oxidative stress and inflammatory response (358, 360). Considering that CVDs are a leading cause of death globally, it is of great importance to recognise that women with history of PE are at significant risk of future CVDs and need to be monitored closely and treated aggressively for modifiable risk factors, especially in developing countries with a higher incidence of PE.

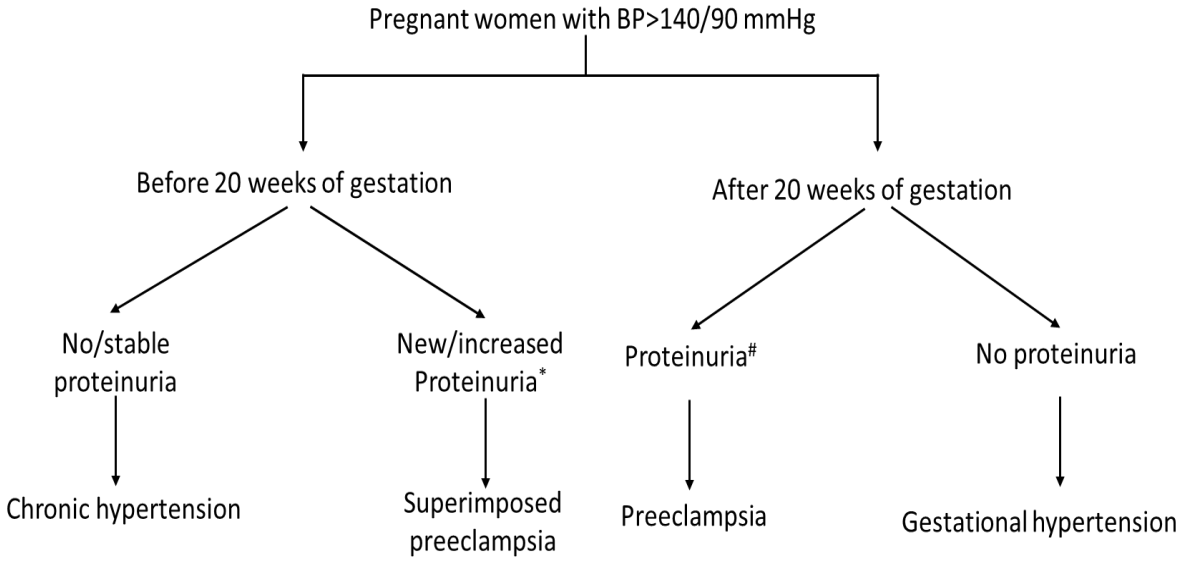

Figure 1.13 Hypertensive disorders of pregnancy. Based on the temporal relationship between hypertension and gestation, and the coexisting symptoms, hypertensive disorders of pregnancy are subclassified into four groups: chronic hypertension, preeclampsia superimposed on chronic hypertension, preeclampsia and gestational hypertension. *It also includes an acute increase of BP, and development of HELLP syndrome (haemolysis, elevated liver enzymes, and low platelet) (349, 361). # In the absence of proteinuria, diagnosis of PE requires evidence of systemic disease, such as thrombocytopenia, renal insufficiency, impaired liver function, pulmonary oedema and cerebral/visual symptoms.

1.2.9.2 General pathophysiology of preeclampsia

The pathology of early-onset PE, also referred to as placental PE was reported as a three-stage process, which starts with defective trophoblastic invasion leading to a failed transformation of the uterine spiral arteries. Physiological remodelling of spiral artery is

necessary during implantation, to accommodate increased blood flow to nourish the developing foetus, while incomplete spiral artery remodelling results in decreased placental perfusion, causing a state of relative ischemia of placenta (Stage 1) (348, 362). Consequently, placental ischemia and the resulting oxidative stress induce release into the maternal circulation of anti-angiogenic factors, such as soluble vascular endothelial growth factor receptor-1 (sFlt-1) and soluble endoglin (sEng) (Stage 2) (362, 363). Excessive circulating sFlt-1 blocks VEGF and PIGF, important players to maintain normal endothelial function and development of the placental vasculature. Soluble Eng inhibits TGF-β, an anti-inflammatory and vasodilator growth factor in vasculature and induces systemic endothelial dysfunction affecting multiple organs including the heart, kidney, liver and brain, and ultimately contribute to the clinical syndrome observed in the mother (Stage 3) (Figure 1.14) (348, 362-364).

For late-onset PE, also referred to as maternal PE, which mainly occurs in women with vascular dysfunction prior to pregnancy, there is little evidence of impaired arterial remodelling and the placental perfusion is preserved or even increased, associated with minimal placental stress, indicating that the level of pathology does not seem to be at the placenta. In addition, circulating levels of sFlt-1 and PIGF, highlighted as important biomarkers in early-onset PE, are close to the normal range in late-onset PE (362). Thus, the late-onset PE is now thought to arise from the interaction between a relatively normal placenta and maternal risk factors such as hypertension, diabetes and obesity, resulting in a maternal pre-disposition to cardiovascular disease (348, 362, 364). However, despite the pathophysiological differences between the two subtypes, it is worth noting that the distinction is not always clear cut and most patients with PE have elements of both causal pathways.

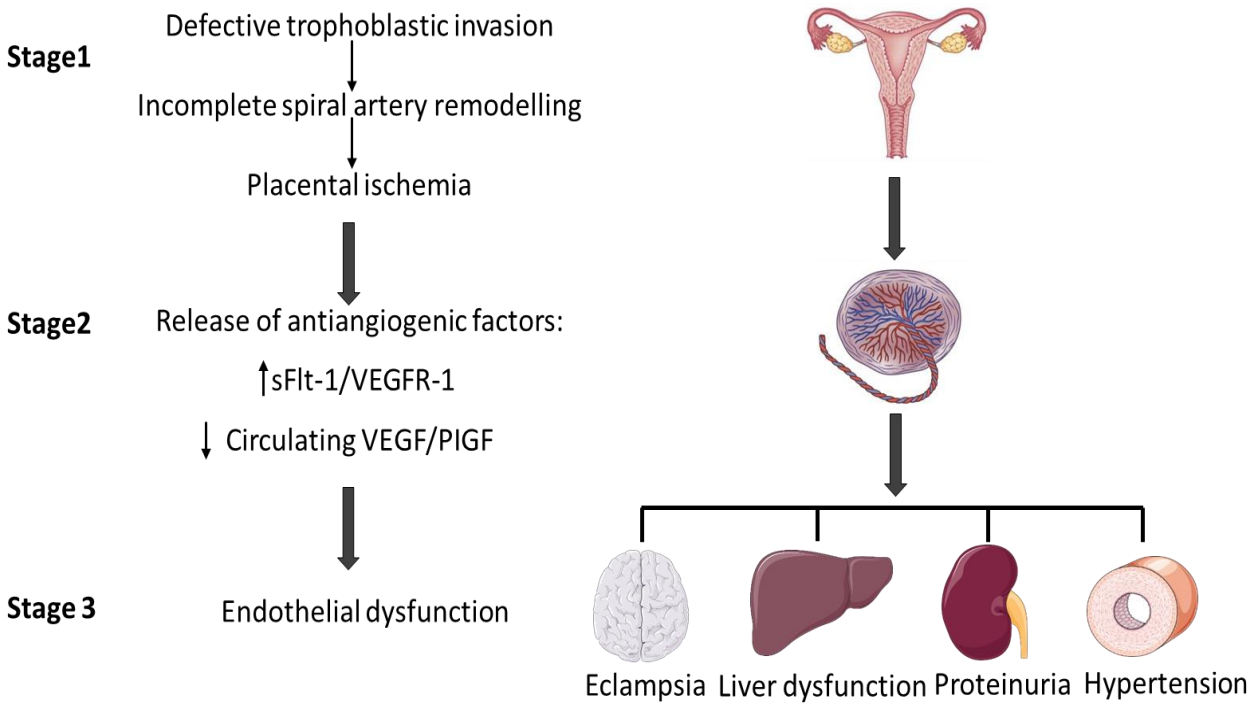

Figure 1.14 Pathogenesis of preeclampsia: three-stage model. The early-onset PE is described as a three-stage disease. It starts from defective trophoblastic invasion followed by impaired spiral artery remodelling, resulting in placental ischemia and oxidative stress, which consequently triggers the release of anti-angiogenic factors to the maternal circulation. Excessive circulating sFlt-1 and sEng were able to antagonize activity of VEGF/PIGF and TGF-β respectively, causing endothelial dysfunction in multiple organs, which contributes to the clinical manifestations observed in the mother with PE.

1.2.9.3 VEGF signalling and PE

1.2.9.3.1 VEGF family and their receptors

VEGF family contains several members, including VEGF-A, VEGF-B, VEGF-C, VEGF-D, VEGF-F and placental growth factor (PIGF) (365). The most widely studied member is VEGF-A, also known simply as VEGF, which presents various isoforms such as $VEGF_{121}$, $VEGF_{145}$, $VEGF_{148}$, $VEGF_{165}$, $VEGF_{183}$, $VEGF_{189}$ and $VEGF_{206}$ (366). PIGF is predominantly produced by the placenta (367), with low expression levels in other tissues including heart, lung, thyroid, liver, skeletal muscle and bone (368). VEGF and PIGF stimulate cellular responses through binding to and activating VEGFRs, which are typical receptor tyrosine kinases as described in previous chapter. The VEGFR family contains three full-length receptors, including VEGFR-1, also known as fms-like tyrosine kinase-1 (Flt-1), VEGFR-2, commonly referred to as fetal liver kinase 1(Flk-1) and

VEGFR-3, and one splice variant of VEGFR-1, soluble VEGFR-1 (sVEGFR-1, also known as sFlt-1), which lacks the transmembrane and intracellular signalling domain (366, 369). VEGF-A is able to bind VEGFR-1, sVEGFR1 and VEGFR-2, while PIGF only bind to VEGFR-1 and sVEGF-1 (370). In addition, PIGF was also shown to transactivate VEGFR-2 through an intermolecular crosstalk between VEGFR-1 and VEGFR-2 (371). Interestingly, although VEGF-A exhibit higher affinity to VEGFR-1, cellular effects of VEGF-A are mainly through VEGFR-2, whereas VEGFR-1 acts as a decoy receptor (367, 370).

1.2.9.3.2 The VEGF-VEGFR system in normal pregnancy and PE

The VEGF-VEGFR system is an essential regulator of angiogenesis and vascular permeability in physiological and pathological processes of both embryos and adults. In the context of PE, both VEGF and PIGF are critically involved in the placental angiogenesis and development (372, 373). Although the level of circulation VEGF in patients with PE is inconsistently reported in the literature depending on the technique used (374), accumulating evidence shows that VEGF potently stimulates endothelial production of NO in placental artery, recruits pericytes to the newly formed vessels and participates in the continued survival of nascent endothelial cells, all of which contribute to the maturation and stability of newly formed vessels (373). During normal pregnancy, PIGF in the maternal circulation increases significantly from 8 weeks gestation and reaches a maximal concentration during the second trimester, when nonbranching villous angiogenesis and terminal villous formation occur (362, 375). The PIGF-VEGFR-1 pathway is also important in modulating uterine vascular remodelling and blood flow during pregnant state (376). In human PE, circulating level of PIGF, predominantly PIGF-1, has consistently been shown to be significantly reduced, associated with increased circulating maternal levels of sVEGFR-1 (367, 377) and the alterations are believed to occur several weeks before the onset of clinical syndrome (369). Excessive sVEGFR-1 acts a potent scavenger of VEGF and PIGF, preventing their binding to the receptors, which subsequently leads to the suppression of VEGF and PIGF and blocks the downstream signalling. Therefore, the sFlt-1: PIGF ratio is raised in pregnant women before the onset of PE, which has been used clinically to predict the disease progression and guide treatment (378).

1.2.9.3.3 VEGF and PIGF as potential treatments for PE

Since excessive sFlt-1 and the resulting angiogenic imbalance play a critical role in the development of PE, strategies using PIGF and VEGF to restore angiogenic balance as potential therapies have been investigated in different experimental models of PE. Suzuki et al. observed reduced mean blood pressure but with no effect on proteinuria in experimental PE induced by transfection of adenoviral vector containing sFlt-1 in mice (379). In rat reduced uterine placental perfusion (RUPP) model of PE, which disrupts uterine perfusion and flow by clipping the ovarian arteries and abdominal aorta with silver clips (380), Granger et al. found that infusion of recombinant human PIGF for 5 days via intraperitoneal osmotic minipumps reduced blood pressure, proteinuria and improved glomerular infiltration rate (GFR), associated with decreased sFlt-1 level (381). In the same model, Khalil et al. showed that PIGF infusion reversed vascular hyper-reactivity and hypertension to levels comparable to that in control pregnant rats (382). In addition, Makris et al. found that in a uteroplacental ischemia model of PE in non-human primates, administration of recombinant human PIGF reduced blood pressure and proteinuria, without changes in circulating sFlt-1 (383).

Beneficial effects of VEGF therapy have been demonstrated in several animal models of PE. Experimental PE induced in Wistar rats by treatment with Nω-nitro-l-arginine methyl ester (L-NAME), a nitric oxide synthase inhibitor, exhibits many signs of PE, such as high blood pressure, proteinuria, and reduced platelet count, pup weight, and placental weight, while all of these manifestations could be reversed by VEGF treatment (384, 385). Treatment with recombinant human VEGF121 (rhVEGF121) also ameliorated PE phenotype in the sFlt-1 overexpression model of PE (379) without apparent harm to the foetus, supporting VEGF121 as a potential therapeutic agent for PE (386). Similar beneficial effects of VEGF121 were observed in RUPP model and in spontaneous genetic model of PE based on BPH/5 mice (387).

1.2.9.4 Magnesium and PE

1.2.9.4.1 Therapeutic effect of MgSO4

Magnesium sulphate ($MgSO_4$), is an important agent used for treatment and prophylaxis of eclampsia and in patients with severe PE (388, 389). A previous systematic review summarizing 59 publications also recommended initiation of $MgSO_4$ to all women with mild PE (390). Despite concerns about toxicities and side effects including loss of the patellar reflex, respiratory paralysis, arrhythmias and cardiac arrest, $MgSO_4$ has been

proved effective by randomized trials in preventing and treating eclamptic seizures, with superior effectiveness compared to other anticonvulsants such as diazepam and phenytoin (389, 391-393).

1.2.9.4.2 Mechanisms of action: involvement of VEGF

Protective effects of $MgSO_4$ for PE treatment are associated with vasodilator properties, central anticonvulsant, protection of the blood-brain barrier (BBB) and reduction of cerebral oedema formation (393). Additionally, Weintraub and colleagues found that $MgSO_4$ affects placental VEGF expression (394), which may contribute to the therapeutic effect of $MgSO_4$ in PE. However molecular mechanisms induced by $MgSO_4$ remains unclear.

1.2.9.4.3 Mg^{2+} transporters and PE

Dysregulation of Mg^{2+} transporters has been reported in PE. Yang et al. showed reduced gene expression of TRPM7 and TRPM6 in placenta from women suffering from PE during preterm labour and remained lower at term labour (395). Additionally, Kolisek and colleagues found that placentas from PE women exhibit increased expression of SLC41A1, a Na^+/Mg^{2+} exchanger important for Mg^{2+} efflux (15, 22). However, whether the alteration of Mg^{2+} transporters is a direct consequence of changed Mg^{2+} status in the body observed in preeclamptic patients (396-399), or acts as an initial contributor in the aetiology of PE remains unclear, which requires further investigation.

1.3 Cross talk between growth factors and TRPM7

1.3.1 TRPM7-mediated regulation of RTK signalling pathways

Considering the ubiquitous expression of TRPM7, and its dual properties as an ion channel and cytoplasmic kinase, it is not surprising that TRPM7 participates in cell signalling pathways. In particular, an increasing body of evidence, including studies involving pharmacological and genetic modulation of TRPM7, have linked TRPM7 to RTKs downstream signalling cascades (Figure 1.15)

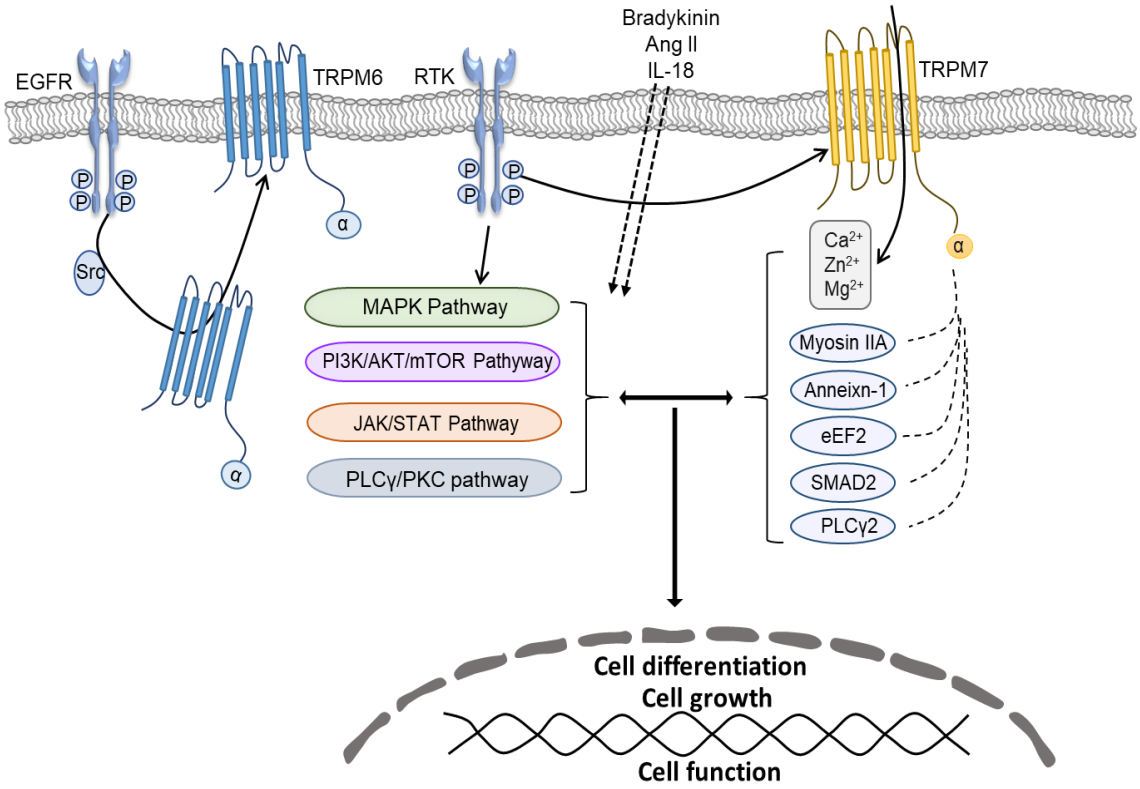

Figure 1.15 Cross-talk between RTK and TRPM7. TRPM7 possesses dual properties acting as an ion channel mainly permeable to Zn^{2+}, Ca^{2+} and Mg^{2+}, and as a cytoplasmic kinase, with identified substrates including ANXA1, myosin IIA heavy chain, eEF2, SMAD2 and PLCγ2. TRPM7 contributes to the regulation of RTK downstream signalling pathways and vice versa. The cross-talk between TRPM7 and RTK signalling plays an important role in cell function, such as cell differentiation and cell growth. Copied from (46).

1.3.1.1 TRPM7 contributes to the regulation of the MAPK pathway

Among the RTKs downstream signalling pathways as discussed above, TRPM7 has been shown to affect the MAPK pathway in different cell types. In human endothelial cells (ECs), silencing TRPM7 by small interfering RNA (siRNA) increased phosphorylation of

ERK1/2 and their upstream kinases MEK1/2, whereas there were no effects on p38 MAPK and JNK activation (400). The opposite was observed in mouse cortical astrocytes, because silencing TRPM7 was associate with decreased ERK phosphorylation. Reduced MEK-ERK activation was also observed in VSMC treated with the TRPM7 non-specific inhibitor 2-Aminoethoxydiphenyl borate (2-APB) (124, 129). In HEK-293 cell line, overexpression of TRPM7 activated p38MAPK and JNK and suppressed ERK phosphorylation (104). In a rat hepatic stellate cell line (HSC-T6), the up-regulation of TRPM7 contributes to PDGF induced activation of ERK and AKT pathways (401). Highly expressed TRPM7 was found to contribute to aberrant cellular proliferation, migration and invasion during tumour development (153). However, despite being discussed in some of the studies, the underlying mechanisms by which TRPM7 interacts with the MAPK pathway remains unclear. Trophic factors such as VEGF and EGF, the PLC pathway, Ca^{2+}/Mg^{2+} status, the TRPM7 α-kinase and reactive oxygen species (ROS) production are proposed with a suspected role, which requires further investigation (104, 400, 402).

1.3.1.2 TRPM7 is involved in the regulation of the PI3K/AKT pathway

The association between TRPM7 and the PI3K/AKT pathway was mainly demonstrated in cancer cells. In glioblastoma cells, inhibition of TRPM7 by carvacrol or silencing TRPM7 significantly reduced the phosphorylation level of AKT, which was associated with reduced cell viability, migration and invasion. Interestingly, the TRPM7 activator naltriben showed no effect on the PI3K/AKT pathway way in these cells (132, 402). In two different cell lines of renal cell carcinoma, TRPM7 silencing was shown to decrease the activation of AKT, a process involved in tumour growth (403). Moreover, TRPM7 was shown to be required for sustained PI3K/AKT signalling activation, which has an indispensable role in regulating lymphocyte growth and proliferation (404). TRPM7 also affects the PI3K/AKT pathway in normal cells. In mouse chondrocytes, TRPM7 overexpression was associated with upregulation of PI3K p85 subunit and AKT expression and phosphorylation, effects that were reduced by silencing TRPM7 (405). In human osteoblasts, mRNA expression of chemotaxis-related genes induced by Mg^{2+} was attenuated by TRPM7 silencing and PI3K inhibitor, suggesting a possible link between TRPM7 and PI3K.

1.3.1.3 TRPM7 and activation of PLC and STAT3

The phosphorylation and regulation of PLC proteins by TRPM7 was observed in 2012, when a study demonstrated that TRPM7 kinase phosphorylates PLCγ2 in its C2-domain at

position Ser1164 and in the linker region at position Thr1045, which might contribute to adjusting the signalling intensity of PLCγ2 dependent pathways (102). The involvement of PLC enzyme as a substrate of the TRPM7 Ser/Thr kinase was also supported by a recent study, which showed that cells expressing specific mutation in the C2 domian of PLCγ2 with an ablated TRPM7 phosphorylation site exhibited a similar phenotype to that of TRPM7 kinase deficient cells (406). However, the molecular targets downstream of TRPM7-phosphorylated PLCγ2 and the physiological function remain unclear.

Studies in cancer cell lines indicated the activation of STAT3 and Src are downstream of TRPM7 activation. In glioblastoma cells, downregulation of TRPM7 by siRNA significantly reduced the phosphorylation of STAT3 at the Tyr705 residue, without changes in total STAT3 levels, contributing to cell proliferation and migration (155). In breast cancer cells, silencing TRPM7 significantly reduced EGF-induced STAT3 activation and decreased the phosphorylation level of Src, and the latter is associated with TRPM7-mediated migration and invasion (407, 408).

Instead of a direct regulatory role, TRPM7 was also implicated in the regulation of RTKs downstream signalling pathways triggered by different stimuli. In VSMCs, high concentration of glucose (HG) induced phenotype switching and proliferation mediated MEK/ERK signalling pathway, effects that were attenuated by TRPM7 knockdown. Similarly, TRPM7 is involved in angiotensin II (Ang II)-induced activation of ERK1/2 and contributes to Ang II-mediated phenotypic change and proliferation of VSMCs (140, 409). In prostate cell lines, cholesterol increased the phosphorylation of AKT and ERK, which was attenuated by both TRPM7 inhibitor 2-APB and TRPM7 silencing RNA (128).

1.3.2 RTK signalling-mediated regulation of TRPM7

1.3.2.1 Activation of RTKs directly regulates TRPM7

In contrast to the widely investigated involvement of TRPM7 in the regulation of RTKs downstream signalling pathways, less studies have focused on the reverse scenario, how RTKs and their downstream effectors could affect TRPM7 functions. An earlier study showed that stimulation of EGFR by EGF initiates PLC-γ activation and PIP2 hydrolysis, which consequently leads to the inhibition of TRPM7 channel activity (410). However, Gao et al. found that in a pulmonary cancer cell lines, EGF through its receptor, enhanced the cell membrane protein expression and currents of TRPM7, a process associated with cell migration (135).

TRPM7 forms heteromers with its homologue TRPM6, and a similar regulatory role of EGF in TRPM6 activity and cell surface expression was observed in HEK293 cells (411, 412). In 2009, Bindels and colleagues found that EGF through binding and activation of EGFR signalling, promotes the activation of TRPM6 and its translocation from cytosol to the plasma membrane in kidney epithelial cells. Blockage of this pathway with Cetuximab abolishes the stimulatory effect of EGF on TRPM6, and eventually causes renal Mg^{2+} waste (Figure 1.16) (259, 411). In hippocampal neurons, nerve growth factor (NGF), reduced the outward rectifying TRPM7-like current, in both dose- and time- dependent manners, and this effect could be blocked by the inhibition of tyrosine kinase activity of TrkA (NGFR) and PLC inhibitor (413). Furtherly, these authors found that NGF activated TrkA, through the PI3K pathway, prevented the up-regulation of TRPM7 expression in hippocampal neurons subjected to ischemic-reperfusion and oxygen-glucose deprivation (414). Moreover, although the underlying mechanisms were not discussed, PDGF stimulation was shown to increase TRPM7 expression in the HSC-T6 hepatic stellate cell line in a time-dependent manner, and TRPM7 inhibitor 2-APB diminished PDGF mediated activation of p-AKT and p-ERK, confirming a regulatory role of TRPM7 upstream of AKT and ERK (401).

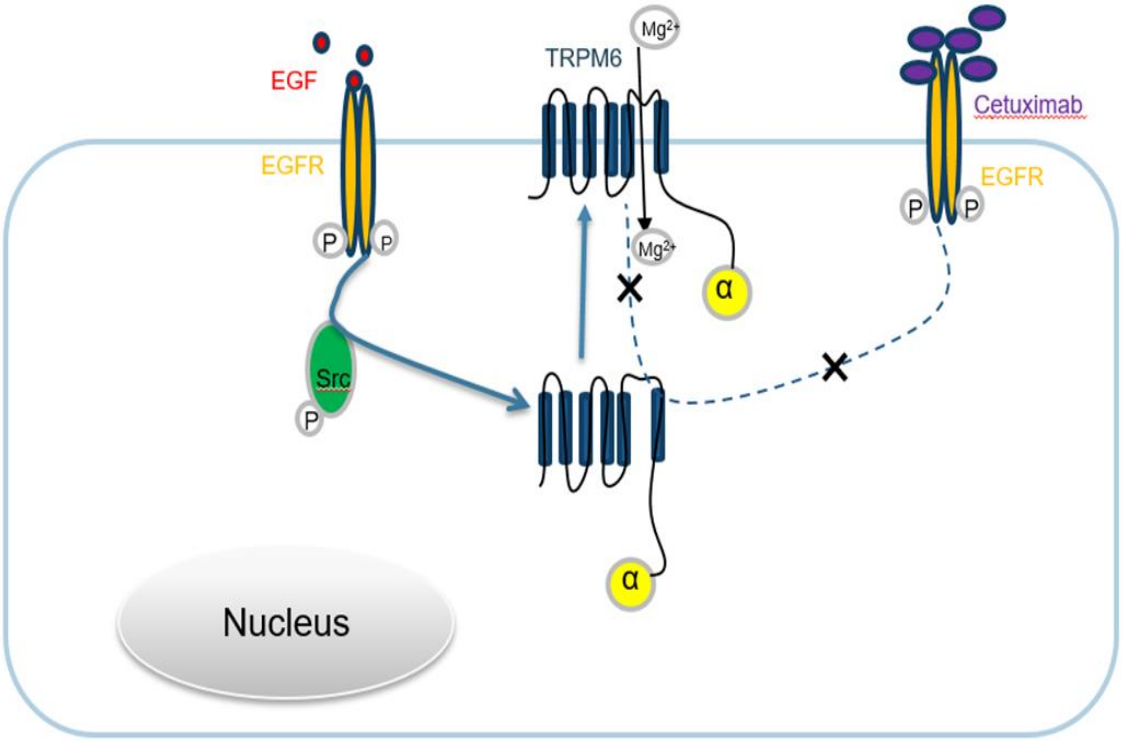

Figure 1.16 EGF regulates TRPM6 in distal convoluted tubule (DCT). TRPM6 is the close sister homologue of TRPM7, and shares ~50% sequences. In HEK 293 cells, EGF activates TRPM6 channel activity through EGFR and Src-family kinase. In DCT, EGF promotes the translocation of TRPM6 from cytosol to cell membrane, mediating renal Mg^{2+} reabsorption. Cetuximab, a monoclonal antibody used to treat cancer, binds to and inhibit EGFR and can cause renal Mg^{2+} wasting leading to hypomagnesemia.

1.3.2.2 RTKs downstream effectors and TRPM7

In addition to the regulation of TRPM7 triggered by ligand-receptor binding, RTKs downstream effectors have been indicated to either individually or through interaction with other stimuli contribute to the modulation of TRPM7 activity. Several studies have shown controversial effects of PLC activation on TRPM7 function in different cell types. Clapham et al. demonstrated PIP2 as a key regulator of TRPM7, and receptor-mediated activation of PLC induced the hydrolysis of localised PIP2 leading to the inactivation of TRPM7 channel (410). However, Langeslag et al. confirmed that when intracellular Mg^{2+} level is reduced, the TRPM7 currents under whole-cell conditions are remarkably inhibited, followed PLC activation. However, under physiological ionic conditions, PLC-activating receptor agonists conversely enhanced TRPM7 currents (415). In prostate cells, Sun et al. found that TRPM7 expression was mediated by Ca^{2+} in a ERK1/2 activation dependent manner, events that were associated with cell proliferation, migration and viability (128). Moreover, RTKs downstream pathways are also involved in the regulation of TRPM7 by

other stimuli. In VSMCs, Ang II increased TRPM7 expression through its AT1 receptor and ERK signalling pathway (409). Bradykinin, another vasoactive peptide, was found to regulate TRPM7 and its downstream target annexin-1 through PLC and c-Src dependent pathways, which has an important role in VSMC Mg^{2+} homeostasis, cell migration and invasion (130). Zhang et al. found that interleukin-18 (IL-18) activated TRPM7 currents, and upregulated TRPM7 expression in an ERK1/2-medated manner, which regulates osteogenic differentiation of VSMCs (142). In HEK293 cells, interleukin-6 (IL-6) inhibits TRPM7 currents through the JAK2-STAT3 signalling pathway and independent of the TRPM7 α-kinase domain. The author speculated that the regulation of TRPM7 by IL-6 signalling may result from JAK2/STAT3-mediated phosphorylation of TRPM7, which requires further investigation (416).

1.4 Objectives, hypothesis and aims

1.4.1 Objectives of the study

The primary objective of the work presented in this thesis was to investigate the interplay between growth factors, RTKs and TRPM7 and specifically to assess how activation of RTKs initiated by growth factors, such VEGF and EGF, influences TRPM7 in the vasculature, and the contribution to ion homeostasis, cellular signalling, and vascular function.

1.4.2 Hypothesis

RTKs, EGFR and VEGFR activated by VEGF and EGF respectively, stimulate TRPM7 activity in vascular smooth muscle cells (VSMC) in a Src dependent manner, and this process plays a role in cellular cation homeostasis and vascular function. The inhibition of RTK signalling reduces TRPM7 expression and trafficking, and changes its channel and α-kinase function, which consequently contributes to ion dysregulation as well as vascular dysfunction (Figure 1.17).

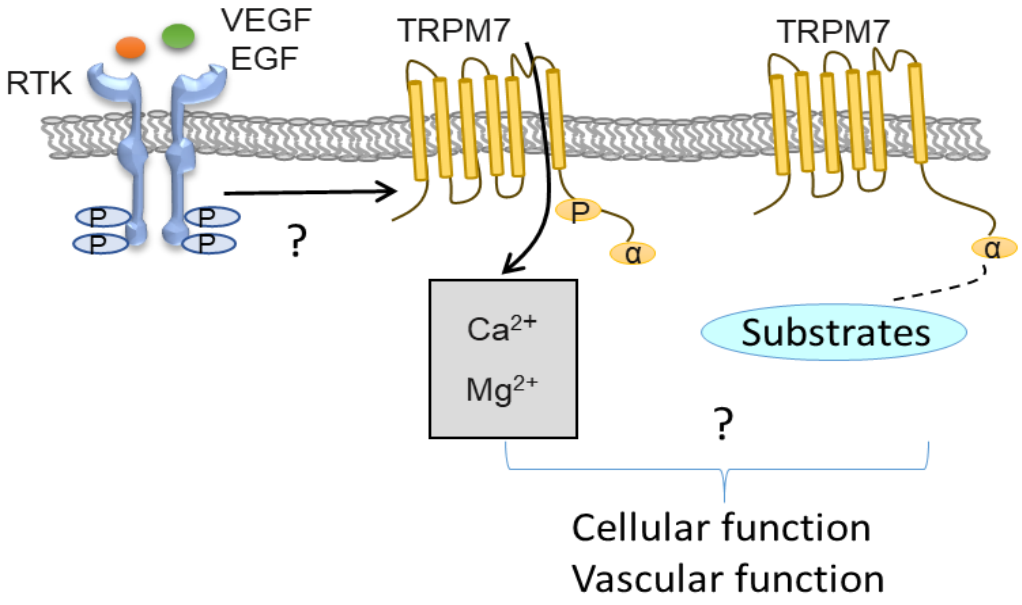

Figure 1.17 We hypothesize that growth factors regulate TRPM7 in the vasculature. This process is supposed to affect the homeostasis of divalent cations such as Ca^{2+} and Mg^{2+} and the activity of TRPM7 substrates, and ultimately contribute to the regulation of cellular function and vascular function.

1.4.3 Specific aims of the study

AIM 1. To study whether RTKs (VEGF receptor and EGF receptor) regulate TRPM7 in VSMCs, and the underlying mechanisms and to explore whether TRPM7 influences RTKs.

AIM 2. To study whether TRPM7 is involved in the downstream signalling of VEGF/EGF, such the MAPK pathway

AIM 3. To investigate whether TRPM7 dysregulation in the vasculature has clinical relevance (hypertension, preeclampsia).

Chapter Two

2 Materials and methods

2.1 General lab practice

All experiments were carried out in laboratories based at the British Heart Foundation Glasgow Cardiovascular Research Centre, Institute of Cardiovascular and Medical Sciences (ICAMS), and in accordance with the Control of Substances Hazardous to Health (COSHH) guidelines specified for each protocol. COSHH Risk Assessment Forms were read carefully and signed before conducting any experiments. All animal experiments were performed in accordance with the United Kingdom Home Office regulations, the National Health and Medical Research Institute Animal Welfare Committee guidelines and the Ethical Principles in Animal Experimentation adopted by the West of Scotland Research Ethics Service (Licence No. 70/9021). Studies at Sapienza University, in collaboration with Prof Savoia, were carried out in accordance with the Italian Law on the protection of animal. All daily activities in the lab are in accordance with proper guidelines developed in the laboratory of Prof Touyz and ICAMS.

2.2 Materials

2.2.1 Reagents and suppliers

Consumables such as cell culture flasks, plates and pipettes, cell culture medium and general chemicals such as ethanol, and chloroform were purchased from Life Technologies (Paisley, Scotland, UK). Other reagents, enzymes and specific drugs were purchased from commercial companies as listed below:

Abcam, Cambridge, UK

Cal-520, AM (ab171868)

BioRad Laboratories, Hertfordshire, UK

Precision Plus Protein^{TM} Dual Xtra Standards

Fisher Scientific, Loughborough, UK

Methanol (#67-56-1); Chloroform (#67-66-3); Glycine (#56-40-6); Tris Base (#77-86-1); D-Glucose anhydrous (#50-99-7); Sodium chloride (#7647-14-5); Sodium hydrogen carbonate ($NaHCO_3$, #144-55-8); Dimethyl Sulfoxide (DMSO)

Life Technologies/Invitrogen, Paisley, UK

Dulbecco's Modified Eagle Medium (DMEM, #22320-022); Smooth Muscle Growth Supplement (SMGS, #S-007-25); Dulbecco's Phosphate Buffered Saline without $CaCl_2$

and $MgCl_2$ (DPBS, #14190-094); Penicillin Streptomycin Dulbecco (#15140-122); Foetal Bovine Serum Heat Inactivated (#10500-064); Phosphate-buffered saline (tablets); DNase1 (Rnase free); 0.5% Trypsin-EDTA (#10500-064)

Qiagen, Manchester, UK

QIAzol Lysis Reagent (#79306)

R & D Systems, Abingdon, UK

Recombinant Human VEGF 165 Protein (293-VE); Recombinant Human EGF Protein; Recombinant Rat VEGF 164 Protein (564-RV); Recombinant Rat EGF Protein (3214-EG)

Sigma-Aldrich, Dorset, UK

NS8593 hydrochloride (N2538); Apamin (A9459); Naltriben methanesulfonate hydrate (N156); N,N,N',N'-tetramethylethane-1,2-diamine (TEMED); Pepstatin; Leupeptin; Aprotinin; Phenylmethylsulfonyl fluoride (PMSF); Ponceau S; Sodium nitroprusside (SNP); Potassium chloride (#7447-40-7); Calcium chloride (#10043-52-4); Triton X-100 (#9002-93-1); Tween 20 (#9005-64-5); Bovine Serum Albumin solution (#9048-46-8); Soybean trypsin inhibitor; F12 medium (N6658); REDExtract-N-Amp™ Tissue PCR Kit

Santa Cruz Biotechnology, Heidelberg, Germany

Gefitinib (sc-202166); Vatalanib Dihydrochloride (sc-202379); Protein A-Agarose (sc-2001); Protein G PLUS-Agarose (sc-2002)

Selleck Chemicals, München, Deutschland

TG100-115 (S1352)

Thermo Fisher Scientific, Renfrew, UK

Pierce™ BCA Protein Assay Kit (#23227); Pluronic™ F-127 (P3000MP); High-Capacity cDNA Reverse Transcription Kit (#4368814); Fast SYBR™ Green Mater Mix (4385612); Magnesium Green™, AM, cell permeant (M3735); Nitrocellulose Membrane (#88018) ; Acrylamide/Bis 19:1, 40% (w/v) solution; CellTrace™ CFSE Cell Proliferation Kit (C34554)

Tocris Bioscience, Bio-Techne Ltd, Abingdon, UK

2-Aminoethoxydiphenylborane (2-APB, #1224)

VWR International, Lutterworth, UK

Ethanol absolute (#64-17-5); N'-2-Hydroxyethylpiperazine-N'-2 ethanesulphonic acid (HEPES, #7365-45-9); Magnesium chloride hexahydrate (#7791-18-6); Sodium dodecyl sulphate (SDS, #151-21-3); $MgSO_4 \cdot 7H_2O$ (#10034-99-8); Potassium dihydrogen phosphate (KH_2PO4, #7778-77-0)

Worthington Biochemical Corp, Lakewood, UK

Collagenase type I; Elastase

2.2.2 Solutions and Media

Protein lysis buffer (pH 7.4)

HEPES (10 mM); Na_3VO_4 (2 mM); Triton X-100 (0.5% v/v); $Na_4P_2O_7$ (50 mM); NaF (50 mM); NaCl (50 mM); Na_2EDTA (5 mM); supplemented with PMSF (1 mM); aprotinin (1 µg/ml); leupeptin (1 µg/ml); pepstatin (1 µg/ml)

6X Laemmli sample buffer

SDS (10%, w/v); β-mercaptoethanol (6% v/v); bromophenol blue (0.012% w/v); glycerol (30% v/v); Tris-HCl (260 mM, pH 6.8)

SDS-PAGE separating gel

Acrylamide/Bis 19:1 (7.5%-12% v/v); Tris-HCl (375 mM, pH 8.8); SDS (0.1% w/v); APS (0.045% w/v); TEMED (0.05% v/v); distilled water

SDS-PAGE stacking gel

Acrylamide/Bis 19:1 (4% v/v); Tris-HCl (125 mM, pH 6.8); SDS (0.1% w/v); APS (0.05% w/v); TEMED (0.1% v/v); distilled water

SDS-PAGE running buffer

Tris-Base (25 mM); glycine (193 mM); SDS (0.1% w/v); distilled water

SDS-PAGE transferring buffer

Tris-Base (25 mM); glycine (193 mM); methanol (20% v/v); distilled water

Tris-buffered saline-Tween 20 (TBS-T)

Tris-Base (20 mM, pH 7.6); NaCl (137 mM); Tween-20 (0.1% v/v); distilled water

BSA-based blocking buffer

BSA in TBS-T (3% w/v)

Non-fat dried skimmed milk-based blocking buffer

Marvel Dried Skimmed Milk in TBS-T (5% w/v)

Stripping buffer

NaOH in distilled water (200 mM)

HEPES physiological saline solution for Ca^{2+} study

NaCl (130 mM); KCl (5 mM); $MgCl_2 \cdot 6H_2O$ (1 mM); $CaCl_2$ (1 mM); d-glucose (10 mM); HEPES (20 mM); distilled water; pH 7.4

HEPES Buffer for Mg^{2+} study

HEPES without Ca^{2+} and Mg^{2+}: NaCl (150 mM); KCl (5 mM); d-glucose (10 mM); HEPES (20 mM); distilled water; pH 7.4

HEPES with Mg^{2+}: NaCl (150 mM); KCl (5 mM); d-glucose (10 mM); HEPES (20 mM); $MgCl_2 \cdot 6H_2O$ (1 mM); distilled water; pH 7.4

Buffer for separation of cell fractions

Buffer A: Tris-Base (50 mM); Na_2EDTA (2 mM); distilled water; pH 7.4

Buffer B: NaCl (300 mM), Triton 100 (1% v/v) and SDS (0.1% w/v) in buffer A. Protease inhibitors including PMSF (1 mM), leupeptin (1 µg/ml), aprotinin (1 µg/ml) and pepstatin (1 µg/ml) were added before use in both buffer A and buffer B.

VSMCs cell culture medium

Human VSMCs cell culture medium: DMEM (1 g/L D-Glucose, L-Glutamine, 25 mM HEPES, Pyruvate); 1X Smooth Muscle Growth Supplement; 1X Penicillin-Streptomycin (1000 U/ml)

Rat VSMCs cell culture medium: DMEM (1 g/L D-Glucose, L-Glutamine, 25 mM HEPES, Pyruvate); 10% (v/v) FBS; 1X Penicillin-Streptomycin (1000 U/ml)

Digestion solution

BSA (0.2% w/v); collagenase (0.2% w/v); elastase (0.012% w/v); soybean trypsin inhibitor (0.036% w/v) in complete F-12 Ham medium

High potassium physiological salt solution (KPSS)

KCl (62.5 mM); $MgSO_4$ (1.2 mM); $NaHCO_3$ (25 mM); KH_2PO_4 (1.2 mM); $CaCl_2$ (2.5 mM); d-glucose (11 mM); distilled water; pH 7.4

Physiological Salt Solution (PSS):

NaCl (119 mM); KCl (4.7 mM); $MgSO_4$ (1.2 mM); $NaHCO_3$ (25 mM); KH_2PO_4 (1.2 mM); $CaCl_2$ (2.5 mM); d-glucose (11 mM); distilled water; pH 7.4

HES Buffer (HES):

HEPES (20 mM); Sucrose (250 mM); EDTA (1 mM); PMSF (1 mM); leupeptin (1 µg/ml); aprotinin (1 µg/ml); pepstatin (1 µg/ml); distilled water; pH 7.4

2.2.3 Antibodies and conditions of use

Primary and secondary antibodies used in this study are summarized in Table 2.1. Primary antibodies used in immunoblotting were diluted 1: 1,000 in TBS-T with 3% BSA (w/v), except for β-actin (1:10,000) and α-tubulin (1:2,000). Secondary antibodies used in immunoblotting were diluted (1: 10,000) in TBS-T with 1% BSA.

Name	Company	Catalogue ID	Host Species	Application
TRPM7	Abcam	ab245408	Rabbit	WB/IP
TRPM6	Abcam	ab79227	Rabbit	WB
MagT1	Abcam	ab90478	Rabbit	WB
SLC41A1	Abcam	ab83701	Rabbit	WB
Annexin-1	Santa Cruz	sc11387	Rabbit	WB
Calpain-2	Santa Cruz	sc373967	Mouse	WB
phospho-VEGFR (Y951)	Cell signalling	4991s	Rabbit	WB
VEGFR	Cell signalling	2479s	Rabbit	WB
phospho-EGFR (Y1068)	Cell signalling	3777S	Rabbit	WB
phospho-EGFR (Y845)	Cell signalling	2231S	Rabbit	WB
EGFR	Cell signalling	2646S	Rabbit	WB

phospho-p38 MAPK (T180/Y182)	Cell signalling	9211S	Rabbit	WB
p38 MAPK	Cell signalling	9212S	Rabbit	WB
phospho-ERK1/2 (T202/Y204)	Cell signalling	9101S	Rabbit	WB
ERK1/2	Cell signalling	9102S	Rabbit	WB
phospho-PKC (T638/641)	Cell signalling	9375S	Rabbit	WB
phospho-Src (Y527)	Cell signalling	2105S	Rabbit	WB
Src	Cell signalling	2109	Rabbit	WB
phospho-MKP1 (S359)	Abcam	ab63548	Rabbit	WB
MKP1	Abcam	ab236501	Mouse	WB
phospho-STAT1 (Y701)	Cell signalling	9167S	Rabbit	WB
STAT1	Cell signalling	9176S	Mouse	WB
phospho-STAT3 (Y705)	Cell signalling	9138S	Mouse	WB
STAT3	Cell signalling	7907	Rabbit	WB
phospho-serine /tyrosine/threonine	/	/	/	/
loading controls				
β-actin	Sigma-Aldrich	A2228	Mouse	WB
α-tubulin	Abcam	ab4074	Rabbit	WB
Na/K-ATPase	/	/	/	/

Second antibodies				
Anti-Mouse Alexa Fluor 680	Thermo Fisher	A21057	Goat	WB
Anti-Rabbit Alexa Fluor 800	Thermo Fisher	A32735	Goat	WB

Table 2.1 Primary and second antibodies used in this study. WB, western blotting; IP, immunoprecipitation.

2.2.4 Oligonucleotides

Nucleotide sequences of the primers used in this study are summarized in Table 2.2.

Targeted gene	Primer Name	Sequence (5' 3)	Application
Transient Receptor Potential Melastatin 7, human	hTRPM7_RW2	CTCTATCCCATGCCAATGTAAGG	qPCR
	hTRPM7_FW2	TGCAGCAGAGCCCGATATTAT	qPCR
Transient Receptor Potential Melastatin 6, human	hTRPM6_FW3	TCCTGTCTGATGATGGGACC	qPCR
	hTRPM6_RW3	TCTTGAGCGGCAGTGTATTTTC	qPCR
Solute carrier family 41 member A1, human	hSLC41A1_FW	TTCTTCAGCCCTGATGTGAA	qPCR
	hSLC41A1_RW	CGAGGAGCTTGCTCAGAGTT	qPCR
Magnesium transporter subtype 1, human	hMagT1_FW	GGGATTGCTTTTGGCTGTTA	qPCR
	hMagT1_RW	TGGTTCCACATTTGACCAGA	qPCR
SGlyceraldehyde-3-phosphate dehydrogenase, human	hGAPDH_Fw	GAGTCAACGGATTTGGTCGT	qPCR
	hGAPDH_Rv	TTGATTTTGGAGGGATCTCG	qPCR

Table 2.2 Oligonucleotides used in this study to detect mRNA levels. All oligonucleotides were purchased from Eurofins Genomics. F, forward; R, reverse; qPCR, quantitative real-time polymerase chain reaction.

2.2.5 Patient characteristics

Primary hVSMCs isolated from small arteries dissected from surplus surgical tissue of patients receiving elective craniofacial surgeries. General characteristics of these patients are summarized in Table 2.3.

BioBank Number	Hypertension	Gender	Age	Type of vessel
BB140323	NO	Male	60	L Facial Artery
BB140473	NO	Female	68	Facial Artery
BB151402	NO	Female	33	L Facial artery
BB151585	NO	Female	66	R Facial Artery
BB160999	NO	Male	43	Facial artery
BB170377	NO	Female	61	R Facial Artery
BB170655	NO	Male	50	Facial Artery
BB171277	NO	Female	48	L Facial Artery
BB171621	NO	Female	67	R Facial Artery
BB181219	NO	Female	45	L Facial Artery
BB181212	NO	Female	78	L Facial Artery
BB180948	NO	Male	68	R Facial Artery

Table 2.3 Characteristics of patients undergoing craniofacial surgery. Small to medium size of surplus arteries were used to establish primary cell culture of hVSMCs. BioBank Number is a unique ID allocated to each patient in Professor Touyz' lab used to track sample information. R, right; L, left.

2.2.6 Software

Software used for data acquisition and analysis in this study is listed below. A webpage link is provided if the software is licence-free.

Lab Chart Reader 8.1.13 Windows: AD Instruments Ltd, Oxford, UK (https://www.adinstruments.com/support/downloads/windows/labchart-reader).

GraphPad Prism 5: GraphPad Software, San Diego, USA

Image Studio Lite Ver 5.2: LI-COR Biotechnology; Cambridge, UK (https://www.licor.com/bio/image-studio-lite/download)

QuantStudio™ Real-Time PCR Software: Applied BioSystems, California, USA

ZEISS ZEN pro Imaging Software for Connected Microscopy: Carl Zeiss Ltd., Cambridge, UK

FlowJo-Win32-10: Tree Star, Inc., Ashland, USA, (https://www.flowjo.com/solutions/flowjo/downloads)

NanoDrop 1000 v3.7.1 software: Thermo Fisher Scientific, Renfrew, UK

2.3 Cell culture procedures

2.3.1 Primary vascular smooth muscle cells

Primary human vascular smooth muscle cells (hVSMCs) were isolated from small arteries dissected from surplus surgical tissue of patients receiving elective craniofacial surgeries. Collection and use of human tissue for research has been approved by the West of Scotland Research Ethics Committee. Primary rat vascular smooth muscle cells (rVSMCs) were isolated from mesenteric arteries dissected from Wistar Kyoto (WKY) rats and stroke-prone spontaneously hypertensive rats (SHRSP). Primary mouse vascular smooth muscle cells (mVSMCs) were isolated from mesenteric arteries dissected from wild type (WT) mice and heterozygous $TRPM7^{+/\Delta kinase}$ mice. The experimental procedure on animals conform to the principles highlighted in Section 2.1. General characteristics of cells and details of cell culture media used in this study are summarized in Table 2.4. In addition, the digestion solution used for primary cell culture was comprised of F12 Ham medium, 1X Penicillin-Streptomycin, 50 ml of FBS and 5ml of 2 M HEPES (pH 7.4).

Cell type	Human vascular smooth muscle cells (hVSMCs)	Rat vascular smooth muscle cells (rVSMCs)	Mouse vascular smooth muscle cells (mVSMCs)
Origin	human: adult facial artery primary culture	Rat: mesenteric artery primary culture	Mouse: mesenteric artery primary culture
Cell Culture Medium	DMEM 1X SMGS 1X Penicillin-Streptomycin (1000 U/ml)	DMEM 10% FBS 1X Penicillin-Streptomycin (1000 U/ml)	DMEM 10% FBS 1X Penicillin-Streptomycin (1000 U/ml)
Starvation Medium	DMEM 0.5% FBS (v/v) 1X Penicillin-Streptomycin (1000 U/ml)	DMEM 0.5% FBS (v/v) 1X Penicillin-Streptomycin (1000 U/ml)	DMEM 0.5% FBS (v/v) 1X Penicillin-Streptomycin (1000 U/ml)
Freezing Medium	DMEM (60%, v/v) FBS (30%, v/v) DMSO (10%, v/v)	DMEM (60%, v/v) FBS (30%, v/v) DMSO (10%, v/v)	FBS (90%, v/v) DMSO (10%, v/v)

Table 2.4 General characteristics of cells and details of cell culture media used in this study. DMEM, Dulbecco's Modified Egle Medium; SMGS, Smooth Muscle Growth Supplement; FBS, Fetal Bovine Serum; DMSO, Dimethyl sulfoxide.

2.3.2 Isolation of vascular smooth muscle cells from human arteries

Surplus surgical tissue obtained from patients undergoing elective craniofacial surgery were kept in phosphate-buffered saline on ice until the isolation procedure. Small arteries were dissected from surrounding fat and adventitial tissue with an effort to pool more vessel segments, which were then transferred to a sterile tube with 12.5 ml of pre-warmed F12 Ham medium containing digestion mix comprised of 25 mg of BSA, 25 mg of collagenase (>200 IU/mg), 1.5 mg of elastase and 4.5 mg of soybean trypsin inhibitor. The vessel segments were digested at 37 ℃ for 30 min and the digested fragments were subsequently passed through a 20G needle to obtain a homogenised solution. The resulting

suspension was centrifuged at 2,000 rpm for 5min at room temperature, and cell pellet was resuspended in 5 ml of complete F12 Ham medium (with antibiotics and FBS), distributed in a T25 tissue culture flask (passage 0) under normal conditions for cell culture. After 24 h, the F12 Ham medium was removed and replaced with basal cell culture medium for hVSMCs. The procedure of isolation and setting up of the primary culture of hVSMCs was performed by the laboratory technician Mrs Jackie Thomson.

2.3.3 Isolation of vascular smooth muscle cells from rat mesenteric arteries

Mesenteric beds were isolated from 10 rats and collected in sterile 50 ml tubes containing 30 ml of F12 Ham medium. Vessels were dissected and the surrounding fat and adventitial tissue were removed. The resulting segments were incubated in 25 ml of F12 Ham medium containing digestion mix comprised of 50 mg of BSA, 50 mg of collagenase, 3 mg of elastase, and 9 mg of soybean trypsin inhibitor, at 37°C for 60-90 min depending on the size of tissue. The digested fragments were subsequently passed through needles in progression from 16G, 18G to 20G to obtain a homogenised solution. The resulting suspension was then filtered through a 100 µm nylon filter and centrifuged for 5 min at 1,500 rpm. Cell pellet was resuspended in 15 ml of basal cell culture medium (DMEM containing 10% FBS and antibiotics), distributed in a T25 tissue culture flask (passage 0) under normal cell culture condition. Medium was changed after 24 and 48 h. The procedure of isolation and setting up of the primary culture of rVSMCs were kindly performed with help from Mrs Wendy Beattie.

2.3.4 Culture and passage of vascular smooth muscle cells

VSMCs from human and rodents were cultured in different incubators under 5% CO_2 at 37°C and 95% humidity. The volume of medium used depends on the size of flasks or dishes (e.g 20 ml for a T150 cell culture flask, 15 ml for a T75 flask, 3 ml for a 60 mm cell culture dish and 7 ml for a 100 mm dish). Cell culture medium was changed every 3 days. Cell morphology and cell confluence were checked by microscope every day and unhealthy or contaminated cells were discarded. VSMCs were passaged at approximately 80% confluence to avoid overconfluence that may cause environmental stress. Culture medium was removed before passaging and cells were then washed twice by pre-warmed and sterile DPBS (without Ca^{2+} and Mg^{2+}). 0.5% trypsin-EDTA solution (2 ml in T150 tissue culture flask) was added and cells were incubated at 37°C for 3 min. Cell detachment was observed using an inverted light microscope. The enzymatic reaction was terminated by the addition of five-times the volume of basal cell culture medium. The

resulting cell suspension was transferred to a sterile tube and centrifuged at 1,200 rpm for 3 min at room temperature. The supernatant was aspirated, and cells were resuspended by either appropriate volume of basal culture medium and then plated in flasks and dishes, or FBS-containing freezing medium for storage (Section 2.3.5) in liquid nitrogen depending on the purpose of the procedure. With help from Mrs Jackie Thomson, every cell culture was tested routinely for mycoplasma contamination and cells were phenotyped on a regular basis as vascular smooth muscle cells using antibodies to probe VSMC-specific proteins, including smoothelin (cat.#: ab8969, Abcam), smooth muscle myosin heavy chain (cat.#: sc-6956, Santa Cruz) and smooth muscle actin (sc-32251, Santa Cruz). In this study, VSMCs at passage 3-8 were used in *in vitro* experiments.

2.3.5 General protocol for freezing and thawing vascular smooth muscle cells

Cells were detached from the flask and centrifuged as described in Section 2.3.4. Cell pellet was resuspended in 1 ml of appropriate freezing medium and transferred to a sterile cryogenic vial. Cryogenic vials were then placed in cryofreezing container (Mr Frosty) in a freezer at -80°C, with a rate of cooling close to 1°C/min. After 24 h, vials were transferred to liquid nitrogen tank for long-term storage. For recovery, vials were removed from liquid nitrogen tank and hold in 37°C water bath. Then, cell suspension was transferred to a 15 ml tube containing 10 ml of complete medium and centrifuged at 1,500 rpm for 3 min. Cell pellet was resuspended in 15 ml of complete medium and transferred to a T75 flask. To avoid potential adverse effects of DMSO, cell culture medium was refreshed immediately after cell attachment was confirmed under microscope.

2.3.6 Experimental protocols

VSMCs at approximately 90% confluence were starved overnight in medium containing 0.5% FBS. Starvation medium was refreshed before experiments. Quiescent cells were stimulated with VEGF (50 ng/ml) or EGF (50 ng/ml), concentration used in previous *in vitro* studies (417, 418), for long term (5 h and 34 h) and short term (1-60 min). Concentrations were selected according to the literature (419, 420), and our concentration-response study. In some experiments, 30 minutes prior to stimulation, quiescent VSMCs were pre-treated with the following inhibitors:

-Gefitinib (EGFR inhibitor, 10^{-6} mol/L)

-Vatalanib (VEGFR inhibitor, 10^{-6} mol/L)

-NS8593 (TRPM7/calcium activated potassium channel inhibitor, 4×10^{-5} mol/L)

-Apamin (calcium activated potassium channel inhibitor, 10^{-6} mol/L)

-2-APB (non-specific TRPM7 inhibitor, 3×10^{-5} mol/L)

-TG100-115 (TRPM7 kinase domain/PI3K inhibitor, 10^{-5} mol/L)

-PP2 (Src family kinase inhibitor, 10^{-5} mol/L)

Concentrations of these compounds were based on previously published data and our preliminary studies (421-427). For cells stimulated with drug diluted in DMSO (≤1%, v/v), DMSO was used as the negative control/vehicle, while for cells stimulated with drug diluted in PBS, equivalent volume of PBS was used. To terminate the stimulation, drug-containing medium was removed by aspiration pump and cells were rinsed with ice-cold DPBS. Plates and dishes were then stored in -20°C freezer until further use. Concentration of pharmacological modulators were based on previously published data on previous studies (428-430).

2.4 Molecular biology methods

2.4.1 Western blot (immunoblotting)

Western blot was used to: i) detect expression of Mg^{2+} transporters including TRPM7, TRPM6, MagT1 and SLC41A1, TRPM7 substrates such as annexin-1 and calpain-2, growth factor receptors such as VEGFR and EGFR, and housekeeping proteins such as α-tubulin, β-actin and Na^{+}/K^{+}-ATPase, ii) examine the activation of cellular kinases such as p38 MAPK, ERK1/2, STAT1 and STAT3, and growth factor receptors such as VEGF and EGFR, and iii) assess the translocation of cytosol proteins such as annexin-1 and calpain-2 to cell membrane.

2.4.1.1 Isolation of total protein from tissue and cells

After stimulation, VSMCs from human and rats were placed on ice and harvested by scrapping in appropriate volume of ice-cold lysis buffer (e.g. 60-80 µl for a 60 mm cell culture dish) using a clean cell scraper. Cell lysates were transferred to a pre-cooled microcentrifuge tube and kept on ice for 30 min for constant agitation, followed by centrifugation at 12,000 rpm for 15 min at 4°C. The resulting supernatant was transferred to a new pre-cooled tube and the protein concentration was assessed.

Tissue samples were homogenised in appropriate volume of lysis buffer using Precellys 24 tissue homogenizer (Bertin Instruments, Montigny-le-Bretonneux, France). The time and speed of homogenization was adjusted depending on the types and amount of tissue. Tissue

lysates were centrifuged at 12,000 rpm for 15 min at 4°C, and the resulting supernatant was transferred to a new pre-cooled tube for later use.

2.4.1.2 Isolation of cytosol and membrane fractions

Human and rat VSMCs cultured in 100 mm cell culture dishes were harvested by scraping in appropriate volume of ice-cold Buffer A (80-100 µl) using a clean cell scraper. Cell lysates were transferred to a pre-cooled tube and centrifuged at 500 g for 10 min at 4°C. The resulting supernatant was collected in a thick-wall polycarbonate tube and ultracentrifuged at 40,000 rpm for 1 hour at 4°C using Optima TL Ultracentrifuge (Beckman Coulter, High Wycombe, UK). The resulting supernatant was collected as cytosolic fraction, and the pellet was resuspended in Buffer B and collected as membrane-rich fraction. Protein concentration of the fractions was determined and samples were storage at -20 °C.

2.4.1.3 Determination of protein concentration and preparation of samples

Protein concentration was measured using Pierce^{TM} BCA Protein Assay Kit according to the manufacturer's instructions. The assay is based on the reduction of Cu^{2+} to Cu^{1+} by protein in alkaline medium and the highly sensitive and selective colorimetric quantification of Cu^{1+} by a unique reagent containing bicinchoninic acid (BCA). The chelation of cuprous ion and BCA results in a purple-coloured reaction complex which exhibit a strong absorbance at 562 nm. For the assay, BSA-based standards were established, comprising a set of diluted standards at 2000 µg/ml, 1000 µg/ml, 500 µg/ml, 250 µg/ml, 125 µg/ml and Milli-Q water as a blank control. Working Reagent (WR) was prepared by mixing BCA Reagent A with BCA Reagent B (dilution 50:1). To measure protein concentration, 5 µl of either standard or sample was added to wells of a clean 96-well plate, followed by the addition of 50 µl of Working Reagent to each well. The plate was incubated at 37°C for 30 min in the dark on an Eppendorf Shaker. The absorbance was measured at 562 nm using VICTORTM X3 Multilabel plate reader (PerkinElmer, Michigan, USA). The obtained standard curve with R-squared > 0.98 was accepted, and protein concentration of samples was determined by the linear equation of the standard curve using Work-Out Wallac software. After protein determination, 20-30 µg of protein lysates were mixed with 6X Laemmli sample buffer with a ratio of 5/1 (5 µl of sample buffer in 25 µl protein lysate). The mixture was then boiled at 95°C for 7 min to denature protein using Eppendorf ThermoMixer, and were stored at -20°C until further use.

2.4.1.4 Sodium dodecyl sulphate polyacrylamide gel electrophoresis (SDS-PAGE)

SDS-PAGE was used to separate proteins according to the molecular weight of the protein of interest. 7.5% SDS/PAGE was used for proteins with molecular weight higher than 150 kDa, 10% SDS/PAGE for proteins of 30-150 kDa and 12% SDS/PAGE for proteins lower than 30 kDa. 25-50 µl of sample containing 20-30 µg of protein loaded using special gel loading tips in pre-casted narrow wells in stacking gel. Standard of protein molecular weight was added in the first lane and positive control was also loaded to testify antibodies. Electrophoresis was performed in SDS-PAGE running buffer, at a constant voltage of 140 V until the blue dye molecule reached the bottom part of the gel. In some experiments, commercial gels (Invitrogen Novex Tris-Glycine Mini Gels, 4-20%) which are capable of separating a wide range of proteins were used depending on the purpose of experiments.

2.4.1.5 Transfer of proteins and immunoblotting

Following the electrophoresis, gel containing proteins was removed from the electrophoresis apparatus and rinsed with SDS-PAGE transferring buffer for 10 min. To transfer proteins from the gel to a hydrophobic, 0.45 µm pore nitrocellulose membrane, gel and membrane were sandwiched between sponge and filter paper sequentially, which were then submerged in transferring buffer in a tank, with the membrane oriented nearest to the positive electrode. Wet transfer was performed at a constant voltage of 110 V for 90 min. For larger proteins such as TRPM7, transfer was performed for 120 min. The efficiency of the electrotransfer was assessed by staining the membrane with Ponceau-S solution for 5-10 sec. Membranes with adequate transfer of proteins were de-stained with distilled water and TBS-T, followed by blockage step using either BSA (3%)-based or non-fat dried milk-based blocking buffer depending on the protein of interest at room temperature for 1 h on a shaker at a gentle speed. Blocked membranes were washed by TBS-T for 3 times and incubated with primary antibody overnight at 4°C. The following day, the primary antibody solution was removed, and the membrane was washed for 5 min with TBS-T (3 times), followed by incubation with appropriate secondary fluorescence-coupled antibodies goat-anti-mouse-IRDye 680 or goat-anti-rabbit-IRDye 800 (LI-COR, Cambridge, UK) for 1 h at room temperature in the dark. Secondary antibody was removed, and the membrane was washed 3×5 min with TBS-T. Immuno-reactive proteins on the membrane were visualized using Odyssey CLx LI-COR imaging system (LI-COR Biosciences, Cambridge, UK). Protein expression levels were analysed by Image Studio Lite software and normalised to housekeeping proteins such as α-tubulin, β-actin and Na^+/K^+-ATPase

depending on the experiments. In some experiments, antibodies were removed from the membranes by treatment with NaOH (200 mM) for 5 min at room temperature. The efficacy of stripping process was assessed using Odyssey CLx LI-COR imaging system. The membrane was then washed 3×5 min with TBS-T, blocked in fresh blocking buffer for 1 h at room temperature and re-probed with new primary antibody.

2.4.2 Immunoprecipitation

Phosphorylation of TRPM7 in VSMCs was detected by immunoprecipitation (IP) followed by immunoblot analysis. VSMCs cultured in 100 mm cell culture dishes were harvested using appropriate volume of proteins lysis buffer (70 µl for one dish). To improve protein concentration, cell lysates harvested from 4 plates were collected as one group. Cell lysates were then subsequently passed through a 26G needle to obtain a homogenised solution and kept on ice for 20 min under constant agitation, followed by centrifugation at 12,000 rpm for 15 min at 4°C. Resulting supernatant was transferred to a new pre-cooled tube, and protein concentration was measured using BCA assay kit, as described in 2.4.1.3. 400-500 µg of protein samples were diluted in 200 µl using Milli-Q water and mixed with the immunoprecipitating antibody according to the manufacturer's datasheet. Appropriate volume of sample solution containing about 10% of protein used for IP was also collected as input control (pre-IP lysate). The reaction mixture for IP was then rotated in a Stuart SB3 Rotator (Camlab Ltd, Cambridge, UK) at a gentle speed overnight at 4°C. The following day, 15 µl of Protein A and 15 µl of Protein G was added to the reaction mixture and rotated at 4°C for 4 h. The IP complex was then centrifuged at 14,000 rpm for 1 min at 4°C and the supernatant was collected as output (post-IP lysate). The IP complex was then washed twice using 1 ml of protein lysis buffer by centrifugation at 14,000 rpm for 30 sec. Supernatant was removed and the final pellet was resuspended with 30 µl of 6X Laemmli sample buffer. Pre-IP lysate control and post-IP lysate control were prepared by making a mixture (30 µl) containing 40-50 µg (~10% of protein used for IP) of sample protein, Milli-Q water and 10 µl of 6X sample buffer. All samples were boiled at 95°C for 7 min before Western blot was performed as described earlier.

2.4.3 RNA analysis

2.4.3.1 Extraction of total RNA using QIAzol ®

Total RNA was extracted using QIAzol ® isolation protocol. VSMCs were harvested by scraping with appropriate volume of QIAzol ® (500 µl for one well of a 6-well plate), while frozen tissues were homogenized in 750 µl of QIAzol ® using Precellys 24 tissue

homogenizer. Subsequently, 200 µl of chloroform was added to each sample and mixed thoroughly. Samples were maintained at room temperature for 2 min to allow phase separation and then centrifuged at 12,000 g for 15 min at 4°C. The aqueous (upper) phase was carefully transferred to a new nuclease-free tube using a pipette setting at 75 µl. 500 µl of isopropanol was added, mixed and maintained at room temperature for 10 min, followed by centrifugation at 12,000 g for 10 min at 4°C. The resulting supernatant was removed, and the pellet was washed with 500 µl of 75% ethanol by centrifugation at 8,000 g for 5 min at 4°C. The supernatant was removed and the pellet was dried by incubation at 37°C for 5 min, followed by resuspension with 20 µl (40 µl for tissue sample) of nuclease-free water. Samples were then left on ice for 1 h followed by incubation at 65°C for 5 min to denature RNA.

2.4.3.2 Measurement of RNA purity and concentration

Total RNA concentration and purity were measured using NanoDrop ND-1000 spectrophotometer (Labtech International, Heathfield, UK) and NanoDrop 1000 v3.7.1 software. Initially, 1.5 µl of RNase-free water was dispensed onto the lower measurement pedestal and measured to wash the system. Next, 1.5 µl of RNase-free water was measured as a blank background control, and equal volume of samples were measured in duplicates. RNA concentration of samples was calculated based on the following formula: RNA concentration = $A/\varepsilon l$, where A indicates the absorbance of samples measured at 260 nm, ε indicates molar extinction coefficient and l is the light path-length. Additional absorbance at 280 nm and 230 nm was measured, and the 260/280 ratio of ~2.0 and the 260/230 ratio in the range of 2.0-2.2 indicate that the purity of RNA is high.

2.4.3.3 Removal of DNA by DNase I treatment

To avoid the contamination of genomic DNA in isolated RNA samples and the impact on following polymerase chain reaction (PCR)-based analysis, DNase I treatment was performed for all RNA samples. Briefly, 10-20 µg of total RNA was incubated with 1X DNase I buffer and 0.1 U of DNase I for 1 h at 37°C and the enzymatic reaction was terminated by 10 min incubation at 70°C. In this study, for RNA samples extracted from cultured VSMCs, 4 µg of total RNA was diluted to a 17 µl mixture in RNase-free water, followed by incubation with 1 µl of DNase I (2 U) and 2 µl of DNase Buffer 10X as described above. Resulting RNA samples were then left on ice and used for cDNA synthesis.

2.4.3.4 cDNA synthesis by reverse transcription of RNA

Complementary DNA (cDNA) was synthesized from isolated RNA sample using High-Capacity cDNA Reverse Transcription Kit based on the manufacturer's instruction. In a 96-well PCR plate, 2 µg of DNase I-treated RNA and a reaction mix including 2 µl of 10X RT buffer, 0.8 µl of 25X dNTP (deoxyribonucleotide triphosphates) mix, 2 µl of 10X RT random primers, 1 µl of multiscribe reverse transcriptase were added to the bottom of the well, which was then topped up to a total volume of 20 µl with RNase-free water. In this study, for RNA samples isolated from cultured VSMCs as described earlier, 10 µl (2 µg) of DNase I-treated sample were added to the reaction mix with extra 4.2 µl of RNase-free water, resulting a total volume of 20 µl. Plate was sealed using adhesive transparent PCR film and vortexed gently followed by a quick centrifugation to spin down the mixture. Subsequently, the cDNA synthesis was performed using a PTC-225 Peltier Thermal Cycler (MJ Research, Massachusetts, USA) under the following condition: 10 min at 25°C (primers annealing), 120 min at 37°C (cDNA synthesis), 5 min at 85°C (inactivation of reverse transcriptase) and 4°C until reaction termination. The synthesized cDNA was stored at -20°C until further use.

2.4.3.5 Determination of mRNA expression levels by quantitative PCR

Gene expression of the Mg^{2+} transporters TRPM7, TRPM6, MagT1 and SLC41A1 in cultured hVSMCs were assessed using SYBR Green-based quantitative PCR (qPCR), also known as real-time PCR. SYBR Green is a commonly applied fluorescent dye and preferentially binds to the minor groove of double-stranded DNA, consequently emitting fluorescence that is directly proportional to the concentration of amplified DNA (431). The fluorescence could be measured at the end of each amplification cycle and the PCR cycle number at which the fluorescence intensity reaches significantly above the background level is termed the threshold cycle (Ct). Consequently, relative gene expression level is calculated by the $2^{-\Delta\Delta CT}$ method using a reference gene (housekeeping gene) as the normaliser (432).

Before qPCR was performed, cDNA samples were diluted in RNase-free water to a concentration of 10 ng/µL. In a 384-well reaction plate, 3 µl of cDNA sample (30 ng), 0.3 µl of primer FW (300 nM), 0.3 µl of primer RW (300 nM), 1.4 µl of nuclease-free water and 5 µl of Fast SYBR Green™ Master mix containing DNA polymerase, SYBR Green I dye, dNTPs, Uracil-DNA Glycosylase (UDG) and ROX™ passive reference dye were added to the bottom of the well, resulting in a final volume of 10 µl. The negative control

of the reaction was performed by adding 3 µL of nuclease-free water instead of cDNA sample. Plate was sealed using adhesive transparent qPCR film and vortexed gently followed by a quick centrifugation to spin down the mixture. PCR reaction was performed using a 7900HT Fast Real-Time PCR System (Applied Biosystems) under the following conditions: 50°C for 2 min, 95°C for 10 min, then 40 cycles of 95°C for 15 sec and 60°C for 1 min, followed by a dissociation curve stage including 95°C for 15 sec, 60 °C for 15 sec and 95°C for 15 sec. The analysis was performed using the $2^{-\Delta\Delta CT}$ method, with GAPDH as the reference gene. Briefly, ΔΔCt was calculated using the following formula: $\Delta Ct = Ct_{GOI} - Ct_{HKG}$, where Ct_{GOI} indicates Ct value of gene of interest and Ct_{HKG} indicates Ct value of the housekeeping gene, and $\Delta\Delta Ct = \Delta Ct_{sample} - \Delta Ct_{control}$, where $\Delta Ct_{control}$ indicates the average ΔCt value of the vehicle-treated control group and ΔCt_{sample} indicates the ΔCt value of stimuli-treated groups. The relative quantity (RQ) value of the target gene was calculated as: $RQ = 2^{-\Delta\Delta Ct}$ (432). Results were reported as fold change relative to the vehicle-treated control group.

2.4.4 Imaging of Ca^{2+} in VSMCs by live cell microscopy

Intracellular Ca^{2+} levels in VSMCs were assessed using fluorescent Ca^{2+} indicator Cal-520 acetoxymethyl ester (Cal-520AM, Abcam) and imaged using live cell microscopy. Cal-520 is a new fluorogenic Ca^{2+} sensitive dye, displaying several critical advantages including significantly higher signal to noise ratio (S/N), improved intracellular retention and convenient spectrum compared to the existing green Ca^{2+} probes such as Fluo-3 AM and Fluo-4 AM. Cal-520 crosses cell membrane and in the intracellular environment, its lipophilic blocking groups are cleaved by esterase, resulting in a negatively charged dye emitting fluorescence that are enhanced upon binding to Ca^{2+}.

Human or rats VSMCs were cultured in 12-well plate and loaded with 5 µM Cal-520 AM in starvation medium (0.5% FBS) at 37 °C for 75 minutes followed by 30 minutes at room temperature. The dye solution was replaced with 800 µl of HEPES buffer (130 mM NaCl, 5 mM KCl, 1 mM CaCl, 1 mM $MgCl_2$, 10 mM D-glucose and 20 mM HEPES, pH 7.4) in each well for 30 min prior to imaging. In some experiments, cells were pre-treated with the pharmacological inhibitors gefitinib, NS8593 and 2-APB during this period according to the purpose of experiments. Fluorescent signals were collected using an inverted epifluorescence microscope (Axio Observer Z1 Live-Cell imaging system, Zeiss, Cambridge, UK) at excitatory wavelength of 490 nm and emission of 535 nm, and images were taken at 2-sec interval for 4 min. Stimuli were added 30 sec after the fluorescent

signal of sample had been collected, and the average fluorescent level in the first 30 sec was considered as the basal level. Data were acquired and analysed using Zen Pro (Zeiss, Cambridge, UK).

2.4.5 Flow cytometry

Flow cytometry is a widely used method to analyse single cells or particles suspended in a buffered salt-based solution, where each particle or cell is measured for visible light scatter and one or multiple fluorescence parameters (Figure 2.1). Through the beam scatter light, cells or particles are analysed for forward scatter (FS) which correlates with cell size and side scatter (SS) which is proportional to the granularity of the cells, allowing to distinguish different cell populations. Within the flow cytometer, the fluorescence from stained cells or particles are channelled by a set of filters and mirrors, consequently detected by different photomultiplier tubes (PMTs).

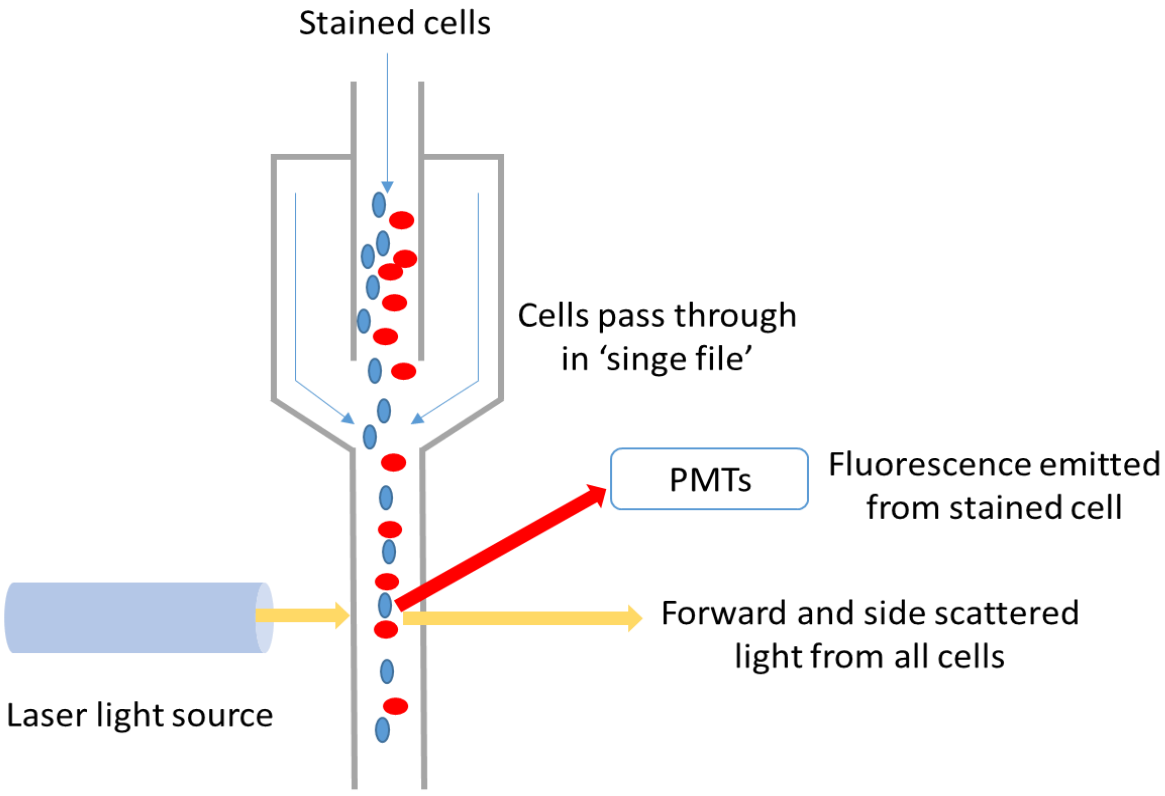

Figure 2.1 Overview of the flow cytometer. In the flow cytometer, cells pass individually through a laser light beam. Forward and side scattered light is detected to distinguish cell populations based on differences in cell size and granularity. Fluorescence from stained cells or particles are channelled by a set of filters and mirrors, consequently detected by different photomultiplier tubes (PMTs).

2.4.5.1 Measurement of intracellular free Mg^{2+} in VSMCs using Magnesium Green

Intracellular free Mg^{2+} levels in VSMCs were assessed using fluorescent Mg^{2+} indicator Magnesium Green (Thermo Fisher Scientific, Renfrew, UK) and flow cytometry. Magnesium Green possesses the o-aminophenol-N, N, O-triacetic acid (APTRA) group, one of the most well-established ligands for targeting Mg^{2+}, and displays a higher affinity for Mg^{2+} than other APTRA-based probes such as mag-fura-2 and mag-indo-1. Magnesium Green has excitation maximum and emission maximum at 490 nm and 520 nm respectively (433). Upon binding to Mg^{2+}, Magnesium Green exhibits increased intensity of the fluorescence emission without any shift in the wavelength. The fluorescent signal can be detected by fluorescence-sensing techniques such as flow cytometry.

VSMCs cultured were detached from a T-75 cell culture flask by 0.5% trypsin-EDTA solution for 3 min at 37°C. The resulting cell suspension was transferred to a 15 sterile tube and washed using 12 ml of sterile DPBS, followed by centrifugation at 1,200 rpm for 3 min at room temperature. Supernatant was removed and the cell pellet was resuspended in 1,400 µl of Mg^{2+} and Ca^{2+} (Ca^{2+}/Mg^{2+})-free HEPES buffer (150 mM NaCl, 5 mM KCl, 10 mM d-glucose and 20 mM HEPES), followed by 10 min incubation at 37°C for stabilisation. Magnesium Green solution was prepared by adding 5 µl of 2.5 mM Magnesium Green diluted in DMSO and 1 µl of Pluronic F127 (20% solution in DMSO) to 2 ml of Ca^{2+}/Mg^{2+}-free HEPES buffer. The final concentration of Magnesium Green is ~6.25 µM and Pluronic F127 is 0.01%**.** Subsequently, 600 µl of the prepared Magnesium Green solution was added to the cell solution, followed by 30 min incubation at 37°C in the dark. To avoid the attachment of VSMCs to the tube wall, the tube was vortexed gently every 5 min. Stained cells were then washed twice with 12 ml of DPBS by centrifugation at 1,200 rpm for 3 min at room temperature. The resulting cell pellet was resuspended in 200 µl of HEPES buffer with Mg^{2+} and no Ca^{2+}(150 mM NaCl, 5 mM KCl, 10 mM d-glucose, 20 mM HEPES and 1 mM $MgCl_2$). Cell suspension was kept at room temperature for 15 min to allow complete de-esterification of intracellular AM esters before measurement. In some experiments, inhibitors such as gefitinib, NS8593, and 2-APB were added to samples during this period according to the purpose of experiments. Stimuli (VEGF or EGF in this study) were then added to samples and mixed by gentle vortex, and after 5 min flow cytometry was performed to assess the intracellular level of free Mg^{2+} using the fluorescein isothiocyanate (FITC, Ex/Em 492/517).

2.4.5.2 Assessment of cell proliferation using CFSE

To assess how growth factors regulate VSMCs proliferation, the cell tracking dye carboxyfluorescein succinimidyl ester (CFSE) was used. CFSE is initially introduced into cells as carboxyfluorescein diacetate succinimidyl ester (CFDA-SE), a colourless nonpolar analogue of fluorescein. After CFDA-SE diffuses into the cytoplasm, its acetate substituents are cleaved by cellular nonspecific esterases, resulting in highly fluorescent and membrane impermeable CFSE, which covalently labels long-lived intracellular molecules through reacting with amine groups on peptides and proteins (434, 435). When CFSE-labelled cell divides, the fluorescein-tagged molecules are split roughly evenly between the two daughter cells, and thus cell division can be indirectly assessed by measurement of the corresponding decrease in the fluorescence intensity by flow cytometry.

Briefly, quiescent VSMCs were trypsinized by 0.5% trypsin-EDTA solution for 3 min at 37°C. The resulting cell suspension was transferred to a 15 sterile tube and washed using 12 ml of starvation medium, followed by centrifugation at 1, 200 rpm for 3 mint at room temperature, and the cell pellet was resuspended by 1 ml of sterile DPBS containing 1% FBS. 1 µl of 5 mM CFSE (Thermo Fisher, Renfrew, UK) diluted in DMSO was added to the cell solution resulting in a final concentration of 5 µM for CFSE, and mixed by gentle vortex, followed by incubation at 37°C for 30 min. The stained cells were then washed twice using basal cell culture medium. Following the second centrifugation, the supernatant was removed and the cell pellet was resuspended using appropriate volume of cell culture medium. CFSE-labelled cells were then plated at 30% confluence and cultured for 24 h in cell culture medium (10% FBS), followed by incubation in DMEM supplemented with 2.5%-5% FBS for 72 h. During this period, cell culture medium was refreshed with the addition of stimuli (e.g. EGF) every 24 h. In some experiments, 30 min prior to the addition of stimuli, inhibitors such as gefitinib, NS8593 and 2-APB were added to the medium. After 72 h, cells were trypsinized using 0.5% trypsin-EDTA, washed using sterile DPBS and resuspended in 300 µl of DPBS containing 1% FBS. Flow cytometry with the FITC PMT (Ex/Em 492/517) was performed to assess cell division by measuring the fluorescence of VSMCs. Data acquisition and analysis were performed using the software FACSDiva (BD Biosciences).

2.4.6 Scratch-wound assay

To investigate how growth factors regulate VSMCs migration, the scratch-wound assay, a two-dimensional (2D) *in vitro* technique was performed. This assay is based on the observation that, upon creation of a cell-free area by scratching a confluent cell monolayer, cells on the edge of the 'wound' will migrate into the gap to close the 'wound' until the establishment of new cell-cell contacts (436, 437). However, this 'wound healing' is considered as a combination of both cell migration and proliferation. To ensure true detection of migration, pre-treating with DNA synthesis inhibitors such as mitomycin C is often recommended (438). In this study, to reduce the effects of cell proliferation, the assay was performed in a medium with low FBS (0.5%), a condition used for cell starvation in our experiments.

VSMCs were counted with a haemocytometer and plated at density of 100, 000 cells/well in a 6-well plate. Cells were cultured in basal culture medium (10% FBS), and when cells were confluent, medium was replaced with starvation medium (0.5% FBS) overnight. Subsequently, a sterile pipette (200 µl) was used to slowly and gently scratch the cells across the centre of the well, resulting a straight 'wound' with equal width. Wells were washed using DPBS to remove the floating cells, and then the 6-well plate was placed on a microscope (EVOS XL Core, Thermo Fisher Scientific, UK). 3 zero-hour (0h) photos were taken at appropriate areas for each well using a 10× objective. Cells were then incubated in fresh starvation medium, with the addition of growth factors (EGF or VEGF, 50 ng/ml) for 20 h. In some experiments, 30 min prior to the addition of stimuli, inhibitors such as gefitinib, NS8593 and 2-APB were added to the medium. After 20 h, the plate was placed on the microscope, and 3 photos were taken at appropriate areas for each well using the 10× objective. The images were collected and analysed using Image J software. Cell migration was determined by the distance travelled from one side of the scratch to the other side during the 20 h.

2.4.7 Proximity ligation assays

rVSMCs from WKY were seeded on cover glasses (13 mm, Thickness No.0; VWR) at a density of 5×104 cells per well in 6-well plates. The following day, cells were stimulated with EGF (50 ng/ml) for 5 min with or without 30 min pretreatment of inhibitors. Cells were fixed with 4% paraformaldehyde in PBS for 15 min at room temperature, and cell membranes were then stained by wheat germ agglutinin (WGA; cat.#: w6748; Invitrogen) for 25 min, followed by permeabilization using 0.1% Triton X-100 (Sigma-Aldrich) in

PBS for 10 min at room temperature. Cells were washed with Buffer A (0.01 M Tris-Base, 0.15 M NaCl, 0.05% Tween-20, pH=7.4) and blocked using Blocking Buffer for 1 hour at 37°C, followed incubation with primary antibodies EGFR (cat.#: 2646S; Cell signalling; 1:100) and TRPM7 (cat.#: MA5-27620; Invitrogen; 1:100) overnight at 4°C. The following day, proximity ligation assay was performed according to the manufacturer's protocol using the Duolink Detection Kit (Sigma-Aldrich). Briefly, cells were washed using Buffer A and incubated with Duolink® In Situ PLA® Probe Anti-Mouse PLUS (cat.#: DUO92001) and Duolink® In Situ PLA® Probe Anti-Rabbit MINUS (cat.#:DUO92005) at 37°C for 1 hour to label TRPM7 and EGFR respectively. Circular DNA molecules were formed in Ligation Buffer (working dilution 1:5) containing DNA Ligase (1:40) at 37°C for 30 min, and were amplified in Amplification Buffer (1:5) containing the rolling circle polymerase (1:80) at 37°C for 100 min. Coverslips were mounted with Duolink® In Situ Mounting Medium with DAPI (cat.#: DUO82040; Sigma-Aldrich). Images were acquired using a laser-scanning confocal microscope (LSM 5 PASCAL ZEISS) under an oil immersion objective (63×/1.4 NA). In order to detect all PLA signals, a series of Z-stack images were collected and were analysed by Image J software.

2.4.8 Confocal microscopy

rVSMCs from WKY were seeded on cover glasses (13 mm, Thickness No. 0; VWR) at a density of 8×104 cells per well in 6-well plates. After stimulation, cells were fixed by 4% paraformaldehyde in PBS for 15 min and permeabilized with Triton X-100 (Sigma-Aldrich) in PBS for 4 min at room temperature. After three washes with Tris-buffered saline (TBS; 150 mM NaCl, 20 mM Tris-HCl, pH 7.6), cells were blocked with 10% goat serum and 2% BSA (w/v) in TBS for 1 h at room temperature. Cells were then washed three times using TBS, and incubated with specific primary antibodies to: TRPM7 (cat.#: MA5-27620; Invitrogen; 1:300) and EGFR (cat.#: 2646S; Cell signalling; 1:300) overnight. The following day, cells were washed and then incubated with 1:400 diluted secondary antibodies Alexa Fluor 555 Goat anti-Rabbit IgG (cat.#: A-21428; Invitrogen) and Alexa Fluor 488 Goat anti-Mouse IgG (cat.#: A-11001; Invitrogen) for 2 hours at room temperature. Coverslips were mounted with Prolong Gold Antifade mounting medium with DAPI (cat.#: P36935; Invitrogen). Staining were visualized using a laser-scanning confocal microscope (ZEISS LSM880) with a 40× (NA 1.1) water-immersion objective. Images were analysed using the open source Fiji software.

2.4.9 Live cell imaging of intracellular TPRM7 movement

Human embryonic kidney (HEK) 293 cells (HEK-293) expressing yellow fluorescent protein (YFP)-tagged wild type mouse TRPM7 (WTmTRPM7-YFP) were kindly provided by Dr. Vladimir Chubanov (Ludwig Maximilian University of Munich, Munich, Germany). The transient transfected HEK-293 cells were maintained in DMEM containing 10% FBS. After EGF (50 ng/ml) treatment, fluorescent signal of TPRM7 in HEK-293 cells were recorded for 15 min by an inverted epifluorescence microscope (Axio Observer Z1 Live-Cell imaging system, ZEISS) at excitatory wavelength of 490 nm and emission of 535 nm. Images were acquired and analysed by Zen Pro software (ZEISS).

2.5 Animals

2.5.1 Housing and husbandry

Wild type TRPM7+/+ (WT) mice (C57BL/6J and SV-129 mixed background) and mice heterozygous for the deletion of TRPM7 kinase domain ($TRPM7^{+/\Delta kinase}$) were housed in the BHF Glasgow Research Centre, Institute of Cardiovascular and Medical Sciences, University of Glasgow. Mice were housed and breed in individual cages under controlled conditions including constant humidity and temperature (22-24°C), a 12-hour light/dark cycle and accessible food and tap water. Cages were cleaned and replaced twice a week by the staff working in animal rooms. SV-129 mice were housed at Sapienza University by Professor Carmine Savoia's research group under controlled conditions.

Ear clipping was used to identify individual adult rodents. Genetically modified animals were confirmed by genotyping performed by Mrs Jackie Thomson and Mrs Wendy Beattie. All *in vivo* procedures were carried out by Dr. Francisco Rios under his personal license (University of Glasgow, UK), and all animal experiments were performed in accordance with proper regulations, guidelines and principles that apply to Scotland as highlighted in Section 2.1. Studies at Sapienza University were performed in accordance with the Italian Law on the protection of animal.

2.5.2 Wild type and TRPM7-kinase heterozygous mice

To investigate how the kinase domain of TRPM7 contributes to TRPM7-mediated signalling pathways and vascular function, WT and $TRPM7^{+/\Delta kinase}$ mice were used. WT mice were generated on the mixed background C57B1/6 and SV-129. The deletion of TRPM7 kinase domain was obtained using a gene-targeting vector through inserting a neomycin resistance gene cassette to replace exons 32-36 encoding the large portion of the

kinase domain (76). As a result of this technique, mutant TRPM7 mRNA encodes a protein containing amino acids 1-1, 537 of TRPM7, which is truncated immediately upstream of the α-kinase domain (Figure 2.2). Homozygous TRPM7Δkinase mice are embryonic lethal, suggesting that the intact kinase domain of TRPM7 is necessary for normal development of mice (76). TRPM7$^{+/\Delta kinase}$ mice were generated through breeding between male WT and female TRPM7$^{+/\Delta kinase}$, and the offspring were either homozygous TRPM7$^{+/+}$ (WT) or heterozygous TRPM7$^{+/\Delta kinase}$, which were confirmed by genotyping after 3 weeks old.

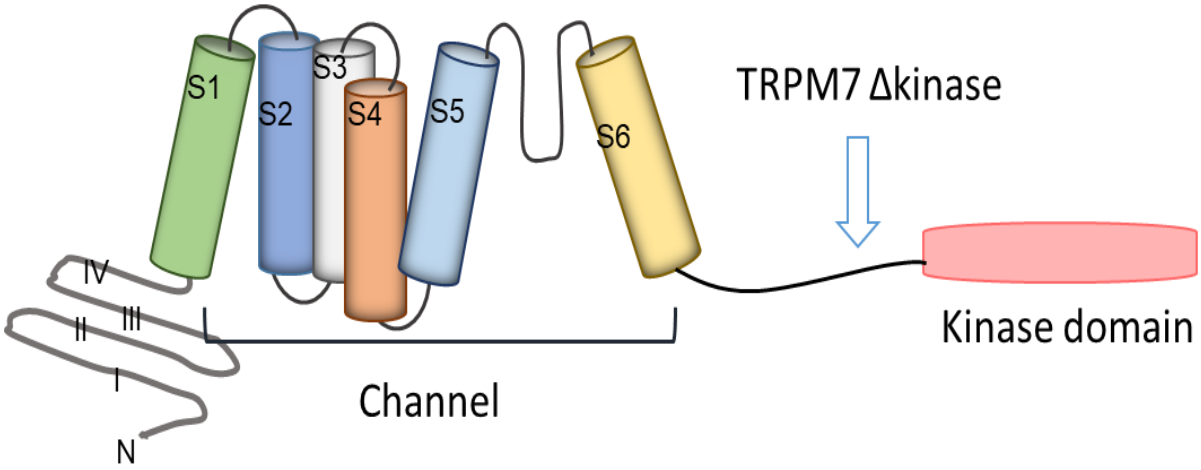

Figure 2.2 A schematic representation of truncated TRPM7 protein. The deletion of TRPM7 kinase domain was obtained using a gene-targeting vector technique. Arrow indicates the position of truncation in TRPM7$^{\Delta kinase}$.

2.5.3 SV-129 mice and drugs administration

The SV-129 mouse strain was first generated by Columbia University in 1928 and has been frequently used in biomedical research either as a background strain (wild type) or in the production of targeted mutations (439). In this study, to investigate the *in vivo* role of RTK inhibitors vatalanib and gefitinib, specific for VEGFR and EGFR respectively, normotensive male SV-129 mice were housed in individual cages under controlled conditions: constant humidity and temperature of 22-24°C, a 12-hour light/dark cycle and accessible standard food and tap water. 8 weeks-old SV-129 mice were divided into 3 groups (n=6 for each group), and treated for 2 weeks, as follows: vehicle-treated group, gefitinib-treated group (Gef, 100 mg/Kg/day) and vatalanib-treated group (Vat, 100 mg/Kg/day). In previous studies, the concentrations were well tolerated by mice and no significant signs of toxicity were observed (440, 441).. Blood pressure (BP) was measured

by tail-cuff before and after the treatment. Mice were sacrificed and tissues including kidney, heart and aorta were collected for further experiments. It should be noted that animal housing, BP measurement, and tissue collection were performed by Professor Carmine Savoia's research group at Sapienza University. Collected tissues were carefully transported to Glasgow under dry ice conditions.

2.5.4 Rat model of preeclampsia

To explore the involvement of the VEGF-VEGFR system and Mg^{2+} transporters in PE, we took advantage of two animal models of PE in this study. SHRSP is an established model of genetic predisposition to hypertension and stroke, which has made a tremendous contribution to cardiovascular research. Graham and her research group have demonstrated that pregnant SHRSP exhibits deficient uterine artery remodelling adversely affecting pregnancy outcome independent of pre-existing hypertension (442). Pregnant SHRSP rats also demonstrate reduced uteroplacental blood flow, increased sFLT-1/PIGF ratio in maternal plasma and increased albumin/creatinine (ACR) ratio in maternal urine, phenotypes that are associated with preeclampsia (442, 443). Thus, pregnant SHRSP is considered as a model of superimposed preeclampsia. The renin-angiotensin system (RAS) has been implicated in the pathogenesis of preeclampsia (444). Pregnant female human angiotensinogen (*h*AGN) transgenic rat (TGR) overexpressing angiotensinogen mated with male hrenin (*h*REN) TGR overexpressing renin displays preeclamptic features including increased blood pressure, proteinuria and placenta alterations of oedema and necrosis (445).

In this study, placental tissues from pregnant WKY and SHRSP, the transgenic preeclampsia model and age-matched Sprague Dawley rats were kindly provided by Dr Delyth Graham and Dr Sheon Samji (Institute of Cardiovascular and Medical Sciences, University of Glasgow). Samples were prepared as described in section 2.4.1 for western blot.

2.5.5 Genotyping

WT and $TRPM7^{+/\Delta kinase}$ mice were genotyped using the REDExtract-N-Amp™ Tissue PCR Kit (Sigma-Aldrich, Dorset, UK). DNA was extracted from the murine ear notches according to manufacturer's instructions, and the concentration and quality of isolated DNA were analysed using the NanoDrop spectrophotometer. The sequence designed to detect the $TRPM7^{+/\Delta kinase}$ is (5' tgc gag gcc aga ggc cac ttg tgt agc 3'; and 5' tgc gag gcc aga ggc cac ttg tgt agc 3'), which specifically amplifies the neighbouring sequence regions of TRPM7 kinase domain. DNA sample isolated from WT mice is not amplified using

these primers, because the PCR conditions in our study do not allow amplification of such a large sequence (TRPM7 plus the neighbouring sequence). Thus, the PCR product is only amplified in TRPM7$^{+/\Delta kinase}$ mice. A control primer set (5' aaa tct tag gct ggt aga cag tg 3'; and 5' ctt atc tct caa gcc aat tta gga g 3') independent of TRPM7+/Δkinase was also used to exclude the possibility that the absence of PCR bands observed in WT mice was caused by poor DNA extraction and/or PCR performance. The PCR reaction was carried out using a PTC-225 Peltier thermal cycle under the following conditions: 94°C for 15 sec; and then 35 cycles of: 94°C for 10 sec (denaturation), 62°C for 30 sec (annealing) and 68°C for 2 min (extension); followed by 68°C for 5 min and 4°C until reaction termination. Subsequently, the amplified PCR products were separated by agarose gel electrophoresis and visualized using a ChemiDoc^{TM} XRS+ System (Bio-Rad Laboratories Ltd, Watford, UK) with Image Lab^{TM} software. Experiments in this part were kindly performed by Mrs Jackie Thomson and Mrs Wendy Beattie.

2.6 Small vessel wire myography

Wire myography is an *in vitro* technique developed by Mulvany and Halpern in 1977, that is widely used to study the functional properties of isolated small arterial vessels (446). Briefly, on a four-channel wire myograph, small vessels were carefully dissected from murine mesenteries and were mounted between two wires that went through the lumen. One wire is connected to a micrometre allowing control of vessel circumference, and the other wire is connected to a force transducer that measures the tension developed by the vessel (Figure 2.3). Followed equilibration and a normalisation procedure, during which the passive length-tension relationship is determined, stimuli were added directly to the bath and vessel tension was monitored.

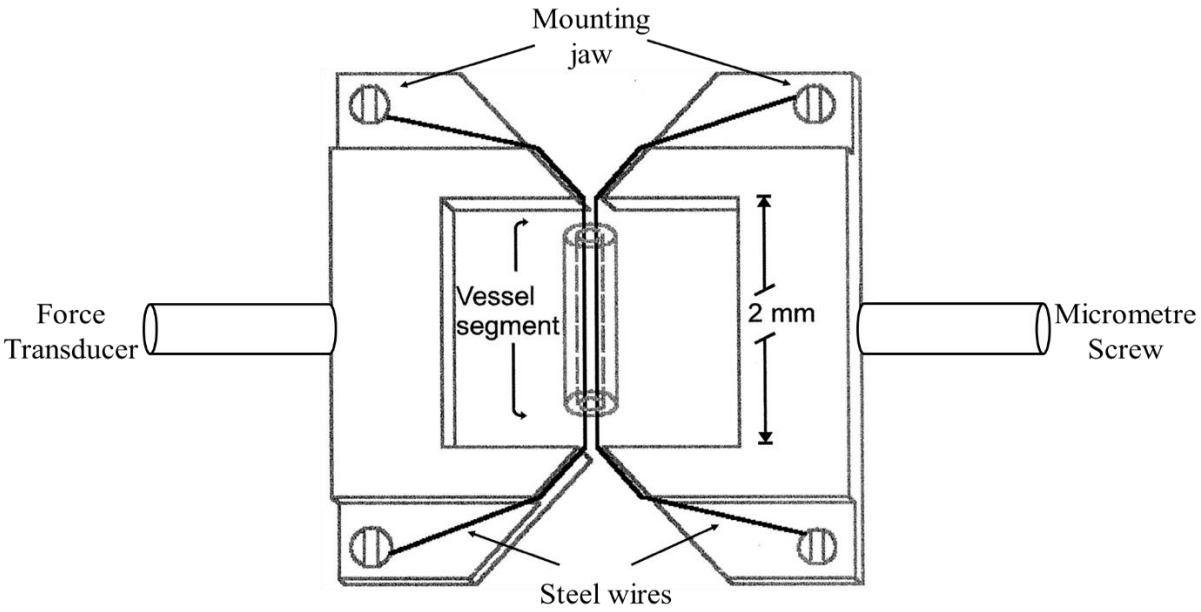

Figure 2.3 Schematic representation of wire myography system. Small vessel segment was mounted by two steel wires, with one connected to a micrometre allowing the control of vessel circumference, and the other connected to a force transducer that records changes in vascular tension. Modified from (447).

2.6.1 Dissection of mesenteric arteries and preparation for myography

Mice were sacrificed by CO_2 inhalation and intestine including the superior mesenteric artery was removed and collected in a 50 ml tube containing cold DPBS. Under a dissecting microscope, the first or second order mesenteric arteries were carefully dissected, cleaned of surrounding perivascular fat using a spring scissor without contacting the vessel wall. Dissected artery was then cut into several segments that were approximately 2 mm in length. Before mounting the vessel segments, the organ bath was washed 4 times with distilled water followed by 4 times with PSS (pH 7.4) leaving PSS in the bath after the final wash and bubbled with 95% O_2/5% CO_2. Subsequently, two wires, approximately 2 cm in length, were inserted through the lumen of the vessel segment minimizing contact with the artery wall. The mounting jaws and micrometre screw were adjusted properly, resulting in a final wire myography system with mounted vessel as shown in Figure 2.3.

Mounted vessels were washed with PSS and left for 30 min equilibration at resting tension before normalisation. To set vessels to standard initial conditions, all vessels were normalised using the normalisation module in LabChart software. Following a rest period of about 20 min after normalisation, to ensure that the technique of isolating and mounting vessels does not cause impairment in functional response, the viability of the vessels was

assessed based on the contractile response to high-potassium (62.5 mM KPSS)-induced depolarization. Vessels were challenged at least twice by KPSS with a 5-minutes interval to achieve a full wake-up. Vessels that failed to maintain a sustained and repeatable contraction were excluded for further experiments, and the maximum response to KPSS was used for further analysis. To check endothelial integrity, vessels were first pre-contracted by U46619 (3×10^{-8} M), followed by a single dose of acetylcholine (ACh, 1×10^{-6} M) to induce endothelium-dependent relaxation. A functional endothelium is defined as a response to attenuate 50% or more of the maximal contractile effect induced by U46619. Vessels without a functional endothelium were not used in this study.

2.6.2 Concentration response curves and data analysis

Subsequently, to investigate how growth factors and TRPM7 affect vascular activity, vessels were incubated with VEGF (50 ng/ml), EGF (50 ng/ml) or Naltriben (TRPM7 activator, 5×10^{-5} M) for 60 min and cumulative concentration-response curves (CCRC) in response to vasoconstrictor (U46619) or vasodilators (acetylcholine and SNP) were performed. It is worth mentioning that U46619 is a stable analogue of thromboxane A2 (TXA2) which stimulates potent vessel contraction through vascular smooth muscle TXA2 receptors (448), ACh induces vasodilation through promoting the release of nitric oxide (NO) from endothelial cells, which diffuses within the vessel wall and causes relaxation of smooth muscle cells (449), and sodium nitroprusside (SNP) is a well-known NO donor and it is able to induce endothelium-independent vascular relaxation (450). Briefly, to assess the contractile response to U46619, vessels were exposed to cumulatively increasing concentrations of U46619 (1×10^{-10} M, 3×10^{-10} M, 1×10^{-9} M, 3×10^{-9} M, 1×10^{-8} M, 3×10^{-8} M, 1×10^{-7} M, 3×10^{-7} M, 1×10^{-6} M, 3×10^{-6} M). The tension developed by vessels was recorded by LabChart software and the contractile response to U46619 was calculated and expressed as a percentage of the maximal response to KPSS measured earlier. Similarly, to assess endothelium-dependent and endothelium-independent relaxation in response to ACh and SNP respectively, vessels were first pre-contracted to 80% of its maximum level using U46619 (3×10^{-8} M). Following a plateau of the contractile response to U46619, vessels were exposed to cumulatively increasing concentration of ACh or SNP (1×10^{-9} M, 3×10^{-9} M, 1×10^{-8} M, 3×10^{-8} M, 1×10^{-7} M, 3×10^{-7} M, 1×10^{-6} M, 3×10^{-6} M, 1×10^{-5} M, 3×10^{-5} M). The tension level immediately achieved after pre-contraction with the addition of U46619 was set as 0% relaxation, and the relaxation in response to ACh or SNP was expressed as a percentage of relaxation relative to the presumed maximum relaxation (the distance between the stable tension recorded prior to the addition of

U46619 and the tense recorded at 0% relaxation). Dose-response curves were then converted and expressed as the percentage of contraction or relaxation to the log concentration of the stimulus (U46619, ACh, or SNP) using a log (stimulus) vs response model in the GraphPad Prism software, which were then analysed using the nonlinear regression model and extra sum-of-squares F test.

2.7 Histology

Aorta tissues from WT and TRPM7$^{+/\Delta kinase}$ mice were fixed in 10% buffered-formalin and embedded in paraffin. Histological sections (5 µm thickness) were stained with Haematoxylin and Eosin (HE). Briefly, aorta sections were deparaffinized and rehydrated in two 7-min changes of Histo-Clear (Fisher Scientific Ltd) and graded ethanol solutions (100%, 95% and 70%, 7 min each), followed by 7 min in distilled water. Next, nuclei were stained with Harris' modified haematoxylin (Cell Pathology Ltd) for 2 min and then rinsed in running tap water for 5 min followed by 30 seconds in 70% ethanol. Cytoplasmic structures were stained using Eosin Y solution (Sigma-Aldrich) for 2 min. Consequently, tissue sections were rinsed in graded ethanol solutios (95% for 30 seconds ×2; 100% for 1 min and 7 min separately), followed by two 5-min changes in Histo-Clear. Tissue sections were then mounted with glass coverslips using DPX non-aqueous mounting medium (Merck Millipore). Images were acquired using a light microscope (ZEISS) with 20× and 40× objective and were analysed using Image J software.

2.8 Statistical analysis

All quantitative data were analysed using commercially available GraphPad 5/6 software package (San Diego, USA). Results were expressed as mean ± standard error of the mean (SEM), with sample size (n) indicating independent experiments specified in each figure. For comparisons between two treatment groups, unpaired and two-tailed Student t-test was performed. When more than two groups were compared, one-way analysis of variance (ANOVA) was performed, followed by Dunnett's or Tukey's post-test. To compare vascular reactivity between groups, the maximal effect (top or bottom parameter) and the agonist concentration (Log agonist) that produced 50% of the maximal response (Log EC50) were calculated and compared using nonlinear regression (curve fit). To compare intracellular Ca^{2+} level between groups, results were converted and expressed as areas under curve (AUC), followed by comparison using Student t-test or ANOVA. Statistical significance was determined as a p value <0.05 and was indicated by special symbols in each figure.

Chapter Three

3 Investigating the Interaction Between EGFR and TRPM7 in VSMCs

3.1 Overview

Epidermal growth factor (EGF) belongs to the EGF family that binds to EGF receptor (EGFR) family (ErbB1, ErbB2, ErbB3, and ErbB4) (451). After binding, EGFR undergoes conformational changes and dimerization, which consequently leads to the autophosphorylation of tyrosine residues in the carboxyl terminal portion of the EGFR (452). Activated EGFR is able to trigger different downstream signalling pathways including PLCγ/PKC, RAS/RAF/MEK/MAPK, PI3K/AKT/mTOR, JAK/STAT and SFKs(46). The EGF-EGFR system exerts significant biological effects on many cellular processes including cell division, proliferation, migration, differentiation and ion homeostasis, and plays a pivotal role in embryo development, wound healing and tumour biology (261, 314, 453-455).

EGFR has been identified in vascular smooth muscle cells (VSMCs) and endothelial cells with indispensable role in maintaining organ and cellular homeostasis (314). The crucial importance of EGFR to the cardiovascular system is observed experimentally in waved-2 (wa-2) mice, a genetic model that exhibits reduced activity of EGFR tyrosine kinase and develops defects in the aortic valve, left ventricular hypertrophy and heart failure (313). Additionally, these mice exhibit reduced vasoconstriction induced by aldosterone and salt with no effects on vascular remodelling (323). Inhibition of EGFR with erlotinib, a widely used anti-cancer drug, was shown to attenuate vascular hypertrophy and perivascular fibrosis induced by Angiotensin II (Ang II) infusion in C57BL/6 mice through mechanisms involving metalloproteinase ADAM17 and endoplasmic reticulum (ER) stress (456). Of importance, vasoactive agents such as aldosterone, endothelin-1 (ET-1) and Ang II have been shown to transactivate EGFR and consequently induce VSMCs hypertrophy, proliferation and migration through mechanisms involving EGFR downstream signalling pathways such as ERK1/2, p38 MAPK and Src kinase (457-460).

The relevance of TRPM7 in the cardiovascular system has been demonstrated by an increasing number of studies. Early cardiac TRPM7-deletion results in congestive heart failure and death at embryonic day 11.5 due to hypo-proliferation of the compact myocardium (138). TRPM7 contributes to cardiac rhythm, with evidence showing that TRPM7 is required to maintain cardiac automaticity in sinoatrial node (SAN) and regulates SAN fibrosis induced by Ang II by mechanisms dependent on Smad signalling (158, 159). In previous studies, we identified TRPM7 as a key regulator of Mg^{2+} homeostasis and

growth in VSMCs (2, 78). Using TRPM7 kinase-deficient mice with malfunction of the channel ($TRPM7^{+/\Delta kinase}$), we found that TRPM7 exerts protective effects against Ang II-induced hypertension, endothelial dysfunction and cardiac hypertrophy. $TRPM7^{+/\Delta kinase}$ mice also exhibit pro-inflammatory and pro-fibrotic cardiovascular phenotype (77, 461). The implication of TRPM7 in regulating blood pressure was also highlighted in a recent study by Polotsky and colleagues, showing that leptin induces hypertension through TRPM7 in carotid body (462).

EGF-EGFR pathway has been shown to regulate TRPM7 expression and channel activity in different cancer cell lines by mechanisms involving phosphatidylinositol 4,5-bisphosphate (PIP_2) hydrolysis and mediate cell migration (135, 410). EGFR inhibitors, such as cetuximab and panitumumab, are widely used in cancer treatment, however, patients develop severe hypomagnesemia as a side effect (3). Bindels and colleagues demonstrated that EGF regulates activity and translocation of TRPM6, the TRPM7 homologue, in kidney epithelial cells through mediating EGFR, SFKs and MAP kinase (259, 411).

TRPM7 is ubiquitously expressed and plays important role in vascular cells, however, whether the interaction between TRPM7 and the EGFR signalling exists in the vasculature has not been investigated yet. Here, we hypothesized that in the vasculature the EGF-EGFR ligand-receptor system interacts with TRPM7, and this process regulates TRPM7 activity and influences vascular homeostasis, VSMCs function and cellular signalling.

3.2 Objective and aims

Objective

The overall objective of the *in-vitro* based studies presented in chapter 3 was to explore the crosstalk between the EGFR signalling and TRPM7 in the vasculature, mainly in VSMCs, and how this interaction affects cellular signalling pathways, VSMCs function and vascular homeostasis.

Specific aims

1. *To study whether EGF induces VSMC signalling and $Ca^{2+}$and Mg^{2+} mobilisation by mechanisms dependent on TRPM7 activation.*

TRPM7 protein expression and phosphorylation were used to assess TRPM7 activity. Effects of pharmacological inhibition of TRPM7 on EGF-induced ion homeostasis were studied.

2. To study whether TRPM7 affects the intracellular signalling activation induced by EGFR in VSMCs.

EGFR and c-Src kinase phosphorylation were assessed in vessels from WT, TRPM7 kinase-deficient and TRPM7 kinase-dead mice. Effects of pharmacological inhibition of TRPM7 on the ERK1/2 activation induced by EGF were assessed. Physical interaction between EGFR and TRPM7 in VSMCs was also investigated.

3. To explore the importance of EGFR-TRPM7-ERK1/2 pathway in VSMC function and vessel homeostasis.

Effects of pharmacological inhibition of EGFR, TRPM7 and ERK1/2 on EGF-induced VSMC migration and proliferation were assessed. Additionally, we investigated the effects of genetic deficiency of TRPM7 on vessel structure and expression of the proliferation marker PCNA

For this study we used VSMCs from rats, mice and human. We also investigated the cross-talk of EGFR and TRPM7 in the following mice models: i) SV129 mice treated with the EGFR inhibitor gefitinib (463); ii) TRPM7 kinase-deficient mice with malfunction of the channel ($TRPM7^{+/\Delta kinase}$) (461) and iii) the TRPM7 "kinase-dead" mice ($TRPM7^{R/R}$) carrying a global K1646R point mutation (106, 157).

3.3 Results

3.3.1 TRPM7 is expressed in VSMCs and contributes to Ca^{2+} homeostasis

TRPM7 is a ubiquitously expressed channel and mediates Ca^{2+} and Mg^{2+} influx in different cell types (46). Firstly, we confirmed TRPM7 protein expression in VSMCs derived from humans and rats (Figure 3.1A). In previous study, we demonstrated that TRPM7 is able to mediate Mg^{2+} influx in VSMCs (2). Here we showed that TRPM7 is also involved in Ca^{2+} homeostasis in VSMCs. Naltriben, is a TRPM7 channel activator that affects channel gating rather than permeation characteristics of the TRPM7 pore through mechanisms involving PIP_2 (430, 464). Naltriben was able to induce intracellular Ca^{2+} elevation in VSMCs, effect that was attenuated by TRPM7 inhibitors NS8593 and 2-APB (Figure 3.1B and C). To test the specificity and efficacy of the Ca^{2+} indicator Cal-520 acetoxymethyl ester (Cal-520AM, Abcam) used in this study, VSMCs labelled by Cal-520 were treated with ionomycin, a calcium ionophore that facilitates Ca^{2+} transport across cell membrane (465), and Ang II that rapidly induces intracellular Ca^{2+} elevation in VSMCs (466). Ang II and ionomycin induced rapid enhancement of fluorescent signals that were captured by live cell microscope and the fluorescent signals in VSMCs were also sensitive to changes of extracellular Ca^{2+} concentrations (data not shown). Thus, our data supported that the usage of Cal-520 to observe Ca^{2+} mobilisation in VSMCs is acceptable.

3.3.2 Optimizing the protocol to detect Mg^{2+} in VSMCs

To visualize Mg^{2+} mobilisation in VSMCs, we first tried the selective fluorescent probe Magnesium Green. hVSMCs stained with Magnesium Green (5μM and 20 μM) were imaged by live cell microscope. Addition of different concentrations of $MgCl_2$ did not induce any changes of fluorescent Mg^{2+}-probe signal, as shown in Figure 3.1D. The dual wavelength intracellular magnesium indicator Mag-Fura-2 was also tested in hVSMCs, however, we did not detect fluorescent signals upon stimulation of $MgCl_2$ at different concentrations (Figure 3.1D). Finally, we decided to apply flow cytometry to investigate Mg^{2+} status in our study. As shown in Figure 3.1E, hVSMCs stained with Magnesium Green were incubated with $MgCl_2$ of different concentrations for 5 min and using flow cytometry we were able to observe changes of intracellular Mg^{2+} levels.

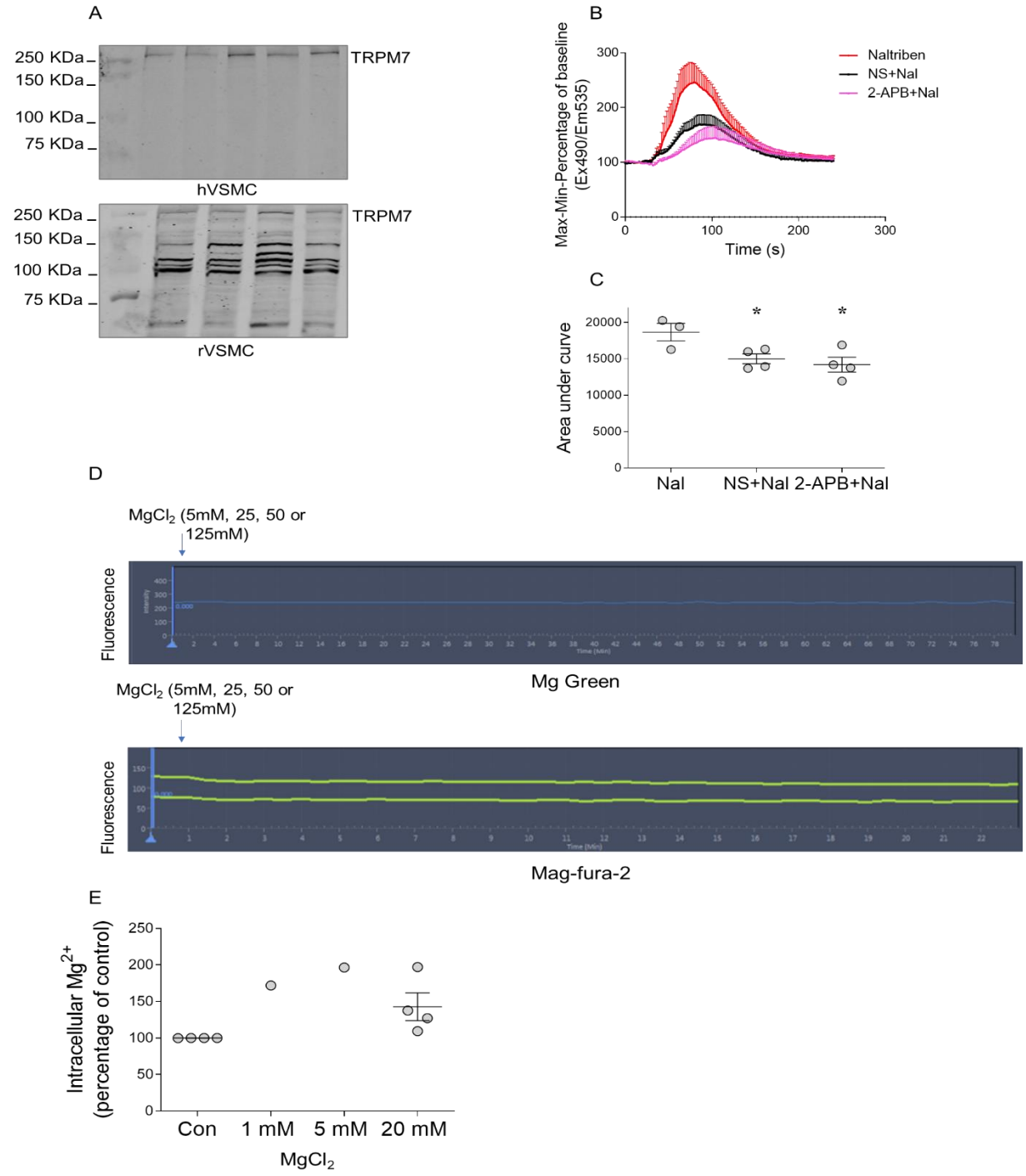

Figure 3.1 TRPM7 has a role in mediating Ca^{2+} and Mg^{2+} homeostasis in VSMCs. TRPM7 protein expression in hVSMC (upper panel) and rVSMC (lower panel) were examined by immunoblotting (**A**). Intracellular Ca^{2+} levels induced by naltriben (50 μM) were measured in the presence and absence of TRPM7 inhibitors NS8593 (NS, 40 μM) and 2-APB (30 μM) in hVSMCs. Data are expressed in Fluorescent Cal-520AM-Ca^{2+} signals (percentage of baseline)-time curve and in Area under curve (**B-C**). Fluorescent Mg^{2+} probes Mg Green and Mag-Fura-2 were tested in hVMSCs by live cell microscope (**D**). Detection of intracellular Mg^{2+} levels using Mg Green by flow cytometry (**E**). **P*<0.05 compared to naltriben.

3.3.3 EGF regulates Ca^{2+} and Mg^{2+} homeostasis through TRPM7 in VSMCs

EGFR expression was confirmed by immunoblotting in VSMCs derived from rats and humans (Figure 3.2A). Stimulation of rVSMCs with EGF induced Ca^{2+} mobilisation and significantly increased intracellular Ca^{2+} levels ($[Ca^{2+}]_i$), effects that were attenuated by EGFR inhibitor gefitinib and the non-specific TPRM7 inhibitor 2-APB, but not NS8593, a well-known potent and relatively specific inhibitor for TRPM7 (Figure3.2B and C) (157, 430). In addition, EGF increased intracellular free Mg^{2+} concentration ($[Mg^{2+}]_i$), effect that was attenuated by gefitinib, NS8593 and 2-APB (Figure 3.2D). NS8593 was also reported to block Ca^{2+}-activated channels (SK channels) (406), to clarify whether the inhibitory effect of NS8593 is via TRPM7, apamin, an SK channel inhibitor, was added as a control for NS8593. As shown in Figure 3.2D, apamin did not attenuate effects of EGF on $[Mg^{2+}]_i$, further supporting the importance of TRPM7 to the Mg^{2+} influx induced by EGF.

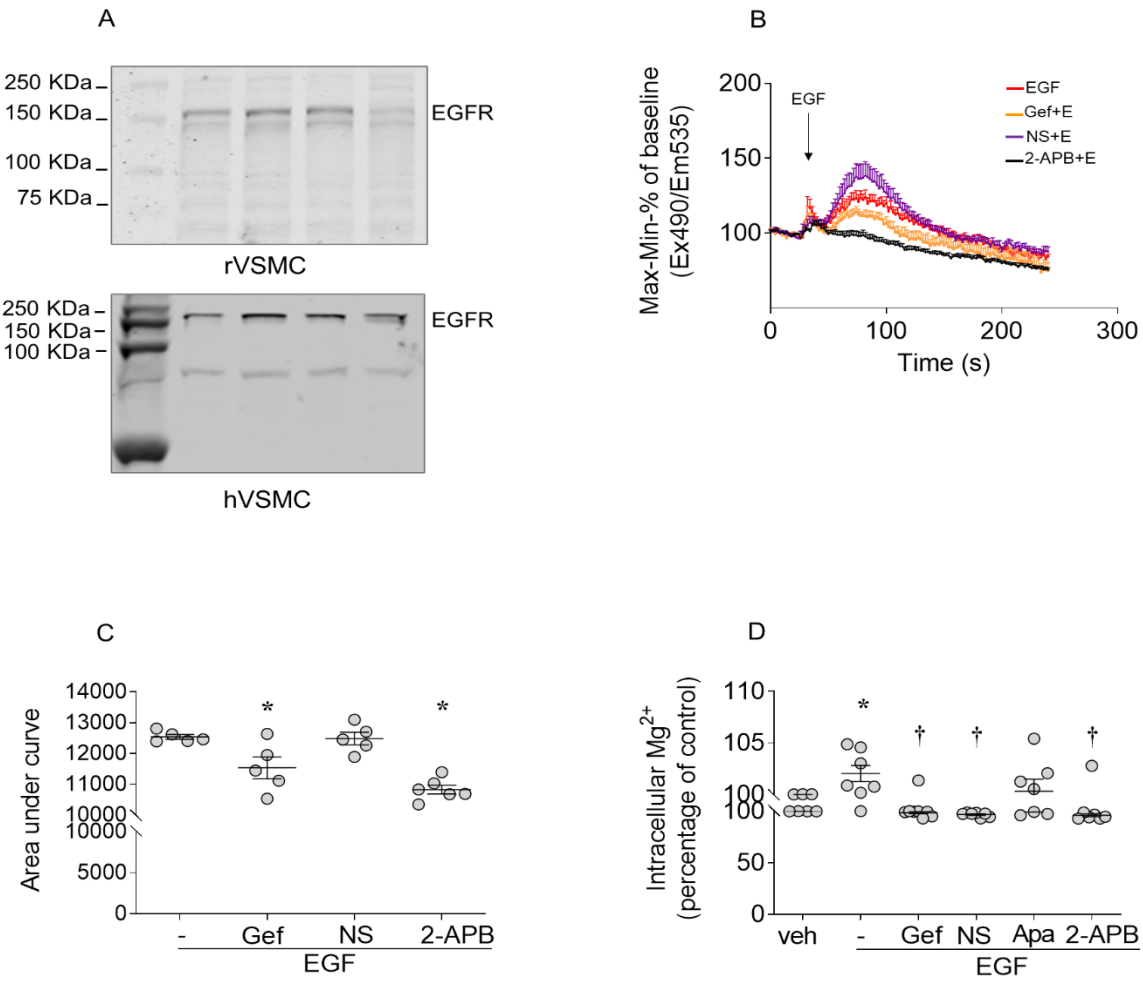

Figure 3.2 EGF regulates Ca^{2+} and Mg^{2+} homeostasis through EGFR and TRPM7. EGFR expression in rVSMCs (upper panel) and hVSMCs (lower panel) was examined by immunoblotting (**A**). Intracellular Ca^{2+} levels induced by EGF (50 ng/ml) were measured in the presence and absence of gefitinib (Gef, 1 μM), NS8593 (NS, 40 μM) and 2-APB (30 μM) in rVSMCs. Data are expressed in Fluorescent Cal-520AM-Ca^{2+} signals (percentage of baseline)-time curve and in Area under curve (**B-C**). Intracellular free Mg^{2+} concentration ($[Mg^{2+}]i$) after EGF (50 ng/ml) treatment (5 min) in the presence and absence of gefitinib (1 μM), NS (40 μM) , Apamin (Apa, 1 μM) and 2-APB (30 μM) (**D**). **P*<0.05 compared to vehicle (veh) and † *P*<0.05 compared to EGF treated cells.

3.3.4 EGF regulates TPRM7 activation and expression in VSMCs through EGFR by c-Src-dependent mechanisms

Next, we investigated whether EGF exerts regulatory effects on TRPM7. Thus, TRPM7 phosphorylation and total protein expression were investigated after EGF stimulation for 5 min and 24 h respectively. As shown in Figure 3.3A and B, EGF treatment significantly increased TRPM7 phosphorylation at Ser1511 (21%) and total expression (47%) in rVSMCs, effects that were abolished by gefitinib (21% and 70% respectively). SFKs, including Src, Fyn and Yes, are important downstream signalling pathways of EGFR (46), and EGF is known to stimulate TRPM6 activity though Src kinase (411). To determine whether c-Src is necessary for EGFR-mediated regulation of TRPM7, rVSMCs were preincubated with PP2, a selectively inhibitor c-Src (467). In the presence of PP2, EGF failed to stimulate TRPM7 phosphorylation (Figure 3.3A) and protein expression (Figure 3.3B).

Additionally, we investigated whether EGF regulates other Mg^{2+} transporters, including TRPM6, magnesium transporter subtype 1 (MagT1), an important transporter involved in Mg^{2+} influx, and the 41st family of solute carrier member 1 (SLC41A1) which critically contributes to Mg^{2+} efflux (19). Long-term (24 h) stimulation with EGF did not change expression levels of TRPM6 (Figure 3.3C) and SLC41A1 (Figure 3.3D). However, it was found that EGF significantly increased expression of MagT1 (49%), effects there attenuated by inhibitors of EGFR (37%) and c-Src (46%) (Figure 3.3E).

The importance of EGFR on TRPM7 expression was also investigated in wild type SV129 mice treated with vehicle or gefitinib (100 mg/Kg/day) for two weeks. TRPM7 expression in aorta was assessed by immunoblotting. Aortas from animals treated with gefitinib exhibited reduced TRPM7 expression (73%) compared to the vehicle group (Figure 3.3F).

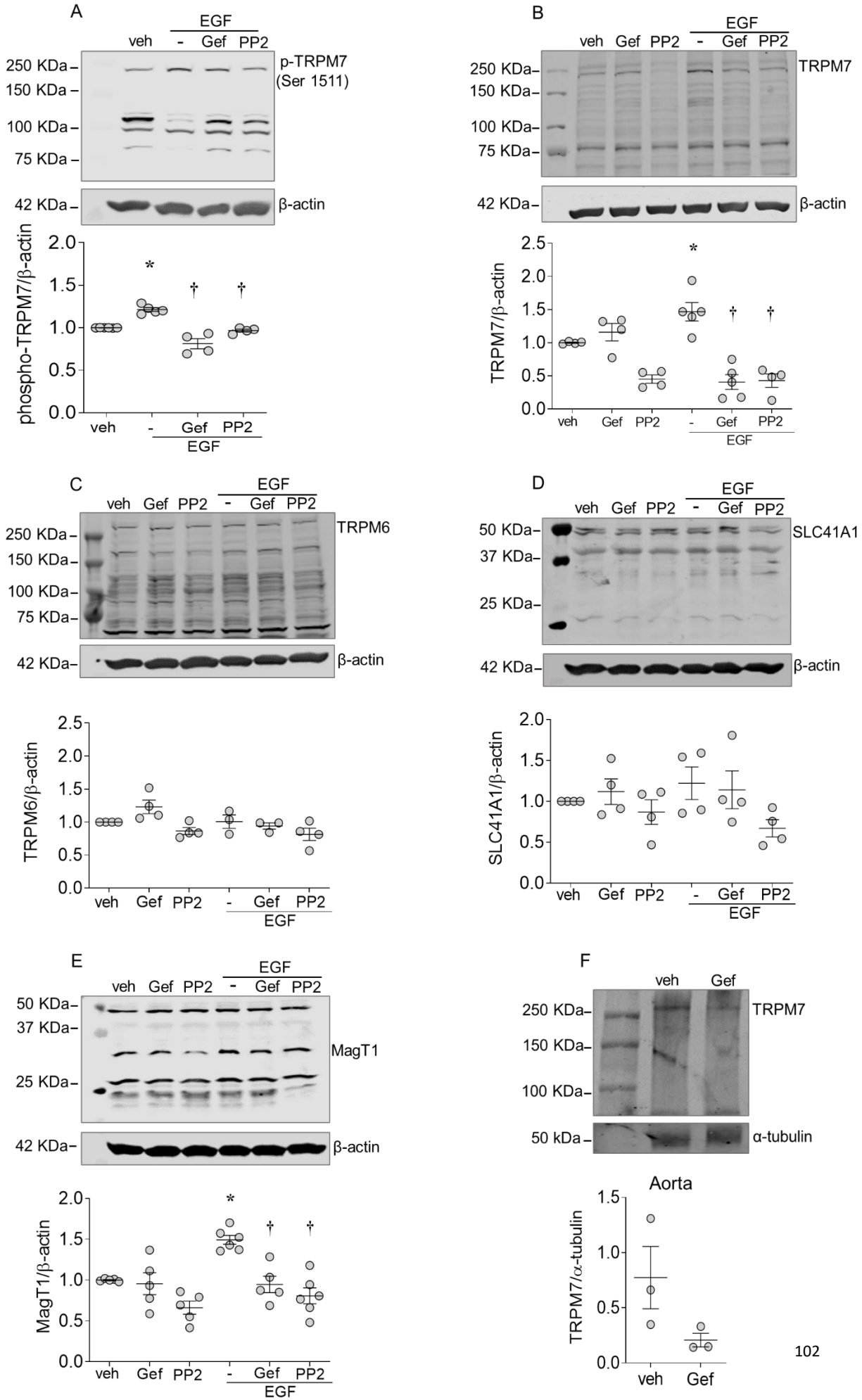
A
EGF
veh - Gef PP2
250 KDa
150 KDa
100 KDa
75 KDa
p-TRPM7
(Ser 1511)
42 KDa
β-actin
phospho-TRPM7/β-actin
2.0
1.5
1.0
0.5
0.0
*
†
†
veh - Gef PP2
EGF
B
EGF
veh Gef PP2 - Gef PP2
250 KDa
150 KDa
100 KDa
75 KDa
TRPM7
42 KDa
β-actin
TRPM7/β-actin
2.5
2.0
1.5
1.0
0.5
0.0
*
†
†
veh Gef PP2 - Gef PP2
EGF
C
EGF
veh Gef PP2 - Gef PP2
250 KDa
150 KDa
100 KDa
75 KDa
TRPM6
42 KDa
β-actin
TRPM6/β-actin
2.5
2.0
1.5
1.0
0.5
0.0
veh Gef PP2 - Gef PP2
EGF
D
EGF
veh Gef PP2 - Gef PP2
50 KDa
37 KDa
25 KDa
SLC41A1
42 KDa
β-actin
SLC41A1/β-actin
2.0
1.5
1.0
0.5
0.0
veh Gef PP2 - Gef PP2
EGF
E
EGF
veh Gef PP2 - Gef PP2
50 KDa
37 KDa
25 KDa
MagT1
42 KDa
β-actin
MagT1/β-actin
2.0
1.5
1.0
0.5
0.0
*
†
†
veh Gef PP2 - Gef PP2
EGF
F
veh Gef
250 KDa
150 KDa
100 KDa
TRPM7
50 kDa
α-tubulin
Aorta
TRPM7/α-tubulin
1.5
1.0
0.5
0.0
veh Gef

Figure 3.3 Effects of EGF on magnesium transporters in rVSMCs. rVSMCs were stimulated with EGF (50 ng/ml) for 5 min and 24 in the presence and absence of 30 min pretreatment of gefitinib (Gef, 1 μM) or PP2 (10 μM). Expression of phosphorylated TRPM7 (Ser1511) was accessed by immunoglotting after 5 min EGF stimulation (**A**). Expression of TRPM7 (**B**), TRPM6 (**C**), SLC41A1 (**D)** and MagT1 (**E**) was assessed after 24 h EGF stimulation. TRPM7 expression in aorta (**F**) from mice treated with gefitinib (Gef, 100 mg/Kg/day) or vehicle for two weeks. **P*<0.05 compared to vehicle (veh) and † *P*<0.05 compared to EGF.

3.3.5 Expression and activation of TRPM7 substrates

To explore whether EGF regulates the expression of the TRPM7-kinase substrates annexin-1 and calpain-2, rVSMCs were treated with EGF (50 ng/ml) for 24 h in the presence and absence of gefitinib and PP2. As shown in Figure 3.4, long-term EGF treatment did not affect expression of annexin-1 (A) or calpain-2 (B). Annexin-1 and calpain-2 are well known downstream targets of TRPM7, and upon activation translocate to the plasma membrane (468). Thus, rVSMCs were treated with EGF for 1 min, 5 min, 30 min and 60 min. Cell lysates were separated into membrane and cytosol rich fractions by ultracentrifugation. Protein expression in membrane fractions was normalised by membrane specific protein Na/K-ATPase. As shown in Figure 3.4, no statistical significance was found in the expression of annexin-1 (C) or calpain-2 (D) in cell membrane compared to unstimulated control group.

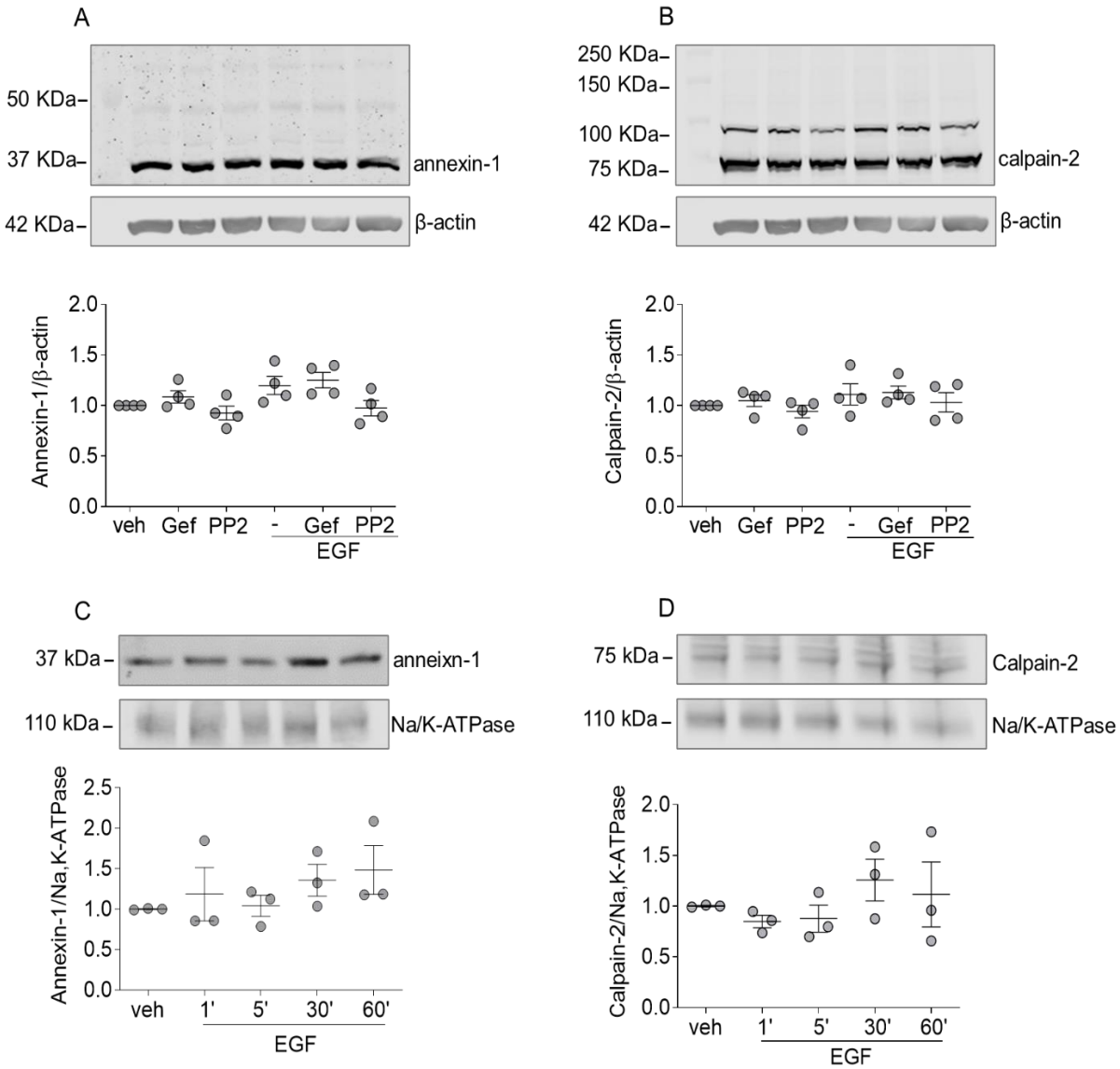

Figure 3.4 Expression and activation of TRPM7 substrates after EGF treatment. rVSMCs were pre-treated with gefitinib (Gef, 1 µM) or PP2 (10 µM) for 30 min and stimulated with EGF (50 ng/ml) for 24 h. The expression of annexin-1 **(A)** and calpain-2 (**B**) was investigated by immunoblotting. Protein expression was normalised by the housekeeping protein β-actin. rVSMCs were stimulated with EGF (50 ng/mL) for 1, 5, 30and 60 min. Membrane fractions were obtained by ultracentrifugation and investigated for the presence of annexin-1 (**C**) and calpain-2 (**D**). Na/K ATPase was used as housekeeping protein for the membrane fractions.

3.3.6 Expression of EGFR and c-Src activity is dependent on TRPM7-kinase

Using an specific antibody to amino acids 1817-1863 of the kinase domain (cat.#: MA5-27620; Invitrogen), the kinase deficiency was confirmed in cells from $TRPM7^{+/\Delta kinase}$ mice by the reduction (80%) in immunoblotting signals (Figure 3.5A). At basal level, mVSMCs from $TRPM7^{+/\Delta kinase}$ mice exhibit reduced EGFR expression (68%) (Figure 3.5B) and c-Src phosphorylation (40%) at the activation motif Tyr416 (Figure 3.5C). $TRPM7^{R/R}$ mice that express a global "kinase-dead" K1646R point mutation and consequent deficiency of the catalytic activity was used to assess the role of the TRPM7-kinase (469). Relative to wild type C57BL/6 mice, aorta tissue from $TRPM7^{R/R}$ mice exhibited significantly reduced phosphorylation of EGFR (66%) on tyrosine 845 (Y845), a well-known Src-dependent phosphorylation site (Figure 3.5D) (470). Taken together, our experiments suggest that TRPM7 interacts with EGFR and its downstream c-Src kinase, which is required for VSMCs to maintain EGFR and c-Src activity, and this process is dependent on a functional TRPM7-kinase.

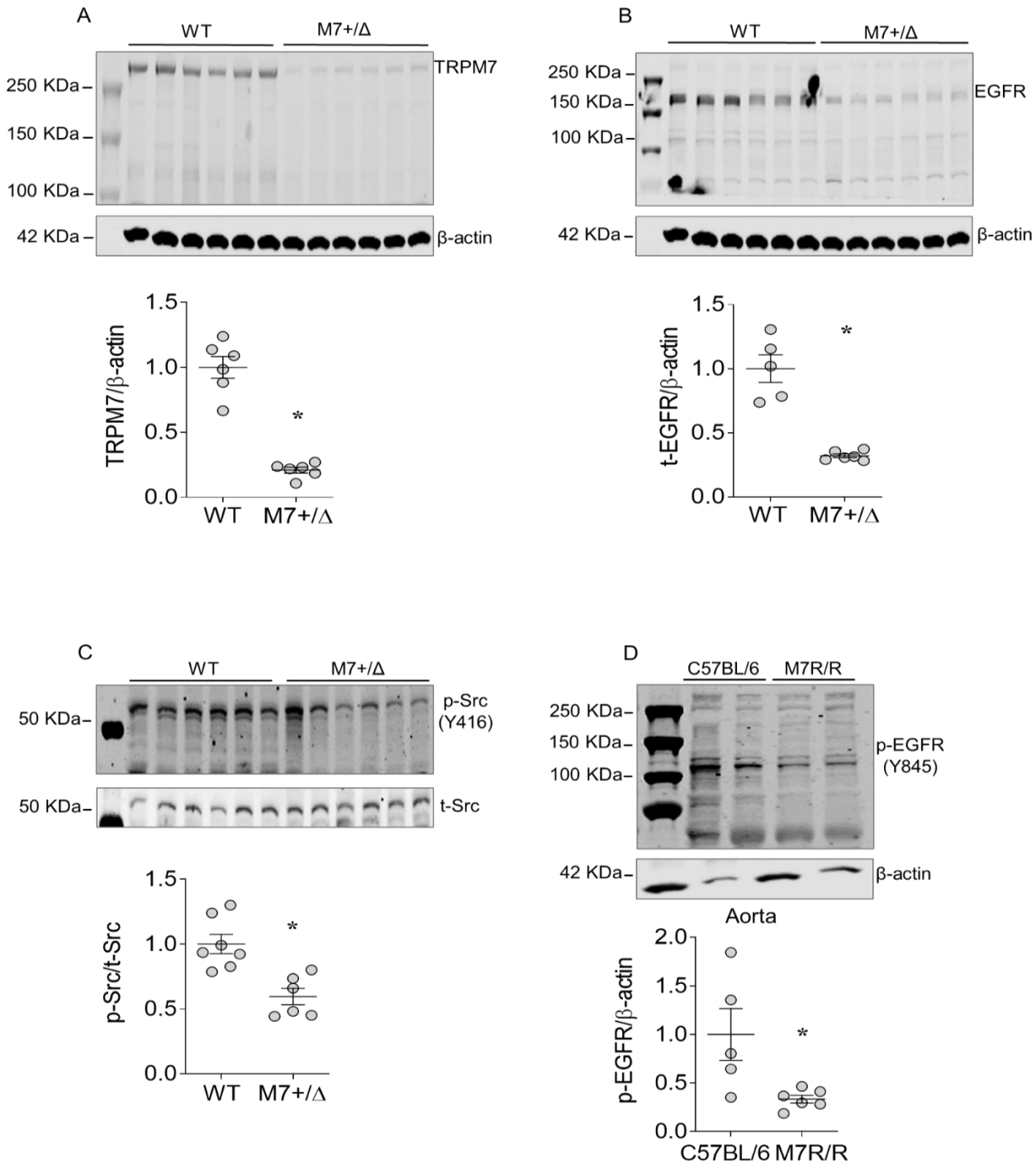

Figure 3.5 TRPM7 is required for EGFR and c-Src activity in VSMCs. Protein expression and phosphorylation levels in VSMCs and aorta tissue derived from mouse models were assessed by immunoblotting, with representative images (upper panels) and quantification (lower panels). mVSMCs from WT and TRPM7 kinase-deficient mice ($TRPM7^{+/\Delta kinase}$, M7+/Δ) were investigated for the expression of TRPM7 (**A**), EGFR (**B**) and phosphorylated c-Src (p-Src) (**C**) at basal level. Aortas from TRPM7 kinase-dead ($TRPM7^{R/R}$, M7R/R) and wild type C57BL/6 mice were investigated for EGFR phosphorylation at tyrosine 845 (Y845) (C57BL/6 n=5, M7R/R n=6) (**D**). **P*<0.05 compared to WT mice.

3.3.7 EGFR directly interacts with TRPM7 in VSMCs in a c-Src-dependent manner

Next we further investigated the interaction between TRPM7 and EGFR, given our previous observations that suggest a crosstalk between these proteins. Firstly, co-immunoprecipitation experiments were performed in rVSMCs (Figure 3.6A). EGFR was detected when TRPM7 was immunoprecipitated with a TRPM7 specific antibody. The presence of TRPM7 was also detected when EGFR was immunoprecipitated using an EGFR specific antibody. The colocalization of EGFR and TRPM7 was also confirmed by immunofluorescence using confocal microscopy (Figure 3.6B). Finally, we performed proximity ligation assay (PLA) using antibodies against EGFR and TRPM7 in rVSMCs, which is a sensitive technique to detect and visualise protein-protein interactions (471). At basal level, there was significant PLA signals mainly distributed at cell membrane in rVSMCs, suggesting a direct interaction between EGFR and TRPM7 at cell surface (Figure 3.6C). Because EGF was shown to enhance TRPM7 expression and phosphorylation, we then questioned whether EGF regulates the interaction between EGFR and TRPM7. As shown in Figure 3.6C and D, 5 min EGF treatment increased 51% PLA signals in rVSMCs, and the effects were attenuated by gefitinib (34%) and PP2 (25%), suggesting that c-Src mediated the association between EGFR and TRPM7.

3.3.8 Intracellular trafficking of TRPM7 in HEK293 cells

EGF has been shown to promote translocation of TRPM6 from cell cytosol to membrane (411). It was also observed that TRPM7 translocates from the cytosol to the plasma membrane in VSMCs (141) and thus we tried to investigate whether the enhanced EGFR-TRPM7 interaction is accompanied by TRPM7 translocation upon EGF stimulation. HEK-293T cells (kindly provided by Dr. Will Fuller and Xing Gao) overexpressing yellow fluorescent protein (YFP)-tagged TRPM7 (YFP-TRPM7) were stimulated with EGF for 15 min. The fluorescent signal was captured by live cell microscopy. As shown in Figure 3.7A, there were no significant TRPM7 movements towards cell membrane after EGF stimulation, suggesting that the regulation of EGFR-TRPM7 interaction by EGF may not depend on TRPM7 trafficking.

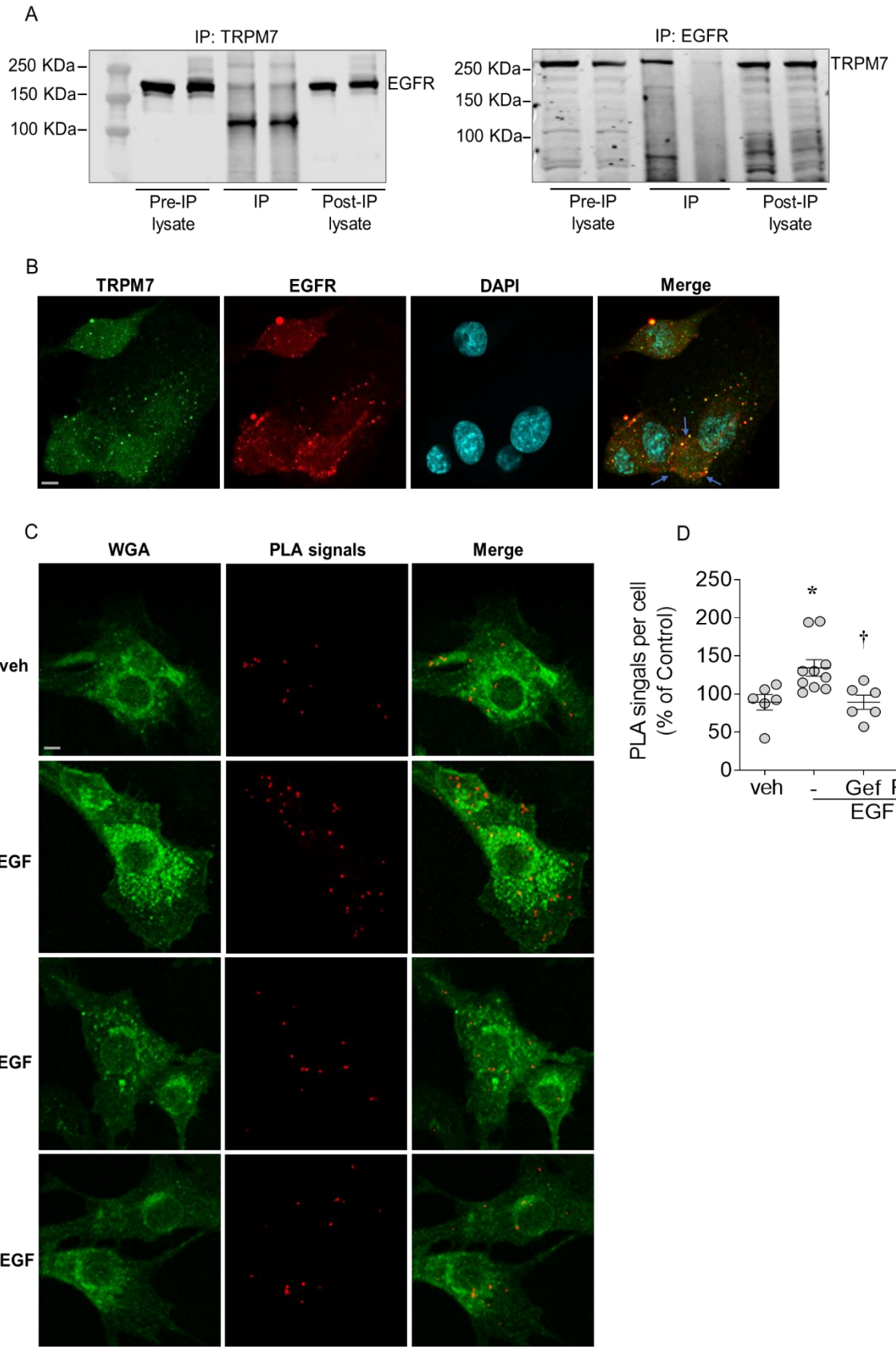
A
IP: TRPM7
250 KDa–
150 KDa–
100 KDa–
EGFR
Pre-IP lysate
IP
Post-IP lysate
IP: EGFR
250 KDa–
150 KDa–
100 KDa–
TRPM7
Pre-IP lysate
IP
Post-IP lysate
B
TRPM7
EGFR
DAPI
Merge
C
WGA
PLA signals
Merge
veh
EGF
Gef+EGF
PP2+EGF
D
PLA singals per cell (% of Control)
250
200
150
100
50
0
*
†
†
veh
-
Gef
PP2
EGF

Figure 3.6 Direct interaction between EGFR and TRPM7 in VSMCs. EGFR was detected when TRPM7 was immunoprecipitated from rVSMCs using anti-TRPM7 antibody (left panel) and TRPM7 was detected when EGFR was immunoprecipitated from rVSMCs using anti-EGFR antibody (right panel) (**A**). Representative confocal microscopy images of rVSMCs co-immunostained for TRPM7 (Alexa 488, green) and EGFR (Alexa 555, red). Nuclei were stained with DAPI (**B**). Proximity ligation assay was used to visualize and quantify TRPM7-EGFR interaction in rVSMCs stimulated with vehicle (Veh), and EGF (50 ng/mL) for 5 min in the presence and absence of gefitinib (1 μM) and PP2 (10 μM). Wheat germ agglutinin (WGA, Alexa 488, green) was used to stain cell membranes. Red dots are identified as PLA positive signals. Orange dots in the merge figure identify the colocalization in the cell membrane (**C** and **D**). Scale bar=5 μm. Arrows indicate colocalization of EGFR and TRPM7. **P*<0.05 compared to vehicle (veh) and † P<0.05 compared to EGF treated cells.

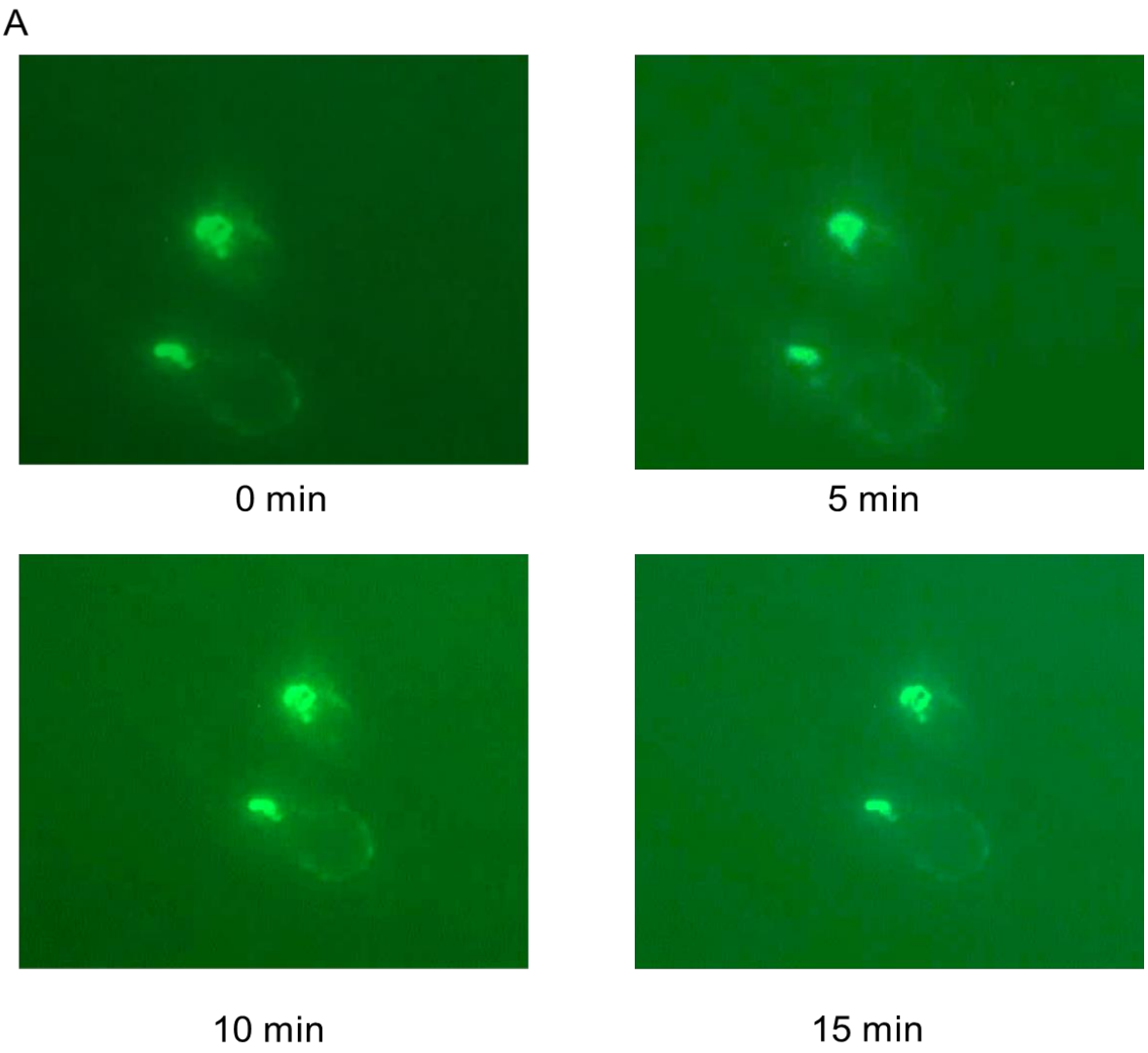

Figure 3.7 Observation of intracellular TRPM7 movements upon EGF stimulation. HEK cells overexpressing YFP-TRPM7 was stimulated with EGF (50 ng/ml) for 15 min. Cellular location of fluorescent TRPM7 was recorded by an inverted epifluorescence microscope (Axio Observer Z1 Live-Cell imaging system, ZEISS) at excitatory wavelength of 490 nm and emission of 535 nm.

3.3.9 The effects of TRPM7 on ERK1/2 activation induced by EGF

Growth factors such as EGF and VEGF through binding to their receptors activate a wide range of downstream signalling pathways, including the MAP kinase pathway (46). MAP kinase ERK1/2 is now known to play an important role in the vasculature (223, 472). In rVSMCs EGF stimulation for 5 min increased ERK1/2 phosphorylation (2-fold), effects that were reduced by pre-treatment with inhibitors of EGFR (gefitinib, 55%), c-Src (PP2, 56%) and TRPM7 (NS8593 and 2-APB, 46% and 57% respectively) (Figure 3.8A). Next, the phosphorylation of ERK1/2 was investigated in mVSMCs derived from WT and $TRPM7^{+/\Delta kinase}$ mice. At basal level, there was remarkably reduced ERK1/2 phosphorylation (90%) in mVSMCs from $TRPM7^{+/\Delta kinase}$ mice relative to WT (Figure 3.8B). While EGF still triggered ERK1/2 phosphorylation in $TRPM7^{+/\Delta kinase}$ mice (EGF 1.54±0.97 vs veh 0.095±0.037), the extent was significantly reduced compared to WT (M7+/Δ 1.54 ±0.97 vs WT 5.09 ±0.26) (Figure 3.8B).

As TRPM7 is a chanzyme comprising an α-kinase domain linked to its channel segment, and the kinase domain has been shown to influence TRPM7 channel activity and mediate cellular functions (107, 108). Thus, we questioned whether TRPM7 kinase catalytic activity is involved in the regulation of ERK1/2 activity. ERK1/2 phosphorylation was examined in aortic tissue from C57BL/6 and the "kinase-dead" $TRPM7^{R/R}$ mice. There was significantly reduced ERK1/2 phosphorylation (37%) in aorta isolated from $TRPM7^{R/R}$ mice, confirming that the effect is kinase dependent (Figure 3.8C).

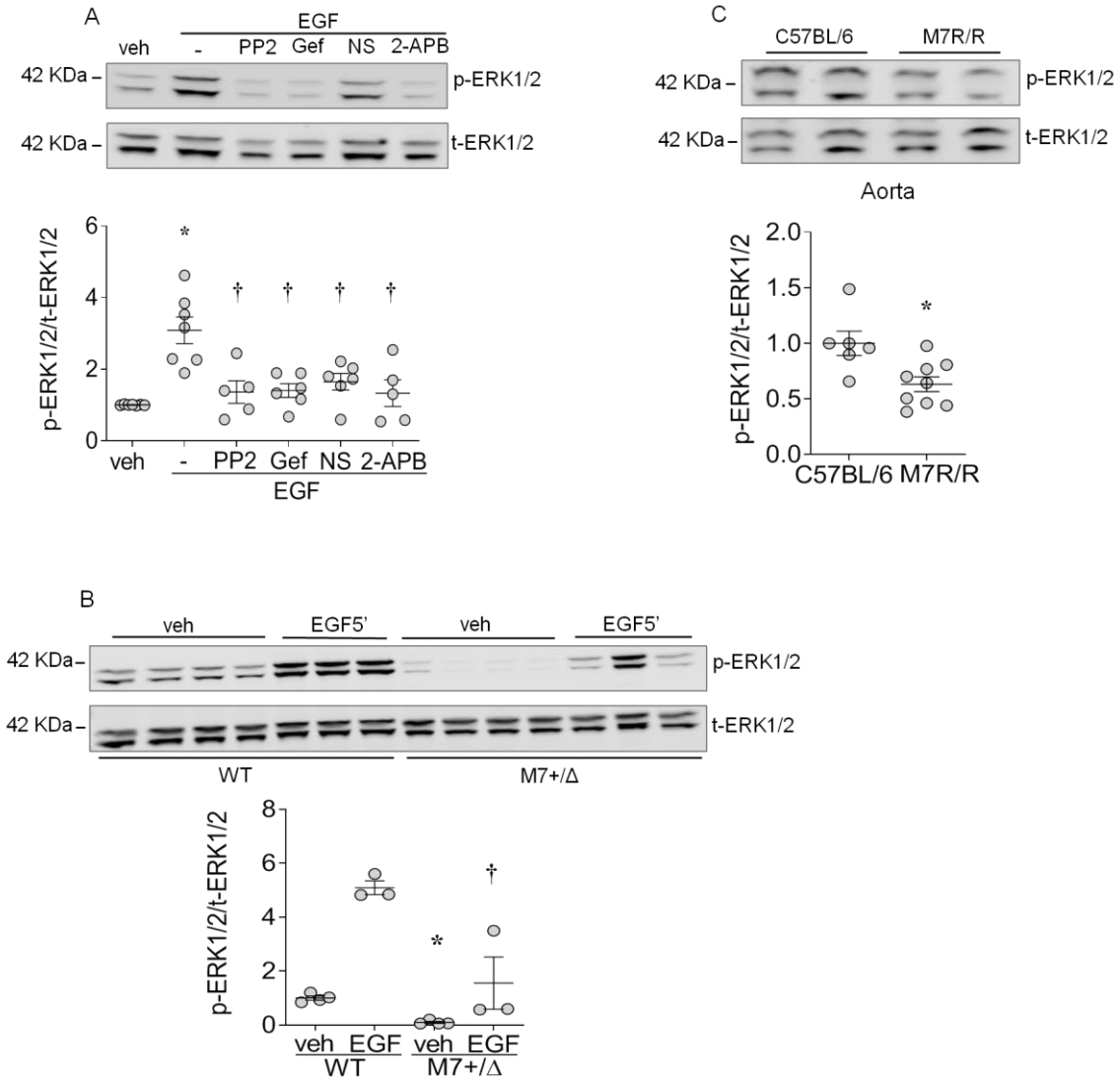

Figure 3.8 EGF induces ERK1/2 phosphorylation through TRPM7 in VSMCs. rVSMC were pre-treated with inhibitors of EGFR (gefitinib, Gef, 1 μM), c-Src (PP2, 10 μM), TRPM7 (NS8593, 40 μM), non-selective TRPM7 (2APB, 30 μM) for 30 min, followed by EGF (50 ng/ml) stimulation for 5 min (**A**). **P*<0.05 compared to veh and † *P*<0.05 compared to EGF. mVSMCs derived from WT and TRPM7$^{+/\Delta kinase}$ (M7+/Δ) mice were stimulated with vehicle or EGF (50 ng/mL) for 5 min (**B**). **P*<0.05 compared to WT veh and † *P*<0.05 compared to WT EGF. Aortic tissues isolated from TRPM7$^{R/R}$ (M7R/R) and wild type C57BL/6 mice (C57BL/6 n=6, M7R/R n=9) (**C**). **P*<0.05 compared to wild type. ERK1/2 phosphorylation was assessed by immunoblotting and normalised by total protein expression.

3.3.10 EGF enhances VSMCs proliferation and migration through TRPM7 and ERK1/2

VSMCs proliferation and migration are key processes in VSMCs phenotypic modulation, contributing to physio(patho)logic processes in the vasculature (473, 474). We explored whether EGF regulates VSMCs migration and proliferation and the involvement of EGFR downstream kinases, TRPM7 and ERK1/2. Using CFSE proliferation assay, we found that EGF promoted rVSMCs proliferation (17%), effects that were attenuated by gefitinib (7%), NS8593 (20%), 2-APB (11%) and PD98059 (10%), an ERK1/2 inhibitor (Figure 3.9A). VSMCs migration was investigated by Scratch-wound assay. Because EGF was found to enhance rVSMCs proliferation, serum-free medium was used throughout the study to reduce the effects of cell proliferation. As shown in Figure 3.9B, EGF significantly increased rVSMCs migration (27%), which was inhibited by gefitinib (26%), NS8593 (53%), 2-APB (18%) and PD98059 (35%) (Figure 3.9B).

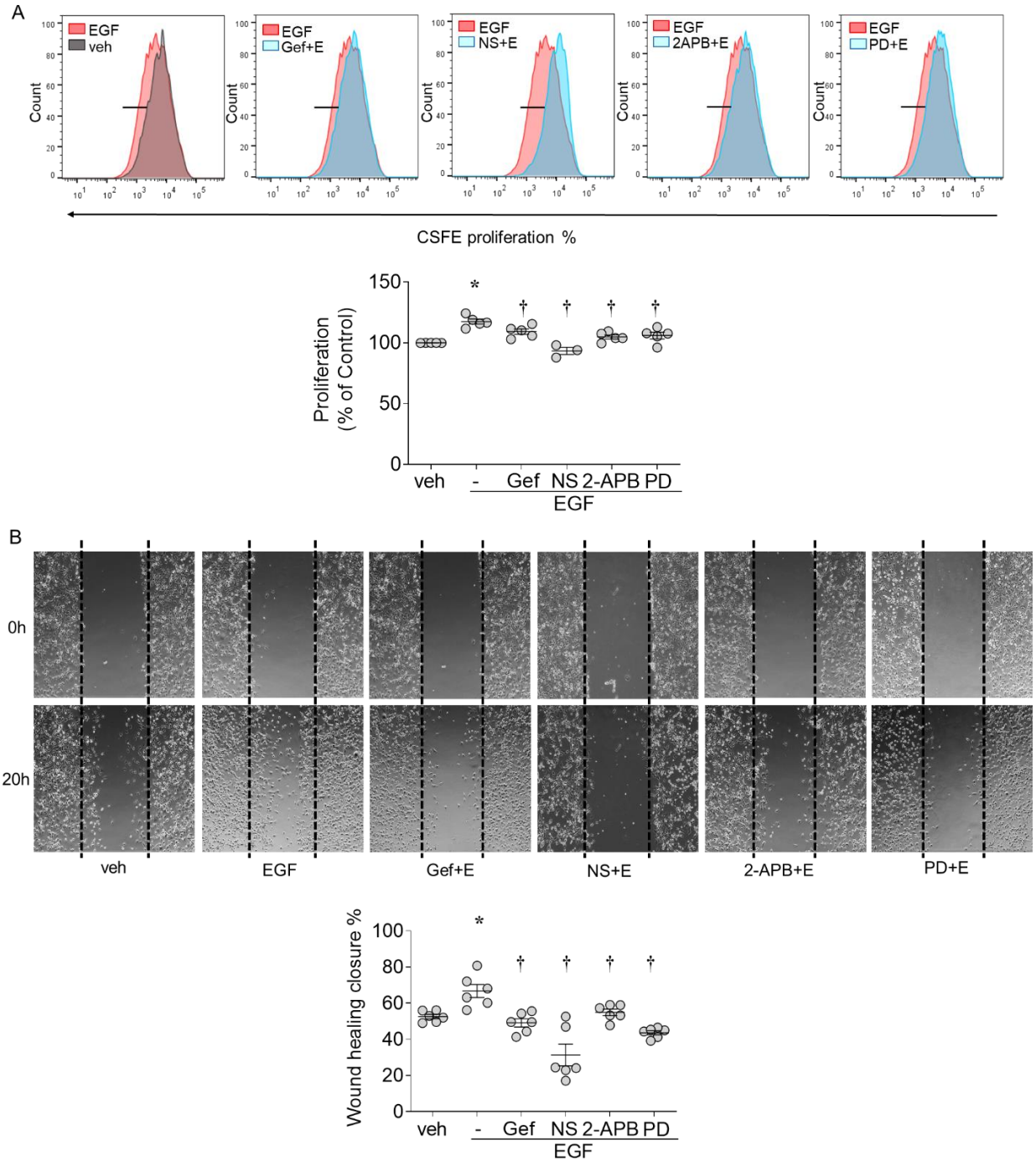

Figure 3.9 EGF regulates VSMCs proliferation and migration through TRPM7 and ERK1/2. rVSMCs were treated with EGF (50 ng/ml) for 20 h (migration study) or 72 h (proliferation study) in the absence and presence of gefitinib (Gef, 1 µM), NS8593 (NS, 40 µM), 2-APB (30 µM) and PD98059 (PD, 20 µM). rVSMCs proliferation was examined by CFSE assay using flow cytometry. Upper panel: Representative flow cytometry histograms. Lower panel: Quantification of proliferation rate (percentage of control) (**A**). rVSMCs migration was assessed by Scratch-wound assay. Upper: Representative images. Lower: Quantification of migration as wound healing closure (**B**). **P*<0.05 compared to vehicle (veh) and † *P*<0.05 compared to EGF.

3.3.11 The effects of TRPM7 deficiency on vascular structure

Since TRPM7 interacts with the EGF-EGFR system and plays an important role in VSMCs migration and proliferation, we studied the effects of TRPM7-deficiency on vessel morphology. Aortas were isolated from WT and TRPM7$^{+/\Delta kinase}$ mice and stained with Haematoxylin and Eosin (HE). As shown in Figure 3.10A and B, there was significantly reduced vessel wall thickness in TRPM7$^{+/\Delta kinase}$ (35%), which was associated with reduced TRPM7 phosphorylation (67%) (Figure 3.10C) and expression of proliferating cell nuclear antigen (PCNA) (66%), a widely used cell proliferation marker (475) (Figure 3.10D). To further investigate the underlying mechanisms of altered vessel structure in TRPM7$^{+/\Delta kinase}$ mice, we investigated the expression of NOTCH3, a cell surface receptor predominantly expressed in hVSMCs regulating vascular development (476). NOTCH3 protein expression was remarkably reduced in mVSMCs derived from TRPM7$^{+/\Delta kinase}$ mice (92%) (Figure 3.10E), and there was a decreased trend ($p=0.053$) of NOTCH3 expression in aortic tissues isolated from TRPM7$^{+/\Delta kinase}$ mice (WT 1.04 ±0.19 vs M7+/Δ 0.33±0.17) (Figure 3.10F).

3.3.12 The effects of TRPM7 in vascular relaxation and contraction induced by EGF

To investigate whether EGF influences vascular reactivity, small mesenteric arteries were isolated from wild type (WT) and heterozygous TRPM7$^{+/\Delta kinase}$ mice. The arteries were incubated with EGF (50 ng/ml) for 30 min and vascular reactivity was assessed by wire myography. As shown in Figure 3.11, vessels exposed to EGF were less responsive to acetylcholine (ACh)-induced relaxation in both WT (maximum response: veh 97%±3% vs EGF 63%±10%, $p<0.05$), and TRPM7$^{+/\Delta kinase}$ mice (maximum response: veh 89%±5% vs EGF 69%±5%, $p<0.05$) (A), while there were no significant differences in sodium nitroprusside (SNP)-induced vessel relaxation (B) and U46619-induced contraction (C) among groups of the two mice strains.

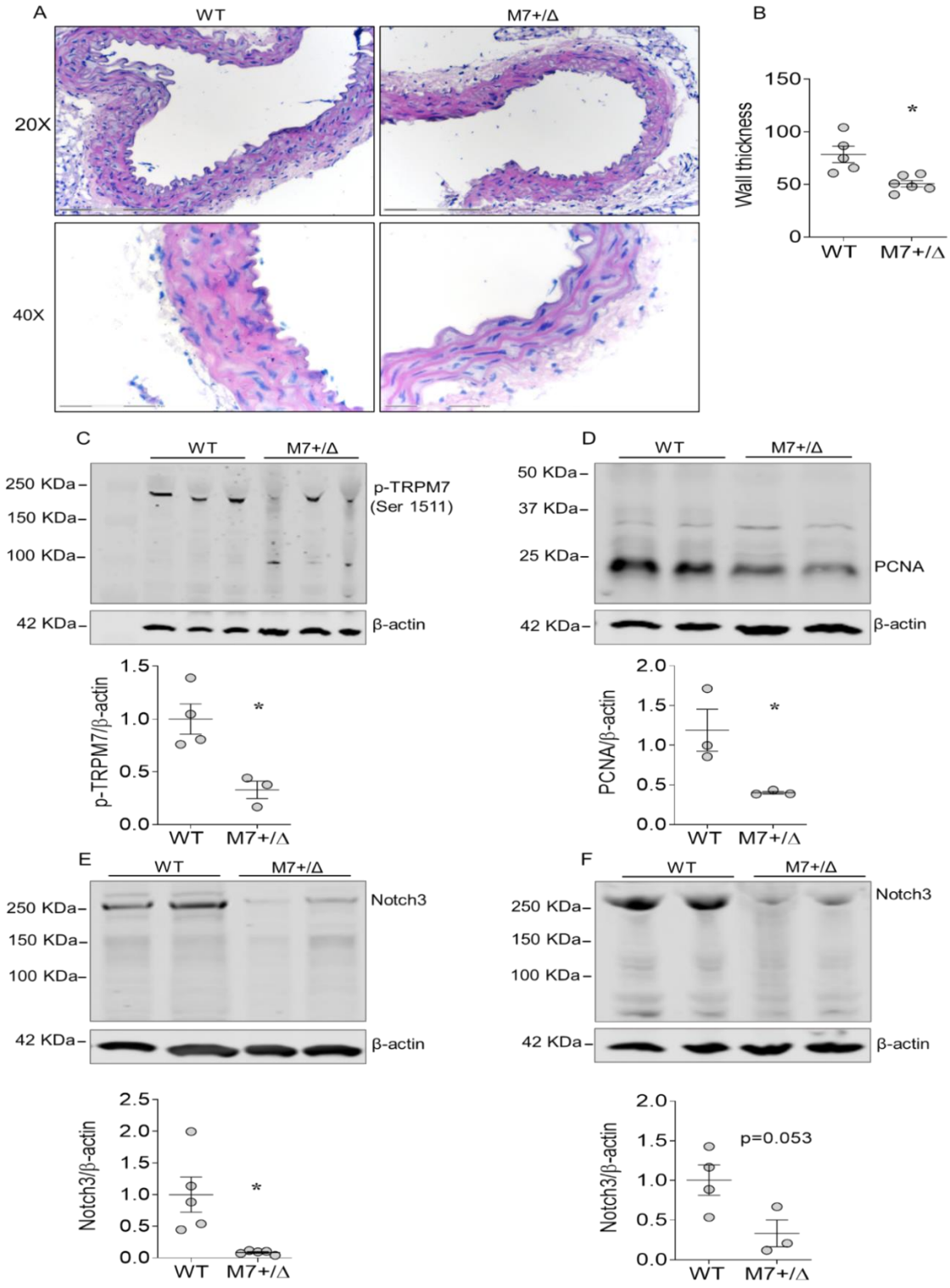

Figure 3.10 TRPM7 deficiency is associated with structural alterations of vessel walls. Aortas were isolated from WT and TRPM7$^{+/\Delta kinase}$ (M7+/Δ) mice. Tissues were stained with Haematoxylin and Eosin (HE) to study aortic wall thickness. 20X objective: Scale bar=150 µm. 40X: Scale bar=75 µm (**A** and **B**). Total tissue lysates of aortas were examined for phosphor-TRPM7 (**C**), PCNA (**D**) and NOTCH3 (**F**) by immunoblotting. NOTCH3 expression in VSMCs derived from WT and M7+/Δmice was examined by immunoblotting (**E**). **P*<0.05 compared to WT.

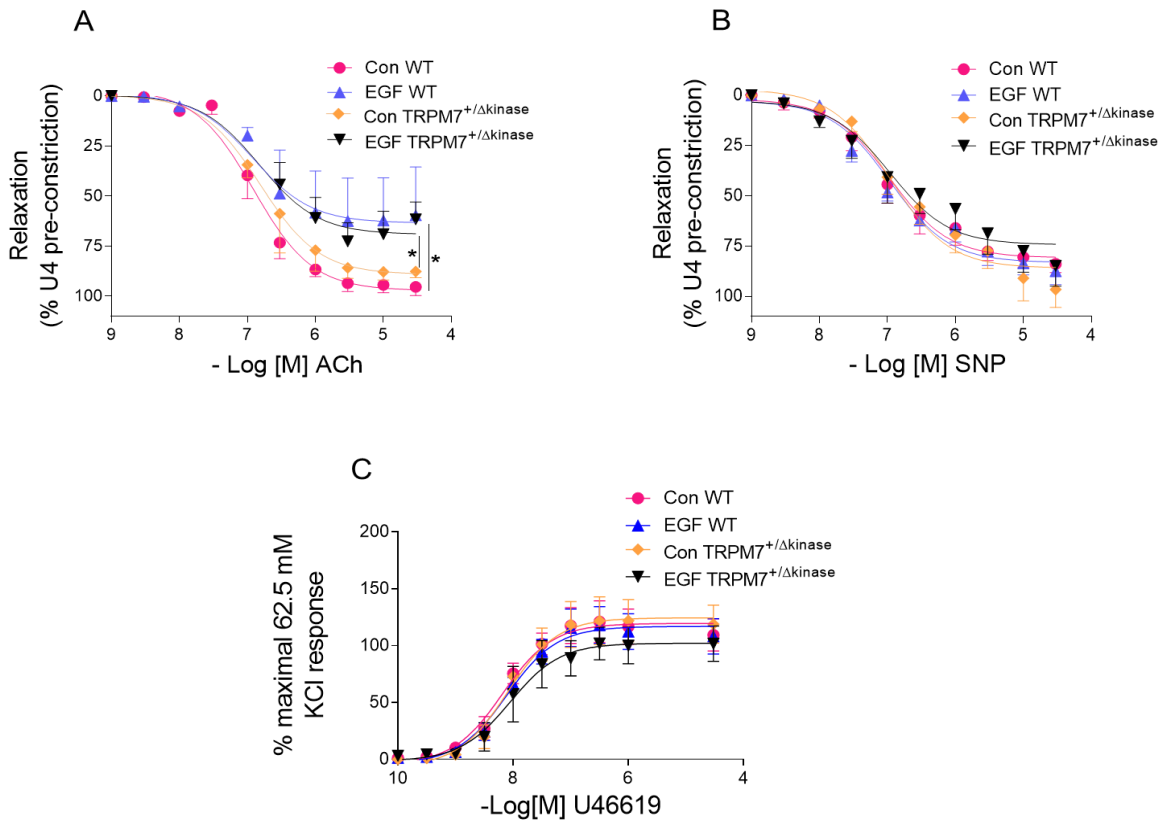

Figure 3.11 EGF regulates vascular relaxation independently of TRPM7 kinase. Isolated vessels were treated with EGF (50 ng/ml) for 30 min and vascular activity was assessed by wire myography. Endothelium-dependent vascular relaxation was assessed by concentration-response curve to acetylcholine (ACh, 1 nM – 100 µM) (**A**). Endothelium-independent vascular relaxation was assessed by concentration-response curve to sodium nitroprusside (SNP, 10 nM – 10 µM) (**B**). Vascular contractility was assessed by concentration-response curve to U46619 (10 nM – 1 µM) (**C**). **P*<0.05, maximum response: EGF vs vehicle (Con) counterparts.

3.3.13 The effects of TRPM7 on Mg^{2+} homeostasis, ERK1/2 activation and migration induced by EGF in human VSMCs

We questioned whether the novel pathway (EGFR-c-Src-TRPM7-ERK) observed in rodent cells and tissues are present in human cells. hVSMCs were derived from normotensive male and female human subjects (Table 3.1). Initially, we observed that 5h EGF stimulation increased expression of TRPM7 (67%) compared to vehicle treated controls, and the pre-treatment with gefitinib was able to reduce the effect (14%) (Figure 3.12A). EGF treatment induced increased $[Mg^{2+}]_i$ (6%) effects that were reduced the treatment with gefitinib (11%), NS8593 (19%) and 2-APB (29%) (Figure 3.12B). Next, we observed the phosphorylation of ERK1/2, which was increased by EGF (2-fold), which was reduced by pre-treatment with gefitinib (22%), NS8593 (19%) and 2-APB (17%) (Figure 3.12C). Cell migration assay demonstrated that EGF enhanced hVSMCs migration (99%), and the effect was reduced by gefitinib (57%), PP2 (69%) and NS8593 (65%), 2-APB (25%) and PD98059 (39%) as shown in Figure 3.12D.

BioBank Number	Hypertension	Gender	Age	Type of vessel
BB140323	NO	Male	60	L Facial Artery
BB140473	NO	Female	68	Facial Artery
BB151402	NO	Female	33	L Facial artery
BB151585	NO	Female	66	R Facial Artery
BB160999	NO	Male	43	Facial artery
BB170377	NO	Female	61	R Facial Artery
BB170655	NO	Male	50	Facial Artery
BB171277	NO	Female	48	L Facial Artery
BB171621	NO	Female	67	R Facial Artery
BB181219	NO	Female	45	L Facial Artery
BB181212	NO	Female	78	L Facial Artery
BB180948	NO	Male	68	R Facial Artery

Table 3.1 Characteristic of human patients undergoing craniofacial surgery. Small arteries were isolated from surplus surgical tissue of patients receiving elective craniofacial surgeries. Primary cell culture was established by Wendy Beatie and Jackie Thomson using the method we previously described (477). Hypertension is defined as a systolic blood pressure ≥140 mmHg and/or a diastolic pressure ≥ 90 mm Hg (478, 479). Biobank number is a unique ID allocated to each patient and is used to track sample information in Professor Touyz' lab. L, left; R, right.

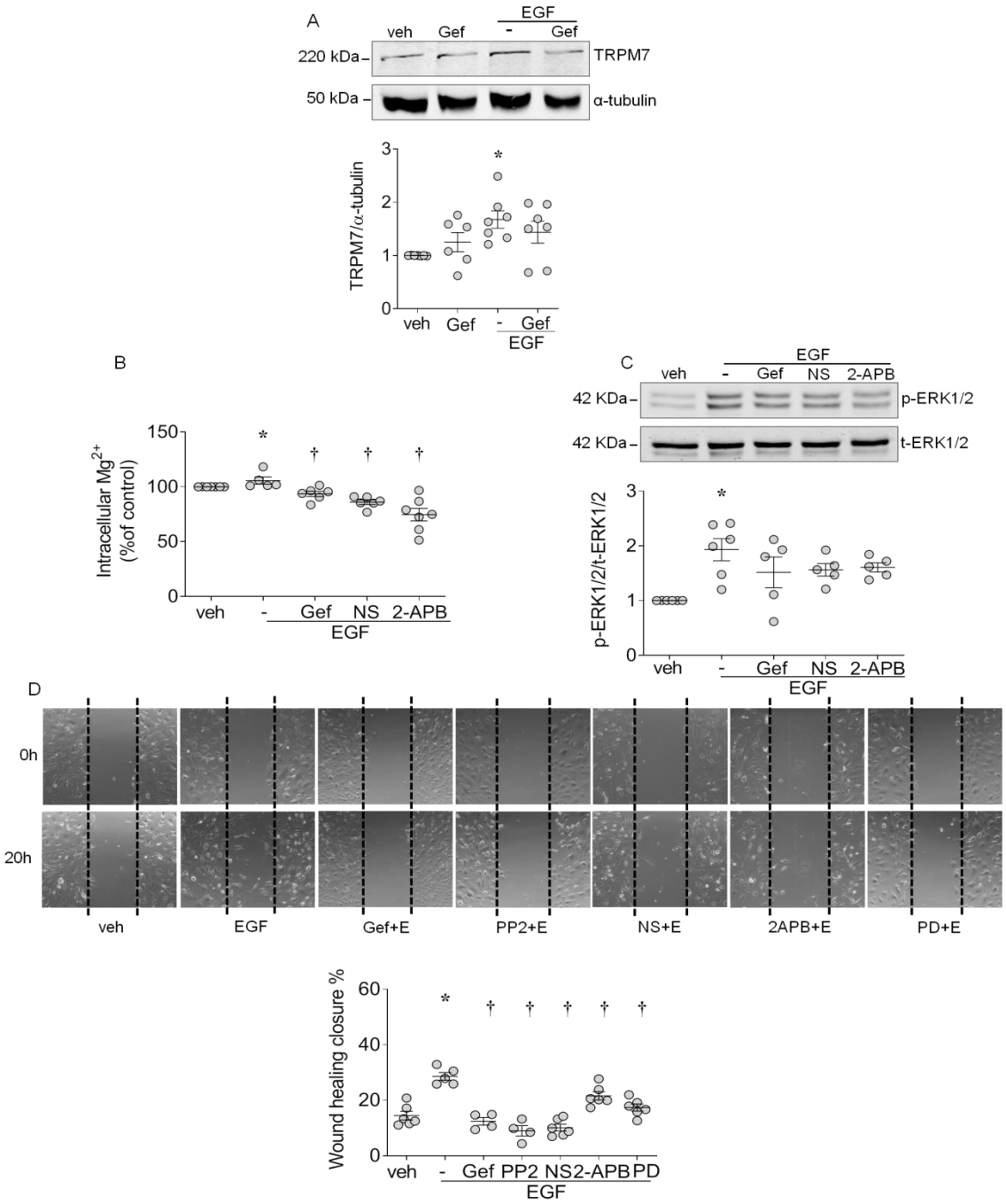

Figure 3.12 Effects of EGF on Mg^{2+} homeostasis, ERK1/2 activation and cell migration are mediated by TRPM7. Human VSMCs were treated with EGF (50 ng/ml) for short term (5 min) and long term (5 h and 20h) in the presence and absence of gefitinib (Gef, 1 µM), PP2 (10 µM), NS8593 (NS, 40 µM), 2-APB (30 µM) and PD98059 (PD, 20 µM). TRPM7 expression after 5 h EGF stimulation was examined by immunoblotting using α-tubulin as the house keeping protein (**A**). $[Mg^{2+}]_i$ after 5 min EGF treatment was assessed by flow cytometry using specific Mg^{2+} indicator Magnesium Green (**B**). ERK1/2 phosphorylation after 5 min EGF stimulation was assessed by immunoblotting (**C**). Scratch-wound assay was used to check hVSMCs migration after 20 h EGF treatment (**D**). **P*<0.05 compared to vehicle (veh) and † *P*<0.05 compared to EGF.

3.4 Chapter Discussion

This study demonstrates the direct interaction between EGFR and the chanzyme TRPM7, which involves c-Src kinase and plays an important role in VSMCs function and vessel morphogenesis. Firstly, in primary VSMCs and aortic vessels from humans and different rodent models, we show that i) the EGF-EGFR pathway regulates TRPM7 expression and phosphorylation in a c-Src-dependent manner and ii) EGFR is also regulated by TPRM7, supported by the fact that genetic TRPM7-defiency leads to reduced EGFR expression. To delineate the underlying molecular mechanisms, with several different approaches including PLA, immunocytochemistry and co-immunoprecipitation, we have shown that EGFR directly interacts with TRPM7 mainly at cell membrane and the interaction is enhanced by EGF stimulation in a c-Src kinase dependent pathway. Our data also suggest that the interaction between EGFR and TRPM7 regulates VSMCs function: i) EGF-EGFR regulates the activation of ERK1/2 via c-Src and TPRM7; ii) EGF-EGFR regulates cell migration and proliferation via TRPM7 and ERK1/2 and iii) TRPM7 kinase-deficient mice exhibited reduced wall thickness.

EGF exerts important regulatory roles in Mg^{2+} and Ca^{2+} homeostasis. Bindels et al. found that EGF through activating TRPM6 channel, which is localised along the apical membrane of distal convoluted tubule, stimulates renal Mg^{2+} absorption and handles systemic Mg^{2+} balance (52, 259, 411). Mutation in the *EGF* gene is associated with isolated recessive renal hypomagnesemia (IRH), and patients receiving cetuximab, an antagonist of EGFR, display gradually reduced serum Mg^{2+} level (259). EGF also mediates cellular Ca^{2+} homeostasis, with evidencing showing that EGF promotes both Ca^{2+} release from intracellular store and Ca^{2+} influx from the outer medium (252, 480). TRPM7 was identified as a Mg^{2+}-and Ca^{2+}- permeable channel essential for Mg^{2+} balance in mammals, and we previously found that TRPM7 functions as an important regulator of vascular Mg^{2+} homeostasis, while dysregulation of TRPM7 is associated with inherited hypomagnesemia (2, 67, 76, 78). TRPM7 also regulates the entry of Ca^{2+} in many cell types, such as platelet, atrial fibroblast and cancer cells (83, 84, 481). In particular, the TRPM7 kinase domain exerts important effects on store-operated Ca^{2+} entry (86, 87). Our study further expands the role of EGF in mediating cellular Mg^{2+}, particularly in VSMCs via a TRPM7-dependent manner. Additionally, our data showed that EGF regulates the expression of MagT1, an important transporter for Mg^{2+} influx, which in combination with TRPM7 impacts Mg^{2+} uptake and cell proliferation (62, 63). Interestingly, although in our experiments EGF induced intracellular Ca^{2+} elevation, the effect was only abolished by 2-

APB, and not by a relatively more specific TRPM7 inhibitor NS8593. 2-APB has been shown to exert nonspecific inhibitory effects on Ca^{2+} channels including TRPM2 and store-operated Ca^{2+} channels (482, 483). Taken together, our findings suggest that in VSMCs, EGFR activation regulates Mg^{2+} homeostasis via TRPM7, while the Ca^{2+} mobilisation is mediated by EGF through other Ca^{2+} channels, which may include other TRP channels or store-operated Ca^{2+} channel, as they are inhibited by 2-APB (482, 483).

EGFR belongs to the large RTKs family, and we have recently reviewed the cross-talk between TRPM7 and RTKs downstream signalling pathways (46). In the present study, we explored the effect of TRPM7 on EGFR and c-Src. Experiments were performed using cells and tissues from two mouse models, $TRPM7^{+/\Delta kinase}$ which is heterozygous for deletion of TRPM7-kinase with channel malfunction and $TRPM7^{R/R}$ which carries a mutant "dead" kinase domain. It was found that TRPM7 is important to maintain EGFR and c-Src activity at both cell and tissue levels with a critical involvement of the TRPM7 catalytic activity. It is worth noting that, our experiments focused on the phosphorylation of c-Src at tyrosine 416 (Y416), which is associated with high kinase activity, and phosphorylation of EGFR on Y845, a Src-dependent phosphorylation site (470, 484). c-Src is downstream of EGFR, and the colocalization of EGFR and Src has been previously elucidated and supported by our co-IP experiment (data not shown) (485). Thus, the reduced EGFR phosphorylation (Y845) and c-Src (Y416) observed in TRPM7-deficient mouse models by our study also suggest a role of TRPM7 in the interaction between EGFR and c-Src.

A key finding of this study is that EGFR directly interacts with TRPM7 at plasma membrane of VSMCs, and the interaction is enhanced by EGF in a c-Src-dependent manner. Proximity ligation assay is a powerful technique to detect, localise and quantify protein-protein interaction, which in combination with co-IP and confocal immunofluorescence, provided firm evidence of the EGFR-TRPM7 interaction. Importantly, our data confirmed TRPM7 expression at plasma membrane of VSMCs. Clapham and colleagues have shown that TRPM7 is most abundant on intracellular vesicles, with undetected level at the plasma membrane in multiple cell types. In our investigations, TRPM7 co-localised with EGFR, a well-known cell surface receptor, and the positive PLA signal mainly occurred at cell membrane. Thus, cellular location of TRPM7 may depend on cell types, while in VSMCs there is a relatively high expression at cell membrane. We also investigated mechanisms underlying the enhancement of EGFR-TRPM7 interaction upon EGF stimulation. Bindels et al. demonstrated that EGF increased

TRPM6 cell surface expression (411), and thus we explored whether EGF-induced TRPM7 trafficking to cell membrane, which would consequently contributes to the EGFR-TRPM7 interaction. Using HEK-293T cells overexpressing YFP-TRPM7, we tracked TRPM7 movement upon EGF stimulation, however, there was no significant TRPM7 trafficking towards cell membrane. Therefore, our data suggest that EGF-induced enhancement of EGFR-TRPM7 interaction might mainly depend on membrane-localised TRPM7.

TRPM7 possesses dual properties as an ion channel and a cytoplasmic kinase, and thus it is not surprising that TRPM7 participates in cellular signalling activation. TRPM7 has been shown to affect the activity of RTKs downstream signalling cascades including the MAP kinase pathway (46). However, results have been contrasting and seems to be cell dependent. Xiong *et al.* found that silencing TRPM7 promotes proliferation via activating ERK1/2 in endothelial cells, while in mouse cortical astrocytes, silencing TRPM7 inhibits proliferation via ERK1/2 and c-Jun N-terminal kinases (JNK) pathways (124, 400). In HEK-293 cell line, overexpression of TRPM7 activated p38 MAPK and JNK, and reduced phosphorylation of ERK1/2 (104). Through modulating the MAP kinase pathway, particularly ERK1/2, EGF regulates cellular functions such as migration and proliferation in different types of cells (288-290). This pathway was confirmed in the present study, as PD98059, a pharmacological inhibitor of ERK1/2, attenuated EGF-induced VSMCs migration and proliferation. Importantly, our data demonstrate that TRPM7 is involved in ERK1/2 activation downstream of the EGF-EGFR system, and this pathway plays a critical role in regulating VSMCs function.

Although EGF has been consistently demonstrated as a potent vasoconstrictor by several studies (319, 320), we did not observe any regulatory effects of EGF on vascular contraction. Interestingly, our data showed that EGF reduced ACh-induced relaxation, which is also endothelium dependent, in both WT and $TRPM7^{+/\Delta kinase}$ mice, suggesting a TRPM7 kinase-independent manner. Since the deletion of TRPM7 kinase domain did not change the channel expression in plasma membrane, but significantly reduced the channel currents, which is associated with altered Mg^{2+} status in plasma, urine and bones of the mice (76), it is difficult to conclude whether or not TRPM7 channel property is involved in EGF-regulated vessel relaxation. It would be interesting to investigate the contribution of TRPM7 substrates such as calpain-2, because calpain has been shown to affect endothelial function, NO production and endothelial adhesiveness (171). To further study the involvement of TRPM7 channel, chelators of Mg^{2+} and Ca^{2+} such as EGTA and EDTA can be applied accordingly in future experiments. In addition, to confirm that EGF mediate

endothelium-dependent relaxation, experiments can be repeated using endothelium-denuded vessels.

VSMCs are the main components of the artery media layer, maintaining the integrity and structure of mature vascular wall (486). Abnormal proliferation and migration of VSMCs have been associated with a number of vascular diseases including hypertension, atherosclerosis and in-stent restenosis (474, 487, 488). The observation that EGFR and TRPM7, two proteins with critical cardiovascular relevance, interact at the membrane of VSMCs and mediate migration and proliferation, leads us to explore the effect of TRPM7 deficiency on vascular wall. Using the $TRPM7^{+/\Delta kinase}$ mouse model, we showed that vascular wall thickness was reduced when there was a lack of TRPM7-kinase, which was associated with a decreased expression of PCNA, a proliferation marker. Notch3 functions as a critical regulator of developmental and pathological blood vessel formation, and our recent study found that mutation in Notch3 is associated with aberrant vascular function (489, 490). Here, we demonstrated that that Nothc3 expression was reduced in $TRPM7^{+/\Delta kinase}$ mice at both cell and tissue level. Therefore, our data suggest that TRPM7 might have an important role during blood vessel morphogenesis. This process is associated with aberrant VSMCs proliferation resulting from TRPM7 deficiency and the dysregulation of Notch3.

In summary, utilizing a combination of pharmacological, biochemical and genetic tools, and taking advantage of different animal models, we provide new evidence that EGFR directly interacts with TRPM7 at the plasma membrane in VSMCs. These effects are dependent on c-Src kinase, influence the activation of EGFR downstream signalling pathway and regulate VSMCs migration and proliferation. Importantly, TRPM7 deficiency is associated with reduced EGFR signalling pathway and reduced thickness of the vascular wall compared to WT animals. These findings define a novel pathway in VSMCs and expand the knowledge of EGFR and TRPM7 in vascular biology, which might contribute to a better understanding of pathology of cardiovascular diseases (Figure 3.13). Moreover, these data suggest that there is important interplay between EGF/EGFR and TRPM7

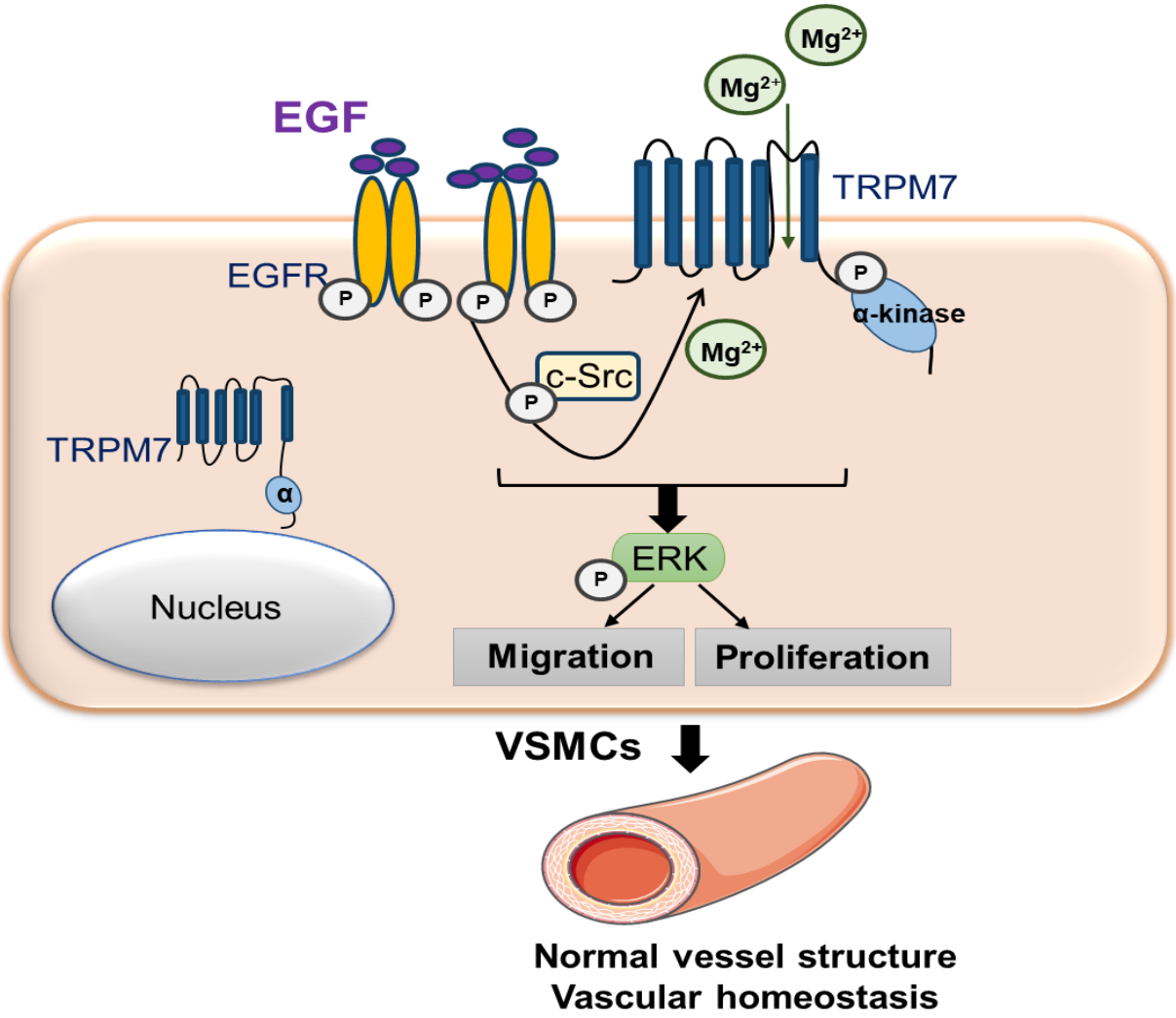

Figure 3.13 Schematic figure demonstrating the novel EGFR- and TRPM7- related signalling pathway in the vasculature. In VSMCs, growth factor EGF though activating EGFR, interacts with TRPM7 at cell membrane in a c-Src-dependent manner. The interaction influences TRPM7 activity (phosphorylation and expression) and consequently regulates Mg^{2+} homeostasis, ERK1/2 activation and VSMCs migration and proliferation. Crosstalk between the EGF-EGFR ligand-receptor system and TRPM7 in VSMCs may also exert important role in vascular homeostasis.

Chapter Four

4 VEGF regulates TRPM7 through VEGFR, a process mediating ion homeostasis and vascular reactivity

4.1 Overview

Vascular endothelial growth factor receptor (VEGFR), which belongs to the receptor tyrosine kinases (RTK) family, together with the ligand VEGF are important signalling molecules involved in vascular development and regulation (491, 492). VEGF regulates cellular functions such as migration, proliferation and apoptosis has been studied thoroughly in endothelial cells (493). *In vivo* studies have demonstrated that VEGF is protective by promoting endothelial regeneration and accelerates the recovery of endothelium-dependent relaxation (335).

Growth factors through activating RTKs have been shown to regulate TRPM7 activity in different types of cells. In hippocampal neurons, nerve growth factor (NGF), reduced the outward rectifying TRPM7-like current and this effect could be blocked by the inhibition of tyrosine kinase activity of TrkA (NGFR) and PLC inhibitor (413). In the HSC-T6 hepatic stellate cell line, PDGF stimulation was shown to increase TRPM7 expression in a time-dependent manner (401). VEGF has been shown to regulate Mg^{2+} homeostasis in endothelial cells by releasing Mg^{2+} from intracellular stores (263). On the other hand, alterations in Mg^{2+} status are associated with imbalance of the VEGF-VEGFR system. Uysal et al. showed that chronic use of magnesium reduces VEGF levels in the uterine tissue in rats, and magnesium sulfate was reported to affect VEGF expression in placental tissue from normotensive and preeclamptic patients (394, 494). Underlying mechanisms of the close relationship between VEGF and Mg^{2+} remain unknown, and it is unclear whether Mg^{2+} transporters such as TRPM7 are involved in this process.

VEGF-induced intracellular Mg^{2+} elevation was observed in HUVECs, where Hong et al. showed that VEGF-A165 released Mg^{2+} from intracellular store in a dose-dependent manner, without impact on Mg^{2+} influx (263). PDGF was found to increase intracellular Mg^{2+} in human osteoblast cells only in the presence of extracellular Mg^{2+}, suggesting a dependence on Mg^{2+} influx (264). It was furthermore shown that PDGF is able to affect the expression of TRPM7, and mediate Mg^{2+} influx through TRPM7, a process associated with cell proliferation, migration and adhesion (264).

In the current chapter, we will focus on whether VEGF through activating its receptor, regulates TRPM7 in VSMCs and consequently influences ion homeostasis, activation of cellular kinases and vascular reactivity.

4.2 Objective and aims

Objective

The overall objectives of the studies presented in Chapter 4 were to explore whether VEGF regulates TRPM7 channel and kinase in VSMCs and to investigate the importance of TRPM7 on vascular reactivity induced by VEGF.

Specific aims

1**.** *To elucidate whether VEGF regulates TRPM7 expression and activity in VSMCs*

Human VSMCs were stimulated with VEGF in the absence and presence of vatalanib for short (5 min) and long (5 h) term. TRPM7 expression and phosphorylation were examined by immunoblotting to assess TRPM7-kinase activity.

2. *To study whether VEGF regulates* Mg^{2+} *and* Ca^{2+} *homeostasis in VSMCs through TRPM7*

Human VSMCs were stimulated with VEGF for a short period (1-60 min) in the absence and presence of vatalanib and TRPM7 inhibitors NS8593 and 2-APB. Using specific fluorescent indicators, Ca^{2+} mobilization was examined by live cell microscope, and intracellular free Mg^{2+} was assessed by flow cytometry.

3. *To explore whether TRPM7 is important for MAP kinase activation induced by VEGF*

Human VSMCs were stimulated with VEGF for 5 min in the absence and presence of vatalanib and TRPM7 inhibitors NS8593 and 2-APB. Both total and phosphorylated forms of the MAP kinases (p38 MAPK and ERK1/2) and protein kinase C (PKC) were examined by immunoblotting.

4. *To examine effects of TRPM7 on the vascular activity induced by VEGF*

Mesenteric arteries were derived from mice wild type and TRPM7 kinase-deficient with channel malfunction ($TRPM7^{+/\Delta kinase}$). Vessels were treated with VEGF and vascular reactivity (contraction and relaxation) was assessed by wire myography.

4.3 Results

4.3.1 The effects of VEGF on TRPM7 expression and activity on VSMCs

Human VSMCs stimulated with VEGF for 5 h exhibit a significant increase in TRPM7 expression (50%). These effects were attenuated by VEGFR inhibitor vatalanib (11%) (Figure 4.1A). No significant changes were found after 24 h stimulation with VEGF. Treatment with vatalanib for 24 h reduced TRPM7 (24%) expression compared to vehicle-treated group (Figure 4.1B). TRPM7 mRNA expression was checked by qPCR. 5h treatment with VEGF increased TRPM7 mRNA (77%), effects that were attenuated by vatalanib (48%) (Figure 4.1C and D).

TRPM7 can be phosphorylated at several serine and threonine sites and the process is associated with TRPM7-kinase activity and cellular localization (96, 495). Thus, we questioned whether VEGF influences TRPM7 by modulating phosphorylation of the kinase domain. VSMC cell lysate was immunoprecipitated using a specific anti-TRPM7 antibody, and phosphorylation of TRPM7 was assessed by immunoblotting using a specific anti-phosphor tyrosine/serine/threonine antibody. As shown in Figure 4.1E, 5 min VEGF stimulation increased TRPM7 phosphorylation in a VEGFR-dependent manner. Because, TRPM7 has been identified in cell plasma membrane and in the intracellular vesicles and TRPM7 trafficking may play an important role in cell function (64, 66), we next explored whether VEGF regulates TRPM7 translocation by examining cell surface expression of TRPM7. As shown in Figure 4.1F, VEGF increased the presence of TRPM7 in the cell membrane after 5 min stimulation.

To further confirm the regulatory role of VEGF on TRPM7 expression, wild type SV129 mice were treated with vatalanib (Vat, 100 mg/Kg/d) and the expression of TRPM7 was assessed in aortas and kidneys. There was a trend for decreased TRPM7 expression in the aorta (50%, Figure 4.1G) and kidney (38%, Figure 4.1H) tissues derived from the vatalanib-treated mice compared to the vehicle-treated group.

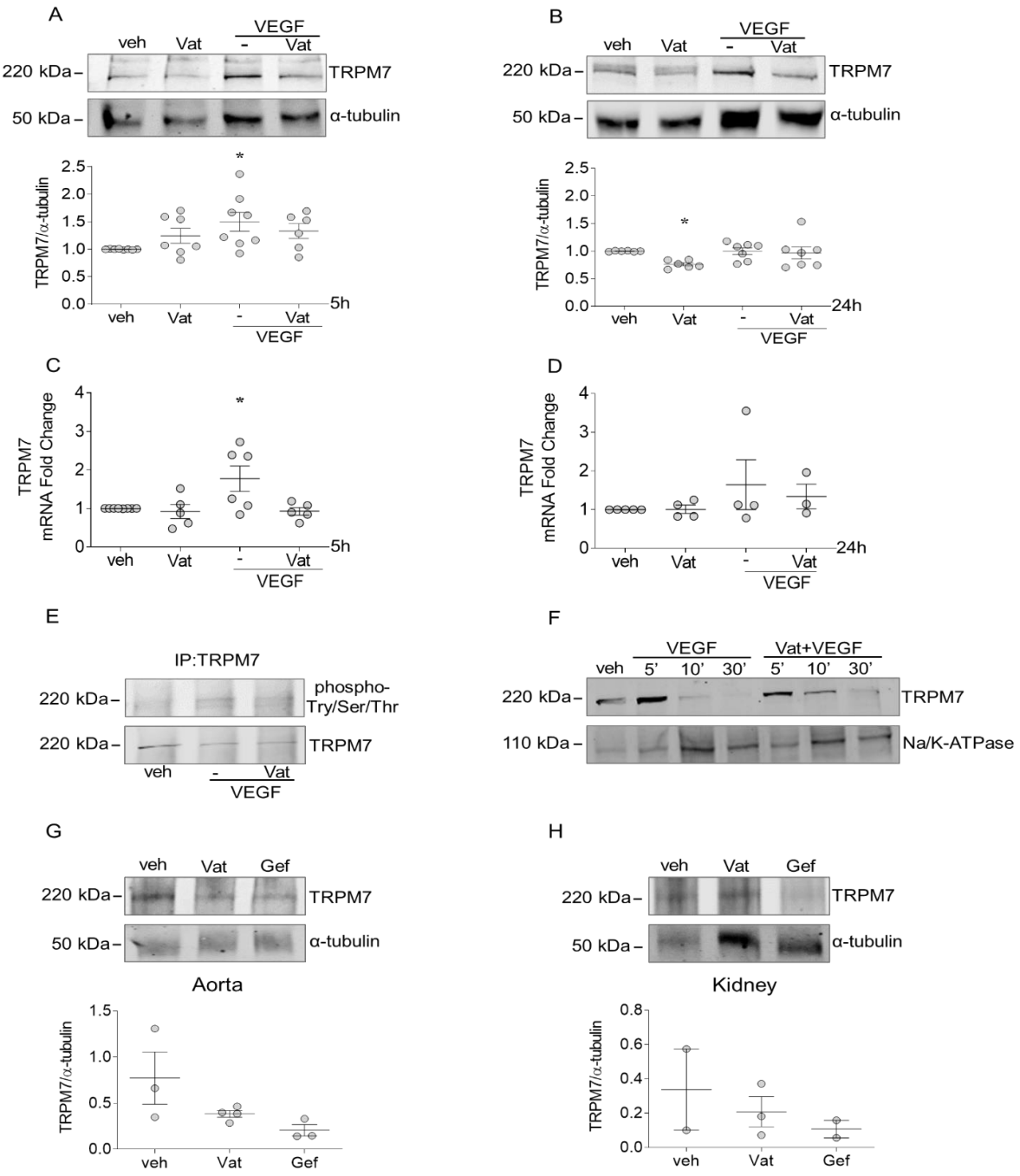

Figure 4.1 VEGF regulates TRPM7 expression and phosphorylation in hVSMCs. hVSMCs were treated with VEGF (50 ng/ml) for long term (5 h or 24 h) and short term (5, 10 and 30 min) in the presence and absence of vatalanib (Vat, 1 μM). TRPM7 protein (**A** and **B**) and gene (**C** and **D**) expression after 5 h and 24 h treatment were assessed by immunoblotting and qPCR respectively. TRPM7 phosphorylation at Try/Ser/Thr residues after 5 min VEGF treatment was normalised by total TRPM7 expression (n=2, **E**). TRPM7 expression in membrane-rich cell fractions after VEGF treatment for 5, 10 and 30 min was examined by immunoblotting, normalised by the cell membrane-specific protein Na/K-ATPase (n=1, **F**). TRPM7 expression in aortas and kidneys from mice treated with vehicle (veh), vatalanib and gefitinib, 100 mg/Kg/d (**G** and **H**). * P<0.05 compared to veh.

4.3.2 The effects of VEGF on the expression of Mg^{2+} transporters in VSMCs

VEGF has been shown to mediate intracellular Mg^{2+}, and we recently found that EGF regulates the Mg^{2+} transporters TRPM7 and MagT1 (263). Thus, we explored whether VEGF exerts regulatory effects on Mg^{2+} transporters MagT1, TRPM6 and SLC41A1. As shown in Figure 4.2A and B, 5 h VEGF treatment significantly increased MagT1 protein expression (1.2-fold) in hVSMCs and the effect was attenuated by vatalanib (26%), without affecting MagT1 expression at mRNA levels. Protein expression of TRPM6, was not significantly changed after 5h and 24h stimulation of VEGF (Figure 4.2C and D). No changes in gene expression of SLC41A1 were observed in hVSMCs stimulated with VEGF (Figure 4.2E).

4.3.3 The effects of VEGF on activation of TRPM7-kinase substrates annexin-1 and calpain-2 in hVSMCs

TRPM7 as a kinase is able to phosphorylate several cellular substrates including annexin-1 and calpain-2 (46). These two proteins are predominantly located in the cytosol and upon activation translocate to the plasma membrane (468). We checked annexin-1 and calpain-2 expression in membrane-rich fractions of hVSMCs stimulated with VEGF for different time periods. As shown in Figure 4.3, VEGF treatment for short term (1, 5, 30 and 60 min) did not change annexin-1 expression in the cell membrane (A), while there was significantly reduced calpain-2 expression after 1 min and 5 min VEGF treatment (30% and 35% respectively) (B). To further investigate whether VEGF exerts the effect through VEGFR, hVSMCs were stimulated with VEGF in the presence and absence of vatalanib for different time periods. VEGF might regulate calpain-2 expression in the cell membrane in a time-dependent manner, and the effect might be reduced by the pre-treatment with vatalanib (Figure 4.3C).

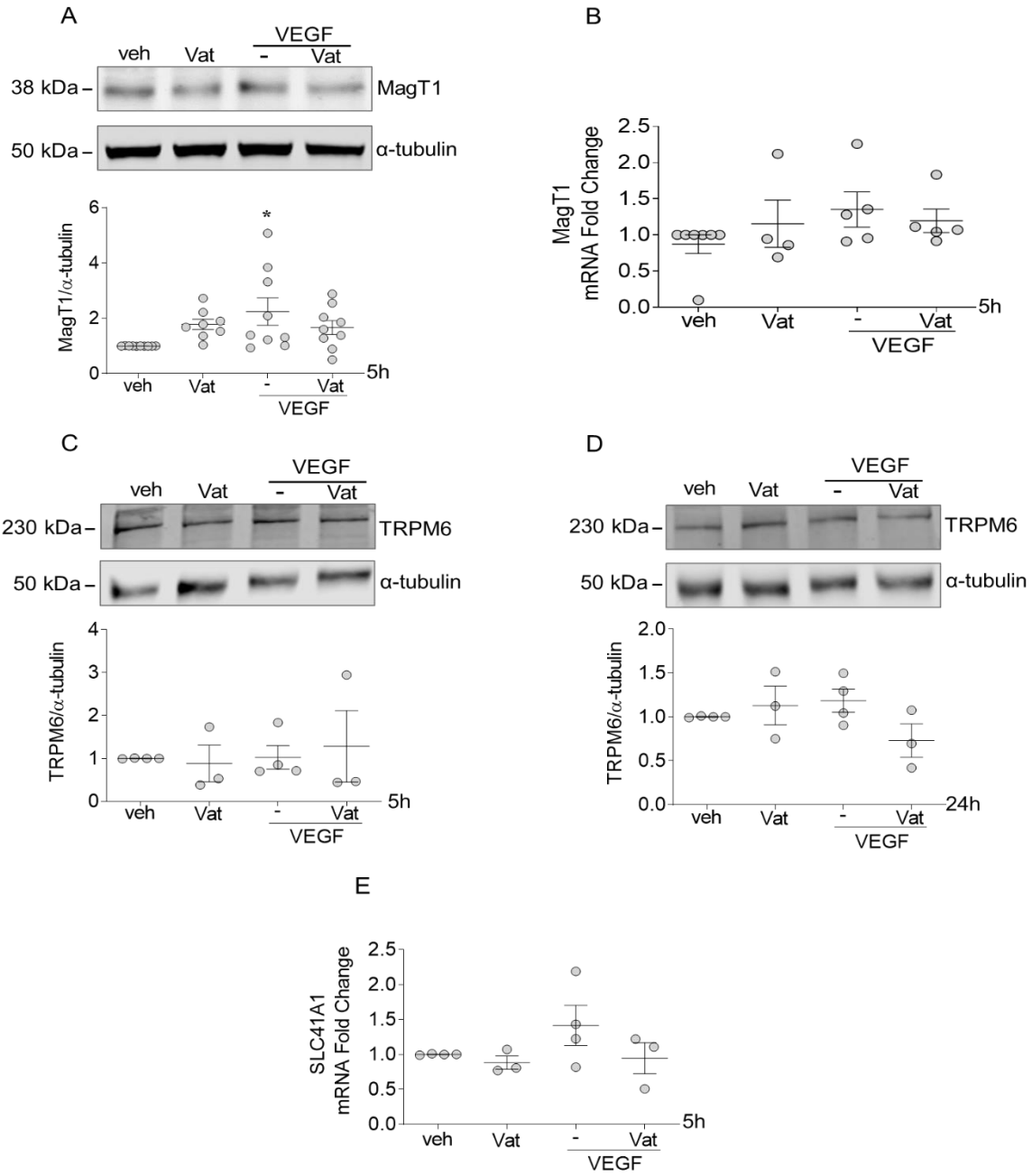

Figure 4.2 Expression of magnesium transporters induced by VEGF in hVSMCs. hVSMCs were treated with VEGF (50 ng/ml) for 5 h or 24 h in the presence and absence of vatalanib (Vat, 1 μM). Protein expression levels of MagT1 (**A**) and TRPM6 (**C** and **D**) after VEGF treatment were assessed by immunoblotting using α-tubulin as the house keeping protein, with representative images (upper panels) and quantification (lower panels). Gene expression of MagT1 (**B**) and SLC41A1 (**E**) in hVMSCs simulated with VEGF was assessed by q-PCR. * P<0.05 compared to vehicle (veh).

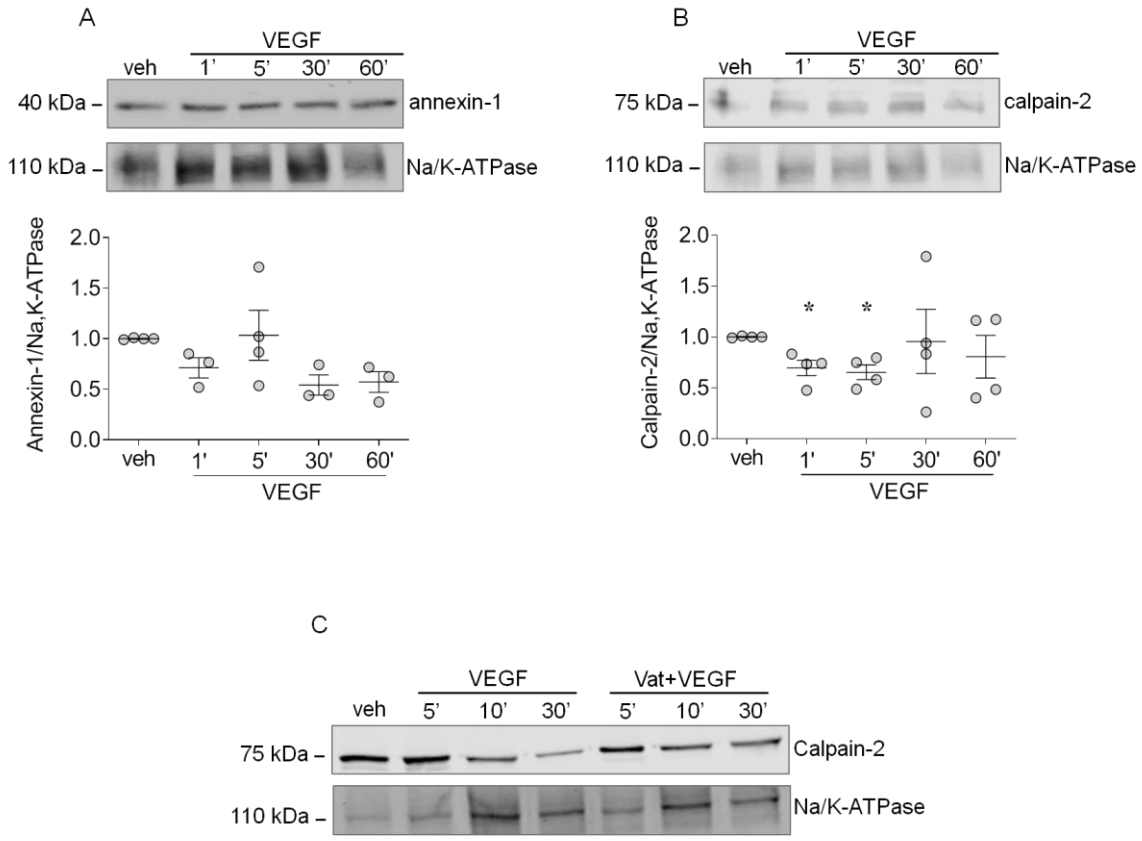

Figure 4.3 Effects of VEGF on the activation of annexin-1 and calpain-2 in hVSMCs. hVSMCs were treated with VEGF (50 ng/ml) for 1, 5, 10, 30 and 60 min in the presence and absence of vatalanib (Vat, 1 μM). Membrane-rich cell fractions were isolated by ultracentrifugation. Activity of annexin-1 and calpain-2 was assessed by the expression in cell membrane. Protein expression levels of annexin-1 (**A**) and calpain-2 (**B)** and (**C**) (n=1) in membrane-rich fractions of cell lysates were examined by immunoblotting. Sodium/potassium ATPase (Na/K-ATPase) was used as a loading control for protein expression in the cell membrane. * $P<0.05$ compared to vehicle (veh).

4.3.4 VEGF regulates Mg^{2+} and Ca^{2+} mobilisation through TRPM7 activation in hVSMCs

TRPM7 acts as a functionally important regulator of Mg^{2+} homeostasis in VSMCs and as shown in Chapter 3, we found that EGF mediates Mg^{2+} mobilisation through TRPM7 in VSMCs (2). Next, we explored whether VEGF regulates Mg^{2+} influx in a TRPM7-dependent manner in hVSMCs. First, we tested the efficacy of using the indicator Magnesium Green by Flow cytometry to detect intracellular free Mg^{2+} by adding different concentrations (1 mM, 5 mM and 20 mM) of extracellular Mg^{2+} for 5 min. $MgCl_2$ was used as extracellular source of Mg^{2+}. As shown in Figure 4.4A, intracellular Mg^{2+} was detectable and reached a plateau at 5 mM extracellular Mg^{2+} concentration. Thus, in the following experiments, the 1 mM extracellular Mg^{2+} concentration was chosen as the best experimental condition. To further investigate Mg^{2+} mobilization upon VEGF stimulation in hVSMCs, we measured intracellular Mg^{2+} for 60 min after VEGF treatment. VEGF mediated intracellular Mg^{2+} in a time-dependent manner, and there was a trend (4%) towards increased intracellular Mg^{2+} after 5-10 min (Figure 4.4B). To study whether the changes of intracellular Mg^{2+} level was induced by Mg^{2+} influx or intracellular store release, experiment was repeated at 0 extracellular Mg^{2+}. There was a decline of intracellular Mg^{2+} in the absence of extracellular Mg^{2+}, suggesting the involvement of Mg^{2+} influx (Figure 4.4C). Next, we stimulated hVSMCs with VEGF for 5 min in the presence and absence of inhibitors of VEGFR and TRPM7. VEGF increased Mg^{2+} influx and the effect was abolished by vatalanib, NS8593 and 2-APB (Figure 4.4D).

We also studied the effect of VEGF on Ca^{2+} homeostasis. Stimulation of hVSMCs with VEGF induced Ca^{2+} mobilization and significantly increased intracellular Ca^{2+} levels, effects that were abolished by NS8593 and 2-APB. Vatalanib also attenuated the effect of VEGF, however the difference was not significant (Figure 4.4E and F).

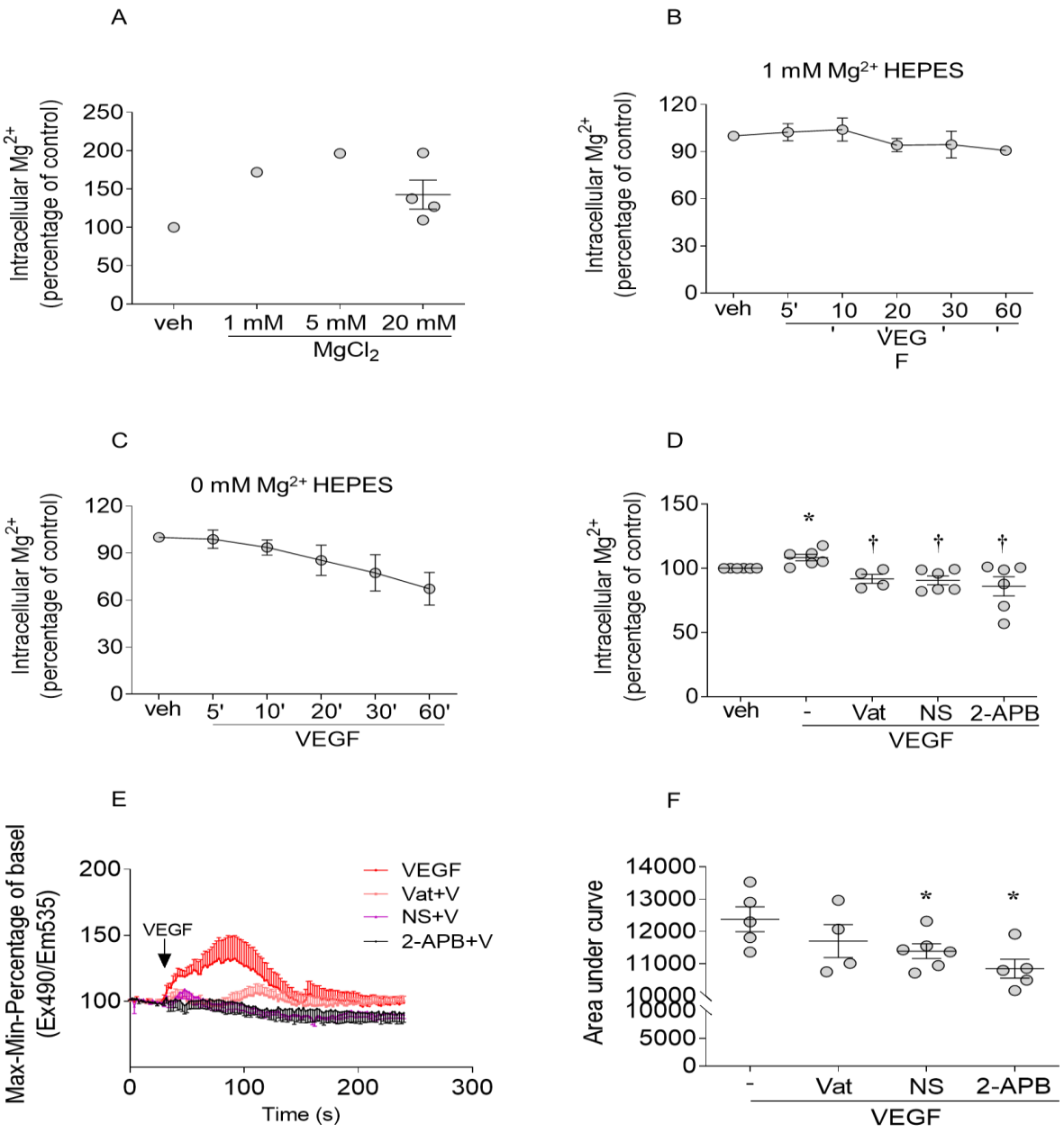

Figure 4.4 TRPM7 medicates Mg^{2+} and Ca^{2+} mobilisation induced by VEGF in hVSMCs. Intracellular free Mg^{2+} ($[Mg^{2+}]_i$) in hVSMCs was measured by flow cytometry using Magnesium green. $[Mg^{2+}]_i$ in hVSMCs after adding different concentrations of extracellular Mg^{2+} for 5 min (**A**). $[Mg^{2+}]_i$ in hVSMCs at different time points under 1 mM (**B**) and 0 mM (**C**) extracellular Mg^{2+}, n=3. $[Mg^{2+}]_i$ in hVSMCs stimulated with VEGF (5 min) in the presence and absence of vatalanib (Vat, 1 μM), NS8593 (40 μM) and 2-APB (30 μM) (**D**).*P<0.05 vs vehicle (veh) and † P<0.05 vs VEGF. Intracellular Ca^{2+} levels induced by VEGF were measured in the presence and absence of vatalanib (Vat, 1 μM), NS8593 (40 μM) and 2-APB (30 μM). Data are expressed in Fluorescent Cal-520AM-Ca^{2+} signals (percentage of control)-time curve and in Area under curve (**E** and **F**). *P<0.05 vs VEGF.

4.3.5 Investigate whether VEGF mediates activation of MAP kinase and PKC through TRPM7

Next we investigated whether VEGF modulates the activity of ERK1/2, p38 MAPK and protein kinase C (PKC) in hVSMCs, downstream signalling pathways of VEGFR that have been well studied in endothelial cells (496-498). Firstly, to determine the optimal time point for experiments, hVSMCs were stimulated with VEGF for different time periods and phosphorylation of ERK1/2 was checked by immunoblotting. Interestingly, we found reduction in ERK1/2 phosphorylation with maximal effect after 5 min (36% reduction) (Figure 4.5A). Next, we stimulated hVSMCs with VEGF for 5 min in the presence and absence of vatalanib, NS8593 and 2-APB. As shown in Figure 4.5, VEGF significantly reduced ERK1/2 phosphorylation (58%), effect that was not changed by VEGFR and TRPM7 inhibitors (B), however, there were no significant differences in the phosphorylation of p38 MAPK (C) and PKC (D) between groups. These findings suggest that VEGF exhibits different effects on ERK1/2 phosphorylation in VSMCs compared with endothelial cells, with mechanisms that may not involve VEGFR and TRPM7.

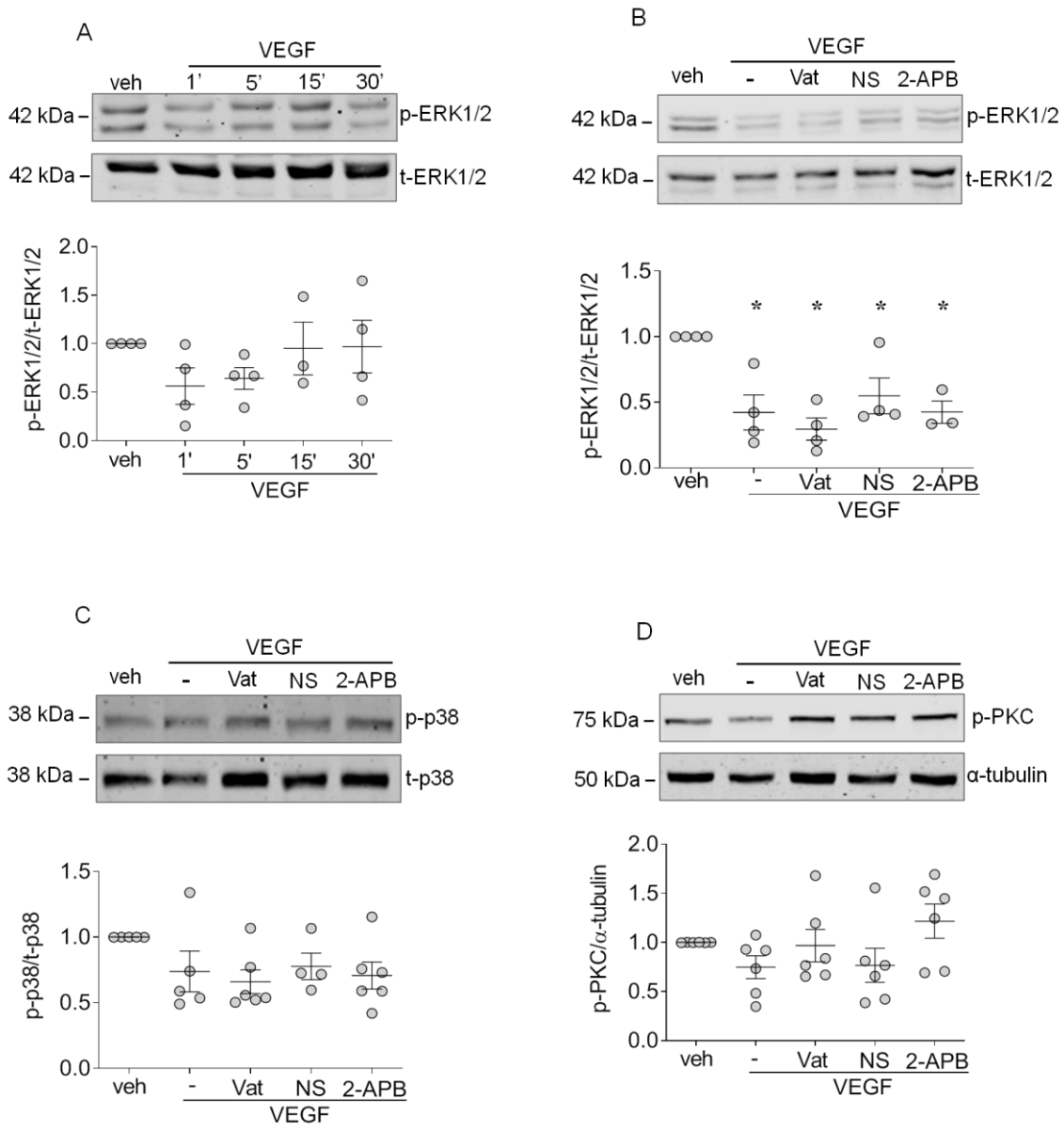

Figure 4.5 Phosphorylation of ERK1/2, p38 MAPK and PKC in hVSMCs. hVSMCs were stimulated with VEGF (50 ng/ml) for 5 min in the presence and absence of vatalanib (Vat, 1 μM), NS8593 (40 μM) and 2-APB (30 μM)**.** Protein expression and phosphorylation were assessed by immunoblotting with representative images (upper panels) and quantification (lower panels). Phosphorylation of ERK1/2 in hVSMCs after VEGF stimulation for 1, 5, 15 and 30 min (**A**). Phosphorylation of ERK1/2 (**B**), p38 MAPK (**C**) and PKC (**D**) in hVSMCs after 5 min VEGF treatment. **P*<0.05 vs vehicle (veh).

4.3.6 Effects of TRPM7 on vascular reactivity induced by VEGF in mesenteric resistance arteries

To investigate whether VEGF influences vascular reactivity, we isolated small mesenteric resistance arteries from wild type (WT) and heterozygous $TRPM7^{+/\Delta kinase}$ mice. Arteries were incubated with VEGF (50 ng/ml) or naltriben (50 μM), a pharmacological activator of TRPM7, for 30 min and vascular reactivity was assessed by wire myography. Cumulative concentration-response curves (CCRC) in response to vasoconstrictor (U46619) or vasodilators acetylcholine (ACh) and sodium nitroprusside (SNP) were used to assess vessel contraction and relaxation relatively. Pre-treatment with VEGF did not change U46619-induced vascular contraction (maximum response: WT veh 120%±6% vs VEGF 127%±9%, $p>0.05$; $TRPM7^{+/\Delta kinase}$ veh 124%±7% vs VEGF 124%±7%, $p>0.05$) (Figure 4.6A) and ACh-induced (endothelium-dependent) vascular relaxation (maximum response: WT veh 97%±3% vs VEGF 96%±5%, $p>0.05$; $TRPM7^{+/\Delta kinase}$ veh 89%±3% vs VEGF 89%±4%, $p>0.05$) (Figure 4.6B) in both WT and $TRPM7^{+/\Delta kinase}$ mice. However, VEGF-pretreated vessel was more sensitive to SNP-induced/endothelium-independent vascular relaxation in WT mice (LogEC50: veh 7±0.13 vs VEGF 7.4±0.12, $p<0.05$) and exhibited reduced maximal relaxation in $TRPM7^{+/\Delta kinase}$ mice (maximum response: veh 89%±5% vs VEGF 74%±2%, $p<0.05$) (Figure 4.6C), suggesting that VEGF might influence vessel relaxation via the TRPM7 kinase. To further confirm the involvement of TRPM7 in the regulation of vascular reactivity, vessels were pretreated with the TRPM7 activator naltriben. As shown in Figure 4.6D, naltriben-pretreated vessel was more sensitive to SNP-induced relaxation compared to vehicle (Con)-pretreated group in WT mice but not in vessels from $TRPM7^{+/\Delta kinase}$ mice (LogEC50: WT veh 7.0±0.13 vs naltriben 7.7±0.09, $p<0.05$; $TRPM7^{+/\Delta kinase}$ veh 6.8±0.15 vs naltriben 7.1±0.11, $p>0.05$).

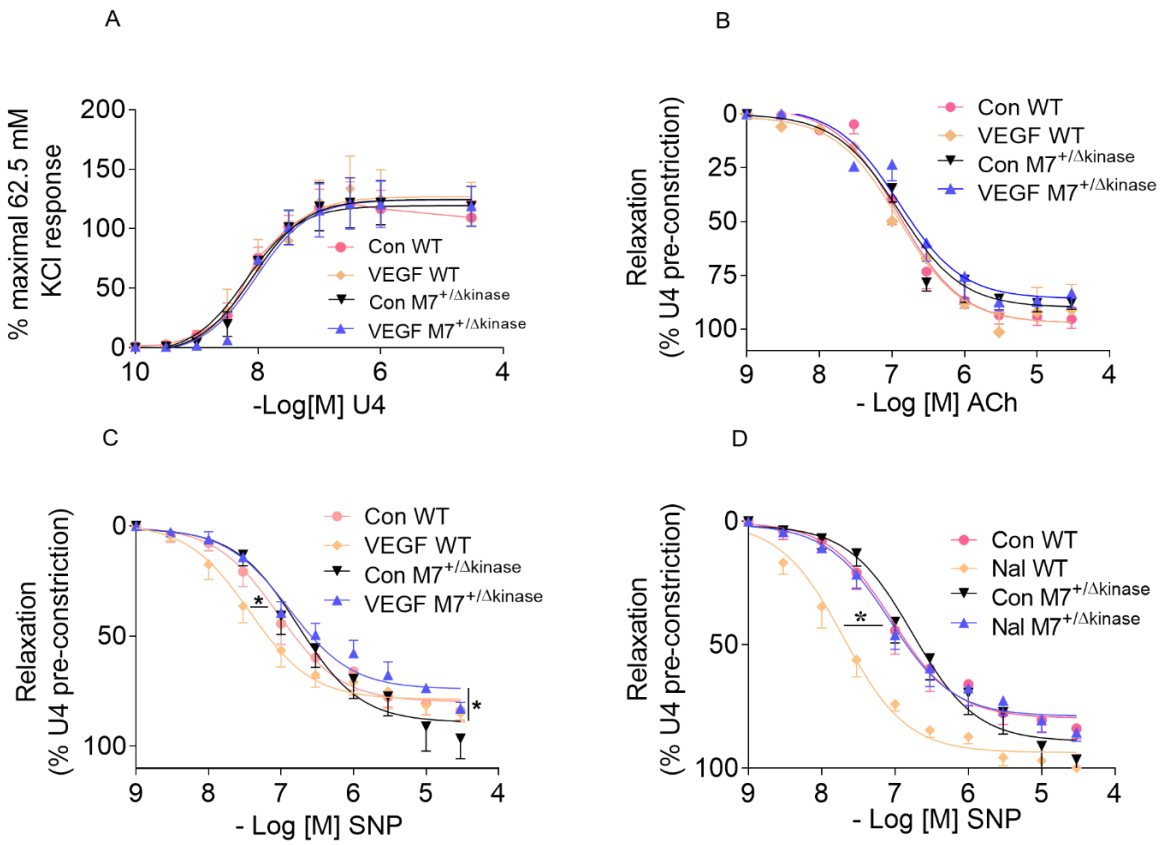

Figure 4.6 Vascular reactivity induced by VEGF in WT and TRPM7$^{+/\Delta kinase}$ mice. Isolated vessels were treated with vehicle (Con), EGF (50 ng/ml) or naltriben (Nal, 50 µM) for 30 min and vascular reactivity was assessed by wire myography. Cumulative concentration-response curve (CCRC) was performed in response to the vasoconstrictor U46619 (U4) and results were expressed as a percentage of the maximal response to 62.5 mM KCl (**A**). CCRC in response to the vasodilator acetylcholine (ACh) (**B**). CCRC in response to the vasodilator sodium nitroprusside (SNP) in vessels pretreated with vehicle (Con), VEGF (**C**) and naltriben (**D**). Results were expressed as a percentage of relaxation relative to the presumed maximum relaxation. n=4-5. *P<0.05 vs vehicle (Con) counterparts.

4.4 Discussion

Major findings from this chapter demonstrate that in human VSMCs: 1) VEGF regulates TRPM7 expression, phosphorylation and trafficking through VEGFR; 2) regulation of TRPM7 by VEGF mediates Mg^{2+} influx and Ca^{2+} homeostasis and 3) VEGF affects endothelium-independent vasodilation in a TRPM7 kinase-mediated manner. Taken together, these data highlight an important role for VEGF which involves the bifunctional chanzyme TRPM7, in the regulation of cation homeostasis in VSMCs and vascular relaxation.

TRPM7 was established as a membrane-bound ion channel, however, Clapham and colleagues found that TRPM7 is most abundant as intracellular vesicles (66). In this study, we isolated membrane-rich fractions from VSMCs lysate by ultracentrifugation and showed that TRPM7 was expressed in the membrane-rich fractions, which was upregulated by VEGF with a maximal effect at 5 min. The expression, phosphorylation and trafficking may contribute differently to the functional effects of TRPM7 in VSMCs, which still requires further investigation.

Our group has previously identified TRPM7 as a functionally important regulator of Mg^{2+} homeostasis in VSMCs, playing a role in angiotensin II (Ang II)-induced Mg^{2+} influx (2). The critical role of TRPM7 in the regulation of Mg^{2+} was further supported by recent advances in the cyro-electron microscopy (cyro-EM) structure elucidation of mouse TRPM7, which shows that the centre of the TRPM7 conduction pore is occupied by partially hydrated Mg^{2+} ions (42). In addition to TRPM7, we also found that MagT1, another important Mg^{2+} transporter with important role in Mg^{2+} influx was also increased after VEGF stimulation, and whether MagT1 contributes the Mg^{2+} influx observed here is still elusive. TRPM7 is also an important Ca^{2+} permeable channel. In cardiac fibroblasts TRPM7 is functionally active and controls both Mg^{2+} and Ca^{2+} influx induced by Ang II at different time periods (69). In neuroblastoma cells, activated TRPM7 following bradykinin stimulation mediates Ca^{2+} influx in a kinase-independent manner (84). Here, we found that VEGF induces elevation of intracellular Ca^{2+} concentration in a TRPM7-mediated manner.

Calpain-2 is a Ca^{2+} dependent cysteine protease, which remains inactive in the cytosol. In response to increased intracellular Ca^{2+} level, calpain-2 translocates to cell membrane, where it undergoes autoproteolysis with removal of 9 to 15 amino acids of the N-terminus domain (171, 183). Many studies have built a reverse association between calpain-2 activity and endothelial function (171, 499). Our data showed that short-term treatment

with VEGF reduced the presence of capain-2 in cell membranes, indicating a reduced calpain-2 activity. Although Su et al. pointed out that TRPM7 overexpression was associated with increased calpain-2 activity in HEK-293 cells, there is still a lack of detailed information of how TRPM7 regulates calpain-2, and whether the TRPM7 α-kinase directly phosphorylates capain-2 remains unclear (104). Another possibility is that the increased intracellular Mg^{2+} concentration would antagonise the Ca^{2+} effects on calpain-2 activation.

TRPM7 plays a critical role in cardiovascular system. Clapham et al. found that early cardiac-targeted knockout of TRPM7 impaired ventricular function, conduction and repolarization (138). Our previous study showed that TRPM7 kinase deficiency resulted exaggerated hypertension, pronounced cardiac hypertrophy and worsened left ventricular function in Ang II treated mice (77). In addition, vasoactive agents such as aldosterone, angiotensin II and bradykinin have been involved in the regulation of TRPM7 activity, including channel function, plasma membrane expression and substrates activation (77, 130, 500). In the current study, we showed that VEGF increases the sensitivity of vascular relaxation in response to SNP (endothelium-independent) only in WT mice, while in TRPM7 kinase-deficient mice, VEGF impairs maximal relaxation of vessels in response to SNP, suggesting that VEGF influences vascular relaxation in a TRPM7 kinase-dependent manner. The involvement of TRPM7 in the regulation of vascular reactivity was also confirmed by the finding that vessels pretreated with naltriben, the pharmacological TRPM7 activator, are more sensitive to SNP induced relaxation, and the effect was not observed in TRPM7 kinase-deficient mice. Interestingly, similar effects were not observed for ACh-induced vascular relaxation. It is worth noting that mechanisms underlying SNP- and ACh- induced vascular response are different. ACh has been shown to relax vessels through endothelial release of both NO and endothelium-derived hyperpolarizing factor (EDHF) (501), whereas SNP induces vascular smooth muscle relaxation with mechanisms involving a decrease in intracellular Ca^{2+} concentration and a reduction of the sensitivity of the contractile apparatus to Ca^{2+} (502). Thus, further studies can be performed to explore whether TRPM7-meidated Ca^{2+} is specifically involved in SNP-induced vascular relaxation. In addition, Bonaventura *et al.* demonstrated that the relaxation and Ca^{2+} decrease induced by SNP in VSMCs is potentiated by endothelial production of NO (450), and several studies reported that endothelium exerts an inhibitory effects on the vasodilation induced by SNP (503). Thus, it would be necessary to expand the study using

endothelium-denuded vessels, to better understand the role of VEGF and TRPM7 in vascular relaxation.

In summary, the present study provides new data on the regulation of TRPM7 by VEGF in VSMCs. Our data indicate that TRPM7 is expressed in the cell membrane and is positively regulated by VEGF/VEGFR. The process is functionally linked to vascular Mg^{2+} and Ca^{2+} homeostasis and cellular translocation of calpain-2 and may have an important role in the modulation of vascular relaxation. In particular VEGF-induced vasorelaxation seems to require functional TRPM7, because TRPM7 deficiency was associated with impaired VEGF-induced vasorelaxation. Exact mechanisms underlying this are unclear but seem to be endothelium-independent and likely involve altered signalling in vascular smooth muscle cells as we demonstrate in this study.

Chapter Five

5 Investigating the potential role of vascular TRPM7 in hypertension and preeclampsia

5.1 Overview

5.1.1 The EGFR-TRPM7-ERK1/2 pathway and hypertension

Hypertension or high blood pressure (BP) is a chronic disease manifesting as elevated arterial blood pressure. According to the Seventh Joint National Committee Guidelines, hypertension is defined as a systolic blood pressure ≥140 mmHg and/or a diastolic pressure ≥ 90 mm Hg and patients with systolic BPs between 130 and 139 mmHg are classified as high normal or prehypertensive (478, 479). Despite many decades of research, the aetiology stills remains unknown in >95% of patients with hypertension, hence termed essential hypertension (504). However, alterations in the vascular system seem to play a major pathophysiological role (505). In previous chapters we established the importance of the EGFR-TRPM7-ERK1/2 pathway in the regulation of VSMC function. Importantly, components of this pathway, including the EGF-EGFR ligand-receptor system, TRPM7 and ERK1/2 have all been associated with the regulation of blood pressure.

EGF was first demonstrated as a vasoconstrictor in 1985 when Berk et al. reported that EGF was able to induce contraction of rat aortic strips with a maximum extent equivalent to 40% of that caused by Ang II (319). The vasoconstrictive effect of EGF was also confirmed in experimental model of hypertension by mechanisms dependent on L-type voltage-gated calcium channel (318, 320). Studies focusing on the EGF receptor (EGFR) show consistent results: enhanced EGFR activity was observed in the cardiovascular system of spontaneously hypertensive rats (SHR), while specific knockout of EGFR in VSMCs results in arterial hypotension in mice (314, 321, 322).

TRPM7 involvement in hypertension was highlighted using a TRPM7 kinase-deficient mice ($TRPM7^{+/\Delta kinase}$) model by our group (77). These animals exhibit exaggerated Ang II-induced hypertension with amplified cardiac remodelling and left ventricular dysfunction compared to wild type (77). Additionally, $TRPM7^{+/\Delta kinase}$ mice exhibit cardiovascular inflammation and fibrosis, through mechanisms involving macrophage activation and intracellular Mg^{2+} status (461). TRPM7 was also found to contribute to the pathology of hypertension. Polotsky and colleagues demonstrated that leptin, a hormone that plays an important role in obesity-related hypertension, induces high blood pressure through activating TRPM7 in carotid bodies (506).

ERK1/2 belongs to the mitogen-activated protein kinase (MAPK) family and increased ERK activity has been demonstrated in various animal models of hypertension (472, 507). Mechanisms whereby ERK1/2 is involved in contraction are related to

phosphorylation of myosin light chain (MLC) (472, 508). The phosphorylated MLC forms cross-bridge with actin, resulting in phosphorylated actomyosin, which leads to muscle contraction (509). Moreover, ERK1/2 can cause vascular contraction through the phosphorylation of caldesmon, an actin-binding protein that inhibits the adenosine triphosphatase activity of actomyosin. Upon ERK1/2-induced phosphorylation, the activity of caldesmon is reduced leading to removal of the inhibitory effect on adenosine triphosphate (472).

5.1.2 VEGF, magnesium and preeclampsia

Preeclampsia (PE) is a clinical syndrome characterized by new-onset of hypertension and proteinuria after 20 weeks of gestation (510). Based on the time of onset, PE can be classified as early onset PE (<34 weeks of gestation) and late onset PE (>34 weeks of gestation) (511), which affects 2%-8% pregnancies and is responsible for around 14% of maternal deaths (512). PE can progress to eclampsia, which represents the consequence of brain injury caused by PE and manifests as new onset of generalized tonic colonic seizures (355). PE carries an increased risk for the mother to develop cardiovascular disease. A recent study based on a large UK pregnancy cohort showed that compared to women without hypertension in pregnancy, women affected by PE had higher hazard ratios for atherosclerosis, peripheral artery disease, atrial fibrillation, heart failure and cardiovascular deaths (513).

VEGF family members VEGF-A (VEGF) and placental growth factor (PIGF) are critically required for placental vascular formation and development during normal pregnancy. Human placental VEGF expression increases with gestational age and plays a paracrine and autocrine role in the regulation of extensive angiogenesis that occurs in late gestation (373). PIGF in the maternal circulation increases significantly from 8 weeks gestation and reaches a maximal concentration during the second trimester, when nonbranching villous angiogenesis and terminal villous formation occur (362, 375). In the context of PE, reduced bioavailability of VEGF and PIGF has been critically involved in the pathological processes. It has been demonstrated that placental ischemia resulting from incomplete spiral artery remodelling induces release of soluble vascular endothelial growth factor receptor-1 (sFlt-1), which acts as potent scavenger of VEGF and PIGF, leading to endothelial dysfunction in multiple organs (348, 362-364). Raised sFlt-1: PIGF ratio was reported in pregnant women before the onset of PE, which has been used clinically to predict the disease progression and guide treatment (378).

Magnesium sulphate ($MgSO_4$) is the drug of choice used to prevent seizures in pre-eclamptic women (514, 515). Mechanisms of action of magnesium in treating PE remain unclear. It has been proposed that magnesium acts as a vasodilator, with actions lowering total peripheral vascular resistance and protecting the blood-brain barrier (BBB) to decrease cerebral oedema formation. Additionally, Mg^{2+} acts centrally to inhibit N-methyl-D-aspartate (NMDA) receptors and provides anticonvulsant activity (393). Is was also shown that perfusion with $MgSO_4$ normalises concentrations of placental VEGF in patients with PE but has no effect on VEGF levels in normotensive placentas (394).

TRPM7 and TRPM6 were identified in the placenta of pregnant women, with predominant expression in the syncytiotrophoblast layers (395). Importantly, reduced gene expression of TRPM7 and TRPM6 were found in preeclamptic placenta tissues during preterm labour, which remained lower at term labour (395). Whether these magnesium transporters are involved in the pathophysiological processes of PE and act as potential therapeutic targets remain unclear.

In Chapters 3 and 4, we investigated the relationship between RTKs (VEGFR and EGFR) and TRPM7 and the functional implications in VSMCs under physiological conditions. In the current chapter, we will explore the RTK-TRPM7 axis under pathological conditions including hypertension and preeclampsia.

5.2 Objective and aims

Objective

The overall objectives of the studies presented in Chapter 5 are to explore whether the RTK (VEGFR and EGFR)-TRPM7 axis is dysregulated in animal models of hypertension and preeclampsia.

Specific aims

1. *To study whether EGF/EGFR regulates TRPM7 expression and activity in VSMCs in the context of hypertension*

Primary VSMCs were derived from SHRSP rat and simulated with EGF in the presence and absence of gefitinib (EGFR inhibitor), PP2 (c-Src inhibitor) and NS8593 (TRPM7 inhibitor). Phosphorylation of TRPM7 and ERK1/2 were assessed by immunoblotting.

2 *To explore the importance of the EGFR-TRPM7-ERK1/2 pathway in VSMCs from hypertensive animals*

Activity of EGFR, c-Src, TRPM7 and ERK1/2 at basal level in VSMCs from WKY and SHRSP rats was checked by immunoblotting. Ca^{2+} and Mg^{2+} homeostasis upon EGF stimulation in VSMCs from WKY and SHRSP rats were assessed by live cell microscopy and flow cytometry relatively. Cell migration was evaluated using scratch wound assay.

3. *To investigate the importance of the VEGFR/TRPM7 pathway and magnesium transporters in placenta from animal models of preeclampsia*

Placental tissues were isolated from wild type and two different animal models of PE. Activity of VEGFR2 assessed as p-VEGFR2/total VEGFR2 and expression of magnesium transporters (TRPM7, TRPM6, MagT1, SLC41A1) and TRPM7 substrates (annexin-1 and calpain-2) were examined by immunoblotting.

5.3 Results

5.3.1 The vascular EGFR-TRPM7-ERK1/2 pathway in hypertension

5.3.1.1 Activity of the EGFR-TRPM7-ERK1/2 pathway is enhanced in SHRSP VSMCs

VSMCs from SHRSP exhibited increased phosphorylation of EGFR at the autophosphorylation site tyrosine 1068 (Y1068) (2-fold), which was associated with reduced expression of total EGFR (58%) compared to WKY (Figure 5.1A and B). Next, we investigated the activity of c-Src kinase, at the inhibitory tyrosine phosphorylation site 527 (Y527) which is associated with an inactive c-Src conformation (516). There was significantly reduced phosphorylation of c-Src at Y527 in VSMCs from SHRSP rats (62%), indicating enhanced c-Src activity (Figure 5.1C). Basal level of ERK1/2 phosphorylation was also increased in VSMCs from SHRSP rats (70%) compared to WKY (Figure 5.1D).

To assess activity and amounts of TRPM7, we examined both TRPM7 phosphorylation and expression levels in VSMCs from WKY and SHRSP rats. As shown in Figure 5.2A and B, there were significant increase of TRPM7 phosphorylation (93%) and expression (1.1-fold) in VSMCs from SHRSP compared to WKY rats. In addition, we also checked expression of TRPM7 substrates calpain-2 and annexin-1. Increased expression of calpain-2 (73%) and decreased expression of annexin-1 (61%) were observed in VSMCs from SHRSP relative to WKY (Figure 5.2C and D).

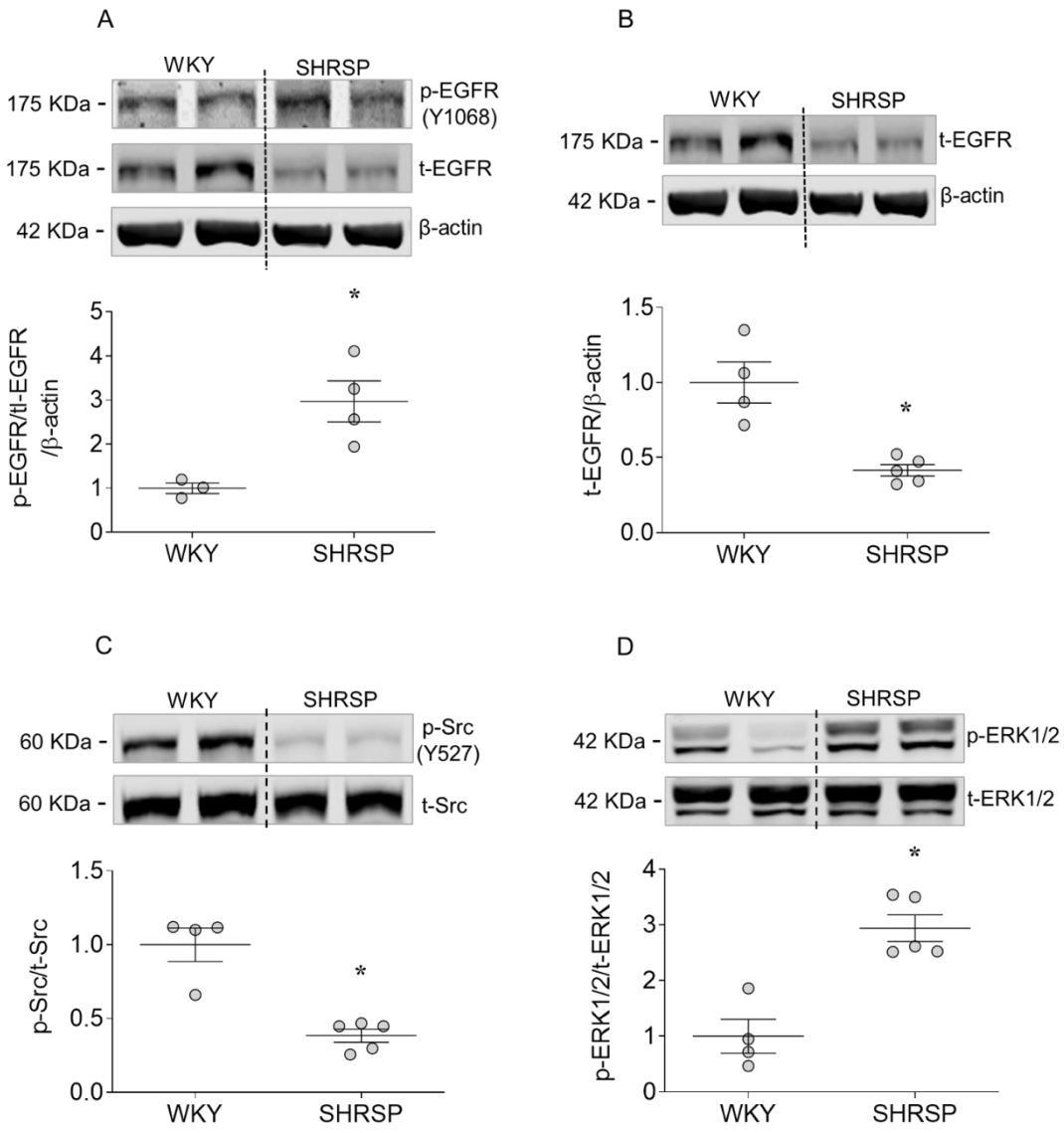

Figure 5.1 Activity of EGFR, c-Src and ERK1/2 in VSMCs from WKY and SHRSP rats. Protein expression and phosphorylation levels in VSMCs derived from WKY and SHRSP rats were examined by immunoblotting, with representative images (upper panels) and quantification (lower panels). Phosphorylation of EGFR (p-EGFR) at tyrosine 1068 (Y1068) was normalised by total EGFR (t-EGFR) and β-actin (**A**). Total EGFR expression was normalised by β-actin(**B**). Phosphorylation of c-Src (p-Src) at the tyrosine phosphorylation site 527 (Y527) (**C**) and phosphorylation of ERK1/2 (p-ERK1/2) (**D**) were normalised by total protein expression. **P*<0.05 compared to WKY.

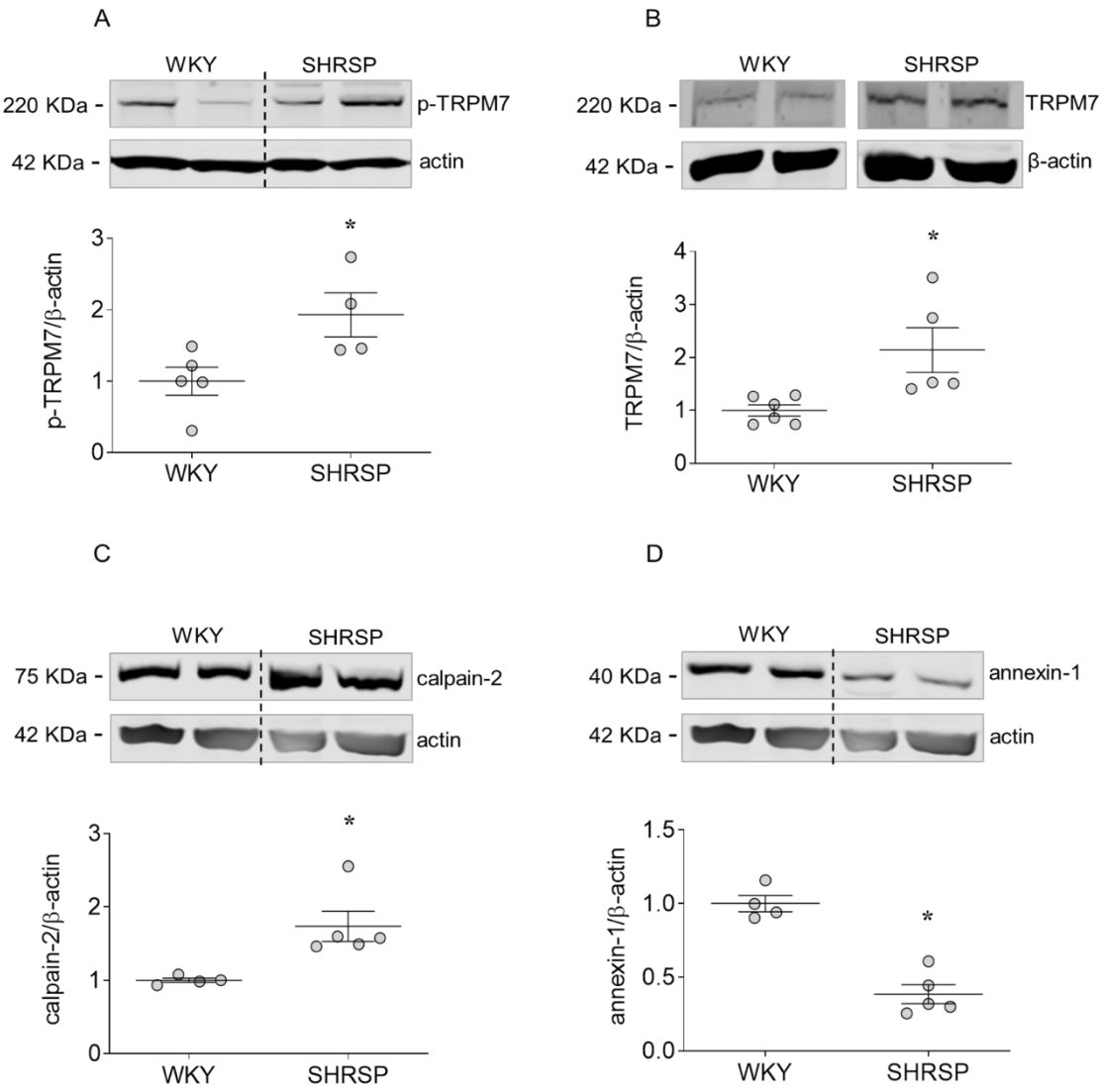

Figure 5.2 Dysregulation of TRPM7 and its substrates in VSMCs from SHRSP rats. Protein expression and phosphorylation levels in VSMCs derived from WKY and SHRSP rats were examined by immunoblotting, with representative images (upper panels) and quantification (lower panels). Phosphorylation of TRPM7 (p-TRPM7) (**A**) and protein expression of TRPM7 (**B**), calpain-2 (**C**) and annexin-1 (**D**) in primary VSMCs derived from WKY and SHRSP rats. Results were normalised by β-actin. **P*<0.05 compared to WKY.

5.3.1.2 The effects EGFR-TRPM7-ERK1/2 pathway in VSMCs from SHRSP

In chapter 3, we demonstrated that EGFR interacts with TRPM7 at cell membranes in a c-Src dependent manner, which consequently mediates activation of ERK1/2 in VSMCs. Here, we studied the importance of this pathway in VSMCs derived from SHRSP rats, a well-known animal model of essential hypertension (517). As shown in Figure 5.3A, EGF stimulation (5 min) enhanced phosphorylation of TRPM7 (27%), effects that were reduced by c-Src inhibitor, PP2 (61%) and EGFR inhibitor gefitinib (40%). EGF also significantly increased the phosphorylation of ERK1/2 (2-fold) and the effect was attenuated by gefitinib (21%). There was a trend to reduced ERK1/2 phosphorylation in cells pretreated with the TRPM7 inhibitor NS8593 (14%) compared to EGF, however, there was no differences in cells pretreated with apamin (Figure 5.3B). Both apamin and NS8593 inhibit calcium activated potassium (SK) channels (518), and thus apamin was used to exclude the involvement of SK channel. Treatment with EGF did not change the phosphorylation of p38 MAPK and no further changes were observed in cell pretreated with gefitinib or NS8593 (Figure 5.3C).

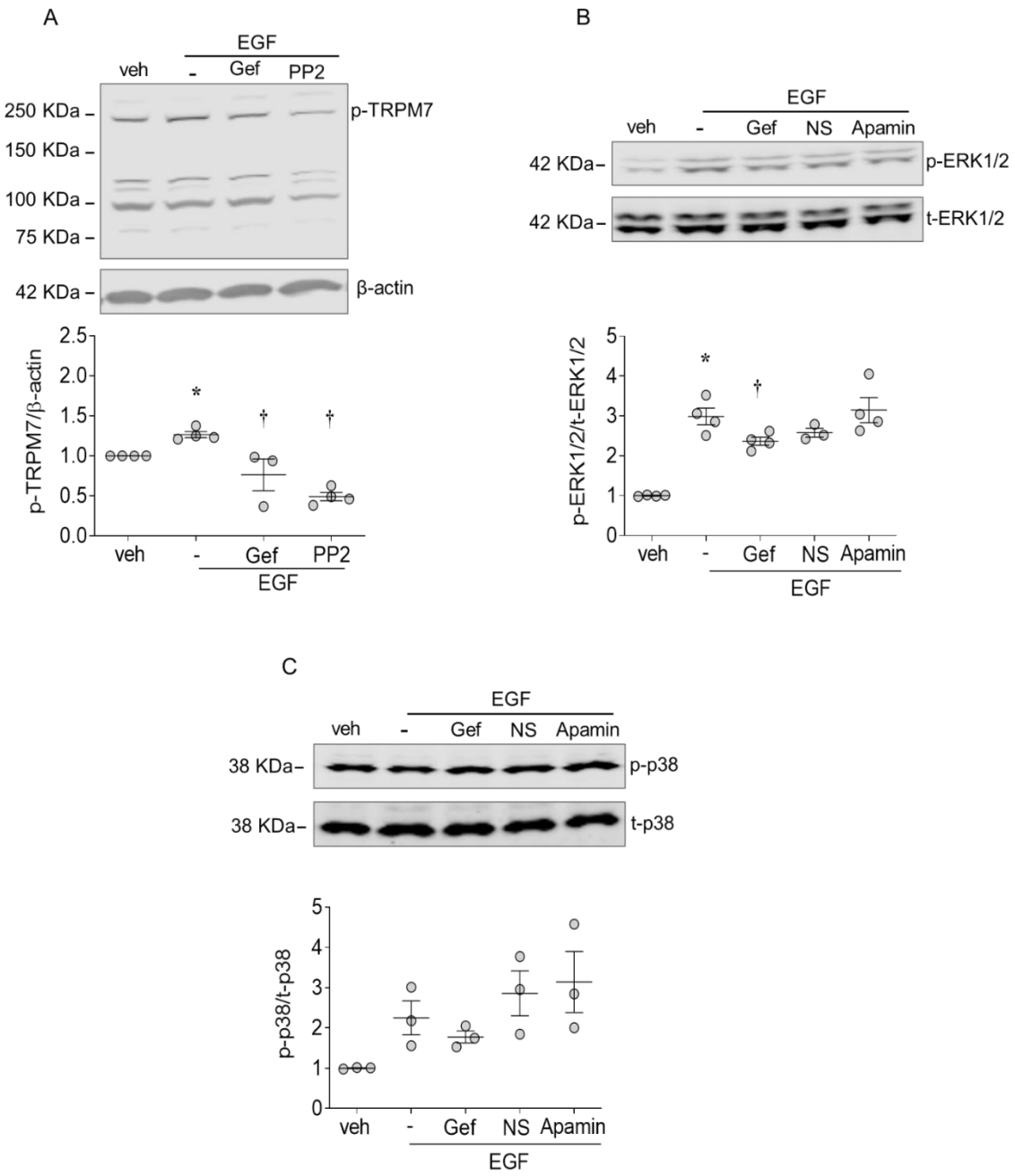

Figure 5.3 EGF regulates TRPM7 through EGFR and c-Src leading to ERK1/2 phosphorylation. rVSMCs derived from SHRSP rat were treated with EGF (50 ng/ml) for 5 min in the presence and absence of gefitinib (Gef, 1 μM), PP2 (10 μM), NS8593 (NS, 40 μM), and apamin (1 μM). Protein expression and phosphorylation levels were examined by immunoblotting, with representative images (upper panels) and quantification (lower panels). Phosphorylation of TRPM7 (p-TRPM7) was normalised using the house keeping protein β-actin (**A**). Phosphorylation of ERK1/2 (p-ERK1/2) (**B**) and p38 MAPK (p-p38) (**C**) was normalised by the total protein expression. **P*<0.05 compared to vehicle (veh) and † P<0.05 compared to EGF.

5.3.1.3 The effects of TRPM7 on Ca^{2+} and Mg^{2+} mobilisation induced by EGF in VSMCs from SHRSP

We have shown that EGF significantly increased intracellular Ca^{2+} levels ($[Ca^{2+}]_i$) in VSMCs from WKY rats and the effects were attenuated by the non-specific TPRM7 inhibitor 2-APB, but not NS8593, a well-known potent inhibitor for TRPM7 (Figure 5.4A). Since 2-APB also inhibits other Ca^{2+} channels such as TRPM2 (482), our data suggest that there might be alternative mechanisms contributing to EGF-induced Ca^{2+} mobilisation in VSMCs from normotensive rats. Experiments were repeated in VSMCs from SHRSP rats under similar conditions described in Chapter 3. As shown in Figure 5.4B, EGF stimulation increased intracellular Ca^{2+} concentration. These effects were attenuated by gefitinib ($p=0.06$) and abolished by NS8593 and 2-APB, suggesting that TRPM7 is involved in this process.

We also compared the regulation of Mg^{2+} homeostasis by EGF in VSMCs from WKY and SHRSP rats. At basal level there was reduced intracellular Mg^{2+} in VSMCs from SHRSP (61%) compared to WKY (Figure 5.5A). EGF exerts similar effects on intracellular free Mg^{2+} in VSMCs from the two rat strains. As shown in Figure 5.5B and C, in VSMCs from WKY and SHRSP rats, EGF increased intracellular Mg^{2+} and the effect was attenuated by pharmacological inhibitors of EGFR (gefitinib) and TRPM7 (NS8593 and 2-APB), but not by the SK channel inhibitor apamin.

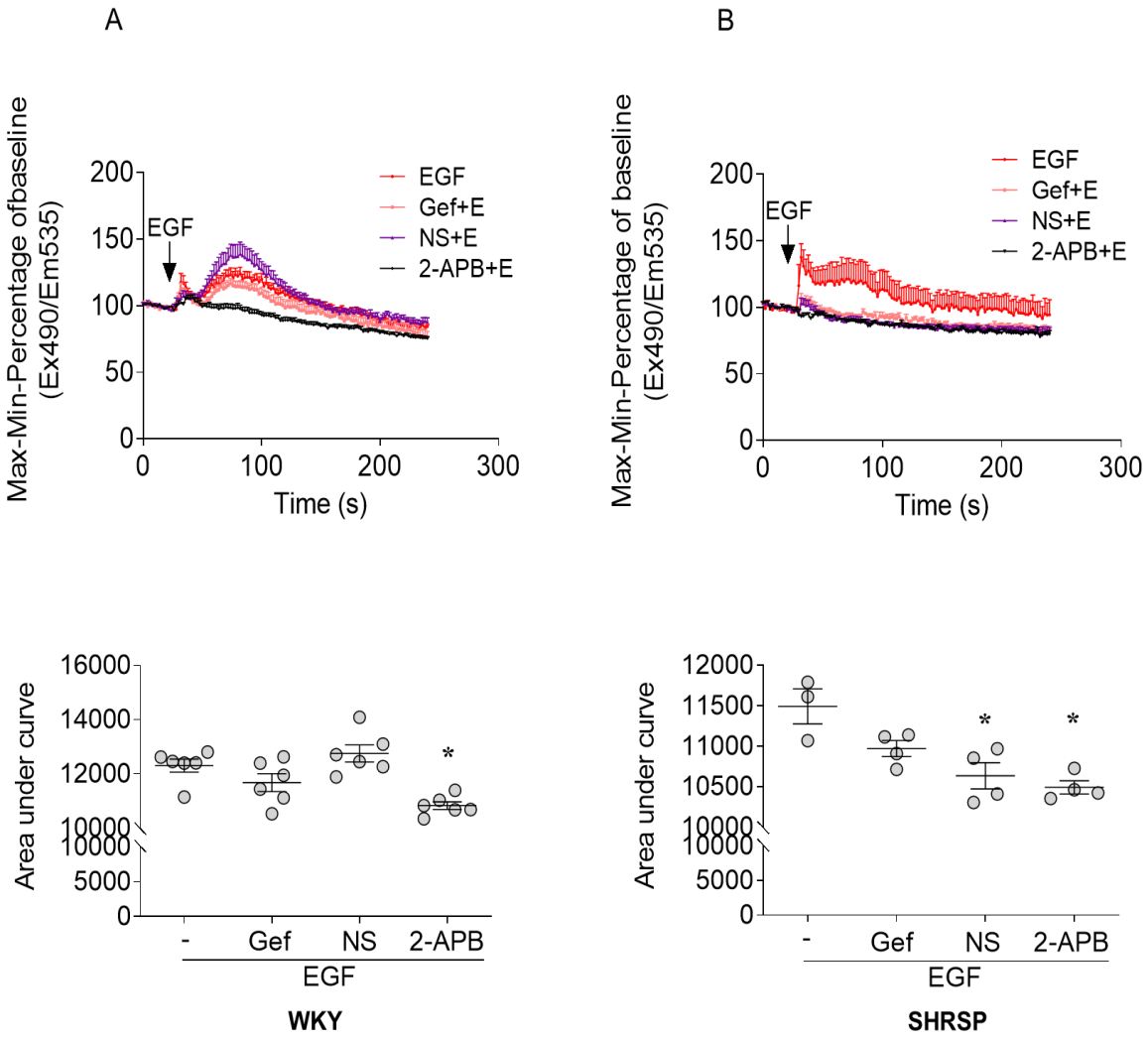

Figure 5.4 EGF-induced Ca^{2+} mobilization is enhanced through TRPM7 in VSMCs from SHRSP. In rVSMCs derived from WKY (**A**) and SHRSP (**B**) rats, intracellular Ca^{2+} levels induced by EGF (50 ng/ml) were measured in the presence and absence of gefitinib (Gef, 1 µM), NS8593 (NS, 40 µM) and 2-APB (30 µM). Data are expressed in Fluorescent Cal-520AM-Ca^{2+} signals (percentage of baseline)-time curve (Upper panel) and in Area under curve (Lower panel). **P*<0.05 compared to EGF.

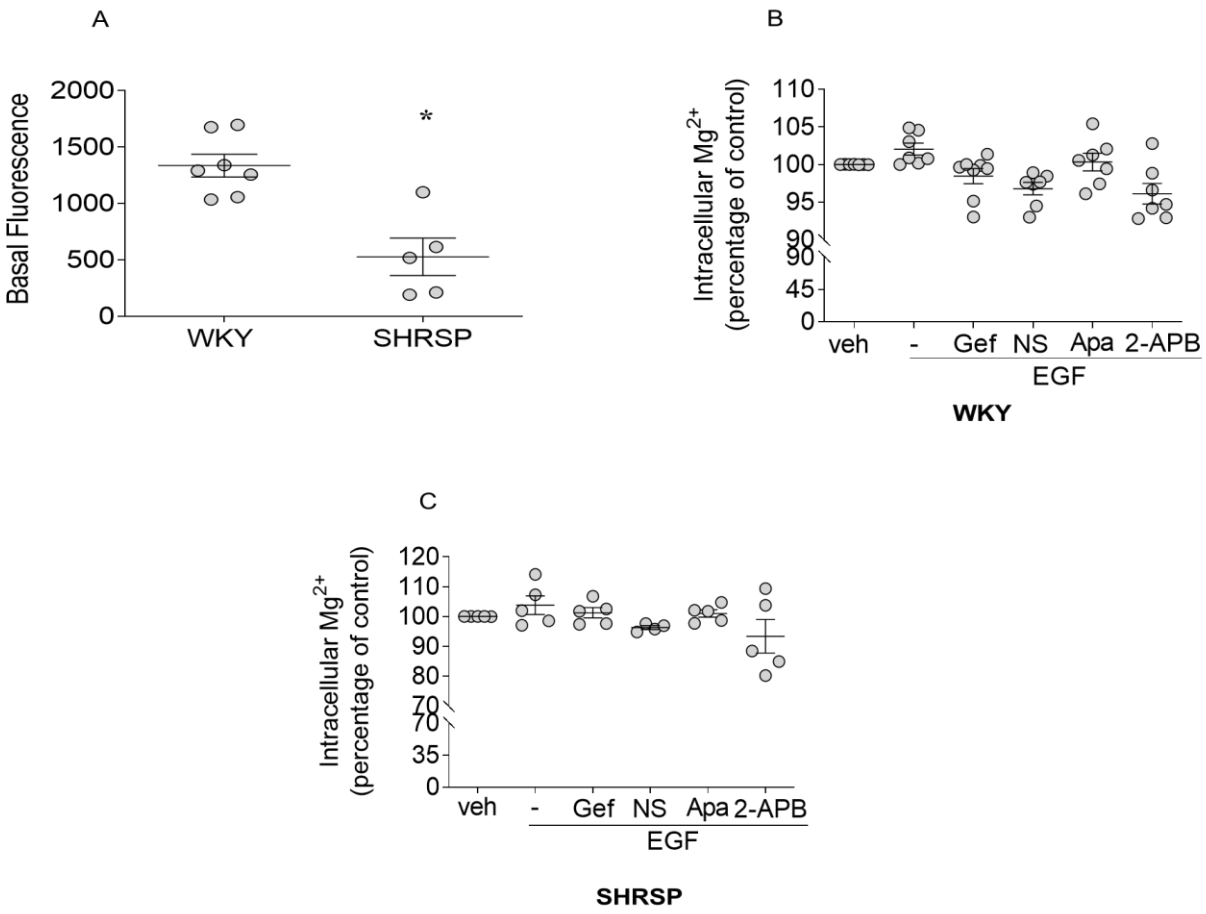

Figure 5.5 EGF mediates Mg^{2+} homeostasis in a similar manner in VSMCs from WKY and SHRSP. Basal levels of Magnesium Green fluorescence indicating intracellular Mg^{2+} concentration were measured in VSMCs from WKY and SHRSP rats (**A**). In VSMCs from WKY (**B**) and SHRSP (**C**) rats, intracellular free Mg^{2+} concentration ($[Mg^{2+}]i$) after EGF (50 ng/ml) treatment (5 min) in the presence and absence of gefitinib (1 μM), NS8593 (NS, 40 μM) , apamin (Apa, 1 μM) and 2-APB (30 μM) were measured by flow cytometry using Magnesium Green. **P*<0.05 compared to WKY.

5.3.1.4 The effects of TRPM7 on cell migration and proliferation induced by EGF in VSMCs from SHRSP rats

Although the number of experiments is low, we found that at basal levels there might be a trend of increased cell migration in VSMCs from SHRSP compared to WKY rats. EGF might further enhance the cell migration, effects that were blunted by pretreatment with gefitinib, NS8593 and PD98059 (Figure 5.6A). There might be a trend of increased cell proliferation after EGF treatment (20%) in VSMCs from SHRSP and the effect was attenuated by gefitinib (20%), NS8593 (71%) and PD98059 (20%) (Figure 5.7A). Sample size was small in these studies, and experiments need to be repeated before any clear conclusions can be drawn.

Next we questioned whether blocking EGFR with gefitinib could attenuate activity of the downstream TRPM7 and ERK1/2 in VSMCs from SHRSP rats. As shown in Figure 5.8A and B, short-term (5 min) treatment with gefitinib significantly reduced phosphorylation of TRPM7 (54%) and ERK1/2 (24%) in VSMCs derived from SHRSP. Gefitinib treatment also decreased ERK1/2 phosphorylation (35%) in VSMCs from WKY rats (Figure 5.8C).

5.3.1.5 The effects of TRPM7 on cell migration induced by EGF in VSMCs from hypertensive patients

Primary VSMCs were isolated as we previously described (477). As shown in Figure 5.9A, at basal level there was a trend of increased cell migration in VSMCs derived from hypertensive patients compared to that of normotensive patients. EGF might further enhance cell migration and the effect was attenuated by gefitinib, NS8593 and PD98059. In addition, we also tested the role of Ca^{2+} in EGF-induced cell migration. Pretreatment with the Ca^{2+} chelator EGTA (2 mM) might blunt EGF-induced migration in VSMCs from hypertensive patients (Figure 5.9A).

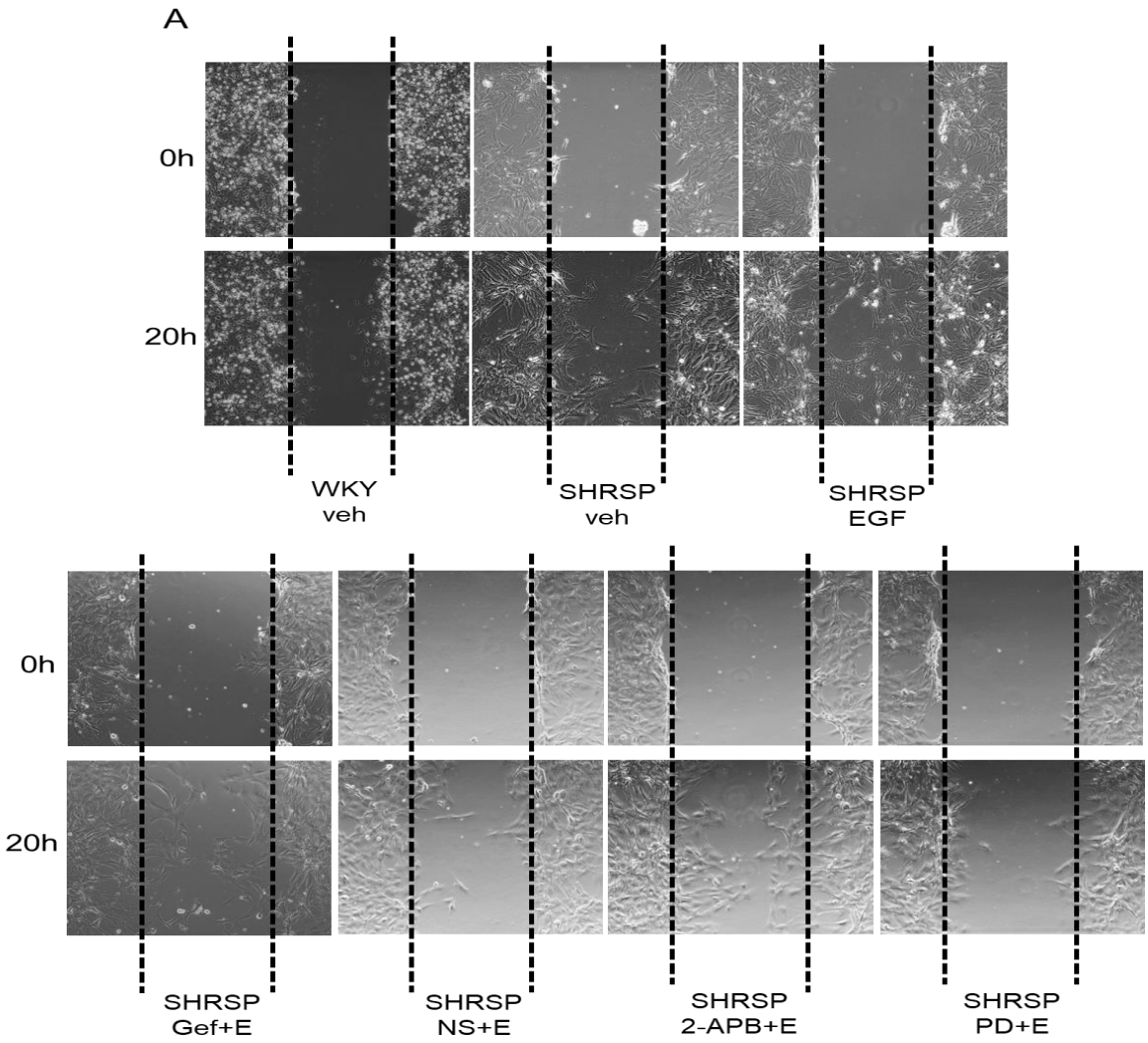

Figure 5.6 EGF-induced cell migration might be enhanced through TRPM7 and ERK1/2 in VSMCs from SHRSP rats. VSMCs derived from SHRSP rats were stimulated with EGF (50 ng/ml) for 20 h in the presence and absence of gefitinib (Gef, 1μM), NS8593 (NS, 40 μM), 2-APB (30 μM) and PD98059 (PD, 20 μM). VSMCs migration was assessed by Scratch-wound assay, with representative images at the 0 h and 20 h time points from 2-4 independent experiments.

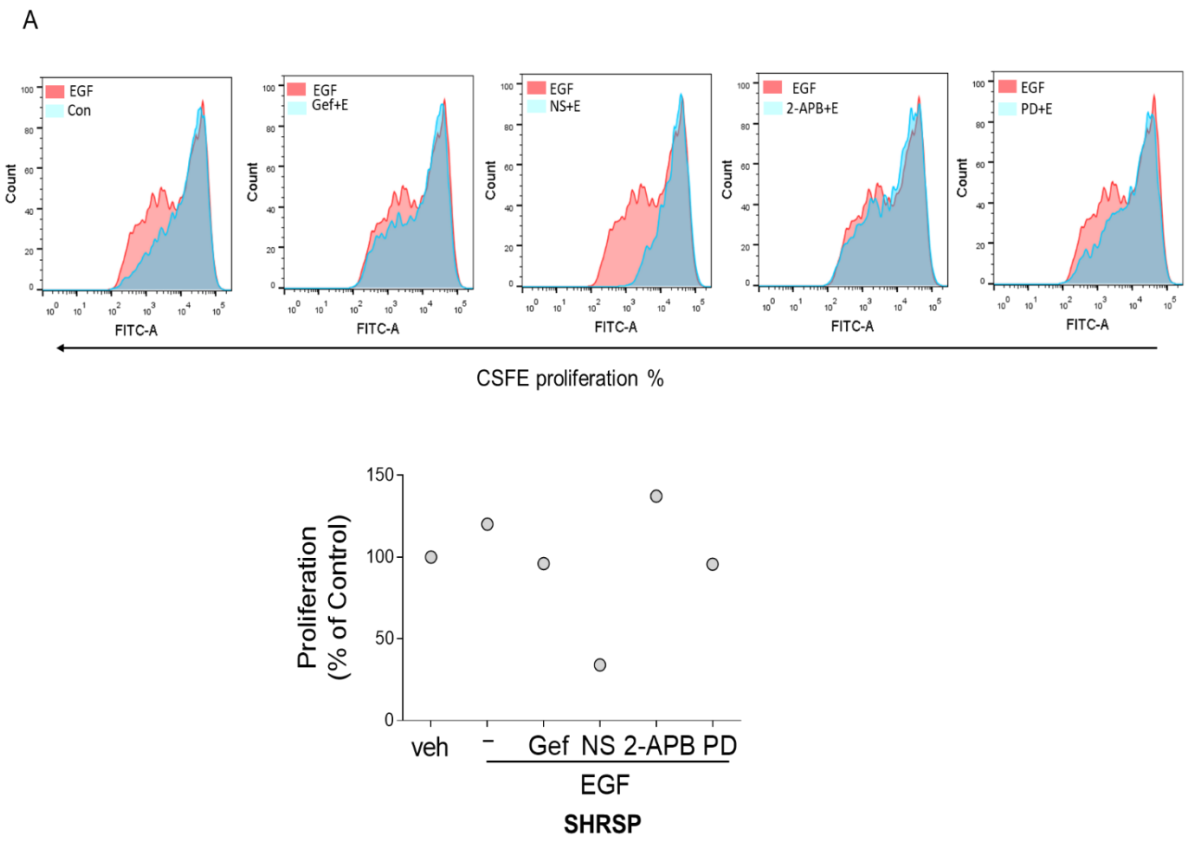

Figure 5.7 EGF-induced proliferation in VSMCs from SHRSP rats. VSMCs derived from SHRSP rats were stimulated with EGF (50 ng/ml) for 72 h in the presence and absence of gefitinib (Gef, 1 µM), NS8593 (NS, 40 µM), 2-APB (30 µM) and PD98059 (PD, 20 µM). VSMCs proliferation was examined by CFSE assay using flow cytometry. Upper panel: Representative flow cytometry histograms. Lower panel: Quantification of proliferation rate (percentage of control). Results are from 1 independent experiment.

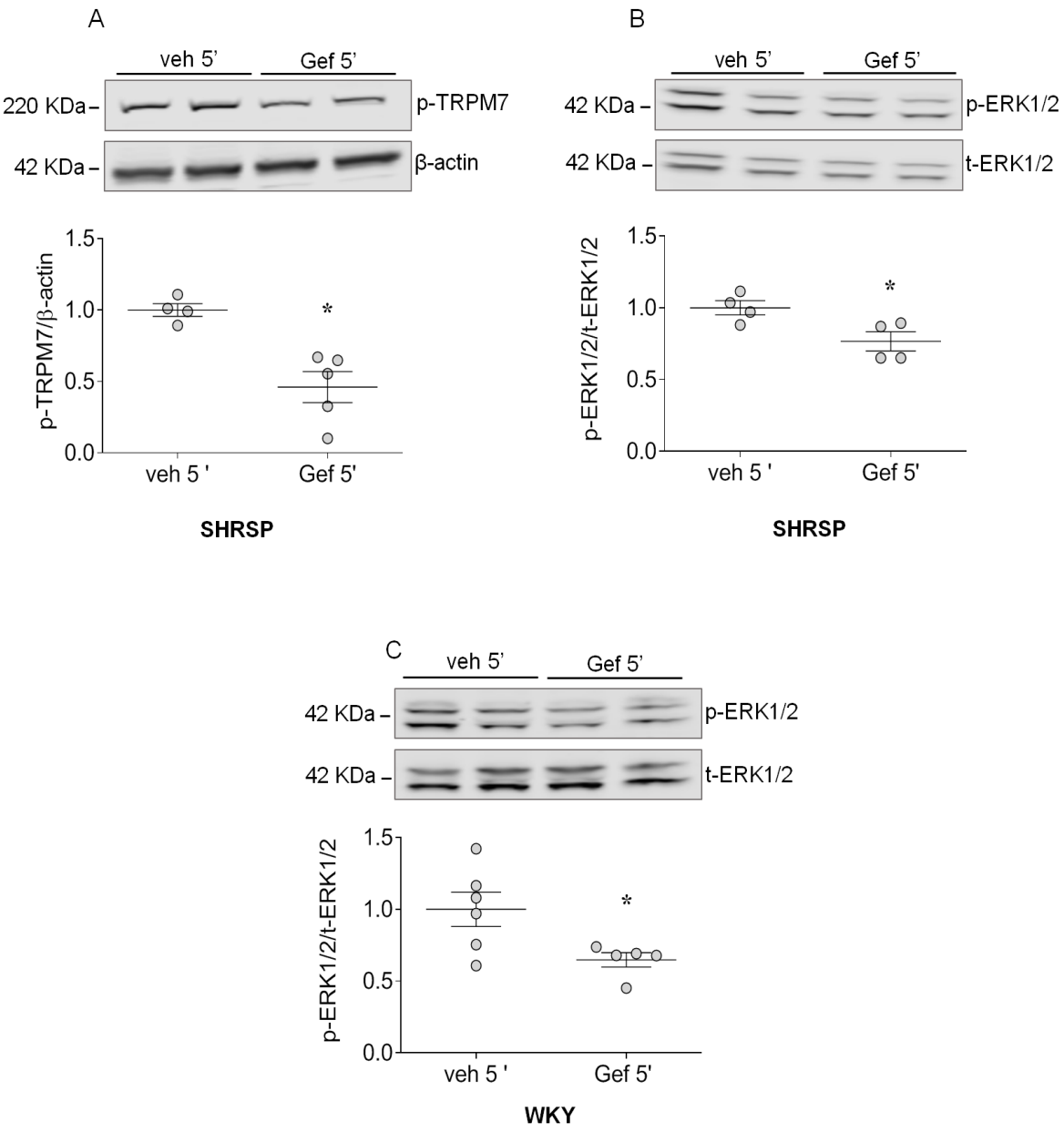

Figure 5.8 Gefitinib attenuates phosphorylation of TRPM7 and ERK1/2 in VSMCs from WKY and SHRSP rats. VSMCs derived from WKY and SHRSP rats were treated with vehicle or gefitinib (Gef, 1 μM) for 5 min. Protein expression and phosphorylation levels were examined by immunoblotting, with representative images (upper panels) and quantification (lower panels). Phosphorylation of TRPM7 (p-TRPM7) was normalised to the expression of β-actin (**A**). Phosphorylation of ERK1/2 (p-ERK1/2) in VSMCs from SHRSP (**B**) and WKY (**C**) rats was normalised to total ERK1/2 (t-ERK1/2). **P*<0.05 compared to vehicle treated cells (veh 5').

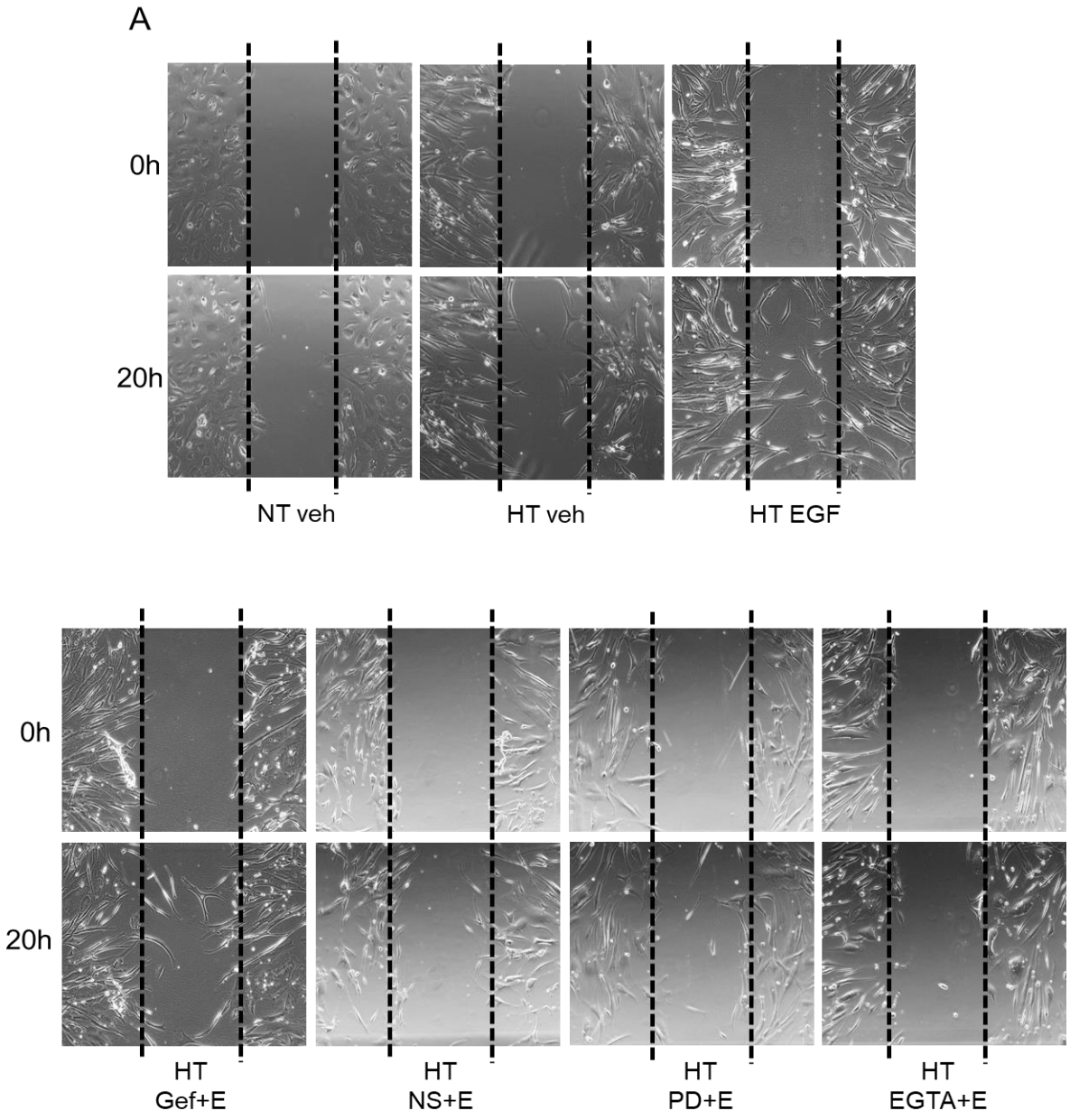

Figure 5.9 Regulation of cell migration by EGF in VSMCs from hypertensive patients. VSMCs were derived from normotensive (NT) and hypertensive patients (HT). VSMCs from HT were stimulated with EGF (50 ng/ml) for 20 h in the presence and absence of gefitinib (Gef, 1 μM), NS8593 (NS, 40 μM), PD98059 (PD, 20 μM) and EGTA (2 mM). Cell migration was assessed by Scratch-wound assay, with representative images at the 0 h and 20 h time points from 4 independent experiments.

5.3.2 The effects of VEGFR-TRPM7 pathway in preeclampsia

5.3.2.1 VEGFR phosphorylation and TRPM7 expression are reduced in a model of superimposed preeclampsia

Dysregulation of the VEGF-VEGFR system is believed to play an important role in preeclampsia development, and altered gene expression of TRPM7 has been found in preeclamptic placenta (395, 519). We have shown that VEGF exerts regulatory effects on TRPM7 through VEGFR2 in VSMCs which influences ion homeostasis and vascular relaxation. Here, we questioned whether the VEGFR2 activity is changed in the placenta tissues from pregnant SHRSP rats, a model of superimposed preeclampsia (442). Placental tissues of this animal model were kindly provided by Dr Delyth Graham and Dr Sheon Samji (University of Glasgow). We first checked the activity of VEGFR2 in the placental tissues. As shown in Figure 5.10A and B, there was reduced phosphorylation of VEGFR2 at tyrosine 951 residue (60%) associated with increased total VEGFR expression (72%) in the placental tissues from pregnant SHRSP rats compared to pregnant WKY rats.

As we demonstrated in the previous chapters, TRPM7 is a downstream target of RTKs including VEGFR and EGFR. The TRPM7 expression was significantly reduced in the placental tissues from pregnant SHRSP (28%) rats compared to WKY rats (Figure 5.11A). Additionally, no differences in protein expression of the TRPM7-kinase substrates calpain-2 and annexin-1 were observed in the two groups (Figure 5.11B and C).

5.3.2.2 TRPM6, MagT1 and SLC41A1 expression in the placental tissues

We also checked protein expression of other magnesium transporters. As shown in Figure 5.12, there was no differences in TRPM6 (**A**) expression, while there was increased expression of MagT1 (55%) (**B**) and SLC41A1 (41%) (**C**) in the placental tissues from pregnant SHRSP rats compared to pregnant WKY rats.

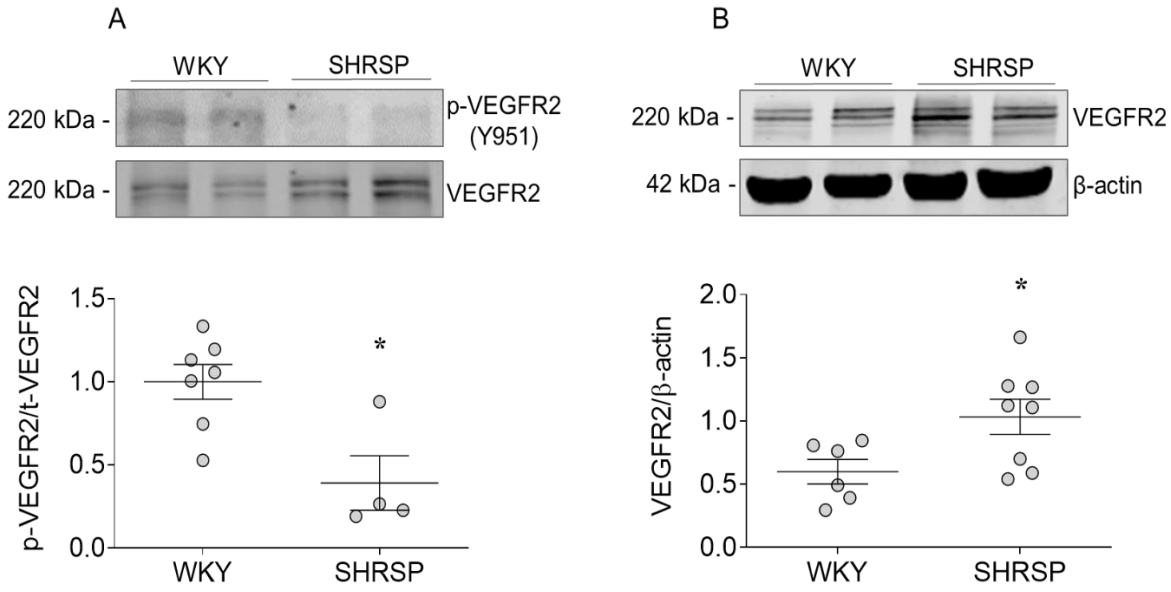

Figure 5.10 VEGFR2 phosphorylation and expression in placenta from pregnant WKY and SHRSP rats. Placental tissues were isolated from pregnant WKY and SHRSP rats. Protein expression and phosphorylation levels were examined by immunoblotting with representative images (upper panels) and quantification (lower panels). Phosphorylation of VEGFR2 (p-VEGFR2) at tyrosine 951 residue was normalised to total VEGFR2 expression (**A**). Expression of VEGFR2 was normalised by the house keeping protein β-actin (**B**). **P*<0.05 compared to WKY.

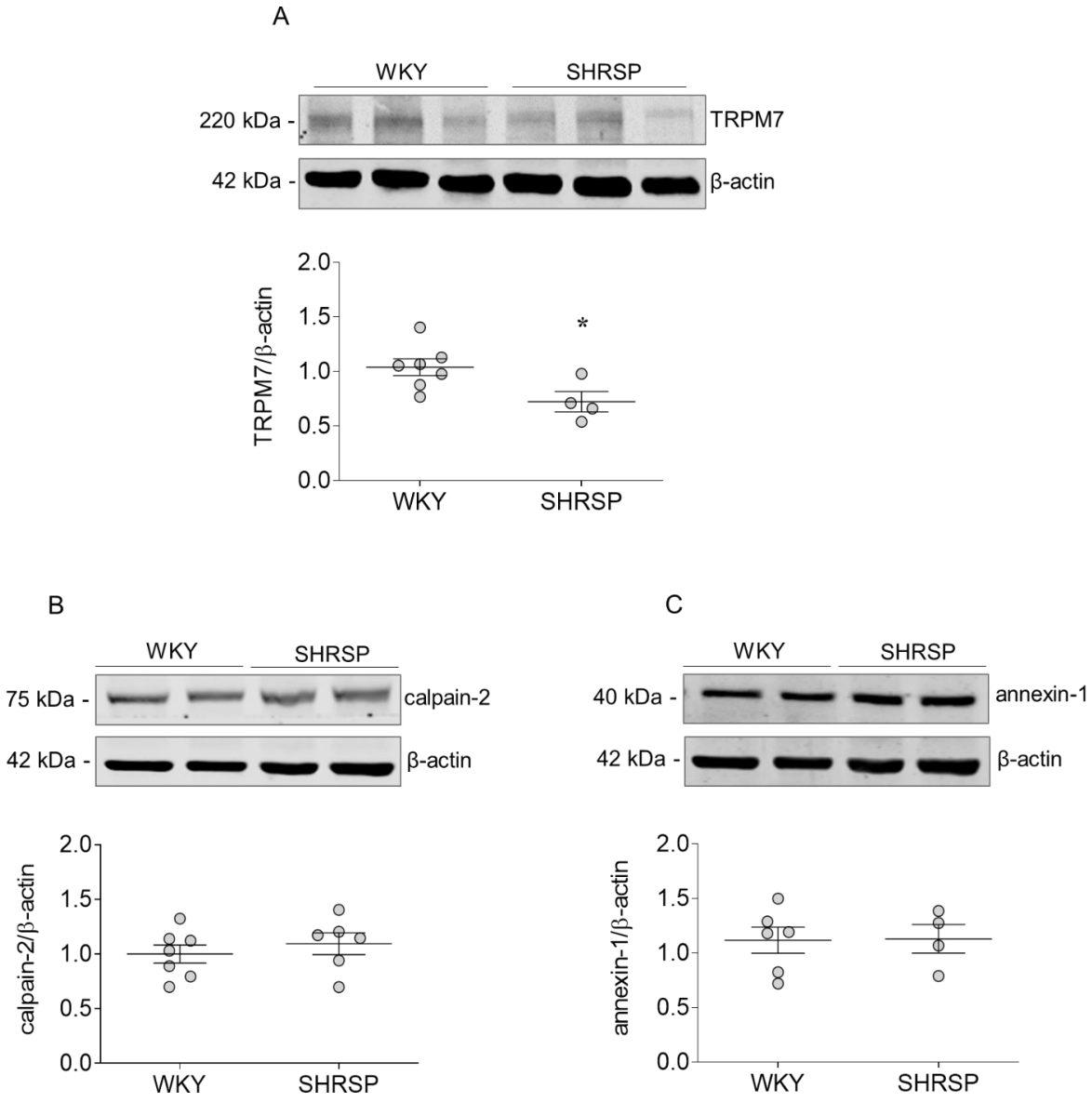

Figure 5.11 Expression of TRPM7 and its substrates in placenta from pregnant WKY and SHRSP rats. Placental tissues were isolated from pregnant WKY and SHRSP rats. Protein expression of TPPM7 (**A**) and its substrates calpain-2 (**B**) and annexin-1 (**C**) were normalised by β-actin expression. Upper panel: Representative images of immunoblotting. Lower panel: results are expressed as scatter-plot graphs. **P*<0.05 compared to WKY.

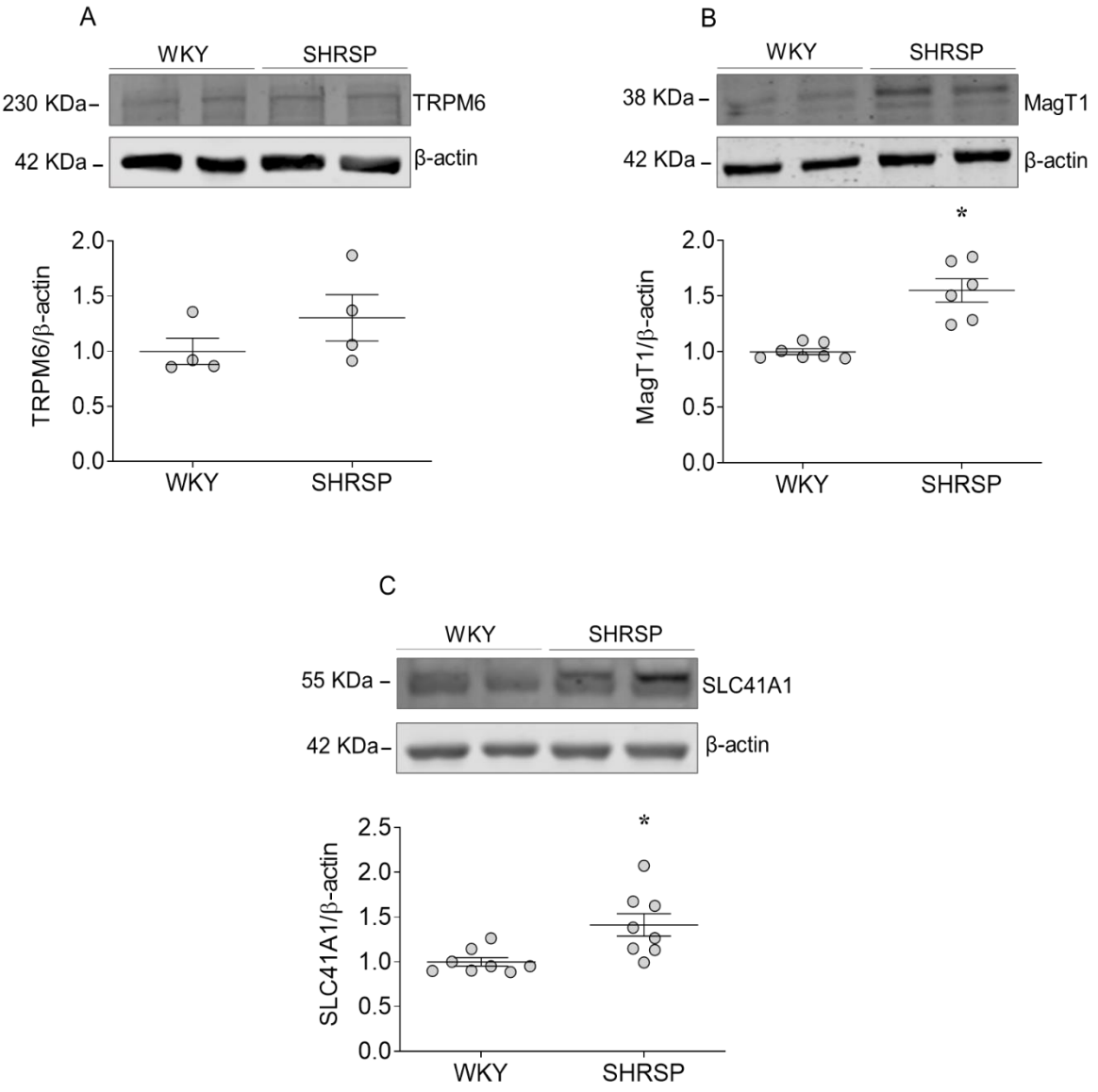

Figure 5.12 Expression of Mg^{2+} transporters in placenta from pregnant WKY and SHRSP rats. Placental tissues were isolated from pregnant WKY and SHRSP rats. Protein expression of TPPM6 (**A**), MagT1 (**B**) and SLC41A1 (**C**) in the placental tissues were normalised by the house keeping protein β-actin. Upper panel: Representative images of immunoblotting. Lower panel: results are expressed as scatter-plot graphs. **P*<0.05 compared to WKY.

5.3.2.3 Expression of VEGFR and TRPM7 in a transgenic model of preeclampsia

To further study whether expression of VEGFR and TRPM7 is altered in preeclamptic placentas, we took advantage of a transgenic rat model of preeclampsia (445). Placental tissues from pregnant female transgenic rats overexpressing angiotensinogen mated with male rats transgenic for human renin and age-matched control rats (Sprague-Dawley) were kindly provided by Dr Delyth Graham and Dr Sheon Samji. As shown in Figure 5.13A, there was reduced VEGFR2 expression in placenta from the preeclampsia rats (PE) (52%) compared to the control rats (Con). There was a trend of increased TRPM7 expression in the PE rats (Figure 5.13B). Similar to what we found in the model of PE in SHRSP, no differences were found regarding to the expression of calpain-2 and annexin-1 in the two groups (Figure 5.13C and D).

We also examined expression of MagT1 in the placental tissues. As shown in Figure 5.14A, there was increased MagT1 expression in placenta from the transgenic PE rats (54%) compared to the control rats.

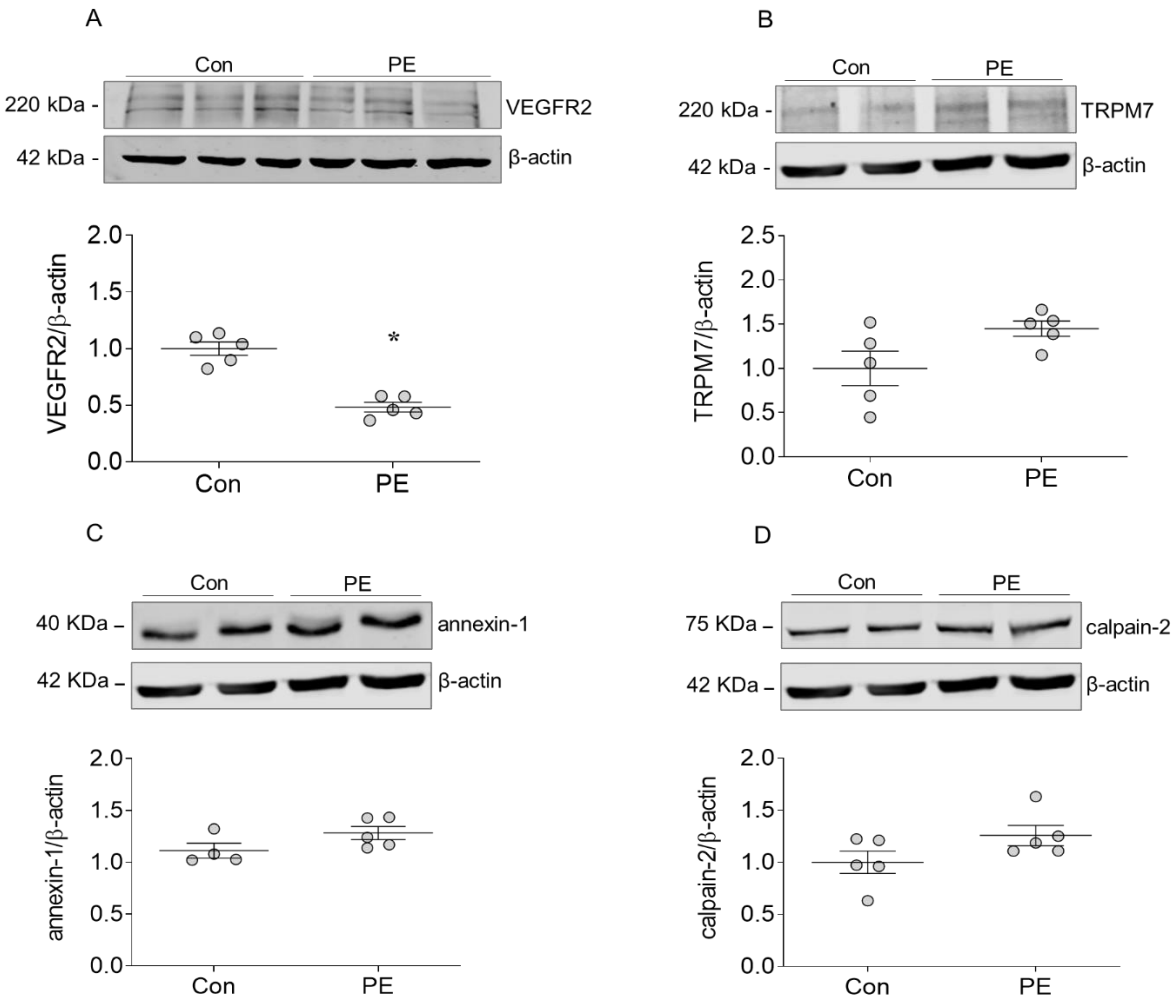

Figure 5.13 Altered VEGFR2 and TRPM7 expression in a transgenic model of preeclampsia. Placental tissues were isolated from age-matched wild type rats (Con) and the transgenic rat model of preeclampsia (PE). Protein expression levels of VEGFR (**A**), TRPM7 (**B**), annexin-1 (**C**) and calpain-2 (**D**) in placental tissues were examined by immunoblotting and normalised by the house keeping protein β-actin, with representative images (upper panels) and quantification (lower panels). **P*<0.05 compared to the control rats.

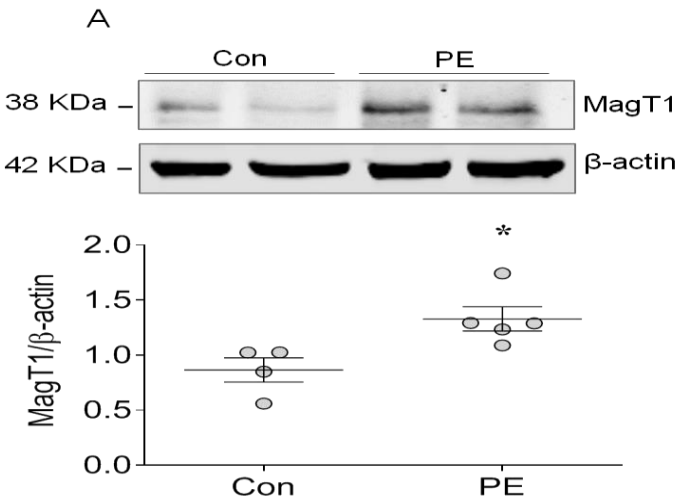

Figure 5.14 Expression of MagT1 in the control rats and the transgenic preeclamptic rats. Protein expression level of MagT1 (**A**) in placental tissues from age-matched control rats (Con) and the transgenic rat model of preeclampsia (PE) was examined by immunoblotting using β-actin as the house keeping protein. Upper panel, representative images of immunoblotting. Lower panel, results are expressed as scatter-plot graphs. **P*<0.05 compared to the control rats.

5.4 Discussion

5.4.1 The effects of EGFR-TRPM7-ERK1/2 pathway in hypertension

Major findings from this chapter demonstrate that: 1) the EGFR-TRPM7-ERK1/2 pathway exists and the activity is enhanced in VSMCs from animal model of hypertension (SHRSP); 2) EGF induces elevation of intracellular Ca^{2+} concentration through TRPM7 in VSMCs from SHRSP rats and 3) the enhanced EGFR-TRPM7-ERK1/2 pathway might lead to increased cell migration and proliferation in VSMCs from SHRSP rats. Taken together, our data support the hypothesis that aberrantly activated EGFR contributes to alterations of ion homeostasis, cell migration and proliferation through TRPM7 in VSMCs under hypertensive conditions, which might play an important role in the pathology of hypertension.

We have previously demonstrated that in VSMCs under physiological conditions, EGF through EGFR and c-Src kinase enhances TRPM7 expression and phosphorylation, which critically regulates ion homeostasis, cell migration and proliferation. Our present data show that this functional pathway in VSMCs is enhanced under hypertensive conditions. In particular, the enhancement of this pathway is associated with elevated intracellular Ca^{2+}. EGF-mediated Ca^{2+} influx has been shown to involve TRP family channels such as TRPP2 and TRPV4 (256). Additionally, we observed that cells from VSMCs from SHRSP exhibit reduced intracellular concentration of Mg^{2+}, which may contribute the deleterious effects of Ca^{2+}. In VSMCs from WKY cells, EGF-induced elevations of intracellular Ca^{2+} concentration were inhibited by 2-APB but not the relatively specific TRPM7 inhibitor NS8593, suggesting the existence of alternative mechanisms under physiological conditions. However, in VSMCs from hypertensive SHRSP rats, EGF-induced Ca^{2+} was inhibited by both 2-APB and NS8593, suggesting the involvement of TRPM7. Ca^{2+} is the final messenger contributing to the contraction vascular muscle (520), and increased Ca^{2+} influx leads to augmented vascular tone and increased vascular resistance (521). Therefore, we suspect that the enhancement of EGFR-TRPM7 activity in VSMCs will lead to elevations of intracellular Ca^{2+}, contributing to increased vascular contraction in hypertension.

In the vascular system, Mg^{2+} negatively regulates vascular tone through its Ca^{2+} antagonistic property and influences VSMCs growth and apoptosis (166). Epidemiological and clinical studies demonstrate a negative correlation between intracellular Mg^{2+} and blood pressure. Hypomagnesemia and decreased tissue Mg^{2+} level have been shown in

various models of experimental hypertension (163-165). In our study, EGF-regulated Mg^{2+} homeostasis through TRPM7 was observed in VSMCs from both WKY and SHRSP rats, however, there was reduced intracellular Mg^{2+} in VSMCs from SHRSP. It was demonstrated that VSMCs treated with Ca^{2+} exhibit reduced TRPM7 in the plasma membrane, which is reverted by Mg^{2+} treatment (141). Taken together, a hypothesis that could explain these differences is that in hypertension there is a reduction of TRPM7 in the plasma membrane, which consequently leads to reduction of intracellular concentration of Mg^{2+} and that increased in Ca^{2+} may be a result of the TRPM7 in the intracellular environment.

Abnormal proliferation and migration of VSMCs have been associated with a number of vascular diseases including hypertension, atherosclerosis and in-stent restenosis (474, 487, 488). In this chapter, our data show that cell migration at basal level might be enhanced in VSMCs derived from hypertensive rats and patients, which was further increased by EGF in an EGFR- and TRPM7- dependent manner. Furthermore, we show that the effect was mediated by Ca^{2+}, since Ca^{2+} chelator EGTA significantly abolished EGF-induced cell migration. Our data provide evidence of novel mechanisms underlying the involvement of TRPM7 and Ca^{2+} in hypertension, which needs further investigation.

5.4.2 VEGFR and magnesium transporters in preeclamptic placenta

PE is a multisystem disorder with clinical manifestations involving different organs such as kidneys, liver, brain, heart, lung, pancreas and the vasculature (355). Compared to normotensive pregnancies, women with a history of preeclampsia are at increased risk for cardiovascular diseases including chronic hypertension, while the underlying mechanisms remain unclear (360). It is believed that the sequestration of circulating VEGF and PIGF by sFlt-1 plays an important role in the development of preeclampsia (362).

Mg^{2+} negatively regulates vascular tone through its Ca^{2+} antagonistic property and influences vascular smooth muscle cell (VSMC) growth and apoptosis (166). Epidemiological and clinical studies demonstrate a negative correlation between intracellular Mg^{2+} and blood pressure. Mg^{2+} may also play a role in the pathology of preeclampsia. It has been demonstrated that serum level of Mg^{2+} is lower in preeclampsia compared to normal pregnant women (396, 522). A small cohort study showed that red cell Mg^{2+} levels is significantly reduced in women with preeclampsia compared with controls (523). Moreover, Carella and colleagues provided direct evidence showing that Mg^{2+} deficiency induces spasm of umbilical vessels isolated from normal pregnant women (524).

Placenta is an organ composed of different types of cells including VSMCs (525), and we have observed that VEGF regulates TRPM7 expression and phosphorylation, a process importantly involved in VEGF-induced Mg^{2+} influx in VSMCs, and that intracellular Mg^{2+} is reduced in VSMCs from SHRSP rats. Thus, we examined the expression of VEGFR and TRPM7 in placental tissues from two animal models of preeclampsia: pregnant SHRSP rats and the transgenic rat model. Alterations in VEGFR and TRPM7 were observed in placental tissues from both models. In particular, there was significantly reduced VEGFR phosphorylation and TRPM7 expression in the model of superimposed preeclampsia (pregnant SHRSP rats). The importance of TRPM7 in regulating Mg^{2+} homeostasis has been explored thoroughly in many cell types, and TRPM7 kinase-deficient mice display low Mg^{2+} status at tissue and cell level and develop cardiovascular impairment (112). However, the transgenic model of preeclampsia displayed opposite patterns of placental TRPM7 expression. It is worth noting that one predominant phenotype of the transgenic model is significantly increased Ang II in the placenta compared to normal pregnancy (445) and upregulation of TRPM7 has been observed in cells derived from mice with Ang II infusion (409). Although elevated Ang II levels are present in SHRSP rats (526), a reduction in RAS component expression has been observed in preeclampsia compared to normal pregnancy, and Graham *et al.* showed that Ang II infusion was required to establish the model of superimposed preeclampsia (443). We assume that different pathological mechanisms contribute to the two models used in this study, and the Ang II level might exert effects on TRPM7 expression in the placenta. Taken together, our study supports that TRPM7 might act downstream of VEGFR with a role in the development of superimposed preeclampsia through Mg^{2+}.

$MgSO_4$ is a therapeutic strategy for preeclampsia, however, the mechanisms of action remain unclear. In our study, alterations in the expression of Mg^{2+} transporters including TRPM7, SLC41A1 and MagT1 were observed in the two models of preeclampsia. Placental Mg^{2+} transporters might contribute to the therapeutic effects of $MgSO_4$ in preeclampsia. Of importance, Mg^{2+} supplement has been shown to reverse phenotypes displayed in TRPM7 kinase-deficient mice (76, 112). MagT1 is an important transporter for Mg^{2+} influx and knockdown of MagT1 is associated with reduced intracellular free Mg^{2+} concentration (20). Loss of MagT1 abrogates Mg^{2+} influx required for T cell signalling and leads to human primary immunodeficiency (21). Interestingly, an altered immune response has been associated with the development of preeclampsia (527). We found that MagT1 protein expression was consistently increased in the placental tissue

from both experimental models of preeclampsia. Thus, MagT1 might be involved in preeclampsia through effects on immune function, which deserves more attention in future studies. In addition, MagT1 has been shown to rescue cell growth and Mg^{2+} uptake in cells lacking TRPM7 (62). Further investigation is necessary to determine whether the overexpression of MagT1 in placenta was an adaptive and compensatory reaction in the context of preeclampsia.

It is worth noting that we only checked the expression of VEGFR and TRPM7 in placental tissues of the two models and there is a paucity of information exploring the pathway in trophoblast, which is the major component of placenta (528). Therefore, to elucidate the role of VEGFR-TRPM7 axis in preeclampsia, further studies are required, especially in the trophoblasts.

In this chapter we explored whether vascular RTK-TRPM7 interplay is altered in pathological conditions. We specifically focused on two conditions, hypertension and preeclampsia, which are known to involve pathological processes linked to growth factors, Mg^{2+} and Mg^{2+} transporters. Our findings clearly show that EGFR/TRPM7 and VEGFR/TRPM7 are important molecular players in hypertension and preeclampsia respectively. Our studies are limited by the fact that we did not comprehensively study EGF and VEGF together in both models. Such studies would be important since EGFR and VEGFR signal through similar pathways. These important studies will be pursued in the Touyz lab in the future.

Chapter Six

6 General discussion

6.1 Crosstalk between RTKs and TRPM7 and the role in vascular biology

6.1.1 The novel EGF-EGFR-Src-TRPM7-ERK1/2 pathway in VSMCs

Since the discovery of EGF in 1962 by Stanley, remarkable advances have been made in understanding EGF-mediated signalling pathways and the effects on cellular functions (529). In general, EGF through binding to and activating EGFR, which belongs to the RTK family, stimulates several cellular pathways including RAS-RAF-MEK-ERK1/2 and PIK3-AKT cascades, the SRC family kinases, PLCγ-PKC, and STATs (530). The EGF-EGFR ligand-receptor system has been shown to exert important effects on various biological processes including cell division, proliferation, migration, differentiation and ion homeostasis, and plays a pivotal role in embryo development, wound healing and tumour biology (261, 314, 453-455).

EGF and its receptor have been shown to modulate TRPM7 activity in various types of cells and different results have been observed. In CHO-K1 cell line, activation of EGFR by EGF initiates PIP2 hydrolysis, which consequently leads to the inhibition of TRPM7 channel activity (410). In a pulmonary cancer cell line, Gao and colleagues found that EGF-EGFR pathway, significantly upregulated the membrane protein expression of TRPM7 and the amplitude of TRPM7 currents, a process associated with cell migration (135). EGF also regulates TRPM6 which shares about 50% sequence identity with TRPM7 (412). Bindels and colleagues demonstrate that in HEK293 cells, EGF promotes translocation of TRPM6 from cytosol to plasma membrane and consequently regulate renal Mg^{2+} reabsorption (259, 411). This research group further clarified mechanisms underlying the regulation of TRPM6 by EGF and showed that the stimulation of TPRM6 by EGF involves both Src-family kinases, MAP kinase, PI3K and Rac1 (411). In our study, we investigate both acute and long-term impact of EGF on TRPM7 in VSMCs. We demonstrate that EGF enhances TRPM7 channel and kinase activity by mechanisms dependent on EGFR and c-Src kinase pathway. A number of TRPM7 phosphorylation sites have been reported (96) and TRPM7 has been shown to undergo extensive autophosphorylation within the serine/threonine-rich region proximal to the exchange domain of the kinase and the kinase's catalytic core (97). Taking advantage of the antibody designed by Chubanov's lab (101), we specifically examined TRPM7 phosphorylation at Serine-1511 (Ser-1511) in this study. Ser-1511 was identified as one of the major sites of autophosphorylation of TRPM7, however, mutation of this site did not affect TRPM7 channel activity (105). Interestingly, phosphorylation of the TRPM7 kinase domain on Ser-

1511 enhances kinase-substrate interactions leading to their serine/threonine phosphorylation (481). Thus, we suspect that EGF-induced TRPM7 phosphorylation might further affect the phosphorylation of TRPM7 substrates such as annexin-1, calpain-2 and myosin IIA. To further investigate this, specific primary antibodies and immunoprecipitation could be utilised to detect the phosphorylated form of these protein in VSMCs after short-term treatment of EGF.

A novel finding of this study is that EGFR directly interacts with TPRM7 in VSMCs. To date, few studies have focused on structural interaction between TRPM7 and other proteins. Zierler and colleagues performed proximity ligation assay (PLA) in purified $CD4^+$ T cells and found that upon TGF-β1 stimulation TRPM7 colocalises with SMAD2 which is dependent on the catalytic activity of TRPM7 (101). It is worth noting that SMAD2 is a transcription factor downstream to TGFβ receptor, highlighting the importance of TRPM7 to the intracellular signalling pathway (531). Of importance, Clapham showed that TRPM7 is most abundant on intracellular vesicles (66). Our investigation shows that TPRM7 colocalises with the membrane-bound protein EGFR. Taken together, TRPM7 is physiologically expressed in both cell cytosol and plasma membrane and the distribution is dynamically regulated by EGF. However, whether the function of TRPM7 changes according to cell location is still elusive. In fact, in 2005 Clapham and colleagues showed that in HEK-293 cells TRPM7 is less abundant in the plasma membrane compared to its intracellular distribution, while in response to shear force TRPM7 starts to accumulate at the plasma membrane (168). However, in our study, using VSMC from WKY rats and normotensive humans, EGF-induced TRPM7 translocation was not observed in our experiments, suggesting that in normal conditions EGF mediates the TRPM7-EGFR interaction by alternative mechanisms. Whether these effects are also observed in pathologic conditions remains unclear.

TRPM7 was initially proposed to regulate intracellular Mg^{2+} levels, with intracellular level of Mg.ATP below 1 mM strongly activating the channel (67). Cells derived from heterozygous $TRPM7^{+/\Delta kinase}$ mice showed reduced TRPM7 currents with increased sensitivity to Mg^{2+} inhibition (76). In the vascular system, Mg^{2+} influences vascular smooth muscle cell (VSMC) growth and apoptosis and negatively regulates vascular tone through its Ca^{2+} antagonistic properties (166). In our study, we explored EGF-induced Mg^{2+} mobilization and showed that EGF increases intracellular free Mg^{2+} which is specifically mediated by TRPM7, since the effects were reduced by TRPM7 inhibitors NS8593 and 2-APB) which are specific to the channel domain (430). Although EGF was

found to induce only a modest elevation of intracellular free Mg^{2+} (~3%) in VSMCs, we believe that such as a change could be biological significant. It is worth noting that intracellular Mg^{2+} is normally maintained within narrow concentration limits except in extreme situation such as hypoxia or prolonged Mg^{2+} depletion (4). In VSMCs, our group previously showed that basal intracellular Mg^{2+} is tightly maintained at 0.5 to 0.6 mmol/L and the vasoactive agent Ang II-induced changes of intracellular Mg^{2+} were modest but were significantly associated with protein and DNA synthesis (2). However, at present we cannot conclude whether or not EGF mediates Mg^{2+} homeostasis in VSMC through effects on the kinase domain. A significant number of studies support a link between TRPM7 channel and its C-terminal kinase domain. For instance, Scharenberg et al. found that HEK293 cells overexpressing mutant human TRPM7 K1648R and G1799D exhibit deficient Mg^{2+}/Mg.ATP-dependent suppression of channel activity, and concluded that the phosphotransferase activity of the kinase domain could influence channel activity (107). The involvement of TRPM7 kinase domain in cation influx was also demonstrated by the observation that although TRPM7 is not a store-operated channel, the kinase regulates store-operated Ca^{2+} entry (86).

Inhibition of EGFR by monoclonal antibodies targeting an extracellular epitope of the EGFR such as panitumumab (Vectibix) and cetuximab (Erbitux), or by small-molecule that inhibit the RTK on the cytoplasmic side of cells such as erlotinib and gefitinib, has been widely used in anti-cancer treatment (532). However, hypomagnesemia is a common side effect observed in patients receiving anti-EGFR treatment. A meta-analysis in 2013 involving 7,045 patients showed that the relative risk of severe hypomagnesemia in patients receiving cetuximab was 8.60 (95%CI, 5.08-14.54) compared with patients on standard therapy (533). Weglicki and colleagues showed that plasma magnesium decreased progressively after 3-9 weeks of erlotinib administration (532). Mechanisms underlying EGFR inhibitor-induced hypomagnesemia have been well studied and it has been shown that the blockage of EGFR signalling in the kidney impairs renal Mg^{2+} reabsorption through TRPM6 (260). Importantly, inhibition of EGFR is also associated with alterations of cardiovascular phenotypes. Threadgill et al. showed that chronic pharmacologic inhibition of EGFR leads to cardiac dysfunction in C57BL/6J mice (534), while Guang Liang and colleagues found that EGFR inhibitors attenuate cardiac hypertrophy induced by Ang II (330).

In the heart, Mg^{2+} has a critical role in modulating neuronal excitation, intracardiac conduction and myocardial contraction through regulating several ion transporters

including potassium and calcium channels (535). In the vascular system, Mg^{2+} induces VSMC growth and negatively regulates vascular tone via its Ca^{2+} antagonistic property, and through mechanisms involving nitric oxide and oxidative stress (166, 536). Our finding that EGF regulates vascular TRPM7 and consequently affects Mg^{2+} homeostasis supports that Mg^{2+} and its transporter might be important modulators contributing to the alterations of cardiovascular phenotypes observed in cancer patients receiving anti-EGFR treatment. Mg^{2+} and Mg^{2+} transporters should be investigated in the future for studies that aims to improve quality of life in those patients.

EGF-induced Ca^{2+} increase in cytosol was reported to exhibit two components including store-based Ca^{2+} release due to activation of the PLCγ/IP3 pathway, and a net Ca^{2+} influx from the outer medium through store operated channel (SOC) and/or non-SOC (252). TRP family channels TRPP2 and TRPV4 were shown to form a functional complex contributing to EGF-mediated Ca^{2+} influx (256). TRPM7 has also been demonstrated as Ca^{2+} permeable channel in human atrial fibroblasts (83), however, whether TRPM7 has a role in regulating Ca^{2+} in VSMCs has not been clearly elucidated. Here, we show that under physiological conditions EGF induced intracellular Ca^{2+} elevation, an effect abolished by non-specific TRPM7 inhibitor 2-APB, but not the potent and relatively specific TRPM7 inhibitor NS8593. 2-APB is non-selective drug, which interacts with multiple channels including TRPM2 and TRPM7 (537). Thus, we postulate that EGF-induced Ca^{2+} transients in VSMCs can be mediated by other ion channels such as the TRP channels or store-operated Ca^{2+} channels. Of importance, our group has recently shown that TRPM2 is important for Ca^{2+} handling in VSMCs, and the channel activity is upregulated by ROS leading to enhanced Ca^{2+} signalling in hypertension (538).

In addition to the well-characterized mitogenic effects in the vasculature, members of the EGF family have been described as direct vascular mediators (317-320). EGF has been consistently demonstrated as a potent vasoconstrictor by several studies. Berk et al. found that EGF significantly induced contraction of rat aortic strips which maximally was equivalent to 40% of that caused by Ang II (319), Florian and colleagues showed that EGF induced contraction in aorta from rats dependent of MEK and L-type Ca^{2+} channel (320), and Amin et al. showed that myogenic tone of coronary arteriole was significantly reduced under inhibition of either EGFR or the downstream JAK-STAT3 complex (318). However, in this study, we did not observe a regulatory role of EGF in vascular contraction. Instead, we show that EGF reduces ACh-induced relaxation, which is endothelium dependent, in both WT and $TRPM7^{+/\Delta kinase}$ mice. This is very interesting, because our previous study

demonstrated that Ang II reduces ACh-induced relaxation in a TRPM7-mediated manner (77). It is worth noting that Ang II exerts its vascular effects through angiotensin type 1 (AT1) receptor and type 2 (AT2) receptor (539), which belong to the family of G-protein coupled receptor (GPCR), while EGFR is a member of the RTK family (202). Ang II is able to activate EGFR through a mechanism called transactivation as it was observed in VSMCs that Ang II-induced activation of the MAP kinase signalling was inhibited by EGFR antagonist (540). Vascular signalling through GPCR and RTK involves different cellular components. For instance, ROS and reactive nitrogen species (RNS) have been shown to play an important role in GPCR agonist-regulated cell function in the vascular system (541). In addition, differences in the role of TRPM7 in Ang II/EGF regulated vascular relaxation may be attributable to different experimental conditions. In the current study, mesenteric resistance arteries were dissected from mice and were treated with EGF *in vitro*, while in the previous study mesenteric arteries were isolated from mice treated with Ang II *in vivo*.

We have recently reviewed the crosstalk between TRPM7 and RTK downstream signalling pathways including the MAP kinases (46). TRPM7 has been shown to regulate the activity of MAP kinases. Xiong et al. found that silencing TRPM7 promotes proliferation via activating ERK1/2 in endothelial cells, while in mouse cortical astrocytes, silencing TRPM7 inhibits proliferation via ERK1/2 and c-Jun N-terminal kinases (JNK) pathways (124, 400). In HEK-293 cell line, overexpression of TRPM7 activates p38MAPK and JNK, whereas suppressed ERK1/2 phosphorylation (104). It is interesting that in these studies, inhibition of TRPM7 activity via silencing RNA and pharmacological inhibitors show opposite effects on ERK1/2 phosphorylation. Hence, these findings suggest that TRPM7 affects ERK1/2 activation in a cell type-specific manner. Our results reveal that TRPM7 is positively associated with ERK1/2 phosphorylation, and contributes to EGF-induced activation of ERK1/2 in the vasculature. Of importance, in our study the regulatory role of TRPM7 in the activation of ERK1/2 was demonstrated at cell and tissues from mice model of TRPM7 deficiency. We assume that the underlying mechanisms may involve TRPM7 channel activation, involving Ca^{2+} or Mg^{2+} effects. Mg^{2+} deprivation has been shown to decrease phosphorylated ERK1/2 levels and consequently inhibit cell proliferation in kidney cells (542), and EGF increases ERK1/2 activation through regulating Ca^{2+} in corneal epithelia (543).

TRPM7 is closely associated with cell migration. In VSMCs, Zhang et al. found that TRPM7 regulates oxidised low-density lipoprotein (Ox-LDL)-induced migration through

MEK-ERK1/2 pathways (129), and Touyz et al. showed that bradykinin-induced cell migration is mediated by TRPM7 (130). The regulation of cell migration by TRPM7 has been also reported in neuroblastoma cell (133), bladder cancer cell (134), and human non-small cell lung cancer cells (135). Our study, to our knowledge is the first to identify the importance of TRPM7 in migration in human VSMCs. Underlying mechanisms may involve MAP kinase and c-Src. It has been shown that in breast cancer cells, TRPM7 mediates migration and invasion via MAP kinase pathway (407), and c-Src is an well-known regulator in cell migration in different cell types (544, 545). Our experiments demonstrate that TRPM7 kinase is required to maintain c-Src activity in the vasculature and EGF-induced VSMC migration involves TRPM7 and ERK1/2. Those findings together suggest that c-Src and ERK1/2 may contribute to the regulatory role of TRPM7 in cell migration. Of importance, the TRPM7 kinase activity in phosphorylating myosin-IIA heavy chain (MHC-IIA) might influence cell migration (84). Actomyosin contractility driven by Myosin II controls cytoskeletal remodelling, and non-muscle myosin II is believed to take centre stages in cell adhesion and migration and is upregulated in many cancers (546, 547). Regulation of myosin II activity includes dynamic phosphorylation and dephosphorylation of myosin heavy chain (MHC) (548) and TRPM7 phosphorylates MHC-IIA at Thr1800, Ser1803 and Ser1808 (99). Whether the phosphorylation status of MHC-IIA is changed by EGF treatment and exerts effects on cell migration in VSMCs remains unclear, but would be of interest to investigate in future studies.

Mechanisms underlying the regulatory role of TRPM7 in cell proliferation involves its kinase activity. Ryazanova et al. showed that the proliferation arrest phenotype was displayed in embryonic stem cells with deficient TRPM7 kinase domain (76), and that in this study aortic vessels isolated from TRPM7 kinase-deficient mice display reduced proliferation marker associated with decreased wall thickness. Compelling evidence shows that Ca^{2+} and Mg^{2+} and the related signalling pathways play major roles in cell proliferation (118, 549), with a specific involvement of the ion channel TRPM7. It has been shown that TRPM7 regulates non-voltage-gated spontaneous Ca^{2+} influx, facilitating cell growth, while silencing TRPM7 reduces the magnitude of Ca^{2+} influx and reduces the rate of cell proliferation with retarded G(1)/S cell cycle progression (126), and that silencing TRPM7 in fibroblasts enhances cell resistance to apoptotic stimuli in a Mg^{2+}-dependent manner through decreasing ROS levels (125). In the present study, our experiments demonstrate that EGF mediates intracellular levels of Mg^{2+} and Ca^{2+} through TRPM7. In particular, we observe that under physiological condition (WKY), TRPM7 is

not involved in EGF-induced Ca^{2+} elevation, while in VSMCs derived from SHRSP, cells that are characterized by enhanced cell proliferation (505). TRPM7 specifically contributes to EGF-triggered Ca^{2+} mobilisation. All together, we postulate that both the TRPM7 kinase activity and the channel property in permeating Ca^{2+} and Mg^{2+} are involved in EGF-mediated proliferation in VSMCs. However, this modulation might be different according to the cell activation phenotype. Further strategies to clarify the detailed mechanisms include observation of ion homeostasis and cell proliferation in cells with TRPM7 kinase deficiency ($TRPM7^{+/\Delta kinase}$) or "dead" catalytic activity ($TRPM7^{R/R}$) in the presence of EGF and TRPM7 activator (e.g. naltriben).

6.1.2 Regulation of TRPM7 by VEGF in VSMCs

The VEGF family contains several members, including VEGF-A, VEGF-B, VEGF-C, VEGF-D, VEGF-F and placental growth factor (PIGF) (365). The most widely studied member is VEGF-A, also known simply as VEGF. Since the discovery of VEGF in 1983 and the subsequent cloning of the gene in 1989 (550, 551), an increasing amount of knowledge has accumulated on the biological effects of VEGF on blood vessel formation in health and disease (551). VEGF has been described as a potent, endothelial cell-specific mitogen that regulates angiogenesis, vascular permeability and vasodilation (552). VEGF exerts biological effects through binding to RTKs, mainly VEGFR-1 and VEGFR-2, members of the RTK family (553). The VEGF-VEGFR system by increasing microvascular permeability and promoting endothelial cell migration and proliferation, regulates both the normal and pathological angiogenic processes (365). In addition to the classical role in endothelial cells, VEGFR-1 and VEGFR-2 are also expressed in SMCs and the activation has been shown to modulate phenotypes of SMCs (554). Zhang et al. found that VEGF through activating VEGFR2 promotes VSMCs proliferation with mechanisms involving STAT3 (555), while Laitinen and colleagues found that VEGF reduces VSMCs proliferation via a mechanism that involves VEGF-induced NO production from the endothelium (556).

TRPM7 plays a critical role in cardiovascular system. Clapham et al. found that early cardiac-targeted knockout of TRPM7 impaired ventricular function, conduction and repolarization (138). Our previous study showed that TRPM7 is important in regulating vascular Mg^{2+} homeostasis and that Ang II-induced hypertension is exacerbated in TRPM7 kinase-deficient mice, associated with pronounced cardiac hypertrophy and worsened left ventricular function (77). The current study examines the biological effects of the VEGF-

VEGFR system on VSMCs, with a specific focus on the activity of TRPM7. We demonstrate that VEGF through its receptor enhances TRPM7 phosphorylation and expression at gene and protein level, without influencing TRPM6. TRPM7 trafficking has been associated with important cellular functions. Clapham and his group demonstrate that functional TRPM7 accumulates at the plasma membrane in response to fluid flow which might play a role in pathological response to vessel wall injury (168). TRPM7 is also proteolytically cleaved in normal tissue and cell lines, and the TRPM7 cleaved kinase fragments translocate to the nucleus and bind to multiple components of chromatin remodelling complexes, which affects gene expression patterns (557). In our study, we provide preliminary evidence for the translocation of TRPM7 towards the plasma membrane upon VEGF stimulation in VSMCs. Since VEGF-induced Mg^{2+} influx was also observed in VSMCs, we hypothesize that VEGF through VEGFR recruits TRPM7 to the plasma membrane acting as a channel for Mg^{2+} influx.

VEGF has been shown to mediate intracellular Ca^{2+} in different cell types, including endothelial cells (244-246), VSMCs (247), cardiomyocytes (248), neurons (249) and trophoblast cells (250). Angle *et al.* demonstrate that in VSMCs VEGF induces extracellular Ca^{2+} influx but not intracellular Ca^{2+} release (247). In our study, we found that VEGF elevates intracellular Ca^{2+} through TRPM7 in VSMCs. However, in our experiments the VEGFR inhibitor vatalanib only partially attenuated the effect of VEGF, as shown by the Area under curve (AUC) in Figure 4.4. It should be noticed that in our experiments the Ca^{2+}-related events were recorded for approximately 250 seconds and the AUC value was determined by the whole curve. It seems that vatalanib exerts its inhibitory effect mainly in the first 100 seconds (Figure 4.4) and during this period VEGF's effect is abolished, suggesting the involvement of VEGFR. Interestingly, although the specific TRPM7 inhibitor NS8593 attenuates the effect of EGF on Ca^{2+} mobilisation, the extent was less compared to the non-specific TRPM7 inhibitor 2-APB. Thus, we postulate that alternative mechanisms might contribute to VEGF-regulated Ca^{2+} homeostasis in VSMCs. In line with this, TRP family channel TRPC6 has been shown to modulate VEGF-induced intracellular Ca^{2+} elevation in human microvascular endothelial cells (246). In VSMCs, our group recently demonstrate that TRPM2 is an important Ca^{2+} channel, which contributes to the crosstalk between vascular Redox and Ca^{2+} signalling (538). Whether other TRP family channels are involved in VEGF-induced Ca^{2+} mobilisation in VSMCs remains unclear. To further explore this, chemical compounds 8-Br-cADPR and Larixyl Acetate,

inhibitors to TRPM2 (538) and TRPC6 (558) respectively can be utilised in the presence of VEGF in VSMCs for future studies.

VEGF-induced Mg^{2+} mobilisation was observed in endothelial cells. Hong and colleagues show that VEGF promotes Mg^{2+} release from intracellular store in a dose-dependent manner. Here, we demonstrate that VEGF promotes Mg^{2+} influx by mechanisms dependent on VEGFR and TRPM7 activation in VSMCs under a physiological concentration (1 mM) of extracellular Mg^{2+}. Interestingly, VEGF reduces intracellular free Mg^{2+} under 0 extracellular Mg^{2+} in a time-dependent manner in our experiments. These data, together with the observation that there was a trend for increased SLC41A1 expression after VEGF stimulation, suggest that VEGF might promote both Mg^{2+} influx and efflux in VSMCs, a dynamic process depending on the level of extracellular Mg^{2+}. It is worth noting that the indicator Magnesium green used in this study specifically detects intracellular free Mg^{2+} (559). However, only 1-5% intracellular magnesium is ionized, and the remainder is bound to proteins, negatively charged molecules and adenosine triphosphate (ATP) (6). The observation that intracellular free Mg^{2+} was reduced upon VEGF stimulation under 0 extracellular Mg^{2+} can also be explained by the increased binding of Mg^{2+} to ATP and intracellular proteins, which is of interest and deserves more attention.

VEGF through its receptor, mainly VEGFR-2, has been shown to stimulate the activation of diverse signalling proteins in ECs including p38 MAPK and ERK1/2, which consequently regulates processes related to angiogenesis such as endothelial cell migration, proliferation, and vascular permeability (560-562). VEGF also induces the phosphorylation of PKC in ECs and regulates endothelial permeability in a PKC-dependent manner (498, 563). Interestingly, in VSMCs we observe that VEGF has no effect on the phosphorylation of p38 MAPK and PKC, while it reduces the phosphorylation of ERK1/2 in a VEGFR-independent manner. In line with our finding, Freischlag and colleagues demonstrate that VEGF inhibits PDGF-induced phosphorylation of ERK1/2 and exerts negative effect on proliferation in VSMCs (564), and Standley *et al.* showed that the upregulation of MEK and ERK1/2 as proliferative phenotype appears to be abrogated by VEGF in VSMCs (565). Although Zhang *et al.* found that VEGF promotes VSMCs proliferation, the effect is dependent on VEGFR2/STAT3-mediated upregulation of the proliferation makers Cyclin D1 and PNCA (555). In addition, VEGF has been shown to mediate cell function through a crosstalk with G protein-coupled receptor as a novel mode of “transactivation” in the vascular wall (566).

There is emerging evidence that VEGF acts as a potent vasodilator and exerts vasculoprotective effects. In the skin vasculature, VEGF by the activation of VEGFR-2 induces vasorelaxation with postreceptor signalling pathways involving PLC, PKC, Ca^{2+} release from intracellular store, and the synthesis/release of NO (567). In coronary arteries, VEGF triggers endothelium-dependent relaxation by stimulating endothelium-derived relaxing factor (EDRF)/NO release via a Ca^{2+} dependent mechanism (337). Abman and colleagues show that VEGF causes pulmonary vasodilation and the response is likely mediated by the release of NO through activation of PI3K (568). He *et al.* reported that in human internal mammary artery (IMA) and radial artery (RA), VEGF induces similar and potent relaxation that by mechanisms dependent on prostacyclin, endothelium-derived hyperpolarizing factor (EDHF) and NO (569). It is worth noting that these modulators can be closely regulated by Mg^{2+}. For instance, hypomagnesemia has been shown to inhibit NO release from coronary endothelium (570); Mg^{2+} enhances prostacyclin production in both ECs and VSMCs (571) and Mg^{2+} infusion improves endothelium-dependent vasodilation in the human forearm (572). The vasculoprotective role of VEGF has been further supported by the fact that anti-VEGF chemotherapy in cancer patients is associated with significantly increased blood pressure (338). In the current study, we demonstrate that VEGF increases the sensitivity of mesenteric arteries to SNP-induced (endothelium independent) relaxation. Taking advantage of the mice model of TRPM7 deficiency, we show that the VEGF-promoted relaxation is dependent on TRPM7. Application of the TRPM7 activator naltriben produces similar effect on SNP-induced relaxation, suggesting that TRPM7 might be a potential target for diseases associated with vascular dysfunction. Of importance, our experiments show that VEGF promotes Mg^{2+} influx in VSMCs. Thus, we hypothesize that TRPM7 contributes to VEGF-induced vasodilation through Mg^{2+}.

6.1.3 EGF and VEGF have different effects on VSMCs

Growth factors are secreted biologically active molecules that stimulate cell proliferation and mediate (patho)physiological processes including embryogenesis, wound healing and carcinogenesis (573). Growth factors include lipid-soluble steroid hormones such as oestrogen, androgen and progestogen which bind to intracellular protein receptors or nuclear receptors, and protein growth factors such as VEGF and EGF which bind to cell surface receptors (574). There are multiple similarities between VEGF and EGF. Receptors of VEGF and EGF (VEGFR and EGFR) belongs to the RTK family and share a common molecular architecture. Through activating RTKs, VEGF and EGF trigger similar downstream signalling pathways (575, 576). Abnormal activation of RTKs has been found

in a wide range of cancers and small molecule agents targeting VEGFR and EGFR are important anticancer strategies (307, 575, 576).

TRPM7 has been involved in the regulation of downstream signalling pathways of growth factors (VEGF and EGF), such as the PI3K/AKT pathway (46). Contribution of TRPM7 to the PI3K/AKT pathway has been demonstrated in different cell types. In mouse chondrocytes, TRPM7 overexpression was associated with upregulation of PI3K p85 subunit and AKT expression and phosphorylation, effects that were reduced by silencing TRPM7 (405) and in lymphocyte TRPM7 was shown to be required for sustained PI3K/AKT signalling activation, which is important for cell growth (404). Of importance, VEGF and EGF have been shown to induce the activation of PI3K in VSMCs (313, 577). Findings from this study demonstrate that VEGF and EGF exert similar effects on TRPM7 expression and phosphorylation in VSMCs. Thus, we postulate that TRPM7 plays an important role in the activation of downstream signalling pathways shared by VEGF and EGF in VSMCs, such as the PI3K/AKT pathway.

However, we also show that VEGF and EGF differently affect VSMCs: 1) VEGF promotes accumulation of TRPM7 at the plasma membrane isolated by ultracentrifugation in VSMCs while EGF has no effect on TRPM7 movements as observed in HEK cells ; 2) at basal level VEGF but not EGF regulates Ca^{2+} mobilization by TRPM7 specific mechanisms; 3) VEGF reduces ERK1/2 phosphorylation in a VEGFR- and TRPM7-independent manner while EGF enhances ERK1/2 phosphorylation through EGFR and TRPM7 and 4) VEGF potentiates endothelium-independent vascular relaxation by mechanisms depending on TRPM7, whereas EGF inhibits endothelium-dependent vasodilation in a TRPM7 independent manner. Among these different effects, ERK1/2 phosphorylation is of our greatest interest. ERK1/2 causes vascular contraction and increased ERK1/2 activity has been demonstrated in a number of different animal models of hypertension (472, 507). Involvement of TRPM7 in the activation of ERK1/2 depends upon cell type. Silencing TRPM7 increases phosphorylation of ERK1/2 and their upstream kinases MEK1/2 (400) in ECs, whereas in mouse cortical astrocytes silencing TRPM7 is associated with decreased ERK1/2 phosphorylation (124). Understanding how TRPM7 is involved in ERK1/2 activity induced by VEGF/EGF has been complicated by the observation that VEGF and EGF exert similar effects on TRPM7 expression/phosphorylation while opposingly regulate ERK1/2 phosphorylation. However, in our experiments VEGF promotes TRPM7 accumulation at the plasma membrane of VSMCs while EGF has no effect on TRPM7 trafficking in HEK cells. It is worth noting

that cellular location of TRPM7 is associated with distinct biological functions, as supported by the findings that TRPM7 accumulates at the plasma membrane in response to fluid flow and plays a role in pathological response to vessel wall injury (168), and that cleaved TRPM7 kinase fragments translocate to the nucleus and mediate gene expression patterns (557). Taken together, we believe that VEGF and EGF act as vasoactive agents in the vasculature, and distinct effects of VEGF and EGF on ERK1/2 phosphorylation may be attributable to the different TRPM7 location upon VEGF/EGF stimulation.

6.2.1 Dysregulation of EGFR and TRPM7 is involved in hypertension

Epidermal growth factor receptor (EGFR) and its downstream signalling have been widely acknowledged for the influence in cancer development, however, its involvement in cardiovascular disease is poorly understood. Accumulating evidence has highlighted the EGFR signalling as a critical contributor to hypertension. Enhanced EGFR phosphorylation and expression have been observed in experimental hypertension, while specific knockout of EGFR in VSMCs is associated with arterial hypotension in mice (314, 321, 322). Accordingly, EGF has been described as a potent vasoconstrictor by several studies (319, 320). Interestingly, in our study we did not observe a regulatory role of EGF in vascular contraction. Instead, we show that EGF reduces ACh-induced (endothelium dependent) vascular relaxation, a process that does not involve the TRPM7 kinase.

Ca^{2+} is the final messenger contributing to the contraction of vascular muscle (520). Increased Ca^{2+} influx leads to augmented vascular tone and enhanced vascular resistance (521). Mg^{2+} negatively regulates vascular tone through its Ca^{2+} antagonistic property (166). Hypomagnesemia and decreased tissue Mg^{2+} level have been shown in various models of experimental hypertension (163-165). We examined EGF-regulated Ca^{2+} and Mg^{2+} homeostasis in VSMCs from WKY and SHRSP. EGF elevates intracellular Ca^{2+} in VSMCs from both strains and the effect is specifically mediated by TRPM7 in VSMCs from SHRSP. These results suggest that TRPM7 is predominantly involved in EGF-initiated Ca^{2+} elevation in hypertension, which is consistent with our observation that increased TRPM7 expression is present in SHRSP. In addition, our preliminary data also show that Ca^{2+} contributes to the enhanced cell migration observed in VSMCs from hypertensive humans compared to normotensive controls.

Although EGF regulates Mg^{2+} homeostasis in a similar manner in VSMCs from WKY and SHRSP, there is reduced intracellular free Mg^{2+} at basal level in SHRSP, which supports the negative correlation between Mg^{2+} and hypertension. In addition to the Ca^{2+}

antagonistic property, Mg^{2+} is able to affect vascular health via mechanisms involving nitric oxide and oxidative stress. Mg^{2+} exerts direct effects on maintaining endothelial function, by stimulating endothelial proliferation, enhancing the mitogenic response to angiogenic factors and inducing the synthesis of nitric oxide (536). Accordingly, Mg^{2+} supplement lowered arterial blood pressure in nitric oxide synthase (NOS) inhibition-induced hypertension through restoring the agonist-induced relaxation response of the arteries (578). Oxidative stress, defined as an imbalance between oxidants and antioxidants, instigates endothelial dysfunction and inflammation and contributes to cardiac and vascular abnormalities in different types of CVDs (579). Mg^{2+} deficiency has been shown to induces oxidative stress (580), and Mg^{2+} supplementation plays protective role through reducing oxidative stress in diabetic rats (581), in athletes and in young men with sedentary lifestyle (582).

Interestingly, TRPM7 appears to be vascular protective, because $TRPM7^{+/\Delta kinase}$ mice fused with Ang II present with exaggerated blood pressure, worsening of left ventricular function and pronounced cardiac hypertrophy in comparison with Ang II-infused WT mice (77). However, it should be noted that the deletion of TRPM7 kinase domain in this animal model is global, and TRPM7 as a ubiquitously expressed protein has been involved in the physiological functions of several organ systems. Thus, the phenotypes observed in Ang II-infused $TRPM7^{+/\Delta kinase}$ mice might be attributed to the dysfunction of TRPM7 in other organs such as kidney and heart. Since TRPM7 acts as a critical chanzyme involved in a variety of physiological processes, and global TRPM7 deletion results in embryonic lethality, it is not surprising that both TRPM7 deficiency and enhancement can induce abnormalities according to the cell type. Recently, Polotsky and colleagues demonstrate that leptin, a hormone increased in obese humans, induces hypertension through acting on TRPM7 in the carotid body (506). We hypothesize that under physiological conditions, TRPM7 is more permeable to Mg^{2+} in VSMCs and exerts protective effects via Mg^{2+} in the vascular system. While in the context of hypertension, TRPM7 is responsible for agonist (e.g. EGF) -induced Ca^{2+} elevation. We have previously shown that VSMCs treated with Ca^{2+} exhibit reduced TRPM7 in the plasma membrane (141). Enhanced Ca^{2+} signalling might consequently lead to a reduction of TRPM7 in the plasma membrane, which causes the reduction of intracellular concentration of Mg^{2+} in VSMCs. Thus, enhancement of the EGFR-TRPM7 signalling might contribute to the development of hypertension through aberrant alterations of divalent cations.

6.2.2 Possible role for TRPM7 in PE

Preeclampsia (PE) is a multisystem disorder with clinical manifestations involving different organs such as kidneys, liver, brain, heart, lung, pancreas and the vasculature (355). PE negatively affects both the mother and foetus. Deleterious effects on foetus include growth restriction, preterm delivery, respiratory distress, cerebral palsy, necrotizing enterocolitis and still birth (362). For the pregnant women, PE is associated with adult respiratory distress syndrome (ARDS), pulmonary oedema, cerebral thrombosis or haemorrhage, renal dysfunction, hepatic dysfunction, thrombocytopenia and disseminated intravascular coagulopathy (DIC) (350, 355).

The VEGF family and their receptors have been shown to play an important role in normal pregnancy and the pathogenesis of PE. VEGF and PIGF are required for normal placental angiogenesis and development (372, 373). Targeted inactivation of a single *VEGF* allele or disruption of genes encoding VEGF receptor 1 (VEGFR1) resulted in abnormal vessel formation during embryogenesis leading to embryonic death, and PIGF-knockout mice display delays in spiral arterial remodelling and placental development (583). In the context of PE, abnormalities of the VEGF-VEGFR system are believed to contribute to the pathophysiology of PE (367, 377), and the sFlt-1: PIGF ratio has been used clinically to predict the disease progression and guide treatment (378). In addition, inhibition of VEGFR, the classical therapeutic strategy in the management of malignancies, is associated with significant cardiovascular toxicities especially hypertension, which makes VEGF and its receptor more attractive candidates to explore for a better understanding of the pathophysiology of PE (343).

In our study, alterations of VEGFR2 expression and/or phosphorylation are present in two animal models of PE, further supporting involvement of the VEGF-VEGFR system in PE. Given the importance of the VEGF-VEGFR system in PE, using PIGF and VEGF to restore angiogenic balance as potential therapies have been investigated in different experimental models of PE. Infusion of recombinant human PIGF for 5 days via intraperitoneal osmotic minipumps has been shown to reduce blood pressure and proteinuria and improve glomerular infiltration rate (GFR), associated with decreased sFlt-1 level in the RUPP model of PE (381). In a model of PE based on sFlt-1 overexpression, (379), treatment with recombinant human VEGF121 (rhVEGF121) alleviates symptoms and pathological features such as hypertension, proteinuria and glomerular endotheliosis without apparent harm to the foetus (386). It is worth noting that although reduced bioavailability of serum VEGF and PIGF has been shown in animal models of PE, there is a paucity of information about activity of this system in the placenta. Here, we demonstrate

that dysregulated VEGFR is present in the placental tissue from animal model of PE. Moreover, we show that in the placenta alterations of VEGFR activity are associated with changes of Mg^{2+} transporters MagT1 and TRPM7, downstream targets of VEGF/VEGFR that we have demonstrated in the vascular system.

PE has been considered a disease with cardiovascular origins, where the placental dysfunction is secondary to maternal cardiovascular maladaptation in pregnancy (584). Additionally, women with a history of PE have an elevated risk to develop CVDs such as hypertension (513). Our group has demonstrated that TRPM7 exerts vasculoprotective effects, while the lack of TRPM7 in mice can cause exaggerated hypertension in response to Ang II (77), and induce cardiovascular inflammation and fibrosis (112). In the current study, we show that VEGF increases TRPM7 expression and phosphorylation in VSMCs, with an important role in Mg^{2+} homeostasis. Moreover, VEGF promotes the sensitivity to SNP-induced vessel relaxation in a TRPM7-dependent manner. Thus, we hypothesize that TRPM7 might act as an important downstream effector of VEGF, which contributes to the pathogenesis of PE when the bioavailability of VEGF is reduced and mediates the therapeutic effects of VEGF/PIGF shown in animal model of PE.

One novel finding of this study is that Mg^{2+} transporters such as TRPM7 and MagT1 might have an important role in the development of PE. In line with our findings, gene expression of TRPM7 was down-regulated in preeclamptic placenta tissues during preterm labour and remained lower at term labour (395). We also found that MagT1, the important transporter for Mg^{2+} influx, was consistently increased in the placental tissue from both experimental models of PE. As we discussed earlier, MagT1 might be involved in PE through its effects on immune function, while MagT1 could also act as an adaptive and compensatory mechanism to rescue the preeclamptic phenotype caused by the dysregulation of TRPM7.

$MgSO_4$ is the mainstream strategy to prevent and treat PE or eclampsia (388, 389), however, the underlying mechanisms remain unclear. It has been reported that gene expression of TRPM7 and TRPM6 is down-regulated in preeclamptic placenta tissues during preterm labour and remained lower at term labour (395), while Vormann *et al.* show that SLC41A1 is significantly overexpressed in placentas of preeclamptic women compared to pregnant women without preeclampsia with no significant changes in expression levels of TRPM7 and MagT1 (585). Taking advantages of placental tissues from two different animal models of PE, we demonstrate that Mg^{2+} transporters including

TRPM7, MagT1 and SLC41A1 are dysregulated in the preeclamptic group. We believe that alterations of placental Mg^{2+} transporters might be involved in the pathogenesis of PE and contribute to mechanisms underlying the clinical use of $MgSO_4$ in PE. To further explores this, animals can be treated by $MgSO_4$ with or without pretreatment of inhibitors of Mg^{2+} transporters (e.g. TRPM7), and expression of Mg^{2+} transporters in the placenta or other systems such as the vasculature can be examined.

To summarize, our studies identify TRPM7 as a novel signalling target of growth factor VEGF and EGF in the vascular system. In particular, we demonstrate that i) VEGF and EGF through their receptors (RTK) influence TRPM7 expression, phosphorylation and cellular location in VSMCs, important in the regulation of ion homeostasis such as Mg^{2+} and Ca^{2+}, ii) TRPM7 is both upstream and downstream of growth factor/RTK in VSMCs and the direct interaction between TRPM7 and EGFR occurs in the cell membrane and is regulated by EGF in a c-Src-dependent manner, iii) TRPM7 is critically involved in the activation of RTK downstream cascades such as ERK1/2, a process consequently contributing to EGF-induced VSMC migration and proliferation, iv) TRPM7 differently contributes to EGF- and VEGF- regulated vascular reactivity, as EGF reduces ACh-induced (endothelium-dependent) vascular relaxation independently of TRPM7 kinase while VEGF promotes vessel sensitivity to SNP-induced/endothelium-independent vascular relaxation via the TRPM7 kinase and v) the RTK-TRPM7 crosstalk may have significant clinical relevance, as dysregulation of the EGFR-TRPM7-ERK pathway is observed in VSMCs from hypertensive rats and aberrant expression of VEGFR-TRPM7 is identified in placenta from animal model of preeclampsia.

6.3 Limitations of the study

The study has highlighted the involvement of TRPM7 in growth factors VEGF- and EGF- triggered downstream signalling pathways in VSMCs and a possible role of TRPM7 in PE. Different pharmacological inhibitors of TRPM7 including 2-APB and NS8593 and VSMCs derived from TRPM7 kinase-deficient mice were used to explore how TRPM7 contributes to ERK1/2 activation, Ca^{2+} and Mg^{2+} homeostasis, cell migration and proliferation, and vascular reactivity. It was also demonstrated that VEGF and EGF regulate another Mg^{2+} transporter MagT1. In order to confirm that all the effects observed on VSMCs are specifically mediated by TRPM7 rather than MagT1, experiments with the modulation of MagT1 activity should be performed in VSMCs. Currently, there are no

available pharmacological inhibitors of MagT1, and thus gene silencing approaches should be considered in future studies.

Ca^{2+} and Mg^{2+} are intracellular messengers involved in a wide variety of vital cellular processes. TRPM7 and its property acting as Ca^{2+}- and Mg^{2+}- permeable channel have been shown to play important roles in different cell types. In this study, we demonstrate that VEGF and EGF regulate Ca^{2+} and Mg^{2+} homeostasis through TRPM7, however, the importance of Mg^{2+} and Ca^{2+} in ERK1/2 activation, cell migration and proliferation, and vascular reactivity has not been thoroughly investigated. To study whether TRPM7 mediates growth factors-regulated cellular signalling and cell functions through Ca^{2+} and Mg^{2+}, the metal ion chelators such as EGTA and EDTA should be used in some experiments.

To study the role of TRPM7 in VEGF- and EGF- induced signalling and cellular functions, we used pharmacological inhibitors of TRPM7 including 2-APB and NS8593. However, 2-APB is known to inhibit the Ca^{2+} permeable channel TRPM2, and NS8593 can inhibit SK channels. The usage of the two pharmacological inhibitors in most experiments may raise concerns over their specificity. To improve the quality of this study, other techniques such as gene silencing mediated by small interfering RNAs should be utilised in some experiments. In addition, to further highlight the importance of TRPM7 in vascular system, specific knockout of TRPM7 in VSMCs using the Cre-lox system could be considered.

To investigate the role of the VEGFR-TRPM7 axis in PE, we show that VEGF upregulates TRPM7 and subsequently mediates ion homeostasis in VSMCs and demonstrate that dysregulation of VEGFR and TRPM7 is present in preeclamptic placentas. However, VSMC is not the primary component of placenta and there is a paucity of information on serum levels of VEGF and PIGF in this study. The alteration of TPRM7 observed in preeclamptic placenta could not be directly linked to the dysregulation of VEGF/VEGFR. To further investigate whether VEGF/VEGFR exerts similar regulatory effects on TRPM7 in placenta, experiments should also be designed and performed properly in trophoblast, which is the major component of placenta, and serum levels of VEGF/PIGF in the two models need to be examined. Data about PE present in this study are still preliminary, and additional studies should be performed to support our hypothesis.

Finally, the sample size in some experiments is relatively small, which may lead to a low statistical power and low reproducibility. To produce more conclusive results, some

experiments such as the migration and proliferation study in VSMCs from SHRSP rats need to be repeated with a targeted sample size of at least 6.

References:

1.Cunha AR, Umbelino B, Correia ML, Neves MF. Magnesium and vascular changes in hypertension. International journal of hypertension. 2012;2012:754250.

2.He Y, Yao G, Savoia C, Touyz RM. Transient receptor potential melastatin 7 ion channels regulate magnesium homeostasis in vascular smooth muscle cells: role of angiotensin II. Circ Res. 2005;96(2):207-15.

3.Hsieh MC, Wu CF, Chen CW, Shi CS, Huang WS, Kuan FC. Hypomagnesemia and clinical benefits of anti-EGFR monoclonal antibodies in wild-type KRAS metastatic colorectal cancer: a systematic review and meta-analysis. Scientific reports. 2018;8(1):2047.

4.Swaminathan R. Magnesium metabolism and its disorders. Clin Biochem Rev. 2003;24(2):47-66.

5.Seo JW, Park TJ. Magnesium metabolism. Electrolyte Blood Press. 2008;6(2):86-95.

6.Jahnen-Dechent W, Ketteler M. Magnesium basics. Clinical kidney journal. 2012;5(Suppl 1):i3-i14.

7.Wolf FI, Trapani V. Cell (patho)physiology of magnesium. Clin Sci (Lond). 2008;114(1):27-35.

8.Vernon WB. The role of magnesium in nucleic-acid and protein metabolism. Magnesium. 1988;7(5-6):234-48.

9.Grober U, Schmidt J, Kisters K. Magnesium in Prevention and Therapy. Nutrients. 2015;7(9):8199-226.

10.Sissi C, Palumbo M. Effects of magnesium and related divalent metal ions in topoisomerase structure and function. Nucleic Acids Res. 2009;37(3):702-11.

11.Blaszczyk U, Duda-Chodak A. Magnesium: its role in nutrition and carcinogenesis. Rocz Panstw Zakl Hig. 2013;64(3):165-71.

12.Apell HJ, Hitzler T, Schreiber G. Modulation of the Na,K-ATPase by Magnesium Ions. Biochemistry. 2017;56(7):1005-16.

13.Dai Q, Motley SS, Smith JA, Jr., Concepcion R, Barocas D, Byerly S, et al. Blood magnesium, and the interaction with calcium, on the risk of high-grade prostate cancer. PLoS One. 2011;6(4):e18237.

14.Yogi A, Callera GE, Antunes TT, Tostes RC, Touyz RM. Transient receptor potential melastatin 7 (TRPM7) cation channels, magnesium and the vascular system in hypertension. Circulation journal : official journal of the Japanese Circulation Society. 2011;75(2):237-45.

15.Romani A. Regulation of magnesium homeostasis and transport in mammalian cells. Arch Biochem Biophys. 2007;458(1):90-102.

16.Goytain A, Quamme GA. Identification and characterization of a novel mammalian Mg2+ transporter with channel-like properties. BMC Genomics. 2005;6:48.

17.Wolf FI, Trapani V. MagT1: a highly specific magnesium channel with important roles beyond cellular magnesium homeostasis. Magnes Res. 2011;24(3):S86-91.

18.Trapani V, Shomer N, Rajcan-Separovic E. The role of MAGT1 in genetic syndromes. Magnes Res. 2015;28(2):46-55.

19.Romani AM. Cellular magnesium homeostasis. Arch Biochem Biophys. 2011;512(1):1-23.

20.Zhou H, Clapham DE. Mammalian MagT1 and TUSC3 are required for cellular magnesium uptake and vertebrate embryonic development. Proc Natl Acad Sci U S A. 2009;106(37):15750-5.

21.Li FY, Lenardo MJ, Chaigne-Delalande B. Loss of MAGT1 abrogates the Mg2+ flux required for T cell signaling and leads to a novel human primary immunodeficiency. Magnesium research. 2011;24(3):S109-14.

22.Fleig A, Schweigel-Rontgen M, Kolisek M. Solute Carrier Family SLC41, what do we really know about it? Wiley Interdiscip Rev Membr Transp Signal. 2013;2(6).

23.Goytain A, Quamme GA. Functional characterization of human SLC41A1, a Mg2+ transporter with similarity to prokaryotic MgtE Mg2+ transporters. Physiol Genomics. 2005;21(3):337-42.

24.Mandt T, Song Y, Scharenberg AM, Sahni J. SLC41A1 Mg(2+) transport is regulated via Mg(2+)-dependent endosomal recycling through its N-terminal cytoplasmic domain. Biochem J. 2011;439(1):129-39.

25.Hurd TW, Otto EA, Mishima E, Gee HY, Inoue H, Inazu M, et al. Mutation of the Mg2+ transporter SLC41A1 results in a nephronophthisis-like phenotype. J Am Soc Nephrol. 2013;24(6):967-77.
26.Tsao YT, Shih YY, Liu YA, Liu YS, Lee OK. Knockdown of SLC41A1 magnesium transporter promotes mineralization and attenuates magnesium inhibition during osteogenesis of mesenchymal stromal cells. Stem Cell Res Ther. 2017;8(1):39.
27.Mastrototaro L, Smorodchenko A, Aschenbach JR, Kolisek M, Sponder G. Solute carrier 41A3 encodes for a mitochondrial Mg(2+) efflux system. Sci Rep. 2016;6:27999.
28.de Baaij JH, Arjona FJ, van den Brand M, Lavrijsen M, Lameris AL, Bindels RJ, et al. Identification of SLC41A3 as a novel player in magnesium homeostasis. Sci Rep. 2016;6:28565.
29.Schlingmann KP, Waldegger S, Konrad M, Chubanov V, Gudermann T. TRPM6 and TRPM7--Gatekeepers of human magnesium metabolism. Biochim Biophys Acta. 2007;1772(8):813-21.
30.Yee NS, Kazi AA, Yee RK. Cellular and Developmental Biology of TRPM7 Channel-Kinase: Implicated Roles in Cancer. Cells. 2014;3(3):751-77.
31.Montell C, Rubin GM. Molecular characterization of the Drosophila trp locus: a putative integral membrane protein required for phototransduction. Neuron. 1989;2(4):1313-23.
32.Li H. TRP Channel Classification. Adv Exp Med Biol. 2017;976:1-8.
33.Hardie RC, Minke B. The trp gene is essential for a light-activated Ca2+ channel in Drosophila photoreceptors. Neuron. 1992;8(4):643-51.
34.Samanta A, Hughes TET, Moiseenkova-Bell VY. Transient Receptor Potential (TRP) Channels. Subcell Biochem. 2018;87:141-65.
35.Nilius B, Owsianik G. The transient receptor potential family of ion channels. Genome Biol. 2011;12(3):218.
36.Startek JB, Boonen B, Talavera K, Meseguer V. TRP Channels as Sensors of Chemically-Induced Changes in Cell Membrane Mechanical Properties. Int J Mol Sci. 2019;20(2).
37.Tiulpakov A, Kalintchenko N, Semitcheva T, Polyakov A, Dedov I, Sverdlova P, et al. A potential rearrangement between CYP19 and TRPM7 genes on chromosome 15q21.2 as a cause of aromatase excess syndrome. J Clin Endocrinol Metab. 2005;90(7):4184-90.
38.Hara K, Kokubo Y, Ishiura H, Fukuda Y, Miyashita A, Kuwano R, et al. TRPM7 is not associated with amyotrophic lateral sclerosis-parkinsonism dementia complex in the Kii peninsula of Japan. Am J Med Genet B Neuropsychiatr Genet. 2010;153B(1):310-3.
39.Venkatachalam K, Montell C. TRP channels. Annu Rev Biochem. 2007;76:387-417.
40.Nilius B. TRP channels in disease. Biochim Biophys Acta. 2007;1772(8):805-12.
41.Clapham DE. TRP channels as cellular sensors. Nature. 2003;426(6966):517-24.
42.Duan J, Li Z, Li J, Hulse RE, Santa-Cruz A, Valinsky WC, et al. Structure of the mammalian TRPM7, a magnesium channel required during embryonic development. Proc Natl Acad Sci U S A. 2018;115(35):E8201-E10.
43.Levitan IB, Cibulsky SM. Biochemistry. TRP ion channels--two proteins in one. Science. 2001;293(5533):1270-1.
44.Park HS, Hong C, Kim BJ, So I. The Pathophysiologic Roles of TRPM7 Channel. Korean J Physiol Pharmacol. 2014;18(1):15-23.
45.Paravicini TM, Chubanov V, Gudermann T. TRPM7: a unique channel involved in magnesium homeostasis. Int J Biochem Cell Biol. 2012;44(8):1381-4.
46.Zou ZG, Rios FJ, Montezano AC, Touyz RM. TRPM7, Magnesium, and Signaling. Int J Mol Sci. 2019;20(8).
47.Yamaguchi H, Matsushita M, Nairn AC, Kuriyan J. Crystal structure of the atypical protein kinase domain of a TRP channel with phosphotransferase activity. Mol Cell. 2001;7(5):1047-57.
48.Schlingmann KP, Gudermann T. A critical role of TRPM channel-kinase for human magnesium transport. J Physiol. 2005;566(Pt 2):301-8.
49.Chubanov V, Gudermann T. Trpm6. Handb Exp Pharmacol. 2014;222:503-20.
50.Schlingmann KP, Weber S, Peters M, Niemann Nejsum L, Vitzthum H, Klingel K, et al. Hypomagnesemia with secondary hypocalcemia is caused by mutations in TRPM6, a new member of the TRPM gene family. Nat Genet. 2002;31(2):166-70.

51.Astor MC, Lovas K, Wolff AS, Nedrebo B, Bratland E, Steen-Johnsen J, et al. Hypomagnesemia and functional hypoparathyroidism due to novel mutations in the Mg-channel TRPM6. Endocr Connect. 2015;4(4):215-22.
52.Voets T, Nilius B, Hoefs S, van der Kemp AW, Droogmans G, Bindels RJ, et al. TRPM6 forms the Mg2+ influx channel involved in intestinal and renal Mg2+ absorption. J Biol Chem. 2004;279(1):19-25.
53.van der Wijst J, Blanchard MG, Woodroof HI, Macartney TJ, Gourlay R, Hoenderop JG, et al. Kinase and channel activity of TRPM6 are co-ordinated by a dimerization motif and pocket interaction. Biochem J. 2014;460(2):165-75.
54.Thebault S, Cao G, Venselaar H, Xi Q, Bindels RJ, Hoenderop JG. Role of the alpha-kinase domain in transient receptor potential melastatin 6 channel and regulation by intracellular ATP. J Biol Chem. 2008;283(29):19999-20007.
55.Cao G, Thebault S, van der Wijst J, van der Kemp A, Lasonder E, Bindels RJ, et al. RACK1 inhibits TRPM6 activity via phosphorylation of the fused alpha-kinase domain. Curr Biol. 2008;18(3):168-76.
56.Krapivinsky G, Krapivinsky L, Renthal NE, Santa-Cruz A, Manasian Y, Clapham DE. Histone phosphorylation by TRPM6's cleaved kinase attenuates adjacent arginine methylation to regulate gene expression. Proc Natl Acad Sci U S A. 2017;114(34):E7092-E100.
57.Zhang Z, Faouzi M, Huang J, Geerts D, Yu H, Fleig A, et al. N-Myc-induced up-regulation of TRPM6/TRPM7 channels promotes neuroblastoma cell proliferation. Oncotarget. 2014;5(17):7625-34.
58.Clark K, Middelbeek J, Dorovkov MV, Figdor CG, Ryazanov AG, Lasonder E, et al. The alpha-kinases TRPM6 and TRPM7, but not eEF-2 kinase, phosphorylate the assembly domain of myosin IIA, IIB and IIC. FEBS Lett. 2008;582(20):2993-7.
59.Zhang Z, Yu H, Huang J, Faouzi M, Schmitz C, Penner R, et al. The TRPM6 kinase domain determines the Mg.ATP sensitivity of TRPM7/M6 heteromeric ion channels. J Biol Chem. 2014;289(8):5217-27.
60.Chubanov V, Ferioli S, Wisnowsky A, Simmons DG, Leitzinger C, Einer C, et al. Epithelial magnesium transport by TRPM6 is essential for prenatal development and adult survival. Elife. 2016;5.
61.Cai N, Bai Z, Nanda V, Runnels LW. Mass Spectrometric Analysis of TRPM6 and TRPM7 Phosphorylation Reveals Regulatory Mechanisms of the Channel-Kinases. Sci Rep. 2017;7:42739.
62.Deason-Towne F, Perraud AL, Schmitz C. The Mg2+ transporter MagT1 partially rescues cell growth and Mg2+ uptake in cells lacking the channel-kinase TRPM7. FEBS Lett. 2011;585(14):2275-8.
63.Cazzaniga A, Moscheni C, Trapani V, Wolf FI, Farruggia G, Sargenti A, et al. The different expression of TRPM7 and MagT1 impacts on the proliferation of colon carcinoma cells sensitive or resistant to doxorubicin. Scientific reports. 2017;7:40538.
64.Brandao K, Deason-Towne F, Zhao X, Perraud AL, Schmitz C. TRPM6 kinase activity regulates TRPM7 trafficking and inhibits cellular growth under hypomagnesic conditions. Cell Mol Life Sci. 2014;71(24):4853-67.
65.Monteilh-Zoller MK, Hermosura MC, Nadler MJ, Scharenberg AM, Penner R, Fleig A. TRPM7 provides an ion channel mechanism for cellular entry of trace metal ions. J Gen Physiol. 2003;121(1):49-60.
66.Abiria SA, Krapivinsky G, Sah R, Santa-Cruz AG, Chaudhuri D, Zhang J, et al. TRPM7 senses oxidative stress to release Zn(2+) from unique intracellular vesicles. Proceedings of the National Academy of Sciences of the United States of America. 2017;114(30):E6079-E88.
67.Nadler MJ, Hermosura MC, Inabe K, Perraud AL, Zhu Q, Stokes AJ, et al. LTRPC7 is a Mg.ATP-regulated divalent cation channel required for cell viability. Nature. 2001;411(6837):590-5.
68.Gwanyanya A, Amuzescu B, Zakharov SI, Macianskiene R, Sipido KR, Bolotina VM, et al. Magnesium-inhibited, TRPM6/7-like channel in cardiac myocytes: permeation of divalent cations and pH-mediated regulation. J Physiol. 2004;559(Pt 3):761-76.

69.Yu Y, Chen S, Xiao C, Jia Y, Guo J, Jiang J, et al. TRPM7 is involved in angiotensin II induced cardiac fibrosis development by mediating calcium and magnesium influx. Cell Calcium. 2014;55(5):252-60.
70.Castiglioni S, Cazzaniga A, Trapani V, Cappadone C, Farruggia G, Merolle L, et al. Magnesium homeostasis in colon carcinoma LoVo cells sensitive or resistant to doxorubicin. Sci Rep. 2015;5:16538.
71.Stritt S, Nurden P, Favier R, Favier M, Ferioli S, Gotru SK, et al. Defects in TRPM7 channel function deregulate thrombopoiesis through altered cellular Mg(2+) homeostasis and cytoskeletal architecture. Nat Commun. 2016;7:11097.
72.Tashiro M, Inoue H, Konishi M. Physiological pathway of magnesium influx in rat ventricular myocytes. Biophys J. 2014;107(9):2049-58.
73.Abed E, Moreau R. Importance of melastatin-like transient receptor potential 7 and cations (magnesium, calcium) in human osteoblast-like cell proliferation. Cell Prolif. 2007;40(6):849-65.
74.Zhu D, You J, Zhao N, Xu H. Magnesium Regulates Endothelial Barrier Functions through TRPM7, MagT1, and S1P1. Advanced science. 2019;6(18):1901166.
75.Baldoli E, Castiglioni S, Maier JA. Regulation and function of TRPM7 in human endothelial cells: TRPM7 as a potential novel regulator of endothelial function. PloS one. 2013;8(3):e59891.
76.Ryazanova LV, Rondon LJ, Zierler S, Hu Z, Galli J, Yamaguchi TP, et al. TRPM7 is essential for Mg(2+) homeostasis in mammals. Nat Commun. 2010;1:109.
77.Antunes TT, Callera GE, He Y, Yogi A, Ryazanov AG, Ryazanova LV, et al. Transient Receptor Potential Melastatin 7 Cation Channel Kinase: New Player in Angiotensin II-Induced Hypertension. Hypertension. 2016;67(4):763-73.
78.Paravicini TM, Yogi A, Mazur A, Touyz RM. Dysregulation of vascular TRPM7 and annexin-1 is associated with endothelial dysfunction in inherited hypomagnesemia. Hypertension. 2009;53(2):423-9.
79.Jin J, Desai BN, Navarro B, Donovan A, Andrews NC, Clapham DE. Deletion of Trpm7 disrupts embryonic development and thymopoiesis without altering Mg2+ homeostasis. Science. 2008;322(5902):756-60.
80.Li FY, Chaigne-Delalande B, Kanellopoulou C, Davis JC, Matthews HF, Douek DC, et al. Second messenger role for Mg2+ revealed by human T-cell immunodeficiency. Nature. 2011;475(7357):471-6.
81.Krebs J, Agellon LB, Michalak M. Ca(2+) homeostasis and endoplasmic reticulum (ER) stress: An integrated view of calcium signaling. Biochem Biophys Res Commun. 2015;460(1):114-21.
82.Massullo P, Sumoza-Toledo A, Bhagat H, Partida-Sanchez S. TRPM channels, calcium and redox sensors during innate immune responses. Semin Cell Dev Biol. 2006;17(6):654-66.
83.Du J, Xie J, Zhang Z, Tsujikawa H, Fusco D, Silverman D, et al. TRPM7-mediated Ca2+ signals confer fibrogenesis in human atrial fibrillation. Circ Res. 2010;106(5):992-1003.
84.Clark K, Langeslag M, van Leeuwen B, Ran L, Ryazanov AG, Figdor CG, et al. TRPM7, a novel regulator of actomyosin contractility and cell adhesion. The EMBO journal. 2006;25(2):290-301.
85.Schappe MS, Szteyn K, Stremska ME, Mendu SK, Downs TK, Seegren PV, et al. Chanzyme TRPM7 Mediates the Ca(2+) Influx Essential for Lipopolysaccharide-Induced Toll-Like Receptor 4 Endocytosis and Macrophage Activation. Immunity. 2018;48(1):59-74 e5.
86.Faouzi M, Kilch T, Horgen FD, Fleig A, Penner R. The TRPM7 channel kinase regulates store-operated calcium entry. The Journal of physiology. 2017;595(10):3165-80.
87.Beesetty P, Wieczerzak KB, Gibson JN, Kaitsuka T, Luu CT, Matsushita M, et al. Inactivation of TRPM7 kinase in mice results in enlarged spleens, reduced T-cell proliferation and diminished store-operated calcium entry. Sci Rep. 2018;8(1):3023.
88.Inoue K, Branigan D, Xiong ZG. Zinc-induced neurotoxicity mediated by transient receptor potential melastatin 7 channels. J Biol Chem. 2010;285(10):7430-9.
89.Georgiev P, Okkenhaug H, Drews A, Wright D, Lambert S, Flick M, et al. TRPM channels mediate zinc homeostasis and cellular growth during Drosophila larval development. Cell Metab. 2010;12(4):386-97.

90.Yu P, Wang Q, Zhang LH, Lee HC, Zhang L, Yue J. A cell permeable NPE caged ADP-ribose for studying TRPM2. PLoS One. 2012;7(12):e51028.
91.Yang W, Manna PT, Zou J, Luo J, Beech DJ, Sivaprasadarao A, et al. Zinc inactivates melastatin transient receptor potential 2 channels via the outer pore. J Biol Chem. 2011;286(27):23789-98.
92.Manna PT, Munsey TS, Abuarab N, Li F, Asipu A, Howell G, et al. TRPM2-mediated intracellular Zn2+ release triggers pancreatic beta-cell death. Biochem J. 2015;466(3):537-46.
93.Uchida K, Tominaga M. Extracellular zinc ion regulates transient receptor potential melastatin 5 (TRPM5) channel activation through its interaction with a pore loop domain. J Biol Chem. 2013;288(36):25950-5.
94.Middelbeek J, Clark K, Venselaar H, Huynen MA, van Leeuwen FN. The alpha-kinase family: an exceptional branch on the protein kinase tree. Cell Mol Life Sci. 2010;67(6):875-90.
95.Drennan D, Ryazanov AG. Alpha-kinases: analysis of the family and comparison with conventional protein kinases. Prog Biophys Mol Biol. 2004;85(1):1-32.
96.Kim TY, Shin SK, Song MY, Lee JE, Park KS. Identification of the phosphorylation sites on intact TRPM7 channels from mammalian cells. Biochem Biophys Res Commun. 2012;417(3):1030-4.
97.Clark K, Middelbeek J, Morrice NA, Figdor CG, Lasonder E, van Leeuwen FN. Massive autophosphorylation of the Ser/Thr-rich domain controls protein kinase activity of TRPM6 and TRPM7. PLoS One. 2008;3(3):e1876.
98.Dorovkov MV, Ryazanov AG. Phosphorylation of annexin I by TRPM7 channel-kinase. J Biol Chem. 2004;279(49):50643-6.
99.Clark K, Middelbeek J, Lasonder E, Dulyaninova NG, Morrice NA, Ryazanov AG, et al. TRPM7 regulates myosin IIA filament stability and protein localization by heavy chain phosphorylation. Journal of molecular biology. 2008;378(4):790-803.
100.Perraud AL, Zhao X, Ryazanov AG, Schmitz C. The channel-kinase TRPM7 regulates phosphorylation of the translational factor eEF2 via eEF2-k. Cell Signal. 2011;23(3):586-93.
101.Romagnani A, Vettore V, Rezzonico-Jost T, Hampe S, Rottoli E, Nadolni W, et al. TRPM7 kinase activity is essential for T cell colonization and alloreactivity in the gut. Nat Commun. 2017;8(1):1917.
102.Deason-Towne F, Perraud AL, Schmitz C. Identification of Ser/Thr phosphorylation sites in the C2-domain of phospholipase C gamma2 (PLCgamma2) using TRPM7-kinase. Cell Signal. 2012;24(11):2070-5.
103.Su LT, Agapito MA, Li M, Simonson WT, Huttenlocher A, Habas R, et al. TRPM7 regulates cell adhesion by controlling the calcium-dependent protease calpain. J Biol Chem. 2006;281(16):11260-70.
104.Su LT, Chen HC, Gonzalez-Pagan O, Overton JD, Xie J, Yue L, et al. TRPM7 activates m-calpain by stress-dependent stimulation of p38 MAPK and c-Jun N-terminal kinase. J Mol Biol. 2010;396(4):858-69.
105.Matsushita M, Kozak JA, Shimizu Y, McLachlin DT, Yamaguchi H, Wei FY, et al. Channel function is dissociated from the intrinsic kinase activity and autophosphorylation of TRPM7/ChaK1. The Journal of biological chemistry. 2005;280(21):20793-803.
106.Kaitsuka T, Katagiri C, Beesetty P, Nakamura K, Hourani S, Tomizawa K, et al. Inactivation of TRPM7 kinase activity does not impair its channel function in mice. Sci Rep. 2014;4:5718.
107.Schmitz C, Perraud AL, Johnson CO, Inabe K, Smith MK, Penner R, et al. Regulation of vertebrate cellular Mg2+ homeostasis by TRPM7. Cell. 2003;114(2):191-200.
108.Desai BN, Krapivinsky G, Navarro B, Krapivinsky L, Carter BC, Febvay S, et al. Cleavage of TRPM7 releases the kinase domain from the ion channel and regulates its participation in Fas-induced apoptosis. Dev Cell. 2012;22(6):1149-62.
109.Demeuse P, Penner R, Fleig A. TRPM7 channel is regulated by magnesium nucleotides via its kinase domain. J Gen Physiol. 2006;127(4):421-34.
110.Yu H, Zhang Z, Lis A, Penner R, Fleig A. TRPM7 is regulated by halides through its kinase domain. Cell Mol Life Sci. 2013;70(15):2757-71.

111.Takezawa R, Schmitz C, Demeuse P, Scharenberg AM, Penner R, Fleig A. Receptor-mediated regulation of the TRPM7 channel through its endogenous protein kinase domain. Proc Natl Acad Sci U S A. 2004;101(16):6009-14.
112.Rios FJ, Zou ZG, Harvey AP, Harvey KY, Nosalski R, Anyfanti P, et al. Chanzyme TRPM7 protects against cardiovascular inflammation and fibrosis. Cardiovascular research. 2020;116(3):721-35.
113.Maret W. Zinc biochemistry: from a single zinc enzyme to a key element of life. Adv Nutr. 2013;4(1):82-91.
114.Long S, Romani AM. Role of Cellular Magnesium in Human Diseases. Austin J Nutr Food Sci. 2014;2(10).
115.Ikari A, Sawada H, Sanada A, Tonegawa C, Yamazaki Y, Sugatani J. Magnesium deficiency suppresses cell cycle progression mediated by increase in transcriptional activity of p21(Cip1) and p27(Kip1) in renal epithelial NRK-52E cells. J Cell Biochem. 2011;112(12):3563-72.
116.MacDonald RS. The role of zinc in growth and cell proliferation. J Nutr. 2000;130(5S Suppl):1500S-8S.
117.Fukada T, Yamasaki S, Nishida K, Murakami M, Hirano T. Zinc homeostasis and signaling in health and diseases: Zinc signaling. J Biol Inorg Chem. 2011;16(7):1123-34.
118.Capiod T. Cell proliferation, calcium influx and calcium channels. Biochimie. 2011;93(12):2075-9.
119.Resende RR, Andrade LM, Oliveira AG, Guimaraes ES, Guatimosim S, Leite MF. Nucleoplasmic calcium signaling and cell proliferation: calcium signaling in the nucleus. Cell Commun Signal. 2013;11(1):14.
120.Ni HM, Baty CJ, Li N, Ding WX, Gao W, Li M, et al. Bid agonist regulates murine hepatocyte proliferation by controlling endoplasmic reticulum calcium homeostasis. Hepatology. 2010;52(1):338-48.
121.Kawamoto EM, Vivar C, Camandola S. Physiology and pathology of calcium signaling in the brain. Front Pharmacol. 2012;3:61.
122.Hardingham GE, Bading H. Calcium as a versatile second messenger in the control of gene expression. Microsc Res Tech. 1999;46(6):348-55.
123.Huang J, Furuya H, Faouzi M, Zhang Z, Monteilh-Zoller M, Kawabata KG, et al. Inhibition of TRPM7 suppresses cell proliferation of colon adenocarcinoma in vitro and induces hypomagnesemia in vivo without affecting azoxymethane-induced early colon cancer in mice. Cell Commun Signal. 2017;15(1):30.
124.Zeng Z, Leng T, Feng X, Sun H, Inoue K, Zhu L, et al. Silencing TRPM7 in mouse cortical astrocytes impairs cell proliferation and migration via ERK and JNK signaling pathways. PloS one. 2015;10(3):e0119912.
125.Chen HC, Su LT, Gonzalez-Pagan O, Overton JD, Runnels LW. A key role for Mg(2+) in TRPM7's control of ROS levels during cell stress. Biochem J. 2012;445(3):441-8.
126.Hanano T, Hara Y, Shi J, Morita H, Umebayashi C, Mori E, et al. Involvement of TRPM7 in cell growth as a spontaneously activated Ca2+ entry pathway in human retinoblastoma cells. J Pharmacol Sci. 2004;95(4):403-19.
127.Takahashi K, Umebayashi C, Numata T, Honda A, Ichikawa J, Hu Y, et al. TRPM7-mediated spontaneous Ca(2+) entry regulates the proliferation and differentiation of human leukemia cell line K562. Physiol Rep. 2018;6(14):e13796.
128.Sun Y, Sukumaran P, Varma A, Derry S, Sahmoun AE, Singh BB. Cholesterol-induced activation of TRPM7 regulates cell proliferation, migration, and viability of human prostate cells. Biochim Biophys Acta. 2014;1843(9):1839-50.
129.Lin J, Zhou S, Zhao T, Ju T, Zhang L. TRPM7 channel regulates ox-LDL-induced proliferation and migration of vascular smooth muscle cells via MEK-ERK pathways. FEBS Lett. 2016;590(4):520-32.
130.Callera GE, He Y, Yogi A, Montezano AC, Paravicini T, Yao G, et al. Regulation of the novel Mg2+ transporter transient receptor potential melastatin 7 (TRPM7) cation channel by bradykinin in vascular smooth muscle cells. J Hypertens. 2009;27(1):155-66.

131.Chen L, Cao R, Wang G, Yuan L, Qian G, Guo Z, et al. Downregulation of TRPM7 suppressed migration and invasion by regulating epithelial-mesenchymal transition in prostate cancer cells. Med Oncol. 2017;34(7):127.
132.Wong R, Turlova E, Feng ZP, Rutka JT, Sun HS. Activation of TRPM7 by naltriben enhances migration and invasion of glioblastoma cells. Oncotarget. 2017;8(7):11239-48.
133.Lange I, Koomoa DL. MycN promotes TRPM7 expression and cell migration in neuroblastoma through a process that involves polyamines. FEBS Open Bio. 2014;4:966-75.
134.Gao SL, Kong CZ, Zhang Z, Li ZL, Bi JB, Liu XK. TRPM7 is overexpressed in bladder cancer and promotes proliferation, migration, invasion and tumor growth. Oncol Rep. 2017;38(4):1967-76.
135.Gao H, Chen X, Du X, Guan B, Liu Y, Zhang H. EGF enhances the migration of cancer cells by up-regulation of TRPM7. Cell Calcium. 2011;50(6):559-68.
136.Guilbert A, Gautier M, Dhennin-Duthille I, Rybarczyk P, Sahni J, Sevestre H, et al. Transient receptor potential melastatin 7 is involved in oestrogen receptor-negative metastatic breast cancer cells migration through its kinase domain. Eur J Cancer. 2013;49(17):3694-707.
137.Jin J, Wu LJ, Jun J, Cheng X, Xu H, Andrews NC, et al. The channel kinase, TRPM7, is required for early embryonic development. Proc Natl Acad Sci U S A. 2012;109(5):E225-33.
138.Sah R, Mesirca P, Mason X, Gibson W, Bates-Withers C, Van den Boogert M, et al. Timing of myocardial trpm7 deletion during cardiogenesis variably disrupts adult ventricular function, conduction, and repolarization. Circulation. 2013;128(2):101-14.
139.Liu YS, Liu YA, Huang CJ, Yen MH, Tseng CT, Chien S, et al. Mechanosensitive TRPM7 mediates shear stress and modulates osteogenic differentiation of mesenchymal stromal cells through Osterix pathway. Sci Rep. 2015;5:16522.
140.Yang M, Fang J, Liu Q, Wang Y, Zhang Z. Role of ROS-TRPM7-ERK1/2 axis in high concentration glucose-mediated proliferation and phenotype switching of rat aortic vascular smooth muscle cells. Biochem Biophys Res Commun. 2017;494(3-4):526-33.
141.Montezano AC, Zimmerman D, Yusuf H, Burger D, Chignalia AZ, Wadhera V, et al. Vascular smooth muscle cell differentiation to an osteogenic phenotype involves TRPM7 modulation by magnesium. Hypertension. 2010;56(3):453-62.
142.Zhang K, Zhang Y, Feng W, Chen R, Chen J, Touyz RM, et al. Interleukin-18 Enhances Vascular Calcification and Osteogenic Differentiation of Vascular Smooth Muscle Cells Through TRPM7 Activation. Arterioscler Thromb Vasc Biol. 2017;37(10):1933-43.
143.Ogunrinde A, Pereira RD, Beaton N, Lam DH, Whetstone C, Hill CE. Hepatocellular differentiation status is characterized by distinct subnuclear localization and form of the chanzyme TRPM7. Differentiation. 2017;96:15-25.
144.Yu M, Huang C, Huang Y, Wu X, Li X, Li J. Inhibition of TRPM7 channels prevents proliferation and differentiation of human lung fibroblasts. Inflamm Res. 2013;62(11):961-70.
145.Cui L, Xu SM, Ma DD, Wu BL. The effect of TRPM7 suppression on the proliferation, migration and osteogenic differentiation of human dental pulp stem cells. Int Endod J. 2014;47(6):583-93.
146.Zhang X, Zu H, Zhao D, Yang K, Tian S, Yu X, et al. Ion channel functional protein kinase TRPM7 regulates Mg ions to promote the osteoinduction of human osteoblast via PI3K pathway: In vitro simulation of the bone-repairing effect of Mg-based alloy implant. Acta Biomater. 2017;63:369-82.
147.Xiao E, Yang HQ, Gan YH, Duan DH, He LH, Guo Y, et al. Brief reports: TRPM7 Senses mechanical stimulation inducing osteogenesis in human bone marrow mesenchymal stem cells. Stem Cells. 2015;33(2):615-21.
148.Cheng H, Feng JM, Figueiredo ML, Zhang H, Nelson PL, Marigo V, et al. Transient receptor potential melastatin type 7 channel is critical for the survival of bone marrow derived mesenchymal stem cells. Stem Cells Dev. 2010;19(9):1393-403.
149.Diaz-Tocados JM, Herencia C, Martinez-Moreno JM, Montes de Oca A, Rodriguez-Ortiz ME, Vergara N, et al. Magnesium Chloride promotes Osteogenesis through Notch signaling activation and expansion of Mesenchymal Stem Cells. Sci Rep. 2017;7(1):7839.
150.Peruzzo R, Biasutto L, Szabo I, Leanza L. Impact of intracellular ion channels on cancer development and progression. Eur Biophys J. 2016;45(7):685-707.

151.Prevarskaya N, Skryma R, Shuba Y. Ion Channels in Cancer: Are Cancer Hallmarks Oncochannelopathies? Physiol Rev. 2018;98(2):559-621.
152.Hantute-Ghesquier A, Haustrate A, Prevarskaya N, Lehen'kyi V. TRPM Family Channels in Cancer. Pharmaceuticals (Basel). 2018;11(2).
153.Yee NS. Role of TRPM7 in Cancer: Potential as Molecular Biomarker and Therapeutic Target. Pharmaceuticals. 2017;10(2).
154.Zhou W, Guo S, Xiong Z, Liu M. Oncogenic role and therapeutic target of transient receptor potential melastatin 7 channel in malignancy. Expert Opin Ther Targets. 2014;18(10):1177-96.
155.Liu M, Inoue K, Leng T, Guo S, Xiong ZG. TRPM7 channels regulate glioma stem cell through STAT3 and Notch signaling pathways. Cell Signal. 2014;26(12):2773-81.
156.Liu K, Xu SH, Chen Z, Zeng QX, Li ZJ, Chen ZM. TRPM7 overexpression enhances the cancer stem cell-like and metastatic phenotypes of lung cancer through modulation of the Hsp90alpha/uPA/MMP2 signaling pathway. BMC Cancer. 2018;18(1):1167.
157.Mittermeier L, Demirkhanyan L, Stadlbauer B, Breit A, Recordati C, Hilgendorff A, et al. TRPM7 is the central gatekeeper of intestinal mineral absorption essential for postnatal survival. Proc Natl Acad Sci U S A. 2019.
158.Sah R, Mesirca P, Van den Boogert M, Rosen J, Mably J, Mangoni ME, et al. Ion channel-kinase TRPM7 is required for maintaining cardiac automaticity. Proc Natl Acad Sci U S A. 2013;110(32):E3037-46.
159.Zhong H, Wang T, Lian G, Xu C, Wang H, Xie L. TRPM7 regulates angiotensin II-induced sinoatrial node fibrosis in sick sinus syndrome rats by mediating Smad signaling. Heart and vessels. 2018;33(9):1094-105.
160.Zhang YH, Sun HY, Chen KH, Du XL, Liu B, Cheng LC, et al. Evidence for functional expression of TRPM7 channels in human atrial myocytes. Basic Res Cardiol. 2012;107(5):282.
161.Ortega A, Rosello-Lleti E, Tarazon E, Gil-Cayuela C, Lago F, Gonzalez-Juanatey JR, et al. TRPM7 is down-regulated in both left atria and left ventricle of ischaemic cardiomyopathy patients and highly related to changes in ventricular function. ESC Heart Fail. 2016;3(3):220-4.
162.Wu Y, Liu Y, Pan Y, Lu C, Xu H, Wang X, et al. MicroRNA-135a inhibits cardiac fibrosis induced by isoproterenol via TRPM7 channel. Biomed Pharmacother. 2018;104:252-60.
163.Whelton PK, Klag MJ. Magnesium and blood pressure: review of the epidemiologic and clinical trial experience. Am J Cardiol. 1989;63(14):26G-30G.
164.Sontia B, Touyz RM. Magnesium transport in hypertension. Pathophysiology. 2007;14(3-4):205-11.
165.Touyz RM, Milne FJ, Reinach SG. Intracellular Mg2+, Ca2+, Na2+ and K+ in platelets and erythrocytes of essential hypertension patients: relation to blood pressure. Clin Exp Hypertens A. 1992;14(6):1189-209.
166.Touyz RM, He Y, Montezano AC, Yao G, Chubanov V, Gudermann T, et al. Differential regulation of transient receptor potential melastatin 6 and 7 cation channels by ANG II in vascular smooth muscle cells from spontaneously hypertensive rats. American journal of physiology Regulatory, integrative and comparative physiology. 2006;290(1):R73-8.
167.Touyz RM. Transient receptor potential melastatin 6 and 7 channels, magnesium transport, and vascular biology: implications in hypertension. Am J Physiol Heart Circ Physiol. 2008;294(3):H1103-18.
168.Oancea E, Wolfe JT, Clapham DE. Functional TRPM7 channels accumulate at the plasma membrane in response to fluid flow. Circulation research. 2006;98(2):245-53.
169.Sontia B, Montezano AC, Paravicini T, Tabet F, Touyz RM. Downregulation of renal TRPM7 and increased inflammation and fibrosis in aldosterone-infused mice: effects of magnesium. Hypertension. 2008;51(4):915-21.
170.Rocha-Penha L, Caldeira-Dias M, Tanus-Santos JE, de Carvalho Cavalli R, Sandrim VC. Myeloperoxidase in Hypertensive Disorders of Pregnancy and Its Relation With Nitric Oxide. Hypertension. 2017;69(6):1173-80.

171.Etwebi Z, Landesberg G, Preston K, Eguchi S, Scalia R. Mechanistic Role of the Calcium-Dependent Protease Calpain in the Endothelial Dysfunction Induced by MPO (Myeloperoxidase). Hypertension. 2018;71(4):761-70.
172.Letavernier E, Perez J, Bellocq A, Mesnard L, de Castro Keller A, Haymann JP, et al. Targeting the calpain/calpastatin system as a new strategy to prevent cardiovascular remodeling in angiotensin II-induced hypertension. Circ Res. 2008;102(6):720-8.
173.Touyz RM, Alves-Lopes R, Rios FJ, Camargo LL, Anagnostopoulou A, Arner A, et al. Vascular smooth muscle contraction in hypertension. Cardiovasc Res. 2018;114(4):529-39.
174.Goulopoulou S, Webb RC. Symphony of vascular contraction: how smooth muscle cells lose harmony to signal increased vascular resistance in hypertension. Hypertension. 2014;63(3):e33-9.
175.Brown MJ, Palmer CR, Castaigne A, de Leeuw PW, Mancia G, Rosenthal T, et al. Morbidity and mortality in patients randomised to double-blind treatment with a long-acting calcium-channel blocker or diuretic in the International Nifedipine GITS study: Intervention as a Goal in Hypertension Treatment (INSIGHT). Lancet. 2000;356(9227):366-72.
176.Vennekens R. Emerging concepts for the role of TRP channels in the cardiovascular system. J Physiol. 2011;589(Pt 7):1527-34.
177.Firth AL, Remillard CV, Yuan JX. TRP channels in hypertension. Biochim Biophys Acta. 2007;1772(8):895-906.
178.Schmidt K, Dubrovska G, Nielsen G, Fesus G, Uhrenholt TR, Hansen PB, et al. Amplification of EDHF-type vasodilatations in TRPC1-deficient mice. Br J Pharmacol. 2010;161(8):1722-33.
179.Liu D, Scholze A, Zhu Z, Krueger K, Thilo F, Burkert A, et al. Transient receptor potential channels in essential hypertension. J Hypertens. 2006;24(6):1105-14.
180.Liu D, Scholze A, Zhu Z, Kreutz R, Wehland-von-Trebra M, Zidek W, et al. Increased transient receptor potential channel TRPC3 expression in spontaneously hypertensive rats. Am J Hypertens. 2005;18(11):1503-7.
181.Scalia R, Gong Y, Berzins B, Freund B, Feather D, Landesberg G, et al. A novel role for calpain in the endothelial dysfunction induced by activation of angiotensin II type 1 receptor signaling. Circ Res. 2011;108(9):1102-11.
182.Goncalves I, Nitulescu M, Saido TC, Dias N, Pedro LM, JF EF, et al. Activation of calpain-1 in human carotid artery atherosclerotic lesions. BMC Cardiovasc Disord. 2009;9:26.
183.Suzuki K, Hata S, Kawabata Y, Sorimachi H. Structure, activation, and biology of calpain. Diabetes. 2004;53 Suppl 1:S12-8.
184.Letavernier B, Zafrani L, Nassar D, Perez J, Levi C, Bellocq A, et al. Calpains contribute to vascular repair in rapidly progressive form of glomerulonephritis: potential role of their externalization. Arterioscler Thromb Vasc Biol. 2012;32(2):335-42.
185.Stalker TJ, Gong Y, Scalia R. The calcium-dependent protease calpain causes endothelial dysfunction in type 2 diabetes. Diabetes. 2005;54(4):1132-40.
186.Stalker TJ, Skvarka CB, Scalia R. A novel role for calpains in the endothelial dysfunction of hyperglycemia. FASEB J. 2003;17(11):1511-3.
187.Kovacs L, Han W, Rafikov R, Bagi Z, Offermanns S, Saido TC, et al. Activation of Calpain-2 by Mediators in Pulmonary Vascular Remodeling of Pulmonary Arterial Hypertension. Am J Respir Cell Mol Biol. 2016;54(3):384-93.
188.Salamino F, Sparatore B, De Tullio R, Pontremoli R, Melloni E, Pontremoli S. The calpastatin defect in hypertension is possibly due to a specific degradation by calpain. Biochim Biophys Acta. 1991;1096(4):265-9.
189.Averna M, De Tullio R, Salamino F, Minafra R, Pontremoli S, Melloni E. Age-dependent degradation of calpastatin in kidney of hypertensive rats. J Biol Chem. 2001;276(42):38426-32.
190.Duffy JY, Schwartz SM, Lyons JM, Bell JH, Wagner CJ, Zingarelli B, et al. Calpain inhibition decreases endothelin-1 levels and pulmonary hypertension after cardiopulmonary bypass with deep hypothermic circulatory arrest. Crit Care Med. 2005;33(3):623-8.
191.Mirsaeidi M, Gidfar S, Vu A, Schraufnagel D. Annexins family: insights into their functions and potential role in pathogenesis of sarcoidosis. J Transl Med. 2016;14:89.

192.Camors E, Monceau V, Charlemagne D. Annexins and Ca2+ handling in the heart. Cardiovasc Res. 2005;65(4):793-802.
193.de Jong R, Leoni G, Drechsler M, Soehnlein O. The advantageous role of annexin A1 in cardiovascular disease. Cell Adh Migr. 2017;11(3):261-74.
194.Purvis GSD, Solito E, Thiemermann C. Annexin-A1: Therapeutic Potential in Microvascular Disease. Front Immunol. 2019;10:938.
195.Drechsler M, de Jong R, Rossaint J, Viola JR, Leoni G, Wang JM, et al. Annexin A1 counteracts chemokine-induced arterial myeloid cell recruitment. Circ Res. 2015;116(5):827-35.
196.Kusters DH, Chatrou ML, Willems BA, De Saint-Hubert M, Bauwens M, van der Vorst E, et al. Pharmacological Treatment with Annexin A1 Reduces Atherosclerotic Plaque Burden in LDLR-/- Mice on Western Type Diet. PLoS One. 2015;10(6):e0130484.
197.Qin CX, Rosli S, Deo M, Cao N, Walsh J, Tate M, et al. Cardioprotective Actions of the Annexin-A1 N-Terminal Peptide, Ac2-26, Against Myocardial Infarction. Front Pharmacol. 2019;10:269.
198.de Jong RJ, Paulin N, Lemnitzer P, Viola JR, Winter C, Ferraro B, et al. Protective Aptitude of Annexin A1 in Arterial Neointima Formation in Atherosclerosis-Prone Mice-Brief Report. Arterioscler Thromb Vasc Biol. 2017;37(2):312-5.
199.Ewing MM, de Vries MR, Nordzell M, Pettersson K, de Boer HC, van Zonneveld AJ, et al. Annexin A5 therapy attenuates vascular inflammation and remodeling and improves endothelial function in mice. Arterioscler Thromb Vasc Biol. 2011;31(1):95-101.
200.Kim BM, Yoon W, Shim JH, Jung H, Lim JH, Choi HJ, et al. Role of Protein Kinases and Their Inhibitors in Radiation Response of Tumor Cells. Curr Pharm Des. 2017;23(29):4259-80.
201.Schwartz PA, Murray BW. Protein kinase biochemistry and drug discovery. Bioorg Chem. 2011;39(5-6):192-210.
202.Segaliny AI, Tellez-Gabriel M, Heymann MF, Heymann D. Receptor tyrosine kinases: Characterisation, mechanism of action and therapeutic interests for bone cancers. J Bone Oncol. 2015;4(1):1-12.
203.Hubbard SR, Miller WT. Receptor tyrosine kinases: mechanisms of activation and signaling. Curr Opin Cell Biol. 2007;19(2):117-23.
204.Yamaoka T, Kusumoto S, Ando K, Ohba M, Ohmori T. Receptor Tyrosine Kinase-Targeted Cancer Therapy. Int J Mol Sci. 2018;19(11).
205.Butti R, Das S, Gunasekaran VP, Yadav AS, Kumar D, Kundu GC. Receptor tyrosine kinases (RTKs) in breast cancer: signaling, therapeutic implications and challenges. Mol Cancer. 2018;17(1):34.
206.Hubbard SR. Structural analysis of receptor tyrosine kinases. Prog Biophys Mol Biol. 1999;71(3-4):343-58.
207.Hubbard SR. Autoinhibitory mechanisms in receptor tyrosine kinases. Front Biosci. 2002;7:d330-40.
208.Baldanzi G, Graziani A. Physiological Signaling and Structure of the HGF Receptor MET. Biomedicines. 2014;3(1):1-31.
209.Hubbard SR. The insulin receptor: both a prototypical and atypical receptor tyrosine kinase. Cold Spring Harb Perspect Biol. 2013;5(3):a008946.
210.Li E, Hristova K. Receptor tyrosine kinase transmembrane domains: Function, dimer structure and dimerization energetics. Cell Adh Migr. 2010;4(2):249-54.
211.Maruyama IN. Mechanisms of activation of receptor tyrosine kinases: monomers or dimers. Cells. 2014;3(2):304-30.
212.Du Z, Lovly CM. Mechanisms of receptor tyrosine kinase activation in cancer. Mol Cancer. 2018;17(1):58.
213.Lemmon MA, Schlessinger J. Cell signaling by receptor tyrosine kinases. Cell. 2010;141(7):1117-34.
214.Lee J, Miyazaki M, Romeo GR, Shoelson SE. Insulin receptor activation with transmembrane domain ligands. J Biol Chem. 2014;289(28):19769-77.

215.Niu XL, Peters KG, Kontos CD. Deletion of the carboxyl terminus of Tie2 enhances kinase activity, signaling, and function. Evidence for an autoinhibitory mechanism. J Biol Chem. 2002;277(35):31768-73.
216.Hadari YR, Gotoh N, Kouhara H, Lax I, Schlessinger J. Critical role for the docking-protein FRS2 alpha in FGF receptor-mediated signal transduction pathways. Proc Natl Acad Sci U S A. 2001;98(15):8578-83.
217.Fraser J, Cabodevilla AG, Simpson J, Gammoh N. Interplay of autophagy, receptor tyrosine kinase signalling and endocytic trafficking. Essays Biochem. 2017;61(6):597-607.
218.Soares-Silva M, Diniz FF, Gomes GN, Bahia D. The Mitogen-Activated Protein Kinase (MAPK) Pathway: Role in Immune Evasion by Trypanosomatids. Front Microbiol. 2016;7:183.
219.Yang S, Liu G. Targeting the Ras/Raf/MEK/ERK pathway in hepatocellular carcinoma. Oncol Lett. 2017;13(3):1041-7.
220.Ying HZ, Chen Q, Zhang WY, Zhang HH, Ma Y, Zhang SZ, et al. PDGF signaling pathway in hepatic fibrosis pathogenesis and therapeutics (Review). Mol Med Rep. 2017;16(6):7879-89.
221.Arkun Y, Yasemi M. Dynamics and control of the ERK signaling pathway: Sensitivity, bistability, and oscillations. PLoS One. 2018;13(4):e0195513.
222.Annenkov A. Receptor tyrosine kinase (RTK) signalling in the control of neural stem and progenitor cell (NSPC) development. Mol Neurobiol. 2014;49(1):440-71.
223.Muslin AJ. MAPK signalling in cardiovascular health and disease: molecular mechanisms and therapeutic targets. Clin Sci (Lond). 2008;115(7):203-18.
224.Katz M, Amit I, Yarden Y. Regulation of MAPKs by growth factors and receptor tyrosine kinases. Biochim Biophys Acta. 2007;1773(8):1161-76.
225.Papadimitrakopoulou V. Development of PI3K/AKT/mTOR pathway inhibitors and their application in personalized therapy for non-small-cell lung cancer. J Thorac Oncol. 2012;7(8):1315-26.
226.Liu P, Cheng H, Roberts TM, Zhao JJ. Targeting the phosphoinositide 3-kinase pathway in cancer. Nat Rev Drug Discov. 2009;8(8):627-44.
227.Paquette M, El-Houjeiri L, Pause A. mTOR Pathways in Cancer and Autophagy. Cancers (Basel). 2018;10(1).
228.Chang L, Graham PH, Ni J, Hao J, Bucci J, Cozzi PJ, et al. Targeting PI3K/Akt/mTOR signaling pathway in the treatment of prostate cancer radioresistance. Crit Rev Oncol Hematol. 2015;96(3):507-17.
229.Rhee SG. Regulation of phosphoinositide-specific phospholipase C. Annu Rev Biochem. 2001;70:281-312.
230.Yang YR, Follo MY, Cocco L, Suh PG. The physiological roles of primary phospholipase C. Adv Biol Regul. 2013;53(3):232-41.
231.Putney JW, Tomita T. Phospholipase C signaling and calcium influx. Adv Biol Regul. 2012;52(1):152-64.
232.Mikoshiba K. IP3 receptor/Ca2+ channel: from discovery to new signaling concepts. J Neurochem. 2007;102(5):1426-46.
233.Fukami K, Inanobe S, Kanemaru K, Nakamura Y. Phospholipase C is a key enzyme regulating intracellular calcium and modulating the phosphoinositide balance. Prog Lipid Res. 2010;49(4):429-37.
234.Zhu M, Leung CY, Shahbazi MN, Zernicka-Goetz M. Actomyosin polarisation through PLC-PKC triggers symmetry breaking of the mouse embryo. Nat Commun. 2017;8(1):921.
235.Chen J, Zheng D, Cui H, Liu S, Zhang L, Liu C. Roles and mechanisms of TRPC3 and the PLCgamma/PKC/CPI-17 signaling pathway in regulating parturition. Mol Med Rep. 2018;17(1):898-910.
236.Yu M, Chen Y, Zeng H, Zheng Y, Fu G, Zhu W, et al. PLCgamma-dependent mTOR signalling controls IL-7-mediated early B cell development. Nat Commun. 2017;8(1):1457.
237.Kazi JU, Ronnstrand L. The role of SRC family kinases in FLT3 signaling. Int J Biochem Cell Biol. 2019;107:32-7.

238.Bromann PA, Korkaya H, Courtneidge SA. The interplay between Src family kinases and receptor tyrosine kinases. Oncogene. 2004;23(48):7957-68.
239.Chen Z, Oh D, Dubey AK, Yao M, Yang B, Groves JT, et al. EGFR family and Src family kinase interactions: mechanics matters? Curr Opin Cell Biol. 2018;51:97-102.
240.Lieu C, Kopetz S. The SRC family of protein tyrosine kinases: a new and promising target for colorectal cancer therapy. Clin Colorectal Cancer. 2010;9(2):89-94.
241.Yang X, Qiao D, Meyer K, Friedl A. Signal transducers and activators of transcription mediate fibroblast growth factor-induced vascular endothelial morphogenesis. Cancer Res. 2009;69(4):1668-77.
242.Rawlings JS, Rosler KM, Harrison DA. The JAK/STAT signaling pathway. J Cell Sci. 2004;117(Pt 8):1281-3.
243.Harrison DA. The Jak/STAT pathway. Cold Spring Harb Perspect Biol. 2012;4(3).
244.Munaron L, Fiorio Pla A. Calcium influx induced by activation of tyrosine kinase receptors in cultured bovine aortic endothelial cells. J Cell Physiol. 2000;185(3):454-63.
245.Faehling M, Kroll J, Fohr KJ, Fellbrich G, Mayr U, Trischler G, et al. Essential role of calcium in vascular endothelial growth factor A-induced signaling: mechanism of the antiangiogenic effect of carboxyamidotriazole. FASEB J. 2002;16(13):1805-7.
246.Hamdollah Zadeh MA, Glass CA, Magnussen A, Hancox JC, Bates DO. VEGF-mediated elevated intracellular calcium and angiogenesis in human microvascular endothelial cells in vitro are inhibited by dominant negative TRPC6. Microcirculation. 2008;15(7):605-14.
247.Chandra A, Angle N. Vascular endothelial growth factor stimulates a novel calcium-signaling pathway in vascular smooth muscle cells. Surgery. 2005;138(4):780-7.
248.Rottbauer W, Just S, Wessels G, Trano N, Most P, Katus HA, et al. VEGF-PLCgamma1 pathway controls cardiac contractility in the embryonic heart. Genes Dev. 2005;19(13):1624-34.
249.Kim BW, Choi M, Kim YS, Park H, Lee HR, Yun CO, et al. Vascular endothelial growth factor (VEGF) signaling regulates hippocampal neurons by elevation of intracellular calcium and activation of calcium/calmodulin protein kinase II and mammalian target of rapamycin. Cell Signal. 2008;20(4):714-25.
250.Ahmed A, Dunk C, Kniss D, Wilkes M. Role of VEGF receptor-1 (Flt-1) in mediating calcium-dependent nitric oxide release and limiting DNA synthesis in human trophoblast cells. Lab Invest. 1997;76(6):779-91.
251.Dawson NS, Zawieja DC, Wu MH, Granger HJ. Signaling pathways mediating VEGF165-induced calcium transients and membrane depolarization in human endothelial cells. FASEB J. 2006;20(7):991-3.
252.Marqueze-Pouey B, Mailfert S, Rouger V, Goaillard JM, Marguet D. Physiological epidermal growth factor concentrations activate high affinity receptors to elicit calcium oscillations. PLoS One. 2014;9(9):e106803.
253.Fleet A, Ashworth R, Kubista H, Edwards H, Bolsover S, Mobbs P, et al. Inhibition of EGF-dependent calcium influx by annexin VI is splice form-specific. Biochem Biophys Res Commun. 1999;260(2):540-6.
254.Hudson PL, Pedersen WA, Saltsman WS, Liscovitch M, MacLaughlin DT, Donahoe PK, et al. Modulation by sphingolipids of calcium signals evoked by epidermal growth factor. J Biol Chem. 1994;269(34):21885-90.
255.Ma R, Sansom SC. Epidermal growth factor activates store-operated calcium channels in human glomerular mesangial cells. J Am Soc Nephrol. 2001;12(1):47-53.
256.Zhang ZR, Chu WF, Song B, Gooz M, Zhang JN, Yu CJ, et al. TRPP2 and TRPV4 form an EGF-activated calcium permeable channel at the apical membrane of renal collecting duct cells. PLoS One. 2013;8(8):e73424.
257.Wallmon A, Fellstrom B, Larsson R, Floege J, Topley N, Ljunghall S. PDGF-BB, but not PDGF-AA, stimulates calcium mobilization, activation of calcium channels and cell proliferation in cultured rat mesangial cells. Exp Nephrol. 1993;1(4):238-44.
258.Saqr HE, Guan Z, Yates AJ, Stokes BT. Mechanisms through which PDGF alters intracellular calcium levels in U-1242 MG human glioma cells. Neurochem Int. 1999;35(6):411-22.

259.Groenestege WM, Thebault S, van der Wijst J, van den Berg D, Janssen R, Tejpar S, et al. Impaired basolateral sorting of pro-EGF causes isolated recessive renal hypomagnesemia. The Journal of clinical investigation. 2007;117(8):2260-7.
260.Dimke H, van der Wijst J, Alexander TR, Meijer IM, Mulder GM, van Goor H, et al. Effects of the EGFR Inhibitor Erlotinib on Magnesium Handling. J Am Soc Nephrol. 2010;21(8):1309-16.
261.Trapani V, Arduini D, Luongo F, Wolf FI. EGF stimulates Mg(2+) influx in mammary epithelial cells. Biochem Biophys Res Commun. 2014;454(4):572-5.
262.Grubbs RD. Effect of epidermal growth factor on magnesium homeostasis in BC3H1 myocytes. Am J Physiol. 1991;260(6 Pt 1):C1158-64.
263.Hong BZ, Kang HS, So JN, Kim HN, Park SA, Kim SJ, et al. Vascular endothelial growth factor increases the intracellular magnesium. Biochem Biophys Res Commun. 2006;347(2):496-501.
264.Abed E, Moreau R. Importance of melastatin-like transient receptor potential 7 and magnesium in the stimulation of osteoblast proliferation and migration by platelet-derived growth factor. Am J Physiol Cell Physiol. 2009;297(2):C360-8.
265.Rodrigues M, Griffith LG, Wells A. Growth factor regulation of proliferation and survival of multipotential stromal cells. Stem Cell Res Ther. 2010;1(4):32.
266.Liang Y, Brekken RA, Hyder SM. Vascular endothelial growth factor induces proliferation of breast cancer cells and inhibits the anti-proliferative activity of anti-hormones. Endocr Relat Cancer. 2006;13(3):905-19.
267.Sun J, Sha B, Zhou W, Yang Y. VEGF-mediated angiogenesis stimulates neural stem cell proliferation and differentiation in the premature brain. Biochem Biophys Res Commun. 2010;394(1):146-52.
268.Wang S, Li X, Parra M, Verdin E, Bassel-Duby R, Olson EN. Control of endothelial cell proliferation and migration by VEGF signaling to histone deacetylase 7. Proc Natl Acad Sci U S A. 2008;105(22):7738-43.
269.Podar K, Tai YT, Davies FE, Lentzsch S, Sattler M, Hideshima T, et al. Vascular endothelial growth factor triggers signaling cascades mediating multiple myeloma cell growth and migration. Blood. 2001;98(2):428-35.
270.Chen H, Shen YF, Gong F, Yang GH, Jiang YQ, Zhang R. Expression of VEGF and its effect on cell proliferation in patients with chronic myeloid leukemia. Eur Rev Med Pharmacol Sci. 2015;19(19):3569-73.
271.Zhang L, Wang JN, Tang JM, Kong X, Yang JY, Zheng F, et al. VEGF is essential for the growth and migration of human hepatocellular carcinoma cells. Mol Biol Rep. 2012;39(5):5085-93.
272.Liu X, Lin CS, Graziottin T, Resplande J, Lue TF. Vascular endothelial growth factor promotes proliferation and migration of cavernous smooth muscle cells. J Urol. 2001;166(1):354-60.
273.Cucina A, Borrelli V, Randone B, Coluccia P, Sapienza P, Cavallaro A. Vascular endothelial growth factor increases the migration and proliferation of smooth muscle cells through the mediation of growth factors released by endothelial cells. J Surg Res. 2003;109(1):16-23.
274.Cai J, Jiang WG, Ahmed A, Boulton M. Vascular endothelial growth factor-induced endothelial cell proliferation is regulated by interaction between VEGFR-2, SH-PTP1 and eNOS. Microvasc Res. 2006;71(1):20-31.
275.Li ZD, Bork JP, Krueger B, Patsenker E, Schulze-Krebs A, Hahn EG, et al. VEGF induces proliferation, migration, and TGF-beta1 expression in mouse glomerular endothelial cells via mitogen-activated protein kinase and phosphatidylinositol 3-kinase. Biochem Biophys Res Commun. 2005;334(4):1049-60.
276.Chavakis E, Dimmeler S. Regulation of endothelial cell survival and apoptosis during angiogenesis. Arterioscler Thromb Vasc Biol. 2002;22(6):887-93.
277.Gupta K, Kshirsagar S, Li W, Gui L, Ramakrishnan S, Gupta P, et al. VEGF prevents apoptosis of human microvascular endothelial cells via opposing effects on MAPK/ERK and SAPK/JNK signaling. Exp Cell Res. 1999;247(2):495-504.
278.Friehs I, Barillas R, Vasilyev NV, Roy N, McGowan FX, del Nido PJ. Vascular endothelial growth factor prevents apoptosis and preserves contractile function in hypertrophied infant heart. Circulation. 2006;114(1 Suppl):I290-5.

279.Pidgeon GP, Barr MP, Harmey JH, Foley DA, Bouchier-Hayes DJ. Vascular endothelial growth factor (VEGF) upregulates BCL-2 and inhibits apoptosis in human and murine mammary adenocarcinoma cells. Br J Cancer. 2001;85(2):273-8.
280.Li Y, Zhang F, Nagai N, Tang Z, Zhang S, Scotney P, et al. VEGF-B inhibits apoptosis via VEGFR-1-mediated suppression of the expression of BH3-only protein genes in mice and rats. J Clin Invest. 2008;118(3):913-23.
281.Mei J, Gao Y, Zhang L, Cai X, Qian Z, Huang H, et al. VEGF-siRNA silencing induces apoptosis, inhibits proliferation and suppresses vasculogenic mimicry in osteosarcoma in vitro. Exp Oncol. 2008;30(1):29-34.
282.Meeson AP, Argilla M, Ko K, Witte L, Lang RA. VEGF deprivation-induced apoptosis is a component of programmed capillary regression. Development. 1999;126(7):1407-15.
283.Narasimhan P, Liu J, Song YS, Massengale JL, Chan PH. VEGF Stimulates the ERK 1/2 signaling pathway and apoptosis in cerebral endothelial cells after ischemic conditions. Stroke. 2009;40(4):1467-73.
284.Andl CD, Mizushima T, Nakagawa H, Oyama K, Harada H, Chruma K, et al. Epidermal growth factor receptor mediates increased cell proliferation, migration, and aggregation in esophageal keratinocytes in vitro and in vivo. J Biol Chem. 2003;278(3):1824-30.
285.Hoelting T, Siperstein AE, Clark OH, Duh QY. Epidermal growth factor enhances proliferation, migration, and invasion of follicular and papillary thyroid cancer in vitro and in vivo. J Clin Endocrinol Metab. 1994;79(2):401-8.
286.Fricker-Gates RA, Winkler C, Kirik D, Rosenblad C, Carpenter MK, Bjorklund A. EGF infusion stimulates the proliferation and migration of embryonic progenitor cells transplanted in the adult rat striatum. Exp Neurol. 2000;165(2):237-47.
287.Zhang H, Nan W, Wang S, Zhang T, Si H, Yang F, et al. Epidermal Growth Factor Promotes Proliferation and Migration of Follicular Outer Root Sheath Cells via Wnt/beta-Catenin Signaling. Cell Physiol Biochem. 2016;39(1):360-70.
288.Kimura H, Okubo N, Chosa N, Kyakumoto S, Kamo M, Miura H, et al. EGF positively regulates the proliferation and migration, and negatively regulates the myofibroblast differentiation of periodontal ligament-derived endothelial progenitor cells through MEK/ERK- and JNK-dependent signals. Cell Physiol Biochem. 2013;32(4):899-914.
289.Zhuang S, Dang Y, Schnellmann RG. Requirement of the epidermal growth factor receptor in renal epithelial cell proliferation and migration. Am J Physiol Renal Physiol. 2004;287(3):F365-72.
290.Jiang Q, Zhou C, Bi Z, Wan Y. EGF-induced cell migration is mediated by ERK and PI3K/AKT pathways in cultured human lens epithelial cells. J Ocul Pharmacol Ther. 2006;22(2):93-102.
291.Frey MR, Golovin A, Polk DB. Epidermal growth factor-stimulated intestinal epithelial cell migration requires Src family kinase-dependent p38 MAPK signaling. J Biol Chem. 2004;279(43):44513-21.
292.Puehringer D, Orel N, Luningschror P, Subramanian N, Herrmann T, Chao MV, et al. EGF transactivation of Trk receptors regulates the migration of newborn cortical neurons. Nat Neurosci. 2013;16(4):407-15.
293.Chiu B, Mirkin B, Madonna MB. Epidermal growth factor can induce apoptosis in neuroblastoma. J Pediatr Surg. 2007;42(3):482-8.
294.Suzuki A, Sekiya S, Gunshima E, Fujii S, Taniguchi H. EGF signaling activates proliferation and blocks apoptosis of mouse and human intestinal stem/progenitor cells in long-term monolayer cell culture. Lab Invest. 2010;90(10):1425-36.
295.Shao H, Yi XM, Wells A. Epidermal growth factor protects fibroblasts from apoptosis via PI3 kinase and Rac signaling pathways. Wound Repair Regen. 2008;16(4):551-8.
296.Kottke TJ, Blajeski AL, Martins LM, Mesner PW, Jr., Davidson NE, Earnshaw WC, et al. Comparison of paclitaxel-, 5-fluoro-2'-deoxyuridine-, and epidermal growth factor (EGF)-induced apoptosis. Evidence for EGF-induced anoikis. J Biol Chem. 1999;274(22):15927-36.
297.Gulli LF, Palmer KC, Chen YQ, Reddy KB. Epidermal growth factor-induced apoptosis in A431 cells can be reversed by reducing the tyrosine kinase activity. Cell Growth Differ. 1996;7(2):173-8.

298.Armstrong DK, Kaufmann SH, Ottaviano YL, Furuya Y, Buckley JA, Isaacs JT, et al. Epidermal growth factor-mediated apoptosis of MDA-MB-468 human breast cancer cells. Cancer Res. 1994;54(20):5280-3.
299.Cao L, Yao Y, Lee V, Kiani C, Spaner D, Lin Z, et al. Epidermal growth factor induces cell cycle arrest and apoptosis of squamous carcinoma cells through reduction of cell adhesion. J Cell Biochem. 2000;77(4):569-83.
300.Grudinkin PS, Zenin VV, Kropotov AV, Dorosh VN, Nikolsky NN. EGF-induced apoptosis in A431 cells is dependent on STAT1, but not on STAT3. Eur J Cell Biol. 2007;86(10):591-603.
301.Jackson NM, Ceresa BP. EGFR-mediated apoptosis via STAT3. Exp Cell Res. 2017;356(1):93-103.
302.Tikhomirov O, Carpenter G. Ligand-induced, p38-dependent apoptosis in cells expressing high levels of epidermal growth factor receptor and ErbB-2. J Biol Chem. 2004;279(13):12988-96.
303.Zhao X, Dai W, Zhu H, Zhang Y, Cao L, Ye Q, et al. Epidermal growth factor (EGF) induces apoptosis in a transfected cell line expressing EGF receptor on its membrane. Cell Biol Int. 2006;30(8):653-8.
304.Ito F. Foreword. Target therapy for cancer: anti-cancer drugs targeting growth-factor signaling molecules. Biol Pharm Bull. 2011;34(12):1773.
305.Zwick E, Bange J, Ullrich A. Receptor tyrosine kinase signalling as a target for cancer intervention strategies. Endocr Relat Cancer. 2001;8(3):161-73.
306.Zwick E, Bange J, Ullrich A. Receptor tyrosine kinases as targets for anticancer drugs. Trends Mol Med. 2002;8(1):17-23.
307.Regad T. Targeting RTK Signaling Pathways in Cancer. Cancers (Basel). 2015;7(3):1758-84.
308.Witsch E, Sela M, Yarden Y. Roles for growth factors in cancer progression. Physiology (Bethesda). 2010;25(2):85-101.
309.Schlessinger J. Cell signaling by receptor tyrosine kinases. Cell. 2000;103(2):211-25.
310.Yogi A, O'Connor SE, Callera GE, Tostes RC, Touyz RM. Receptor and nonreceptor tyrosine kinases in vascular biology of hypertension. Curr Opin Nephrol Hypertens. 2010;19(2):169-76.
311.Dreux AC, Lamb DJ, Modjtahedi H, Ferns GA. The epidermal growth factor receptors and their family of ligands: their putative role in atherogenesis. Atherosclerosis. 2006;186(1):38-53.
312.Harris RC, Chung E, Coffey RJ. EGF receptor ligands. Exp Cell Res. 2003;284(1):2-13.
313.Makki N, Thiel KW, Miller FJ, Jr. The epidermal growth factor receptor and its ligands in cardiovascular disease. Int J Mol Sci. 2013;14(10):20597-613.
314.Schreier B, Gekle M, Grossmann C. Role of epidermal growth factor receptor in vascular structure and function. Curr Opin Nephrol Hypertens. 2014;23(2):113-21.
315.Boyle JJ. Macrophage activation in atherosclerosis: pathogenesis and pharmacology of plaque rupture. Curr Vasc Pharmacol. 2005;3(1):63-8.
316.Wang L, Huang Z, Huang W, Chen X, Shan P, Zhong P, et al. Inhibition of epidermal growth factor receptor attenuates atherosclerosis via decreasing inflammation and oxidative stress. Scientific reports. 2017;8:45917.
317.Zhou Y, Brigstock D, Besner GE. Heparin-binding EGF-like growth factor is a potent dilator of terminal mesenteric arterioles. Microvasc Res. 2009;78(1):78-85.
318.Amin AH, Abd Elmageed ZY, Partyka M, Matrougui K. Mechanisms of myogenic tone of coronary arteriole: Role of down stream signaling of the EGFR tyrosine kinase. Microvasc Res. 2011;81(1):135-42.
319.Berk BC, Brock TA, Webb RC, Taubman MB, Atkinson WJ, Gimbrone MA, Jr., et al. Epidermal growth factor, a vascular smooth muscle mitogen, induces rat aortic contraction. J Clin Invest. 1985;75(3):1083-6.
320.Florian JA, Watts SW. Epidermal growth factor: a potent vasoconstrictor in experimental hypertension. Am J Physiol. 1999;276(3):H976-83.
321.Fujino T, Hasebe N, Fujita M, Takeuchi K, Kawabe J, Tobise K, et al. Enhanced expression of heparin-binding EGF-like growth factor and its receptor in hypertrophied left ventricle of spontaneously hypertensive rats. Cardiovasc Res. 1998;38(2):365-74.

322.Schreier B, Rabe S, Schneider B, Bretschneider M, Rupp S, Ruhs S, et al. Loss of epidermal growth factor receptor in vascular smooth muscle cells and cardiomyocytes causes arterial hypotension and cardiac hypertrophy. Hypertension. 2013;61(2):333-40.
323.Griol-Charhbili V, Fassot C, Messaoudi S, Perret C, Agrapart V, Jaisser F. Epidermal growth factor receptor mediates the vascular dysfunction but not the remodeling induced by aldosterone/salt. Hypertension. 2011;57(2):238-44.
324.Messaoudi S, Zhang AD, Griol-Charhbili V, Escoubet B, Sadoshima J, Farman N, et al. The epidermal growth factor receptor is involved in angiotensin II but not aldosterone/salt-induced cardiac remodelling. PLoS One. 2012;7(1):e30156.
325.Ulu N, Gurdal H, Landheer SW, Duin M, Guc MO, Buikema H, et al. alpha1-Adrenoceptor-mediated contraction of rat aorta is partly mediated via transactivation of the epidermal growth factor receptor. Br J Pharmacol. 2010;161(6):1301-10.
326.Yogi A, Callera GE, Aranha AB, Antunes TT, Graham D, McBride M, et al. Sphingosine-1-phosphate-induced inflammation involves receptor tyrosine kinase transactivation in vascular cells: upregulation in hypertension. Hypertension. 2011;57(4):809-18.
327.Flamant M, Tharaux PL, Placier S, Henrion D, Coffman T, Chatziantoniou C, et al. Epidermal growth factor receptor trans-activation mediates the tonic and fibrogenic effects of endothelin in the aortic wall of transgenic mice. FASEB J. 2003;17(2):327-9.
328.Li Y, Levesque LO, Anand-Srivastava MB. Epidermal growth factor receptor transactivation by endogenous vasoactive peptides contributes to hyperproliferation of vascular smooth muscle cells of SHR. Am J Physiol Heart Circ Physiol. 2010;299(6):H1959-67.
329.Sandoval YH, Li Y, Anand-Srivastava MB. Transactivation of epidermal growth factor receptor by enhanced levels of endogenous angiotensin II contributes to the overexpression of Gialpha proteins in vascular smooth muscle cells from SHR. Cell Signal. 2011;23(11):1716-26.
330.Peng K, Tian X, Qian Y, Skibba M, Zou C, Liu Z, et al. Novel EGFR inhibitors attenuate cardiac hypertrophy induced by angiotensin II. J Cell Mol Med. 2016;20(3):482-94.
331.Kagiyama S, Eguchi S, Frank GD, Inagami T, Zhang YC, Phillips MI. Angiotensin II-induced cardiac hypertrophy and hypertension are attenuated by epidermal growth factor receptor antisense. Circulation. 2002;106(8):909-12.
332.Kagiyama S, Qian K, Kagiyama T, Phillips MI. Antisense to epidermal growth factor receptor prevents the development of left ventricular hypertrophy. Hypertension. 2003;41(3 Pt 2):824-9.
333.Francois H, Placier S, Flamant M, Tharaux PL, Chansel D, Dussaule JC, et al. Prevention of renal vascular and glomerular fibrosis by epidermal growth factor receptor inhibition. FASEB J. 2004;18(7):926-8.
334.Shah S, Akhtar MS, Hassan MQ, Akhtar M, Paudel YN, Najmi AK. EGFR tyrosine kinase inhibition decreases cardiac remodeling and SERCA2a/NCX1 depletion in streptozotocin induced cardiomyopathy in C57/BL6 mice. Life Sci. 2018;210:29-39.
335.Zhao Q, Ishibashi M, Hiasa K, Tan C, Takeshita A, Egashira K. Essential role of vascular endothelial growth factor in angiotensin II-induced vascular inflammation and remodeling. Hypertension. 2004;44(3):264-70.
336.Celletti FL, Waugh JM, Amabile PG, Brendolan A, Hilfiker PR, Dake MD. Vascular endothelial growth factor enhances atherosclerotic plaque progression. Nat Med. 2001;7(4):425-9.
337.Ku DD, Zaleski JK, Liu S, Brock TA. Vascular endothelial growth factor induces EDRF-dependent relaxation in coronary arteries. Am J Physiol. 1993;265(2 Pt 2):H586-92.
338.Robinson ES, Khankin EV, Karumanchi SA, Humphreys BD. Hypertension induced by vascular endothelial growth factor signaling pathway inhibition: mechanisms and potential use as a biomarker. Semin Nephrol. 2010;30(6):591-601.
339.Dienstmann R, Brana I, Rodon J, Tabernero J. Toxicity as a biomarker of efficacy of molecular targeted therapies: focus on EGFR and VEGF inhibiting anticancer drugs. Oncologist. 2011;16(12):1729-40.
340.Evans T. Utility of hypertension as a surrogate marker for efficacy of antiangiogenic therapy in NSCLC. Anticancer Res. 2012;32(11):4629-38.

341.Facemire CS, Nixon AB, Griffiths R, Hurwitz H, Coffman TM. Vascular endothelial growth factor receptor 2 controls blood pressure by regulating nitric oxide synthase expression. Hypertension. 2009;54(3):652-8.
342.Neves KB, Rios FJ, van der Mey L, Alves-Lopes R, Cameron AC, Volpe M, et al. VEGFR (Vascular Endothelial Growth Factor Receptor) Inhibition Induces Cardiovascular Damage via Redox-Sensitive Processes. Hypertension. 2018;71(4):638-47.
343.Touyz RM, Lang NN, Herrmann J, van den Meiracker AH, Danser AHJ. Recent Advances in Hypertension and Cardiovascular Toxicities With Vascular Endothelial Growth Factor Inhibition. Hypertension. 2017;70(2):220-6.
344.Semeniuk-Wojtas A, Lubas A, Stec R, Szczylik C, Niemczyk S. Influence of Tyrosine Kinase Inhibitors on Hypertension and Nephrotoxicity in Metastatic Renal Cell Cancer Patients. Int J Mol Sci. 2016;17(12).
345.Spradley FT, Palei AC, Granger JP. Immune Mechanisms Linking Obesity and Preeclampsia. Biomolecules. 2015;5(4):3142-76.
346.Malik A, Jee B, Gupta SK. Preeclampsia: Disease biology and burden, its management strategies with reference to India. Pregnancy Hypertens. 2019;15:23-31.
347.Gathiram P, Moodley J. Pre-eclampsia: its pathogenesis and pathophysiolgy. Cardiovasc J Afr. 2016;27(2):71-8.
348.Phipps E, Prasanna D, Brima W, Jim B. Preeclampsia: Updates in Pathogenesis, Definitions, and Guidelines. Clin J Am Soc Nephrol. 2016;11(6):1102-13.
349.Portelli M, Baron B. Clinical Presentation of Preeclampsia and the Diagnostic Value of Proteins and Their Methylation Products as Biomarkers in Pregnant Women with Preeclampsia and Their Newborns. J Pregnancy. 2018;2018:2632637.
350.Townsend R, O'Brien P, Khalil A. Current best practice in the management of hypertensive disorders in pregnancy. Integr Blood Press Control. 2016;9:79-94.
351.Osungbade KO, Ige OK. Public health perspectives of preeclampsia in developing countries: implication for health system strengthening. J Pregnancy. 2011;2011:481095.
352.Peres GM, Mariana M, Cairrao E. Pre-Eclampsia and Eclampsia: An Update on the Pharmacological Treatment Applied in Portugal. J Cardiovasc Dev Dis. 2018;5(1).
353.Ghulmiyyah L, Sibai B. Maternal mortality from preeclampsia/eclampsia. Semin Perinatol. 2012;36(1):56-9.
354.Hodgins S. Pre-eclampsia as Underlying Cause for Perinatal Deaths: Time for Action. Glob Health Sci Pract. 2015;3(4):525-7.
355.Chaiworapongsa T, Chaemsaithong P, Yeo L, Romero R. Pre-eclampsia part 1: current understanding of its pathophysiology. Nat Rev Nephrol. 2014;10(8):466-80.
356.Bro Schmidt G, Christensen M, Breth Knudsen U. Preeclampsia and later cardiovascular disease - What do national guidelines recommend? Pregnancy Hypertens. 2017;10:14-7.
357.Chen CW, Jaffe IZ, Karumanchi SA. Pre-eclampsia and cardiovascular disease. Cardiovasc Res. 2014;101(4):579-86.
358.Wu P, Haththotuwa R, Kwok CS, Babu A, Kotronias RA, Rushton C, et al. Preeclampsia and Future Cardiovascular Health: A Systematic Review and Meta-Analysis. Circ Cardiovasc Qual Outcomes. 2017;10(2).
359.Bellamy L, Casas JP, Hingorani AD, Williams DJ. Pre-eclampsia and risk of cardiovascular disease and cancer in later life: systematic review and meta-analysis. BMJ. 2007;335(7627):974.
360.Craici I, Wagner S, Garovic VD. Preeclampsia and future cardiovascular risk: formal risk factor or failed stress test? Ther Adv Cardiovasc Dis. 2008;2(4):249-59.
361.Wagner LK. Diagnosis and management of preeclampsia. Am Fam Physician. 2004;70(12):2317-24.
362.Armaly Z, Jadaon JE, Jabbour A, Abassi ZA. Preeclampsia: Novel Mechanisms and Potential Therapeutic Approaches. Front Physiol. 2018;9:973.
363.Levine RJ, Lam C, Qian C, Yu KF, Maynard SE, Sachs BP, et al. Soluble endoglin and other circulating antiangiogenic factors in preeclampsia. N Engl J Med. 2006;355(10):992-1005.

364.Craici IM, Wagner SJ, Weissgerber TL, Grande JP, Garovic VD. Advances in the pathophysiology of pre-eclampsia and related podocyte injury. Kidney Int. 2014;86(2):275-85.
365.Melincovici CS, Bosca AB, Susman S, Marginean M, Mihu C, Istrate M, et al. Vascular endothelial growth factor (VEGF) - key factor in normal and pathological angiogenesis. Rom J Morphol Embryol. 2018;59(2):455-67.
366.Park SA, Jeong MS, Ha KT, Jang SB. Structure and function of vascular endothelial growth factor and its receptor system. BMB Rep. 2018;51(2):73-8.
367.Bates DO. An unexpected tail of VEGF and PlGF in pre-eclampsia. Biochem Soc Trans. 2011;39(6):1576-82.
368.Chau K, Hennessy A, Makris A. Placental growth factor and pre-eclampsia. J Hum Hypertens. 2017;31(12):782-6.
369.Maynard SE, Karumanchi SA. Angiogenic factors and preeclampsia. Semin Nephrol. 2011;31(1):33-46.
370.Eddy AC, Bidwell GL, 3rd, George EM. Pro-angiogenic therapeutics for preeclampsia. Biol Sex Differ. 2018;9(1):36.
371.Iwasaki H, Kawamoto A, Tjwa M, Horii M, Hayashi S, Oyamada A, et al. PlGF repairs myocardial ischemia through mechanisms of angiogenesis, cardioprotection and recruitment of myo-angiogenic competent marrow progenitors. PLoS One. 2011;6(9):e24872.
372.Takahashi H, Shibuya M. The vascular endothelial growth factor (VEGF)/VEGF receptor system and its role under physiological and pathological conditions. Clin Sci (Lond). 2005;109(3):227-41.
373.Chen DB, Zheng J. Regulation of Placental Angiogenesis. Microcirculation. 2014;21(1):15-25.
374.Bates DO. An unexpected tail of VEGF and PlGF in pre-eclampsia. Biochem Soc T. 2011;39:1576-82.
375.Dover N, Gulerman HC, Celen S, Kahyaoglu S, Yenicesu O. Placental growth factor: as an early second trimester predictive marker for preeclampsia in normal and high-risk pregnancies in a Turkish population. J Obstet Gynaecol India. 2013;63(3):158-63.
376.Osol G, Celia G, Gokina N, Barron C, Chien E, Mandala M, et al. Placental growth factor is a potent vasodilator of rat and human resistance arteries. Am J Physiol Heart Circ Physiol. 2008;294(3):H1381-7.
377.Zeisler H, Llurba E, Chantraine F, Vatish M, Staff AC, Sennstrom M, et al. Predictive Value of the sFlt-1:PlGF Ratio in Women with Suspected Preeclampsia. N Engl J Med. 2016;374(1):13-22.
378.Zeisler H, Llurba E, Chantraine F, Vatish M, Staff AC, Sennstrom M, et al. Predictive Value of the sFlt-1:PlGF Ratio in Women with Suspected Preeclampsia. New Engl J Med. 2016;374(1):13-22.
379.Suzuki H, Ohkuchi A, Matsubara S, Takei Y, Murakami M, Shibuya M, et al. Effect of recombinant placental growth factor 2 on hypertension induced by full-length mouse soluble fms-like tyrosine kinase 1 adenoviral vector in pregnant mice. Hypertension. 2009;54(5):1129-35.
380.Fushima T, Sekimoto A, Minato T, Ito T, Oe Y, Kisu K, et al. Reduced Uterine Perfusion Pressure (RUPP) Model of Preeclampsia in Mice. PLoS One. 2016;11(5):e0155426.
381.Spradley FT, Tan AY, Joo WS, Daniels G, Kussie P, Karumanchi SA, et al. Placental Growth Factor Administration Abolishes Placental Ischemia-Induced Hypertension. Hypertension. 2016;67(4):740-7.
382.Zhu M, Ren Z, Possomato-Vieira JS, Khalil RA. Restoring placental growth factor-soluble fms-like tyrosine kinase-1 balance reverses vascular hyper-reactivity and hypertension in pregnancy. Am J Physiol Regul Integr Comp Physiol. 2016;311(3):R505-21.
383.Makris A, Yeung KR, Lim SM, Sunderland N, Heffernan S, Thompson JF, et al. Placental Growth Factor Reduces Blood Pressure in a Uteroplacental Ischemia Model of Preeclampsia in Nonhuman Primates. Hypertension. 2016;67(6):1263-72.
384.Chen D, Wang H, Huang H, Dong M. Vascular endothelial growth factor attenuates Nomega-nitro-L-arginine methyl ester-induced preeclampsia-like manifestations in rats. Clin Exp Hypertens. 2008;30(7):606-15.
385.Rees DD, Palmer RM, Schulz R, Hodson HF, Moncada S. Characterization of three inhibitors of endothelial nitric oxide synthase in vitro and in vivo. Br J Pharmacol. 1990;101(3):746-52.

386.Li Z, Zhang Y, Ying Ma J, Kapoun AM, Shao Q, Kerr I, et al. Recombinant vascular endothelial growth factor 121 attenuates hypertension and improves kidney damage in a rat model of preeclampsia. Hypertension. 2007;50(4):686-92.
387.Gilbert JS, Verzwyvelt J, Colson D, Arany M, Karumanchi SA, Granger JP. Recombinant vascular endothelial growth factor 121 infusion lowers blood pressure and improves renal function in rats with placentalischemia-induced hypertension. Hypertension. 2010;55(2):380-5.
388.Berzan E, Doyle R, Brown CM. Treatment of preeclampsia: current approach and future perspectives. Curr Hypertens Rep. 2014;16(9):473.
389.Lu JF, Nightingale CH. Magnesium sulfate in eclampsia and pre-eclampsia: pharmacokinetic principles. Clin Pharmacokinet. 2000;38(4):305-14.
390.Berhan Y, Berhan A. Should magnesium sulfate be administered to women with mild pre-eclampsia? A systematic review of published reports on eclampsia. J Obstet Gynaecol Res. 2015;41(6):831-42.
391.English FA, Kenny LC, McCarthy FP. Risk factors and effective management of preeclampsia. Integr Blood Press Control. 2015;8:7-12.
392.Duley L, Gulmezoglu AM, Henderson-Smart DJ, Chou D. Magnesium sulphate and other anticonvulsants for women with pre-eclampsia. Cochrane Database Syst Rev. 2010(11):CD000025.
393.Euser AG, Cipolla MJ. Magnesium sulfate for the treatment of eclampsia: a brief review. Stroke. 2009;40(4):1169-75.
394.Weintraub AY, Amash A, Eshkoli T, Piltcher Haber E, Bronfenmacher B, Sheiner E, et al. The effects of magnesium sulfate on placental vascular endothelial growth factor expression in preeclampsia. Hypertens Pregnancy. 2013;32(2):178-88.
395.Yang H, Kim TH, Lee GS, Hong EJ, Jeung EB. Comparing the expression patterns of placental magnesium/phosphorus-transporting channels between healthy and preeclamptic pregnancies. Mol Reprod Dev. 2014;81(9):851-60.
396.Tavana Z, Hosseinmirzaei S. Comparison of Maternal Serum Magnesium Level in Pre-eclampsia and Normal Pregnant Women. Iranian Red Crescent medical journal. 2013;15(12):e10394.
397.Kanagal DV, Rajesh A, Rao K, Devi UH, Shetty H, Kumari S, et al. Levels of Serum Calcium and Magnesium in Pre-eclamptic and Normal Pregnancy: A Study from Coastal India. J Clin Diagn Res. 2014;8(7):OC01-4.
398.Elmugabil A, Hamdan HZ, Elsheikh AE, Rayis DA, Adam I, Gasim GI. Serum Calcium, Magnesium, Zinc and Copper Levels in Sudanese Women with Preeclampsia. PLoS One. 2016;11(12):e0167495.
399.Jafrin W, Mia AR, Chakraborty PK, Hoque MR, Paul UK, Shaha KR, et al. An evaluation of serum magnesium status in pre-eclampsia compared to the normal pregnancy. Mymensingh Med J. 2014;23(4):649-53.
400.Inoue K, Xiong ZG. Silencing TRPM7 promotes growth/proliferation and nitric oxide production of vascular endothelial cells via the ERK pathway. Cardiovascular research. 2009;83(3):547-57.
401.Fang L, Zhan S, Huang C, Cheng X, Lv X, Si H, et al. TRPM7 channel regulates PDGF-BB-induced proliferation of hepatic stellate cells via PI3K and ERK pathways. Toxicol Appl Pharmacol. 2013;272(3):713-25.
402.Chen WL, Barszczyk A, Turlova E, Deurloo M, Liu B, Yang BB, et al. Inhibition of TRPM7 by carvacrol suppresses glioblastoma cell proliferation, migration and invasion. Oncotarget. 2015;6(18):16321-40.
403.Zhao Z, Zhang M, Duan X, Chen Y, Li E, Luo L, et al. TRPM7 Regulates AKT/FOXO1-Dependent Tumor Growth and Is an Independent Prognostic Indicator in Renal Cell Carcinoma. Mol Cancer Res. 2018;16(6):1013-23.
404.Sahni J, Scharenberg AM. TRPM7 ion channels are required for sustained phosphoinositide 3-kinase signaling in lymphocytes. Cell Metab. 2008;8(1):84-93.

405.Lu D, Qu J, Sun L, Li Q, Ling H, Yang N, et al. Ca2+/Mg2+ homeostasisrelated TRPM7 channel mediates chondrocyte hypertrophy via regulation of the PI3KAkt signaling pathway. Mol Med Rep. 2017;16(4):5699-705.
406.Krishnamoorthy M, Wasim L, Buhari FHM, Zhao T, Mahtani T, Ho J, et al. The channel-kinase TRPM7 regulates antigen gathering and internalization in B cells. Sci Signal. 2018;11(533).
407.Meng X, Cai C, Wu J, Cai S, Ye C, Chen H, et al. TRPM7 mediates breast cancer cell migration and invasion through the MAPK pathway. Cancer letters. 2013;333(1):96-102.
408.Davis FM, Azimi I, Faville RA, Peters AA, Jalink K, Putney JW, Jr., et al. Induction of epithelial-mesenchymal transition (EMT) in breast cancer cells is calcium signal dependent. Oncogene. 2014;33(18):2307-16.
409.Zhang Z, Wang M, Fan XH, Chen JH, Guan YY, Tang YB. Upregulation of TRPM7 channels by angiotensin II triggers phenotypic switching of vascular smooth muscle cells of ascending aorta. Circulation research. 2012;111(9):1137-46.
410.Runnels LW, Yue L, Clapham DE. The TRPM7 channel is inactivated by PIP(2) hydrolysis. Nat Cell Biol. 2002;4(5):329-36.
411.Thebault S, Alexander RT, Tiel Groenestege WM, Hoenderop JG, Bindels RJ. EGF increases TRPM6 activity and surface expression. Journal of the American Society of Nephrology : JASN. 2009;20(1):78-85.
412.Chubanov V, Waldegger S, Mederos y Schnitzler M, Vitzthum H, Sassen MC, Seyberth HW, et al. Disruption of TRPM6/TRPM7 complex formation by a mutation in the TRPM6 gene causes hypomagnesemia with secondary hypocalcemia. Proc Natl Acad Sci U S A. 2004;101(9):2894-9.
413.Tian SL, Jiang H, Zeng Y, Li LL, Shi J. NGF-induced reduction of an outward-rectifying TRPM7-like current in rat CA1 hippocampal neurons. Neurosci Lett. 2007;419(2):93-8.
414.Jiang H, Tian SL, Zeng Y, Li LL, Shi J. TrkA pathway(s) is involved in regulation of TRPM7 expression in hippocampal neurons subjected to ischemic-reperfusion and oxygen-glucose deprivation. Brain Res Bull. 2008;76(1-2):124-30.
415.Langeslag M, Clark K, Moolenaar WH, van Leeuwen FN, Jalink K. Activation of TRPM7 channels by phospholipase C-coupled receptor agonists. J Biol Chem. 2007;282(1):232-9.
416.Liu A, Zhao F, Wang J, Zhao Y, Luo Z, Gao Y, et al. Regulation of TRPM7 Function by IL-6 through the JAK2-STAT3 Signaling Pathway. PLoS One. 2016;11(3):e0152120.
417.Zhou H, Zhang Y. Regulation of in vitro growth of preantral follicles by growth factors in goats. Domest Anim Endocrinol. 2005;28(3):235-42.
418.Buharalioglu CK, Song CY, Yaghini FA, Ghafoor HU, Motiwala M, Adris T, et al. Angiotensin II-induced process of angiogenesis is mediated by spleen tyrosine kinase via VEGF receptor-1 phosphorylation. Am J Physiol Heart Circ Physiol. 2011;301(3):H1043-55.
419.Khan S, Villalobos MA, Choron RL, Chang S, Brown SA, Carpenter JP, et al. Fibroblast growth factor and vascular endothelial growth factor play a critical role in endotheliogenesis from human adipose-derived stem cells. J Vasc Surg. 2017;65(5):1483-92.
420.Aguiar FLN, Lunardi FO, Lima LF, Bruno JB, Alves BG, Magalhaes-Padilha DM, et al. Role of EGF on in situ culture of equine preantral follicles and metabolomics profile. Res Vet Sci. 2017;115:155-64.
421.Zheng D, Hu M, Bai Y, Zhu X, Lu X, Wu C, et al. EGFR G796D mutation mediates resistance to osimertinib. Oncotarget. 2017;8(30):49671-9.
422.Liu S, Xu C, Li G, Liu H, Xie J, Tu G, et al. Vatalanib decrease the positive interaction of VEGF receptor-2 and P2X2/3 receptor in chronic constriction injury rats. Neurochem Int. 2012;60(6):565-72.
423.Norenberg W, Plotz T, Sobottka H, Chubanov V, Mittermeier L, Kalwa H, et al. TRPM7 is a molecular substrate of ATP-evoked P2X7-like currents in tumor cells. J Gen Physiol. 2016;147(6):467-83.
424.Malinowski M, Deja MA, Janusiewicz P, Golba KS, Roleder T, Wos S. Mechanisms of vasodilatatory effect of perivascular tissue of human internal thoracic artery. J Physiol Pharmacol. 2013;64(3):309-16.

425.Choi KJ, Kim KS, Kim SH, Kim DK, Park HS. Caffeine and 2-Aminoethoxydiphenyl Borate (2-APB) Have Different Ability to Inhibit Intracellular Calcium Mobilization in Pancreatic Acinar Cell. Korean J Physiol Pharmacol. 2010;14(2):105-11.
426.Song C, Bae Y, Jun J, Lee H, Kim ND, Lee KB, et al. Identification of TG100-115 as a new and potent TRPM7 kinase inhibitor, which suppresses breast cancer cell migration and invasion. Biochim Biophys Acta Gen Subj. 2017;1861(4):947-57.
427.Chang R, Chicoine LG, Cui H, Kanagy NL, Walker BR, Liu Y, et al. Cytokine-induced arginase activity in pulmonary endothelial cells is dependent on Src family tyrosine kinase activity. Am J Physiol Lung Cell Mol Physiol. 2008;295(4):L688-97.
428.Chen YJ, Huang WC, Wei YL, Hsu SC, Yuan P, Lin HY, et al. Elevated BCRP/ABCG2 expression confers acquired resistance to gefitinib in wild-type EGFR-expressing cells. PloS one. 2011;6(6):e21428.
429.Shin EY, Lee CS, Park MH, Kim DJ, Kwak SJ, Kim EG. Involvement of betaPIX in angiotensin II-induced migration of vascular smooth muscle cells. Experimental & molecular medicine. 2009;41(6):387-96.
430.Chubanov V, Schafer S, Ferioli S, Gudermann T. Natural and Synthetic Modulators of the TRPM7 Channel. Cells. 2014;3(4):1089-101.
431.Tajadini M, Panjehpour M, Javanmard SH. Comparison of SYBR Green and TaqMan methods in quantitative real-time polymerase chain reaction analysis of four adenosine receptor subtypes. Adv Biomed Res. 2014;3:85.
432.Rao X, Huang X, Zhou Z, Lin X. An improvement of the 2^(-delta delta CT) method for quantitative real-time polymerase chain reaction data analysis. Biostat Bioinforma Biomath. 2013;3(3):71-85.
433.Suzuki Y, Yokoyama K. Development of Functional Fluorescent Molecular Probes for the Detection of Biological Substances. Biosensors (Basel). 2015;5(2):337-63.
434.Wallace PK, Tario JD, Jr., Fisher JL, Wallace SS, Ernstoff MS, Muirhead KA. Tracking antigen-driven responses by flow cytometry: monitoring proliferation by dye dilution. Cytometry A. 2008;73(11):1019-34.
435.Quah BJ, Parish CR. The use of carboxyfluorescein diacetate succinimidyl ester (CFSE) to monitor lymphocyte proliferation. J Vis Exp. 2010(44).
436.Liang CC, Park AY, Guan JL. In vitro scratch assay: a convenient and inexpensive method for analysis of cell migration in vitro. Nat Protoc. 2007;2(2):329-33.
437.Entschladen F, Drell TLt, Lang K, Masur K, Palm D, Bastian P, et al. Analysis methods of human cell migration. Exp Cell Res. 2005;307(2):418-26.
438.Vang Mouritzen M, Jenssen H. Optimized Scratch Assay for In Vitro Testing of Cell Migration with an Automated Optical Camera. J Vis Exp. 2018(138).
439.Dos-Santos JS, Firmino-Cruz L, Ramos TD, da Fonseca-Martins AM, Oliveira-Maciel D, De-Medeiros JVR, et al. Characterization of Sv129 Mice as a Susceptible Model to Leishmania amazonensis. Front Med (Lausanne). 2019;6:100.
440.Liu Y, Poon RT, Li Q, Kok TW, Lau C, Fan ST. Both antiangiogenesis- and angiogenesis-independent effects are responsible for hepatocellular carcinoma growth arrest by tyrosine kinase inhibitor PTK787/ZK222584. Cancer Res. 2005;65(9):3691-9.
441.Liu M, Xu S, Wang Y, Li Y, Li Y, Zhang H, et al. PD 0332991, a selective cyclin D kinase 4/6 inhibitor, sensitizes lung cancer cells to treatment with epidermal growth factor receptor tyrosine kinase inhibitors. Oncotarget. 2016;7(51):84951-64.
442.Small HY, Morgan H, Beattie E, Griffin S, Indahl M, Delles C, et al. Abnormal uterine artery remodelling in the stroke prone spontaneously hypertensive rat. Placenta. 2016;37:34-44.
443.Morgan HL, Butler E, Ritchie S, Herse F, Dechend R, Beattie E, et al. Modeling Superimposed Preeclampsia Using Ang II (Angiotensin II) Infusion in Pregnant Stroke-Prone Spontaneously Hypertensive Rats. Hypertension. 2018;72(1):208-18.
444.Shah DM. The role of RAS in the pathogenesis of preeclampsia. Current hypertension reports. 2006;8(2):144-52.

445.Brosnihan KB, Hering L, Dechend R, Chappell MC, Herse F. Increased angiotensin II in the mesometrial triangle of a transgenic rat model of preeclampsia. Hypertension. 2010;55(2):562-6.
446.Mulvany MJ, Halpern W. Contractile properties of small arterial resistance vessels in spontaneously hypertensive and normotensive rats. Circ Res. 1977;41(1):19-26.
447.Wang D, Iversen J, Strandgaard S. Endothelium-dependent relaxation of small resistance vessels is impaired in patients with autosomal dominant polycystic kidney disease. J Am Soc Nephrol. 2000;11(8):1371-6.
448.Dorn GW, 2nd, Becker MW. Thromboxane A2 stimulated signal transduction in vascular smooth muscle. J Pharmacol Exp Ther. 1993;265(1):447-56.
449.del Campo L, Ferrer M. Wire Myography to Study Vascular Tone and Vascular Structure of Isolated Mouse Arteries. Methods Mol Biol. 2015;1339:255-76.
450.Bonaventura D, Lunardi CN, Rodrigues GJ, Neto MA, Bendhack LM. A novel mechanism of vascular relaxation induced by sodium nitroprusside in the isolated rat aorta. Nitric Oxide. 2008;18(4):287-95.
451.Wang S, Zhang Z, Peng H, Zeng K. Recent advances on the roles of epidermal growth factor receptor in psoriasis. Am J Transl Res. 2019;11(2):520-8.
452.Yu X, Sharma KD, Takahashi T, Iwamoto R, Mekada E. Ligand-independent dimer formation of epidermal growth factor receptor (EGFR) is a step separable from ligand-induced EGFR signaling. Mol Biol Cell. 2002;13(7):2547-57.
453.Mitchell RA, Luwor RB, Burgess AW. Epidermal growth factor receptor: Structure-function informing the design of anticancer therapeutics. Exp Cell Res. 2018;371(1):1-19.
454.de Miranda MC, Rodrigues MA, de Angelis Campos AC, Faria J, Kunrath-Lima M, Mignery GA, et al. Epidermal growth factor (EGF) triggers nuclear calcium signaling through the intranuclear phospholipase C delta-4 (PLCdelta4). J Biol Chem. 2019.
455.Zeng F, Harris RC. Epidermal growth factor, from gene organization to bedside. Semin Cell Dev Biol. 2014;28:2-11.
456.Takayanagi T, Kawai T, Forrester SJ, Obama T, Tsuji T, Fukuda Y, et al. Role of epidermal growth factor receptor and endoplasmic reticulum stress in vascular remodeling induced by angiotensin II. Hypertension. 2015;65(6):1349-55.
457.Mazak I, Fiebeler A, Muller DN, Park JK, Shagdarsuren E, Lindschau C, et al. Aldosterone potentiates angiotensin II-induced signaling in vascular smooth muscle cells. Circulation. 2004;109(22):2792-800.
458.Min LJ, Mogi M, Li JM, Iwanami J, Iwai M, Horiuchi M. Aldosterone and angiotensin II synergistically induce mitogenic response in vascular smooth muscle cells. Circ Res. 2005;97(5):434-42.
459.Mugabe BE, Yaghini FA, Song CY, Buharalioglu CK, Waters CM, Malik KU. Angiotensin II-induced migration of vascular smooth muscle cells is mediated by p38 mitogen-activated protein kinase-activated c-Src through spleen tyrosine kinase and epidermal growth factor receptor transactivation. The Journal of pharmacology and experimental therapeutics. 2010;332(1):116-24.
460.Bokemeyer D, Schmitz U, Kramer HJ. Angiotensin II-induced growth of vascular smooth muscle cells requires an Src-dependent activation of the epidermal growth factor receptor. Kidney international. 2000;58(2):549-58.
461.Rios FJ, Zou ZG, Harvey AP, Harvey KY, Nosalski R, Anyfanti P, et al. Chanzyme TRPM7 protects against cardiovascular inflammation and fibrosis. Cardiovasc Res. 2019.
462.Shin MK, Caballero-Eraso C, Mu YP, Gu C, Hyeung BH, Kim LJ, et al. Leptin Induces Hypertension Acting on Transient Receptor Potential Melastatin 7 Channel in the Carotid Body. Circ Res. 2019.
463.Ribback S, Sailer V, Bohning E, Gunther J, Merz J, Steinmuller F, et al. The Epidermal Growth Factor Receptor (EGFR) Inhibitor Gefitinib Reduces but Does Not Prevent Tumorigenesis in Chemical and Hormonal Induced Hepatocarcinogenesis Rat Models. Int J Mol Sci. 2016;17(10).
464.Hofmann T, Schafer S, Linseisen M, Sytik L, Gudermann T, Chubanov V. Activation of TRPM7 channels by small molecules under physiological conditions. Pflugers Arch. 2014;466(12):2177-89.

465.Dedkova EN, Sigova AA, Zinchenko VP. Mechanism of action of calcium ionophores on intact cells: ionophore-resistant cells. Membr Cell Biol. 2000;13(3):357-68.
466.Touyz RM, Schiffrin EL. Angiotensin II regulates vascular smooth muscle cell pH, contraction, and growth via tyrosine kinase-dependent signaling pathways. Hypertension. 1997;30(2 Pt 1):222-9.
467.Brandvold KR, Steffey ME, Fox CC, Soellner MB. Development of a highly selective c-Src kinase inhibitor. ACS Chem Biol. 2012;7(8):1393-8.
468.Yogi A, Callera GE, O'Connor S, Antunes TT, Valinsky W, Miquel P, et al. Aldosterone signaling through transient receptor potential melastatin 7 cation channel (TRPM7) and its alpha-kinase domain. Cell Signal. 2013;25(11):2163-75.
469.Mittermeier L, Demirkhanyan L, Stadlbauer B, Breit A, Recordati C, Hilgendorff A, et al. TRPM7 is the central gatekeeper of intestinal mineral absorption essential for postnatal survival. Proceedings of the National Academy of Sciences of the United States of America. 2019;116(10):4706-15.
470.Wu W, Graves LM, Gill GN, Parsons SJ, Samet JM. Src-dependent phosphorylation of the epidermal growth factor receptor on tyrosine 845 is required for zinc-induced Ras activation. The Journal of biological chemistry. 2002;277(27):24252-7.
471.Poulard C, Rambaud J, Le Romancer M, Corbo L. Proximity ligation assay to detect and localize the interactions of ERalpha with PI3-K and Src in breast cancer cells and tumor samples. Methods Mol Biol. 2014;1204:135-43.
472.Roberts RE. The extracellular signal-regulated kinase (ERK) pathway: a potential therapeutic target in hypertension. J Exp Pharmacol. 2012;4:77-83.
473.Louis SF, Zahradka P. Vascular smooth muscle cell motility: From migration to invasion. Exp Clin Cardiol. 2010;15(4):e75-85.
474.Bennett MR, Sinha S, Owens GK. Vascular Smooth Muscle Cells in Atherosclerosis. Circ Res. 2016;118(4):692-702.
475.Strzalka W, Ziemienowicz A. Proliferating cell nuclear antigen (PCNA): a key factor in DNA replication and cell cycle regulation. Ann Bot. 2011;107(7):1127-40.
476.Wang Q, Zhao N, Kennard S, Lilly B. Notch2 and Notch3 function together to regulate vascular smooth muscle development. PloS one. 2012;7(5):e37365.
477.Montezano AC, Lopes RA, Neves KB, Rios F, Touyz RM. Isolation and Culture of Vascular Smooth Muscle Cells from Small and Large Vessels. Methods Mol Biol. 2017;1527:349-54.
478.Chobanian AV, Bakris GL, Black HR, Cushman WC, Green LA, Izzo JL, Jr., et al. Seventh report of the Joint National Committee on Prevention, Detection, Evaluation, and Treatment of High Blood Pressure. Hypertension. 2003;42(6):1206-52.
479.Poulter NR, Castillo R, Charchar FJ, Schlaich MP, Schutte AE, Tomaszewski M, et al. Are the American Heart Association/American College of Cardiology High Blood Pressure Guidelines Fit for Global Purpose?: Thoughts From the International Society of Hypertension. Hypertension. 2018;72(2):260-2.
480.Moccia F, Berra-Romani R, Tritto S, Signorelli S, Taglietti V, Tanzi F. Epidermal growth factor induces intracellular Ca2+ oscillations in microvascular endothelial cells. J Cell Physiol. 2003;194(2):139-50.
481.Gotru SK, Chen W, Kraft P, Becker IC, Wolf K, Stritt S, et al. TRPM7 Kinase Controls Calcium Responses in Arterial Thrombosis and Stroke in Mice. Arterioscler Thromb Vasc Biol. 2018;38(2):344-52.
482.Togashi K, Inada H, Tominaga M. Inhibition of the transient receptor potential cation channel TRPM2 by 2-aminoethoxydiphenyl borate (2-APB). Br J Pharmacol. 2008;153(6):1324-30.
483.Dobrydneva Y, Blackmore P. 2-Aminoethoxydiphenyl borate directly inhibits store-operated calcium entry channels in human platelets. Molecular pharmacology. 2001;60(3):541-52.
484.Irtegun S, Wood RJ, Ormsby AR, Mulhern TD, Hatters DM. Tyrosine 416 is phosphorylated in the closed, repressed conformation of c-Src. PloS one. 2013;8(7):e71035.
485.Donepudi M, Resh MD. c-Src trafficking and co-localization with the EGF receptor promotes EGF ligand-independent EGF receptor activation and signaling. Cell Signal. 2008;20(7):1359-67.

486.Hu D, Yin C, Luo S, Habenicht AJR, Mohanta SK. Vascular Smooth Muscle Cells Contribute to Atherosclerosis Immunity. Front Immunol. 2019;10:1101.
487.Brown IAM, Diederich L, Good ME, DeLalio LJ, Murphy SA, Cortese-Krott MM, et al. Vascular Smooth Muscle Remodeling in Conductive and Resistance Arteries in Hypertension. Arterioscler Thromb Vasc Biol. 2018;38(9):1969-85.
488.He YH, Wang XQ, Zhang J, Liu ZH, Pan WQ, Shen Y, et al. Association of Serum HMGB2 Levels With In-Stent Restenosis: HMGB2 Promotes Neointimal Hyperplasia in Mice With Femoral Artery Injury and Proliferation and Migration of VSMCs. Arterioscler Thromb Vasc Biol. 2017;37(4):717-29.
489.Liu H, Zhang W, Kennard S, Caldwell RB, Lilly B. Notch3 is critical for proper angiogenesis and mural cell investment. Circ Res. 2010;107(7):860-70.
490.Neves KB, Harvey AP, Moreton F, Montezano AC, Rios FJ, Alves-Lopes R, et al. ER stress and Rho kinase activation underlie the vasculopathy of CADASIL. JCI Insight. 2019;4(23).
491.Ferrara N, Gerber HP, LeCouter J. The biology of VEGF and its receptors. Nat Med. 2003;9(6):669-76.
492.Bogdan S, Klambt C. Epidermal growth factor receptor signaling. Curr Biol. 2001;11(8):R292-5.
493.Eichmann A, Simons M. VEGF signaling inside vascular endothelial cells and beyond. Curr Opin Cell Biol. 2012;24(2):188-93.
494.Hosgorler F, Kizildag S, Ates M, Argon A, Koc B, Kandis S, et al. The Chronic Use of Magnesium Decreases VEGF Levels in the Uterine Tissue in Rats. Biol Trace Elem Res. 2019.
495.Cai N, Lou L, Al-Saadi N, Tetteh S, Runnels LW. The kinase activity of the channel-kinase protein TRPM7 regulates stability and localization of the TRPM7 channel in polarized epithelial cells. J Biol Chem. 2018;293(29):11491-504.
496.Simons M, Gordon E, Claesson-Welsh L. Mechanisms and regulation of endothelial VEGF receptor signalling. Nat Rev Mol Cell Biol. 2016;17(10):611-25.
497.Gee E, Milkiewicz M, Haas TL. p38 MAPK activity is stimulated by vascular endothelial growth factor receptor 2 activation and is essential for shear stress-induced angiogenesis. J Cell Physiol. 2010;222(1):120-6.
498.Harhaj NS, Felinski EA, Wolpert EB, Sundstrom JM, Gardner TW, Antonetti DA. VEGF activation of protein kinase C stimulates occludin phosphorylation and contributes to endothelial permeability. Invest Ophthalmol Vis Sci. 2006;47(11):5106-15.
499.Quiniou C, Sennlaub F, Beauchamp MH, Checchin D, Lahaie I, Brault S, et al. Dominant role for calpain in thromboxane-induced neuromicrovascular endothelial cytotoxicity. J Pharmacol Exp Ther. 2006;316(2):618-27.
500.Valinsky WC, Jolly A, Miquel P, Touyz RM, Shrier A. Aldosterone Upregulates Transient Receptor Potential Melastatin 7 (TRPM7). J Biol Chem. 2016;291(38):20163-72.
501.Martinez-Orgado J, Gonzalez R, Alonso MJ, Marin J. Nitric oxide-dependent and -independent mechanisms in the relaxation elicited by acetylcholine in fetal rat aorta. Life sciences. 1999;64(4):269-77.
502.Cogolludo AL, Perez-Vizcaino F, Zaragoza-Arnaez F, Ibarra M, Lopez-Lopez G, Lopez-Miranda V, et al. Mechanisms involved in SNP-induced relaxation and [Ca+]i reduction in piglet pulmonary and systemic arteries. British journal of pharmacology. 2001;132(4):959-67.
503.Chalon S, Tejura B, Moreno H, Jr., Urae A, Blaschke TF, Hoffman BB. Role of nitric oxide in isoprenaline and sodium nitroprusside-induced relaxation in human hand veins. Br J Clin Pharmacol. 1999;47(1):91-8.
504.Bolivar JJ. Essential hypertension: an approach to its etiology and neurogenic pathophysiology. Int J Hypertens. 2013;2013:547809.
505.Camargo LL, Harvey AP, Rios FJ, Tsiropoulou S, Da Silva RNO, Cao Z, et al. Vascular Nox (NADPH Oxidase) Compartmentalization, Protein Hyperoxidation, and Endoplasmic Reticulum Stress Response in Hypertension. Hypertension. 2018;72(1):235-46.
506.Shin MK, Eraso CC, Mu YP, Gu C, Yeung BHY, Kim LJ, et al. Leptin Induces Hypertension Acting on Transient Receptor Potential Melastatin 7 Channel in the Carotid Body. Circ Res. 2019;125(11):989-1002.

507.Touyz RM, Deschepper C, Park JB, He G, Chen X, Neves MF, et al. Inhibition of mitogen-activated protein/extracellular signal-regulated kinase improves endothelial function and attenuates Ang II-induced contractility of mesenteric resistance arteries from spontaneously hypertensive rats. J Hypertens. 2002;20(6):1127-34.
508.Klemke RL, Cai S, Giannini AL, Gallagher PJ, de Lanerolle P, Cheresh DA. Regulation of cell motility by mitogen-activated protein kinase. J Cell Biol. 1997;137(2):481-92.
509.Kuo IY, Ehrlich BE. Signaling in muscle contraction. Cold Spring Harbor perspectives in biology. 2015;7(2):a006023.
510.Powe CE, Levine RJ, Karumanchi SA. Preeclampsia, a disease of the maternal endothelium: the role of antiangiogenic factors and implications for later cardiovascular disease. Circulation. 2011;123(24):2856-69.
511.Pankiewicz K, Szczerba E, Maciejewski T, Fijalkowska A. Non-obstetric complications in preeclampsia. Prz Menopauzalny. 2019;18(2):99-109.
512.Say L, Chou D, Gemmill A, Tuncalp O, Moller AB, Daniels J, et al. Global causes of maternal death: a WHO systematic analysis. Lancet Glob Health. 2014;2(6):e323-33.
513.Leon LJ, McCarthy FP, Direk K, Gonzalez-Izquierdo A, Prieto-Merino D, Casas JP, et al. Preeclampsia and Cardiovascular Disease in a Large UK Pregnancy Cohort of Linked Electronic Health Records: A CALIBER Study. Circulation. 2019;140(13):1050-60.
514.Smith JM, Lowe RF, Fullerton J, Currie SM, Harris L, Felker-Kantor E. An integrative review of the side effects related to the use of magnesium sulfate for pre-eclampsia and eclampsia management. BMC Pregnancy Childbirth. 2013;13:34.
515.Long Q, Oladapo OT, Leathersich S, Vogel JP, Carroli G, Lumbiganon P, et al. Clinical practice patterns on the use of magnesium sulphate for treatment of pre-eclampsia and eclampsia: a multi-country survey. BJOG. 2017;124(12):1883-90.
516.Mainou BA, Dermody TS. Src kinase mediates productive endocytic sorting of reovirus during cell entry. J Virol. 2011;85(7):3203-13.
517.Ikawa T, Watanabe Y, Okuzaki D, Goto N, Okamura N, Yamanishi K, et al. A new approach to identifying hypertension-associated genes in the mesenteric artery of spontaneously hypertensive rats and stroke-prone spontaneously hypertensive rats. J Hypertens. 2019;37(8):1644-56.
518.Gu M, Zhu Y, Yin X, Zhang DM. Small-conductance Ca(2+)-activated K(+) channels: insights into their roles in cardiovascular disease. Exp Mol Med. 2018;50(4):23.
519.Liberis A, Stanulov G, Ali EC, Hassan A, Pagalos A, Kontomanolis EN. Pre-eclampsia and the vascular endothelial growth factor: a new aspect. Clin Exp Obstet Gynecol. 2016;43(1):9-13.
520.Bruschi G, Regolisti G, Borghetti A. [Cellular calcium, vasoconstriction, hypertension]. Ann Ital Med Int. 1992;7(3 Suppl):119S-23S.
521.Simonetti G, Mohaupt M. [Calcium and blood pressure]. Ther Umsch. 2007;64(5):249-52.
522.Lorenz-Eberhardt G, Kainer F, Sabin K, Haas J. [Magnesium content of serum in pregnancy-induced hypertension]. Gynakologisch-geburtshilfliche Rundschau. 1993;33(2):92-3.
523.Adam B, Malatyalioglu E, Alvur M, Talu C. Magnesium, zinc and iron levels in pre-eclampsia. The Journal of maternal-fetal medicine. 2001;10(4):246-50.
524.Altura BM, Altura BT, Carella A. Magnesium deficiency-induced spasms of umbilical vessels: relation to preeclampsia, hypertension, growth retardation. Science. 1983;221(4608):376-8.
525.Wang Y, Zhao S. Vascular Biology of the Placenta. Integrated Systems Physiology: from Molecules to Function to Disease. San Rafael (CA)2010.
526.Hubner N, Kreutz R, Takahashi S, Ganten D, Lindpaintner K. Altered angiotensinogen amino acid sequence and plasma angiotensin II levels in genetically hypertensive rats. A study on cause and effect. Hypertension. 1995;26(2):279-84.
527.Saito S, Shiozaki A, Nakashima A, Sakai M, Sasaki Y. The role of the immune system in preeclampsia. Molecular aspects of medicine. 2007;28(2):192-209.
528.Evain-Brion D. [The 2 differentiation pathways of the human trophoblast]. Gynecol Obstet Fertil. 2001;29(7-8):497-502.
529.Cohen S. Isolation of a mouse submaxillary gland protein accelerating incisor eruption and eyelid opening in the new-born animal. J Biol Chem. 1962;237:1555-62.

530.Sforza V, Martinelli E, Ciardiello F, Gambardella V, Napolitano S, Martini G, et al. Mechanisms of resistance to anti-epidermal growth factor receptor inhibitors in metastatic colorectal cancer. World J Gastroenterol. 2016;22(28):6345-61.
531.Dai F, Lin X, Chang C, Feng XH. Nuclear export of Smad2 and Smad3 by RanBP3 facilitates termination of TGF-beta signaling. Dev Cell. 2009;16(3):345-57.
532.Mak IT, Kramer JH, Chmielinska JJ, Spurney CF, Weglicki WB. EGFR-TKI, erlotinib, causes hypomagnesemia, oxidative stress, and cardiac dysfunction: attenuation by NK-1 receptor blockade. J Cardiovasc Pharmacol. 2015;65(1):54-61.
533.Fakih MG, Wilding G, Lombardo J. Cetuximab-induced hypomagnesemia in patients with colorectal cancer. Clin Colorectal Cancer. 2006;6(2):152-6.
534.Barrick CJ, Yu M, Chao HH, Threadgill DW. Chronic pharmacologic inhibition of EGFR leads to cardiac dysfunction in C57BL/6J mice. Toxicol Appl Pharmacol. 2008;228(3):315-25.
535.Tangvoraphonkchai K, Davenport A. Magnesium and Cardiovascular Disease. Advances in chronic kidney disease. 2018;25(3):251-60.
536.Maier JA, Bernardini D, Rayssiguier Y, Mazur A. High concentrations of magnesium modulate vascular endothelial cell behaviour in vitro. Biochimica et biophysica acta. 2004;1689(1):6-12.
537.Nilius B, Szallasi A. Transient receptor potential channels as drug targets: from the science of basic research to the art of medicine. Pharmacol Rev. 2014;66(3):676-814.
538.Alves-Lopes R, Neves KB, Anagnostopoulou A, Rios FJ, Lacchini S, Montezano AC, et al. Crosstalk Between Vascular Redox and Calcium Signaling in Hypertension Involves TRPM2 (Transient Receptor Potential Melastatin 2) Cation Channel. Hypertension. 2020;75(1):139-49.
539.Singh KD, Karnik SS. Angiotensin Receptors: Structure, Function, Signaling and Clinical Applications. Journal of cell signaling. 2016;1(2).
540.Touyz RM, Cruzado M, Tabet F, Yao G, Salomon S, Schiffrin EL. Redox-dependent MAP kinase signaling by Ang II in vascular smooth muscle cells: role of receptor tyrosine kinase transactivation. Canadian journal of physiology and pharmacology. 2003;81(2):159-67.
541.Ushio-Fukai M. Vascular signaling through G protein-coupled receptors: new concepts. Current opinion in nephrology and hypertension. 2009;18(2):153-9.
542.Ikari A, Atomi K, Kinjo K, Sasaki Y, Sugatani J. Magnesium deprivation inhibits a MEK-ERK cascade and cell proliferation in renal epithelial Madin-Darby canine kidney cells. Life sciences. 2010;86(19-20):766-73.
543.Leiper LJ, Walczysko P, Kucerova R, Ou J, Shanley LJ, Lawson D, et al. The roles of calcium signaling and ERK1/2 phosphorylation in a Pax6+/- mouse model of epithelial wound-healing delay. BMC biology. 2006;4:27.
544.Chen D, Cao L, Wang X. MPZL1 promotes tumor cell proliferation and migration via activation of Src kinase in ovarian cancer. Oncology reports. 2019;42(2):679-87.
545.Mathew S, George SP, Wang Y, Siddiqui MR, Srinivasan K, Tan L, et al. Potential molecular mechanism for c-Src kinase-mediated regulation of intestinal cell migration. The Journal of biological chemistry. 2008;283(33):22709-22.
546.Vicente-Manzanares M, Ma X, Adelstein RS, Horwitz AR. Non-muscle myosin II takes centre stage in cell adhesion and migration. Nature reviews Molecular cell biology. 2009;10(11):778-90.
547.Halder D, Saha S, Singh RK, Ghosh I, Mallick D, Dey SK, et al. Nonmuscle myosin IIA and IIB differentially modulate migration and alter gene expression in primary mouse tumorigenic cells. Molecular biology of the cell. 2019;30(12):1463-76.
548.Dulyaninova NG, House RP, Betapudi V, Bresnick AR. Myosin-IIA heavy-chain phosphorylation regulates the motility of MDA-MB-231 carcinoma cells. Molecular biology of the cell. 2007;18(8):3144-55.
549.Wolf FI, Cittadini A. Magnesium in cell proliferation and differentiation. Frontiers in bioscience : a journal and virtual library. 1999;4:D607-17.
550.Senger DR, Galli SJ, Dvorak AM, Perruzzi CA, Harvey VS, Dvorak HF. Tumor cells secrete a vascular permeability factor that promotes accumulation of ascites fluid. Science. 1983;219(4587):983-5.

551.Holmes DI, Zachary I. The vascular endothelial growth factor (VEGF) family: angiogenic factors in health and disease. Genome Biol. 2005;6(2):209.
552.He H, Venema VJ, Gu X, Venema RC, Marrero MB, Caldwell RB. Vascular endothelial growth factor signals endothelial cell production of nitric oxide and prostacyclin through flk-1/KDR activation of c-Src. J Biol Chem. 1999;274(35):25130-5.
553.Shibuya M. Vascular Endothelial Growth Factor (VEGF) and Its Receptor (VEGFR) Signaling in Angiogenesis: A Crucial Target for Anti- and Pro-Angiogenic Therapies. Genes Cancer. 2011;2(12):1097-105.
554.Ishida A, Murray J, Saito Y, Kanthou C, Benzakour O, Shibuya M, et al. Expression of vascular endothelial growth factor receptors in smooth muscle cells. J Cell Physiol. 2001;188(3):359-68.
555.Liao XH, Xiang Y, Li H, Zheng L, Xu Y, Xi Yu C, et al. VEGF-A Stimulates STAT3 Activity via Nitrosylation of Myocardin to Regulate the Expression of Vascular Smooth Muscle Cell Differentiation Markers. Sci Rep. 2017;7(1):2660.
556.Laitinen M, Zachary I, Breier G, Pakkanen T, Hakkinen T, Luoma J, et al. VEGF gene transfer reduces intimal thickening via increased production of nitric oxide in carotid arteries. Hum Gene Ther. 1997;8(15):1737-44.
557.Krapivinsky G, Krapivinsky L, Manasian Y, Clapham DE. The TRPM7 chanzyme is cleaved to release a chromatin-modifying kinase. Cell. 2014;157(5):1061-72.
558.Urban N, Wang L, Kwiek S, Rademann J, Kuebler WM, Schaefer M. Identification and Validation of Larixyl Acetate as a Potent TRPC6 Inhibitor. Molecular pharmacology. 2016;89(1):197-213.
559.Fox CH, Timm EA, Jr., Smith SJ, Touyz RM, Bush EG, Wallace PK. A method for measuring intracellular free magnesium concentration in platelets using flow cytometry. Magnesium research. 2007;20(3):200-7.
560.Abhinand CS, Raju R, Soumya SJ, Arya PS, Sudhakaran PR. VEGF-A/VEGFR2 signaling network in endothelial cells relevant to angiogenesis. J Cell Commun Signal. 2016;10(4):347-54.
561.Castilla MA, Caramelo C, Gazapo RM, Martin O, Gonzalez-Pacheco FR, Tejedor A, et al. Role of vascular endothelial growth factor (VEGF) in endothelial cell protection against cytotoxic agents. Life Sci. 2000;67(9):1003-13.
562.Breslin JW, Pappas PJ, Cerveira JJ, Hobson RW, 2nd, Duran WN. VEGF increases endothelial permeability by separate signaling pathways involving ERK-1/2 and nitric oxide. Am J Physiol Heart Circ Physiol. 2003;284(1):H92-H100.
563.Gliki G, Wheeler-Jones C, Zachary I. Vascular endothelial growth factor induces protein kinase C (PKC)-dependent Akt/PKB activation and phosphatidylinositol 3'-kinase-mediates PKC delta phosphorylation: role of PKC in angiogenesis. Cell Biol Int. 2002;26(9):751-9.
564.Dorafshar AH, Angle N, Bryer-Ash M, Huang D, Farooq MM, Gelabert HA, et al. Vascular endothelial growth factor inhibits mitogen-induced vascular smooth muscle cell proliferation. J Surg Res. 2003;114(2):179-86.
565.Schad JF, Meltzer KR, Hicks MR, Beutler DS, Cao TV, Standley PR. Cyclic strain upregulates VEGF and attenuates proliferation of vascular smooth muscle cells. Vasc Cell. 2011;3:21.
566.Igarashi J, Erwin PA, Dantas AP, Chen H, Michel T. VEGF induces S1P1 receptors in endothelial cells: Implications for cross-talk between sphingolipid and growth factor receptors. Proc Natl Acad Sci U S A. 2003;100(19):10664-9.
567.Ashrafpour H, Huang N, Neligan PC, Forrest CR, Addison PD, Moses MA, et al. Vasodilator effect and mechanism of action of vascular endothelial growth factor in skin vasculature. Am J Physiol Heart Circ Physiol. 2004;286(3):H946-54.
568.Grover TR, Zenge JP, Parker TA, Abman SH. Vascular endothelial growth factor causes pulmonary vasodilation through activation of the phosphatidylinositol-3-kinase-nitric oxide pathway in the late-gestation ovine fetus. Pediatr Res. 2002;52(6):907-12.
569.Wei W, Chen ZW, Yang Q, Jin H, Furnary A, Yao XQ, et al. Vasorelaxation induced by vascular endothelial growth factor in the human internal mammary artery and radial artery. Vascul Pharmacol. 2007;46(4):253-9.

570.Pearson PJ, Evora PR, Seccombe JF, Schaff HV. Hypomagnesemia inhibits nitric oxide release from coronary endothelium: protective role of magnesium infusion after cardiac operations. The Annals of thoracic surgery. 1998;65(4):967-72.
571.Satake K, Lee JD, Shimizu H, Uzui H, Mitsuke Y, Yue H, et al. Effects of magnesium on prostacyclin synthesis and intracellular free calcium concentration in vascular cells. Magnesium research. 2004;17(1):20-7.
572.Haenni A, Johansson K, Lind L, Lithell H. Magnesium infusion improves endothelium-dependent vasodilation in the human forearm. American journal of hypertension. 2002;15(1 Pt 1):10-5.
573.Herndon DN, Nguyen TT, Gilpin DA. Growth factors. Local and systemic. Arch Surg. 1993;128(11):1227-33.
574.Stone WL, Varacallo M. Physiology, Growth Factor. StatPearls. Treasure Island (FL)2020.
575.Ono M, Kuwano M. Molecular mechanisms of epidermal growth factor receptor (EGFR) activation and response to gefitinib and other EGFR-targeting drugs. Clin Cancer Res. 2006;12(24):7242-51.
576.Rini BI. Vascular endothelial growth factor-targeted therapy in renal cell carcinoma: current status and future directions. Clin Cancer Res. 2007;13(4):1098-106.
577.Banerjee S, Mehta S, Haque I, Sengupta K, Dhar K, Kambhampati S, et al. VEGF-A165 induces human aortic smooth muscle cell migration by activating neuropilin-1-VEGFR1-PI3K axis. Biochemistry. 2008;47(11):3345-51.
578.Basrali F, Kocer G, Ulker Karadamar P, Nasircilar Ulker S, Sati L, Ozen N, et al. Effect of magnesium supplementation on blood pressure and vascular reactivity in nitric oxide synthase inhibition-induced hypertension model. Clinical and experimental hypertension. 2015;37(8):633-42.
579.Sena CM, Leandro A, Azul L, Seica R, Perry G. Vascular Oxidative Stress: Impact and Therapeutic Approaches. Frontiers in physiology. 2018;9:1668.
580.Morais JB, Severo JS, Santos LR, de Sousa Melo SR, de Oliveira Santos R, de Oliveira AR, et al. Role of Magnesium in Oxidative Stress in Individuals with Obesity. Biological trace element research. 2017;176(1):20-6.
581.Hans CP, Chaudhary DP, Bansal DD. Effect of magnesium supplementation on oxidative stress in alloxanic diabetic rats. Magnesium research. 2003;16(1):13-9.
582.Petrovic J, Stanic D, Dmitrasinovic G, Plecas-Solarovic B, Ignjatovic S, Batinic B, et al. Magnesium Supplementation Diminishes Peripheral Blood Lymphocyte DNA Oxidative Damage in Athletes and Sedentary Young Man. Oxidative medicine and cellular longevity. 2016;2016:2019643.
583.Ratsep MT, Carmeliet P, Adams MA, Croy BA. Impact of placental growth factor deficiency on early mouse implant site angiogenesis. Placenta. 2014;35(9):772-5.
584.Kalafat E, Thilaganathan B. Cardiovascular origins of preeclampsia. Current opinion in obstetrics & gynecology. 2017;29(6):383-9.
585.Kolisek M, Galaviz-Hernandez C, Vazquez-Alaniz F, Sponder G, Javaid S, Kurth K, et al. SLC41A1 is the only magnesium responsive gene significantly overexpressed in placentas of preeclamptic women. Hypertension in pregnancy. 2013;32(4):378-89.